

The Application of Mechanochemical Techniques Towards Organic Synthesis and Catalysis

Andrew C. Jones

This thesis is submitted for the degree of Doctor of
Philosophy (PhD) at Cardiff University



March 2022

Summary

This thesis describes a series of studies of organic synthesis and catalysis under mechanochemical conditions.

Initial investigations outline the development of the first known C-S coupling under mechanochemical conditions, which builds upon previous work in the group describing a mechanochemical C-N coupling. In this study, oxidation of thiols to disulfides proved a detrimental side reaction, which was overcome with the use of a reductant and subsequent studies revealed a possibility for careful control of this interconversion which led to a 2-step, 1-pot coupling of disulfides. Also discussed in this study is the concept of phase transition induced reactivity, which was demonstrated by alteration of the reactor design to promote a melt-phase phenomenon that enabled reactivity in some cases.

Transition metal catalysed cross-electrophile coupling has recently emerged as a powerful strategy for the construction of C-C bonds. Firstly, a mechanochemical cross-electrophile coupling reaction of aryl halides and alkyl halides was developed, demonstrating the excellent capability of ball-milling for the activation of zero-valent metals. A broad scope was shown, including tolerance to a range of metal forms. Further work in this area led to the development of a reductive coupling reaction of twisted amides with alkyl halides for the construction of a range of ketone products. The degree of bond angle distortion for the amide component was examined for its effect in the reaction.

Finally, the reactivity of a fluoroiodane reagent was investigated for use under mechanochemical conditions. Initial work showed excellent reactivity for a known fluorocyclisation of unsaturated carboxylic acids to give fluorinated lactones. These promising results then led to development of mechanochemical protocols for the fluorocyclisation of β,γ unsaturated hydrazones and oximes to access novel fluorinated tetrahydropyridazines and dihydrooxazines respectively.

Related Publications

Some of the work in this thesis is also presented in the following publications.

1. **A Robust Pd-Catalyzed C–S Cross-Coupling Process Enabled by Ball-Milling** Andrew C. Jones, William I. Nicholson, Harry R. Smallman, and Duncan L. Browne, *Org. Lett.*, 2020, **22**, 7433–7438.
2. **A Ball-Milling-Enabled Cross-Electrophile Coupling**
Andrew C. Jones, William I. Nicholson, Jamie A. Leitch, and Duncan L. Browne, *Org. Lett.*, 2021, **23**, 6337–6341.
3. **Accessing novel fluorinated heterocycles with the hypervalent fluoroiodane reagent by solution and mechanochemical synthesis**
William Riley, Andrew C. Jones, Duncan L. Browne, and Alison M Stuart, *Chem. Commun.*, 2021, **57**, 7406–7409.

Acknowledgements

The work in this thesis would not have been possible without the support of many individuals, whom I will be forever grateful for.

Firstly, my MChem, then PhD supervisor Dr Duncan Browne. He has supported me over the past 5 years and has helped me grow and develop my scientific skills for which I am incredibly grateful. He pushed me to achieve my full potential as a part of the DLB group, even from afar in UCL after an institution switch. I'd also like to thank Dr Louis Morrill for welcoming me into his group in the latter stages of my PhD and for the guidance and support he provided me through group meetings as well as taking on administrative responsibilities for me.

Throughout my time in both the DLB and LCM groups, many group members have helped me through the course of my PhD. Firstly, special mention must go to the DLB group that remained in Cardiff as without them, it would have been a completely different journey, particularly given the pandemic. Tom, you helped me navigate through the highs and lows of PhD and became a great friend and housemate along the way, not to mention a fantastic ski instructor as well. Will, who also supervised me through my MChem project, your vast knowledge of chemistry always helped everyone to become the best they could. Roddy, you always made the lab a fun place to be and your constant questioning during my first year really improved my abilities.

A special thanks must also go to Alex from the LCM group, who not only had to put up with me in the lab, but also had the joy of living with me throughout the PhD. You've been a great friend and it was a pleasure to have you there from start to finish.

I would also like to thank other members of the DLB group that have helped me throughout my PhD from both Cardiff and UCL; Joey, Renan, Matt, Tom-LW, Harry, Rob, and Jamie. I'd also like to thank the members of the LCM group with whom I shared 0.30 C with; Deepak, Shyam, Albara, and James.

This project has contained many collaborative elements. Thanks to the group members who worked on some of the projects with me, and to Dr Alison Stuart and Will Riley from Leicester University who worked alongside us on a fluorination project, providing starting materials and advice along the way. I must also give mention to my funders, without which this would not have been possible. Thanks to Cambridge Reactor Designs and Dr Bashir Harji, and to the KESS II scheme.

Finally, a huge thanks for my friends and family outside of Cardiff, especially to my brother Matthew, and my parents Paul and Christine for the continuous support, without

which, this would not have been possible. Thank you also to my girlfriend Hannah for being there through it all and supporting me no matter what.

Abbreviations

1,10-phen	1,10-phenanthroline
acac	Acetylacetone
ACS	American Chemical society
anhyd.	Anhydrous
BINAP	2,2'-bis(diphenylphosphino)-1,1'-binaphthyl
bpy	2,2'-bipyridyl
cod	Cyclooctadiene
d.r.	Diastereomeric ratio
DABCO	1,4-Diazabicyclo[2.2.2]octane
DAST	Diethylaminosulfur trifluoride
dba	Dibenzylideneacetone
DBU	1,8-Diazabicyclo[5.4.0]undec-7-ene
DCC	<i>N,N'</i> -Dicyclohexylcarbodiimide
DCE	1,2-dichloroethane
DFI	2,2-Difluoro-1,3-dimethylimidazolidine
DIPEA	<i>N,N</i> -Diisopropylethylamine
DMA	<i>N,N</i> -Dimethylacetamide
DME	Dimethoxyethane
DMF	<i>N,N</i> -Dimethylformamide
DMI	1,3-Dimethyl-2-imidazolidinone
DMPU	<i>N,N'</i> -Dimethylpropyleneurea
DMSO	Dimethyl sulfoxide
dppe	1,2-Bis(diphenylphosphino)ethane
dppp	1,3-Bis(diphenylphosphino)propane
dtbpy	4,4'-Di- <i>tert</i> -butyl-2,2'-dipyridyl
e.e.	Enantiomeric excess
equiv.	Equivalents
h	Hours
HFIP	1,1,1,3,3,3-Hexafluoropropan-2-ol
HOBt	Hydroxybenzotriazole
HRMS	High resolution mass spectrometry
IPA	Isopropyl alcohol
LAG	Liquid assisted grinding
LRMS	Low resolution mass spectrometry
m. equiv.	Mass equivalents



min	Minutes
MOF	Metal organic framework
NFSI	<i>N</i> -Fluorobenzenesulfonimide
NHC	<i>N</i> -Heterocyclic carbene
NHPI	<i>N</i> -(acyloxy)phthalimides
NMP	<i>N</i> -Methyl-2-pyrrolidone
PC	Photocatalyst
PEPPSI	Pyridine enhanced pre-catalyst preparation stabilisation and initiation
PIDP	bis(tert-butylcarbonyloxy)iodobenzene
Py	Pyridine
rpm	Revolutions per minute
S _N Ar	Nucleophilic aromatic substitution
TBAB	Tetrabutylammonium bromide
TBAI	Tetrabutylammonium iodide
TEMPO	2,2,6,6-Tetramethyl-1-piperidinyloxy, free radical
terpy	2,2':6',2''-terpyridine
TFA	Trifluoroacetic acid
THF	Tetrahydrofuran
TM	Transition-metal
TMS	Trimethylsilyl
TSE	Twin screw extrusion
XEC	Cross-electrophile coupling
	Mixer mill
	Planetary mill

Table of contents

1 Introduction to Mechanochemistry as an Emerging Tool for Organic Synthesis	
1.1 What is Mechanochemistry?	2
1.2 Ball milling Equipment and Reactor Design for Scalable Synthesis.....	2
1.3 Ball-Milling Parameters and Factors for Optimisation	4
1.4 Established Benefits of Mechanochemistry	7
1.4.1 Enhanced Reactivity	8
1.4.2 Altered Reactivity / Selectivity	11
1.4.3 Robust / Operationally Simple Synthesis.....	12
1.4.4 Activation of Zero-valent Metals.....	13
1.5 Emergence of Mechanochemistry in Cross coupling	18
1.6 Conclusions and Outlook	21
1.7 Thesis Aims and Objectives	21
1.8 Bibliography	23
2 A Robust Pd-PEPPSI catalysed Carbon-Sulfur Coupling by Ball-milling	
2.1 Introduction	29
2.1.1 Aryl C-S Bond Formation	29
2.1.2 Development and Utilisation of Pd-PEPPSI Pre-catalysts	34
2.1.3 Carbon-heteroatom Coupling by Ball-milling	38
2.1.4 Project Overview, Aims and Objectives	41
2.2 Results and Discussion	42
2.2.1 Initial Findings	42
2.2.2 Optimisation	42
2.2.3 Reaction Scope and Limitations	47
2.2.4 Exploring Thioether / Disulfide Reactivity	54
2.2.5 Coupling from Disulfides	56
2.2.6 Phase Transition Induced Reactivity	57

2.2.7 Comparison to Solution	61
2.3 Conclusions and Future Outlook.....	63
2.4 Bibliography	64

3 Cross-electrophile Coupling of Alkyl and Aryl Halides under Ball-milling Conditions

3.1 Introduction	69
3.1.1 Ni-catalysed Cross-electrophile Coupling	69
3.1.2 Selectivity and Mechanistic Implications.....	72
3.1.3 Typical Zinc Activation in Solution	75
3.1.4 Mechanical Activation of Zinc	76
3.1.5 Overview, Project Aims and Objectives	79
3.2 Results and Discussion	81
3.2.1 Initial Findings.....	81
3.2.2 Optimisation	81
3.2.3 Aryl (Pseudo)Halide Scope	90
3.2.4 Initial Alkyl Halide Scope and Re-optimisation for Alkyl Bromides.....	92
3.2.5 Alkyl Halide Scope	95
3.2.6 Toleration of Different Reductant Forms	97
3.2.7 Mechanistic Insight.....	98
3.2.8 Scale-up.....	101
3.3 Conclusions and Future Work	103
3.4 Comparisons to Other Ball-milling Cross-electrophile Coupling Reactions	104
3.5 Bibliography	105

4 Mechanochemical Reductive Coupling of Activated Amides with Alkyl Halides

4.1 Introduction	110
4.1.1 Definitions for Non-planar Amides	110
4.1.2 Twisted / Activated Amides – Structure and Reactivity	111
4.1.3 Acyclic Twisted Amides for Use in Synthesis	113
4.1.4 Activated Amides for Reductive Cross-coupling	116
4.1.5 Twisted Amides Under Ball-milling Conditions	118
4.1.6 Outlook and Aims	118
4.2 Results and Discussion	120
4.2.1 Initial Findings	120
4.2.2 Optimisation of Reaction Conditions	120
4.2.3 Alkyl Halide Scope	127
4.2.4 Amide Backbone Scope	129
4.2.5 Assessment of Activated / Twisted Amides	131
4.2.6 Mechanistic Considerations	133
4.2.7 Scale-up	135
4.2.8 Alternative Reactivity	136
4.4 Conclusions and Future Direction	138
4.5 Bibliography	140

5 Mechanochemical Fluorocyclisations Using a Hypervalent Fluoroiodane Reagent to Access Novel Fluorinated Heterocycles

5.1 Introduction	144
5.1.1 Fluorination in Organic Synthesis	144
5.1.2 Fluoroiodane Reagent Synthesis and General Application	146
5.1.3 Fluorocyclisation Using Fluoroiodane Reagent	148
5.1.4 Fluorocyclisation of β,γ-unsaturated Hydrazones and Oximes	149
5.1.5 Mechanochemical Fluorination	151
5.1.6 Outlook and Aims	153

5.2 Results and Discussion	155
5.2.1 Initial Assessment of Fluoroiodane Reagent - Mechanochemical Fluorolactonisation of Carboxylic Acids.....	155
5.2.2 Mechanochemical Amino Fluorocyclisation (Tetrahydropyridazines)....	159
5.2.3 Mechanochemical Oxy Fluorocyclisation (Dihydrooxazines)	163
5.2.4 Proposed Mechanism for Heterocycle Construction	167
5.3 Conclusions and Comparisons.....	170
5.4 Bibliography	172

6 Experimental

6.1 General Information and Milling Equipment.....	175
6.2 A Robust Pd-PEPPSI Catalysed Carbon-Sulfur coupling by Ball-milling.....	177
6.1.1 General Experimental Procedures	177
6.2.2 Characterisation Data of Products.....	178
6.2.3 Comparison to Solution Reactions	188
6.2.4 Trace Metal Analysis.....	190
6.3 Cross-electrophile Coupling of Alkyl and Aryl Halides under Ball-milling Conditions.....	191
6.3.1 General Experimental Procedures	191
6.3.2 Synthesis of substrates	191
6.3.3 Characterisation data of products	193
6.3.4 Mechanistic Studies – Radical Clock and TEMPO Trapping	202
6.3.4 Scale-up Protocol.....	203
6.4 Mechanochemical Reductive Coupling of Activated Amides with Alkyl Halides	205
6.4.1 Synthesis of Starting Materials	205
6.4.2 Mechanochemical Reductive Cross-coupling Procedure and Characterisation Data of Products.....	213
6.4.3 Mechanistic Studies.....	223

6.4.4 Scale Up Protocol.....	225
6.4.5 Other Twisted Amide Reactivity by Ball Milling	226
6.5 Mechanochemical Fluorocyclisations Using a Hypervalent Fluoroiodane Reagent to Access Novel Fluorinated Heterocycles	228
6.5.1 Preparation of Fluoroiodane Reagent	228
6.5.2 Mechanochemical Fluorocyclisation of Unsaturated Carboxylic Acids .	229
6.5.3 Mechanochemical Fluorocyclisation of β,γ -unsaturated Hydrazones	234
6.5.4 Mechanochemical Fluorocyclisation of β,γ -unsaturated Oximes.....	237
6.6 Bibliography	241

1 Introduction to Mechanochemistry as an Emerging Tool for Organic Synthesis

1.1 What is Mechanochemistry?	2
1.2 Ball milling Equipment and Reactor Design for Scalable Synthesis.....	2
1.3 Ball-Milling Parameters and Factors for Optimisation	4
1.4 Established Benefits of Mechanochemistry	7
1.4.1 Enhanced Reactivity	8
1.4.2 Altered Reactivity / Selectivity	11
1.4.3 Robust / Operationally Simple Synthesis.....	12
1.4.4 Activation of Zero-valent Metals.....	13
1.5 Emergence of Mechanochemistry in Cross coupling	18
1.6 Conclusions and Outlook	21
1.7 Thesis Aims and Objectives	21
1.8 Bibliography	23

1.1 What is Mechanochemistry?

For a chemical reaction to occur, energy must be input equal to or greater than the activation energy required. In most cases, this energy is given via conventional methods such as controlled heating of the reaction. However, the emergence of enabling technologies has allowed for the discovery and development of alternative methods for energy input. Photochemical and electrochemical techniques have been extensively applied for improved methodology in organic synthesis.¹⁻⁴ In contrast, mechanochemistry has been less explored with much of its use being in crystallography and manual grinding of materials.^{5,6} The past 20 years has seen accelerated interest in mechanochemistry for use in the synthesis of organic compounds.⁷⁻¹² A mechanochemical reaction is defined as 'a chemical reaction that is induced by the direct adsorption of mechanical energy'.¹³ This definition encompasses several techniques including: sonication, grinding, hammering, extrusion, and ball-milling. The latter is the most explored technique for organic synthesis. Due to the input of energy coming from mechanical forces and not the heating of a solution, the use of a (bulk) reaction solvent is usually by-passed, which addresses a key challenge of solvent reduction for the implementation of green chemistry across chemical industry, as set out by the ACS Green Chemistry Pharmaceutical Roundtable in 2007.^{14,15} The sustainable advantages presented by ball-milling techniques led to its discussion alongside its continuous counterpart (twin screw extrusion) as one of the top ten chemical innovations that could change the world.¹⁶ This approach for greener synthesis is a highly active area of mechanochemistry.¹⁷

1.2 Ball milling Equipment and Reactor Design for Scalable Synthesis

Initial methods for mechanochemical synthesis relied on the use of a mortar and pestle for manual-grinding.¹⁸⁻²⁰ This inherently leads to inconsistency issues due to human error, particularly for long reaction times. This problem was largely solved by the inception of automated devices for controlled and consistent energy input.

Whilst a wide range of devices have become available, the most commonly chosen device is ball mills. A selection of ball mills have been made available and their choice is dependent on the desired energy input. The most chosen are mixer mills and planetary mills.²¹ As a concept, these two devices work in the same way; applying kinetic energy to one or more milling balls which can then transfer the energy to a reaction via collision with the reactant material.

Mixer mills have received significant attention and several brands and models have been made available (Retsch MM400 pictured, Figure 1.1A). A milling jar is mounted

1 - Introduction to Mechanochemistry as an Emerging Tool for Organic Synthesis

horizontally onto the mixer mill and oscillated from side to side, giving kinetic energy to the milling ball to allow for collision and hence energy transfer to the reaction material. The oscillation frequency can be tuned on the machine (most mills operate to a maximum of 30 Hz). Organic reactions are typically run at the maximum frequency available. Studies suggest that the primary energy transfer event takes place through direct impact of the ball with the chemical material at the end of the jar. However, since the ball does not move exactly along a straight path, and instead takes a more random trajectory, other energy transfer events are possible, such as shearing or brief glancing collisions along the side of the jar.^{21,22} Typically, a mixer mill reaction will feature a small number of balls of significant size (1-2 is common), however in some cases, greater amounts of smaller balls may be employed to aid with mixing. A number of jars of different sizes and materials are available (Figure 1.1C) with various compatibility between jars and machines. Milling balls are typically stainless steel.

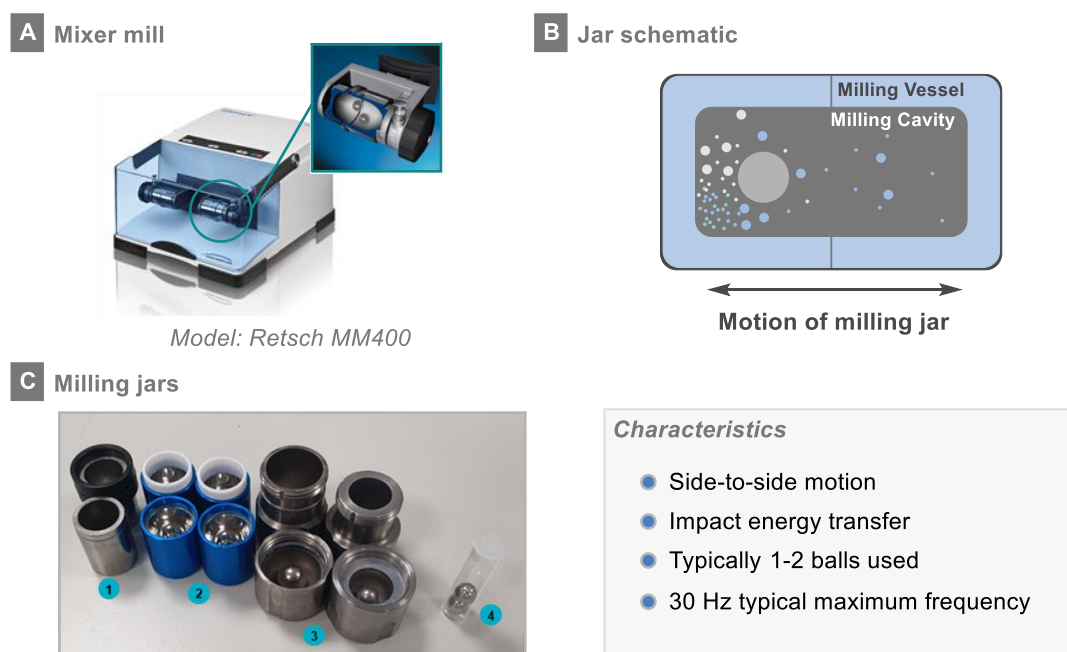


Figure 1.1 Mixer mill equipment

Planetary mills differ in operation, with jars mounted vertically on a rotating plate. The plate is then rotated in one direction (i.e., clockwise) and the jars are counter-rotated (i.e., counter-clockwise) along their central axis. This leads to a large amount of shearing forces. This provides the majority of the energy transfer, with a small amount of direct collision impact energy also provided.²³

Multigram synthesis is possible and has successfully been achieved by using larger jars and balls.^{24–28} Both reactors have an upper limit in reaction scale; <10 g for mixer mills and <100 g for planetary mill, when using standard jar sizes. Reactions on these scales must also be carefully considered from a safety point of view, for example, by product formation. Any thermal dissipation from the reaction is also less likely to be controlled given the absence of solvent. To address these limitations in scale-up of mechanochemical synthesis, different approaches must be explored. To this end, continuous methods for mechanochemical synthesis have been developed through the use of reactive extrusion.^{29–31} The most common methodology for this is twin-screw extrusion (TSE), whereby material is fed onto two parallel screws which rotate in opposite directions by motors. The screws themselves can be configured with “conveying”, “reverse” and “kneading” elements. These elements can be modified along a given system. TSE has been shown to be proficient in large-scale organic reactions, as well as demonstrating beneficial properties in metal organic framework (MOF) synthesis.^{32–36} The use of less common single-screw reactors has been used whereby the reaction takes place between the screw and the outside surface of the device.³⁷

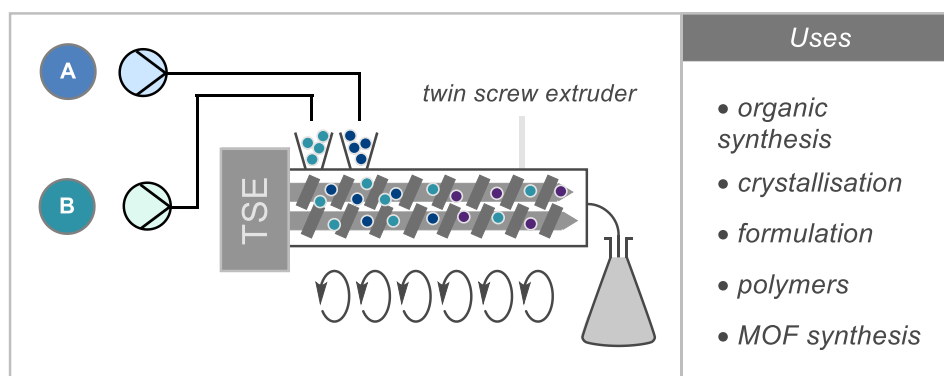


Figure 1.2 Twin screw extrusion (TSE)

1.3 Ball-Milling Parameters and Factors for Optimisation

The key to optimisation of any given reaction lies in understanding the parameters involved. For solution based chemical reactions, these typically include temperature, concentration, and choice of solvent, amongst others. For a ball-milling reaction, there are many atypical parameters that should be considered. These unique parameters include milling frequency, the number and size of the balls, the size of the milling vessel, the material from which the jar and ball are made from, as well as additives (solid and liquid). Taking these with other standard chemical factors (reagent stoichiometry etc.) results in many variables, each affecting one or more of the key mechanochemical

factors for optimisation: energy per collision, mass transfer, efficiency of the energy absorption, and the frequency of collisions.

The frequency of the mill directly affects the energy given to the material with higher frequencies imparting higher kinetic energy onto the milling ball and hence creates higher average energy collisions. This is thought to increase the reaction in the same manner that increasing temperature directly affects a solution-based reaction. The increased frequency of a milled reaction may increase friction inside the jar, hence increasing the temperature. This adds a small amount of thermal energy to the jar as well as kinetic energy. Recently, temperature-controlled devices have been developed for ball milling ranging from a mounted heat gun above the jar to electronically controlled heating sleeves for precise control of the external temperature of the jar. This has led to some profound reactivity previously unattainable in solution, particular for materials that are poorly soluble in common organic solvents.³⁸⁻⁴¹

The number of balls has a direct influence on mechanochemical reactions.⁴² In general, a mixer mill only uses one ball of relatively large mass so as to increase the energy transfer upon impact with the material at one end of the jar. However, a planetary mill is best suited with as many smaller balls as possible (not too small that sufficient energy transfer can't take place) due to the nature of shearing forces that provide the major energy input.

The size of the jar has an important influence on the efficiency of collisions within the jar. By changing the jar size, the space taken up by the reaction material (also called the filling degree) will vary. Lower filling degree reactions with larger amounts of free space suffers from less effective collisions, however reports suggest that the efficiency of each collision is greater.⁴³ Multiple reports have sought to find the optimal loading for a ball-milled reaction. The general consensus is that a third of the jar should be given to each of the reaction mixture, the ball, and free space.⁴⁴ However, this ratio will inevitably change with different reactants or reaction types. Care must also be taken when scaling up to ensure the ratio remains as close to the original as possible.²⁹

There should also be a consideration on the material of the jar and ball(s) used. Typically, a hard, chemically inert material such as stainless steel is used for both the jar and ball(s). The hardness of the material aids with the efficiency of energy transfer. This is extended further to planetary mills whereby zirconium oxide jars and balls are often used due to the increased hardness. The choice of jar / ball(s) is not limited to innocent materials with direct mechanocatalysis emerging as an interesting strategy using Pd, Cu,

or Ni balls to catalyse reactions.^{45–47} Polymer balls have also been shown to produce faster reactions.⁴⁸

The use of additives has also become commonplace in milled reactions. These can take the form of solid grinding auxiliaries or liquid assisted grinding (LAG) agents and affect the reaction in different ways.^{7,10,49}

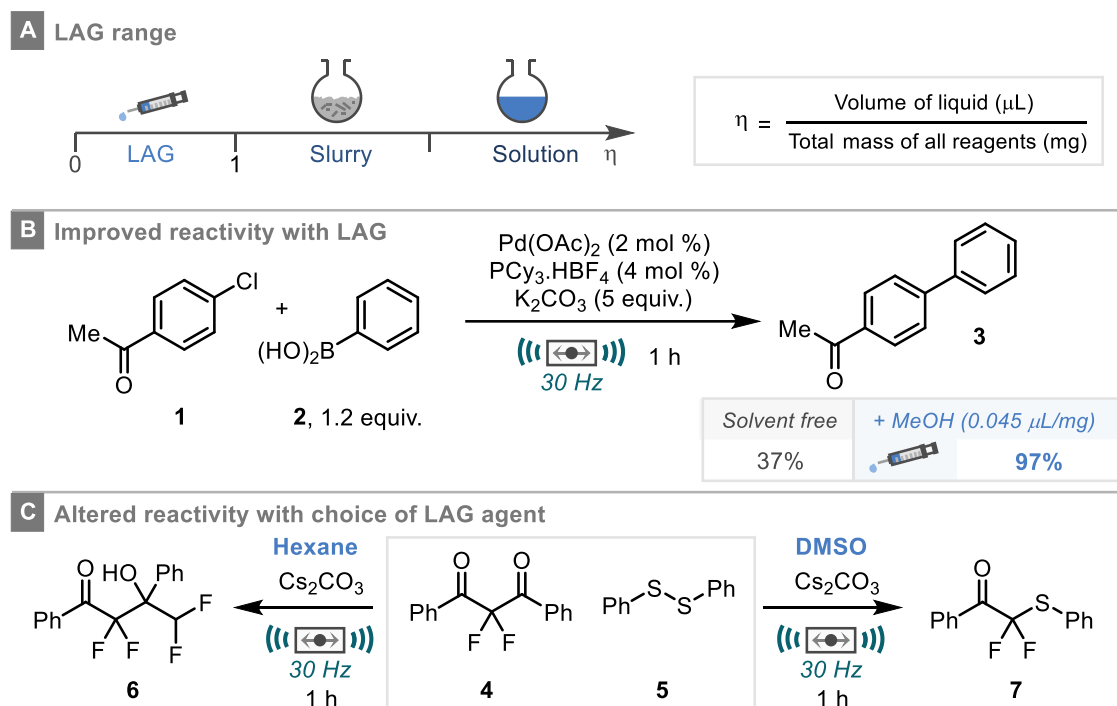
Solid additives are often used to improve mass transfer between liquid reagents by providing a surface to react on. They can also help in the mixing of the reaction, preventing formation of sticky reaction mixtures. This was exemplified in a mechanochemical Buchwald-Hartwig coupling by Browne and co-workers whereby the addition of sand as a grinding auxiliary significantly improved the yield of the coupling reaction.⁵⁰ Friščić and co-workers reported similar findings for a ruthenium catalysed olefin metathesis under ball-milling conditions detailing that in the absence of NaCl, the material clumped together around the milling ball, thereby giving inefficient mixing.⁵¹ With the salt additive, the mixture was seen to be more free-flowing and gave much improved reactivity. Solid additives do not have to be innocent and sometimes have a more direct role within the reaction.^{18,52,53}

The use of a liquid additive is usually referred to as liquid assisted grinding (LAG).^{54–56} Typically, a small amount of liquid (most often a common organic solvent) is added to the milling reaction. Since adding a solvent into a reaction could result in its consideration as a solvent-based reaction, boundaries have been set defining a range in which LAG is operational. The value commonly denoted is η which represents the volume of liquid added in μL divided by the total mass of all reagents in mg. The range for LAG is where η is between 0 and 1 (Scheme 1.1A). Above this, the reaction can start to resemble a slurry texture. Even further and the reagents become solvated, and the reaction is considered as a standard solution reaction.

The use of liquid additives has been shown to enhance reactions as shown by the Suzuki-Miyaura coupling of aryl chlorides from Su and co-workers.⁵⁷ In this study they found that in the complete absence of solvent, the coupling reaction of 4-chloroacetophenone (**1**) and phenylboronic acid (**2**) only proceeds to give 37% desired product **3**. However, the addition of a liquid additive (MeOH) dramatically improved the reaction to give 97% of the desired cross-coupled product (Scheme 1.1B). LAG has also been shown to directly affect the selectivity of a reaction. Browne and co-workers found that the reaction of fluorinated 1,3-diketones with disulfides proceeds via differing mechanisms dependent on liquid additive used (Scheme 1.1C).⁵⁸ Performed neat, or in the presence of a non-polar solvent such as hexane, the reaction proceeds to afford β -

1 - Introduction to Mechanochemistry as an Emerging Tool for Organic Synthesis

hydroxyester **6**. Using a polar solvent (DMSO), the reaction proceeded to give fluorinated thioether **7**.



Considering that each variable in a mechanochemical reaction has an effect on multiple aspects of the reaction, optimisation can become complex quickly for any given system. The interdependence of these variables has been studied across different devices and on different scales using the condensation reaction of vanillin and barbituric acid.^{32,38,59–62} Throughout these studies, different mechanisms are even considered as a result of changing the parameters. For example, James and co-workers suggested a eutectic mixture is formed when one ball is used whereas Užarević discussed the formation of co-crystals using two balls.^{60,62}

1.4 Established Benefits of Mechanochemistry

The initial and perhaps obvious benefit of mechanochemical techniques is the omission of (bulk) reaction solvent. This provides an attractive, sustainable approach towards organic synthesis. This benefit is present across all mechanochemical reactions and represents a large active area for focus in organic mechanochemical synthesis.^{17,63,64}

Outside of this sustainability advantage, other benefits have been outlined throughout the past 15-20 years for the use of mechanochemical methods (Figure 1.3).^{10,65,66} The differing energies imparted in a mechanochemical reaction, as well as the solvent

free/minimised environment have enabled the discovery of these advantages over traditional solution-based protocols.

- Enhanced reactivity
- Alternate reactivity / Selectivity
- Robust protocols / no need for air sensitive techniques

More recently, ball-milling has become a facile tool for the activation of zero-valent metals such as zinc, providing more reliable activation of materials.

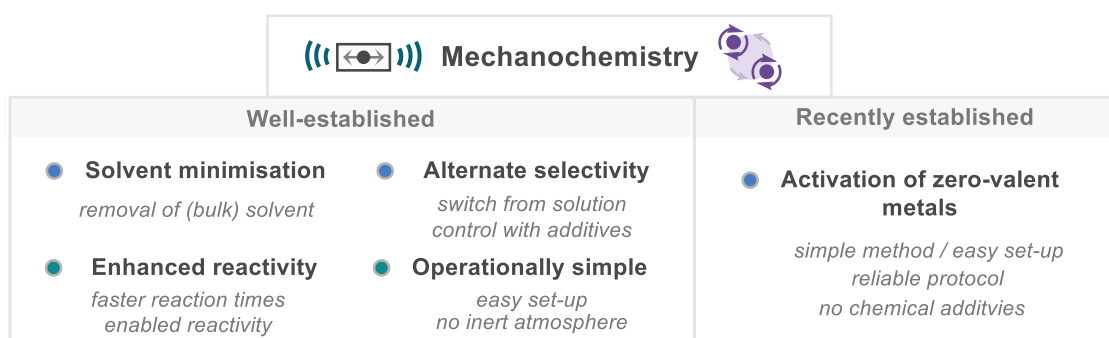


Figure 1.3 Overview of the benefits of mechanochemistry

1.4.1 Enhanced Reactivity

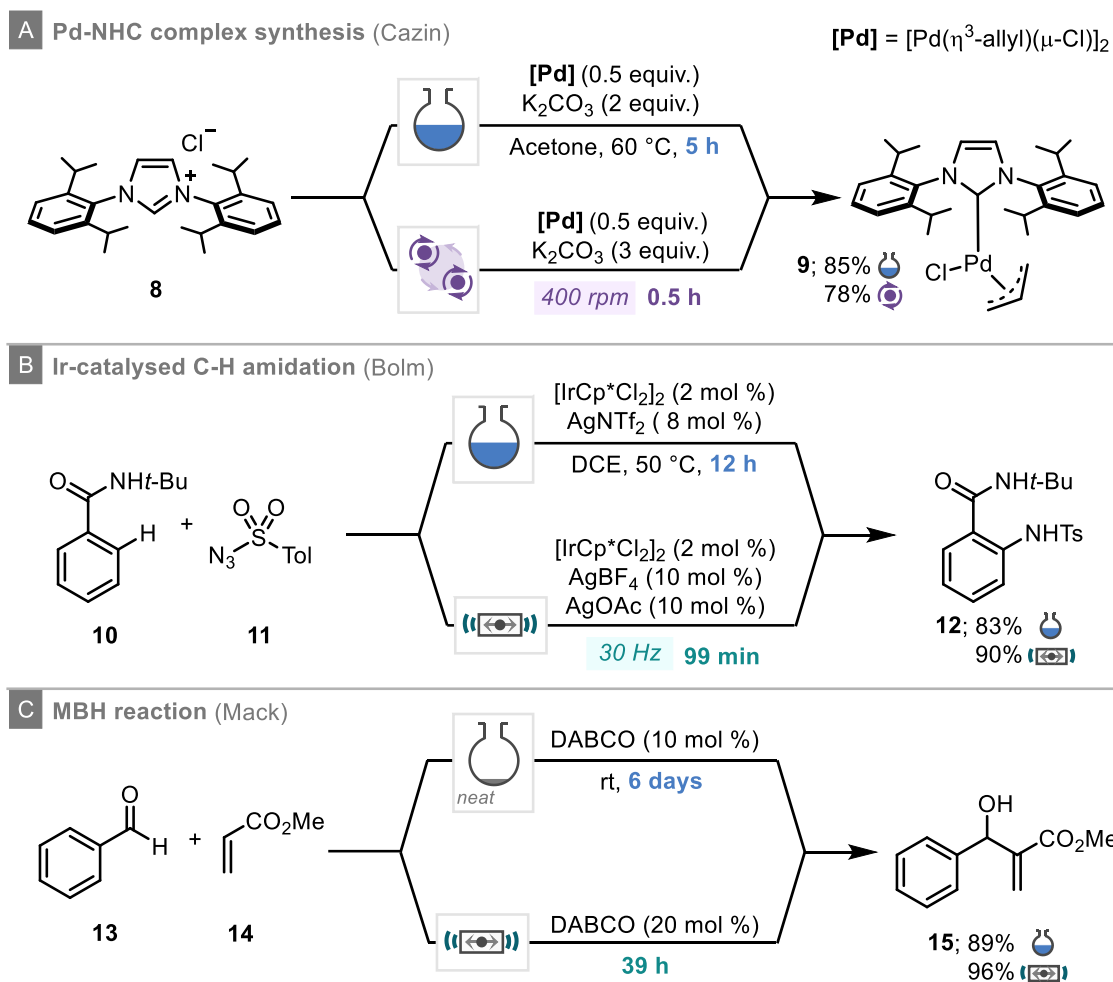
One of the most notable benefits of ball-milling techniques is enhanced reactivity. This is either demonstrated by (greatly) reduced reaction times, improved yields, possibilities for lower catalyst loading, and the enabling of reactivity that is not possible through conventional methods.

One factor for the reduction in reaction times is likely to arise from the dramatically increased concentration. It is also in-part due to the removal of the thermal barrier for desolvation that is present when using solvents.¹² These time-saving benefits are prevalent across a number of areas of organic synthesis and examples have been presented for metal-NHC complex synthesis,⁶⁷⁻⁷⁰ a multitude of cross-coupling reactions,⁷¹⁻⁷³ C-H functionalisation,⁷⁴ and organocatalysis in addition to many other areas.⁷⁵

Pd-NHC complexes have become powerful pre-catalysts for cross-coupling reactions (their use will be discussed in chapter 2 of this thesis). To this end Cazin and co-workers reported a mechanochemical synthesis of Pd(NHC)(η^3 allyl) complexes from imidazolium salts.⁷⁰ This reaction is known in solution and the reaction of the IPr-Imidazolium salt **8** with the palladium source and base requires 5 hours to afford 85% yield of Pd(IPr)(η^3 -allyl)Cl (**9**).⁷⁶ This reaction time is significantly reduced to just 30

minutes to afford **9** in excellent yield (Scheme 1.2A). The authors then proceed to demonstrate that the 30-minute reaction time is sufficient for imidazolium salts with increased steric bulk and examples that require 24 hours using conventional methods.

Bolm and co-workers demonstrate that iridium catalysed C-H bond amidation of benzamide **10** with sulfonyl azide **11** proceeded in just 99 minutes (Scheme 1.2B).⁷⁷ This is a much-improved reaction time on the reported 12 hour reaction time required for solution reactivity by Chang and co-workers.⁷⁸ Key to this reactivity was the fast *in situ* formation of the active iridium species using the mixer mill.

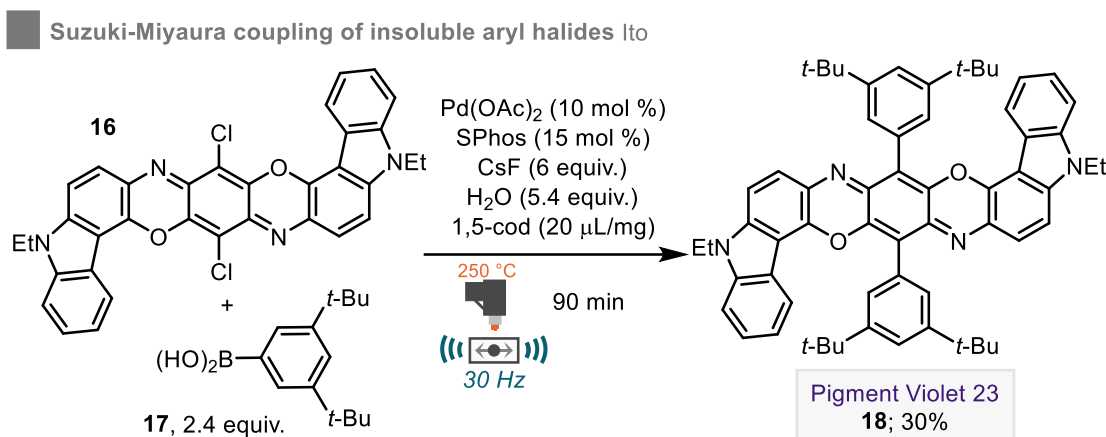


Scheme 1.2 Time-saving using mechanochemistry

Organocatalysis has also been explored for use in mechanochemistry.⁷⁵ A popular organocatalytic reaction is the Morita-Baylis-Hillman (MBH) reaction. This tertiary amine catalysed reaction of Michael acceptors with aldehydes is a synthetically important reaction as it allows functionalisation of the α -position of an acrylate. However, the reaction is typically sluggish as demonstrated by Caubere and co-workers, showing that the DABCO catalysed reaction of benzaldehyde (**13**) and methyl acrylate (**14**) took 6

days to go to completion even when stirring neat.⁷⁹ Mack and co-workers showed that translating these conditions to a mixer mill allowed for almost quantitative conversion to the product (**15**) in 39 hours, which shows a significant improvement (Scheme 1.2C).⁸⁰ Activated benzaldehydes are able to undergo the reaction in just 30 minutes. The aza-MBH reaction has also been developed for use in a mixer mill, proceeding with routine reaction times of just 99 minutes.²⁸

In addition to reducing reaction times, ball-milling has been shown to enable reactivity for the synthesis of previously unattainable molecules. Largely, this is due to solubility issues. To this end, Ito and co-workers reported a Pd-catalysed Suzuki-Miyaura coupling of insoluble aryl halides to form large polyaromatic structures with the aid of a heat gun mounted above the milling jar. The lack of requirement for solvent for ball-milling allowed the synthesis of the novel pigment dye (Pigment Violet 23, **18**) which has previously not been made due to the almost complete insolubility of the starting aryl chloride (**16**) in common organic solvents.



Scheme 1.3 Ball-milling enabled coupling of insoluble aryl halides

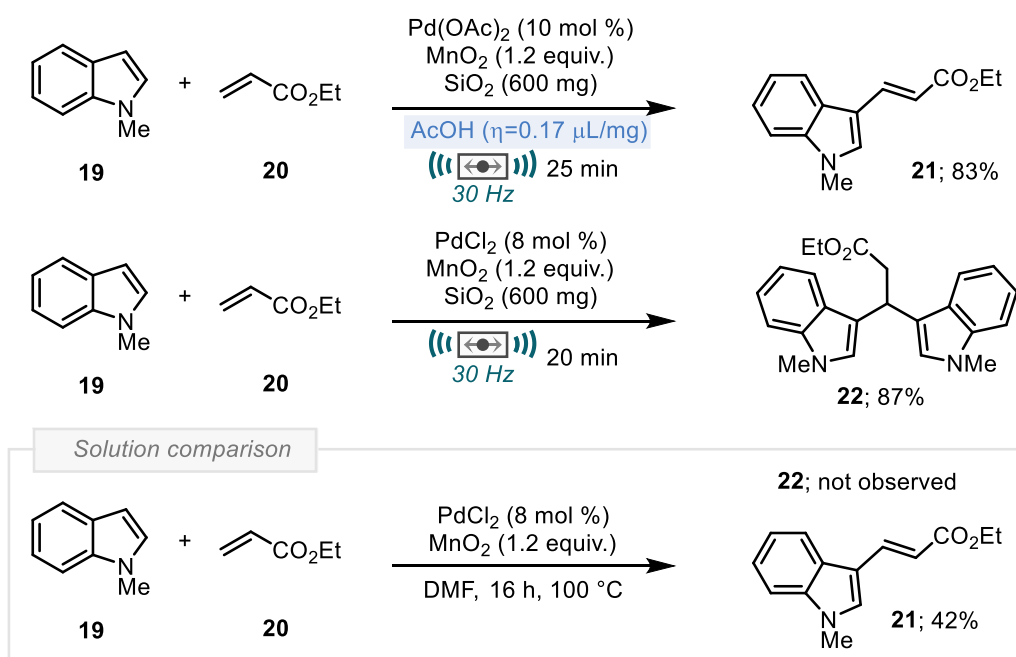
There are other examples of ball-milling being able to achieve products not possible in solution. Mack and co-workers disclosed the silver-catalysed cyclopropanation of alkynes with diazoacetates in tandem with a palladium catalysed Sonogashira coupling. This multi-component reaction cannot be achieved in solution, and instead isolation of the intermediate would be required.⁸¹ Friščić and co-workers also showed that ball-milling could enabled the coupling of sulfonamides with carbodiimides to form *N*-sulfonylguanidines using CuCl as a catalyst and nitromethane as a LAG agent.⁸² This reaction proved impossible under solution conditions, even with increased catalyst loading.

1.4.2 Altered Reactivity / Selectivity

Another possible benefit observed in mechanochemical reactions is that different products can be achieved than that achieved by other techniques.^{11,83} Whilst the rationale for these switches in selectivity is not entirely clear, it is highly desirable for the progression of synthetic chemistry that these different outcomes can be accessed. In addition to selectivity differences observed between solution and mechanochemistry, there have been many cases reported where the selectivity in a mechanochemical system can be controlled, often by the careful use of additives.^{56,58,84}

An excellent example of this is observed through the oxidative coupling of acrylates with indoles. Su and co-workers reported selective synthesis of either 3-vinyl indole **21** or β,β -diindolyl propionate **22** through mechanochemical oxidative coupling with MnO_2 used as oxidant. Key to the outcome of the reaction was the choice of palladium source as well as the additive used (or lack thereof).⁸⁵ Using $\text{Pd}(\text{OAc})_2$ with acetic acid as a liquid additive produced excellent yield (83%) of the 3-vinyl indole **21**. However, using PdCl_2 in the absence of any liquid additive, the reaction selectively formed **22** in excellent yield (87%). Curiously, adapting the reaction to solution conditions by using DMF as the solvent and stirring overnight at 100 °C, only the 3-vinyl indole product was observed. This shows that the diindolyl propionate product **22** is exclusive to milling and is only achieved with careful choice of palladium source and additive.

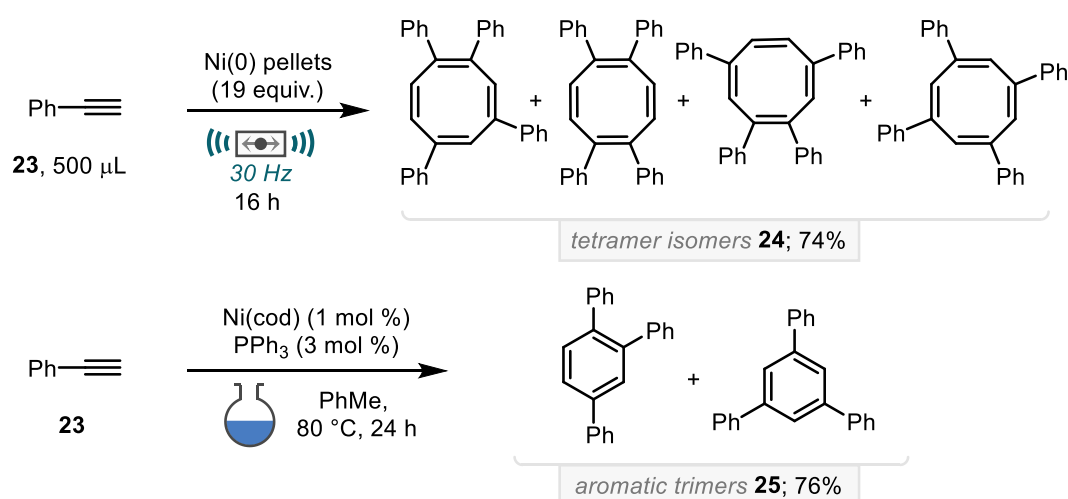
Selective oxidative coupling of indoles with acrylates



Scheme 1.4 Oxidative coupling of indoles and acrylates

Another example exhibiting remarkable selectivity differences from that previously observed is the Ni-catalysed [2+2+2+2] cyclotetramerisation of alkynes developed by Guan, Mack, and co-workers (Scheme 1.5).⁸⁶ In this study, the authors use recyclable Ni(0) pellets to selectively form cyclooctatetraenes (**24**) under ball-milling conditions, thereby removing the need for any air-sensitive nickel complexes. In contrast the solution reaction of alkynes catalysed by a Ni(0) complex does not afford any of the tetramer product, instead showing preference for [2+2+2] trimerisation to give aromatic products (**25**).⁸⁷

Alternate Ni-catalysed cyclo tri/tetra-merisation of alkynes Guan & Mack



Scheme 1.5 Ni-catalysed cyclisations of alkynes

1.4.3 Robust / Operationally Simple Synthesis

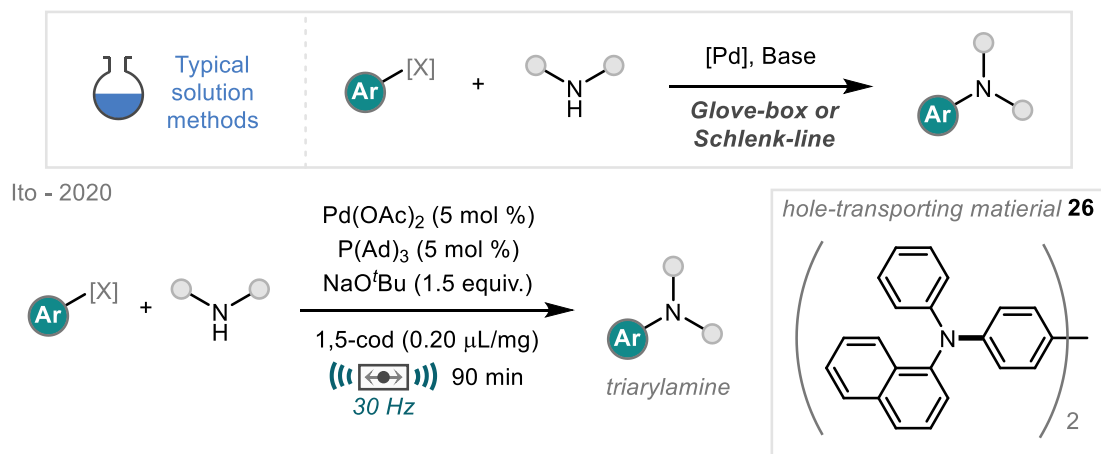
Ball-milling as an enabling technology requires little training, and reactions are straight forward to set up. Whilst some examples of ball-milling reactions are set up within a glovebox or nitrogen bag to maintain an inert environment,^{88–91} the majority of ball-milling protocols circumvent the requirement for inert techniques with materials simply loaded into the jar open to air.^{7,10,73}

This has been shown to be particularly useful for sensitive organometallic reactions, with heavy focus being on cross-coupling reactions. For example, C-N coupling (Buchwald-Hartwig coupling) reactions in solution typically require glove box or Schlenk-line techniques.^{92,93} The developments of ball-milling protocols have allowed for convenient arylamine synthesis under ambient conditions. Initial reports by Su and Browne demonstrate efficient coupling of a wide range of aryl halides and amines with most of the scope being made up from liquid substrates.^{50,94} Ito and co-workers later disclosed a ball-milling C-N coupling protocol focussing on the coupling of solid substrates using

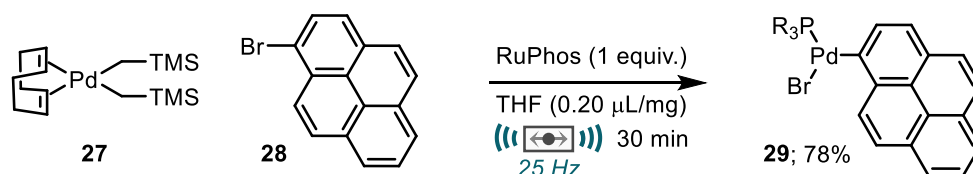
1 - Introduction to Mechanochemistry as an Emerging Tool for Organic Synthesis

P(Ad)₃ as the ligand (Scheme 1.6).⁹⁵ This methodology is also extended to the synthesis of a polyaromatic hole transporting material (**26**).

A Mechanochemical C-N coupling without inert gas protection



B Synthesis of oxidative addition complexes in air



Scheme 1.6 Sensitive synthesis without inert gas protection

Ito and co-workers also present the synthesis of oxidative addition complexes (**29**) from aryl halides and palladium(0) intermediates by ball-milling in air (Scheme 1.6B).⁹⁶

The lack of requirement of inert atmosphere has been a benefit that has been seen across many different types of organic reactions. More recently, it has been that this unique property of ball-milling can successfully be harnessed for use in the activation of zero-valent metals (i.e., zinc, magnesium).

1.4.4 Activation of Zero-valent Metals

Carbon-based nucleophiles play a vital role in the forging of C-C bonds. A common strategy for the generation of carbon nucleophiles is metalation.⁹⁷⁻⁹⁹ This can be achieved in a few different ways:

1. Direct insertion of a zero-valent metal into a C-X bond
2. Metal/halogen exchange (from preformed organometallic)
3. Deprotonation of a C-H bond with a base containing a metal (e.g., Mg(TMP)₂, *n*-BuLi).

Of these options the direct insertion approach requires fewest chemical steps from raw materials and is the most tolerant to the broadest range of functional groups, rendering it one of the more popular strategies. However, it is often unpredictable and unreliable. A decisive factor for the variation of outcomes is the activation of the zero-valent metal. These metals are readily available in a variety of forms and typically have an oxide coating on the outer layer which requires removal to expose the reactive metal surface beneath. Removal of the oxide surface / activation of the metal is regularly achieved through the addition of chemical additives such as iodine, 1,2-dibromoethane, trimethylchlorosilane (TMSCl) and a range of other alternatives (Figure 1.4).^{100–103} Initiation of the activation process is often achieved by thermal input and in the presence of coordinating solvents to aid in breaking up the freshly exposed metal through chemical entrainment.^{104,105} Mechanical activation has previously been achieved by particle size reduction using a mortar and pestle for the energy input.^{106,107} As with all manual grinding, inconsistencies between users causes reliability issues.

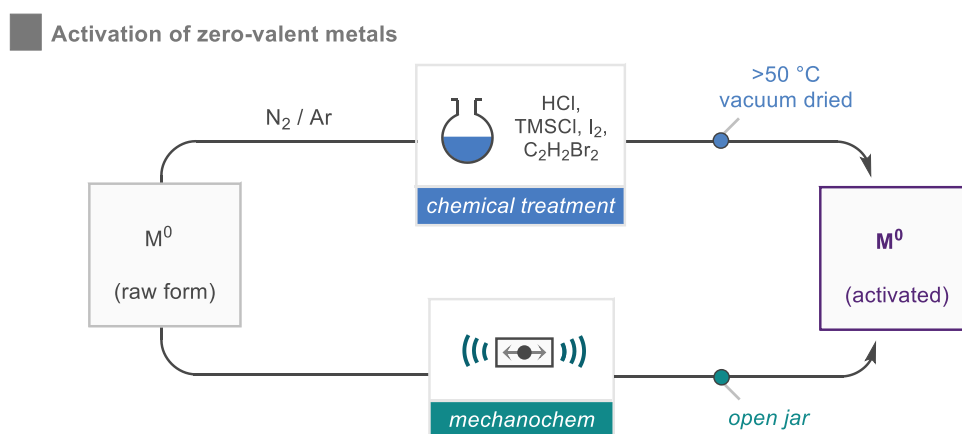
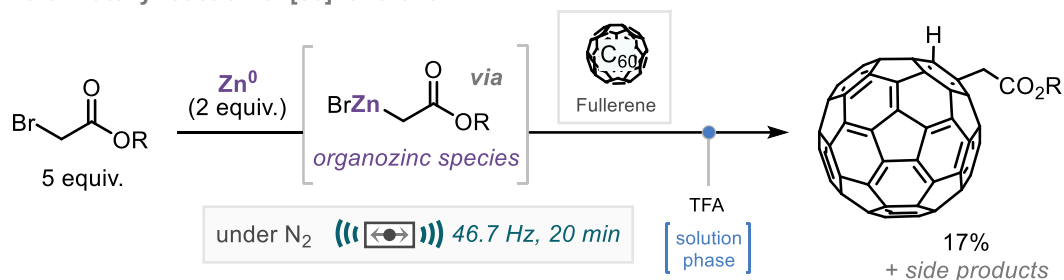


Figure 1.4 Activation of zero valent metals

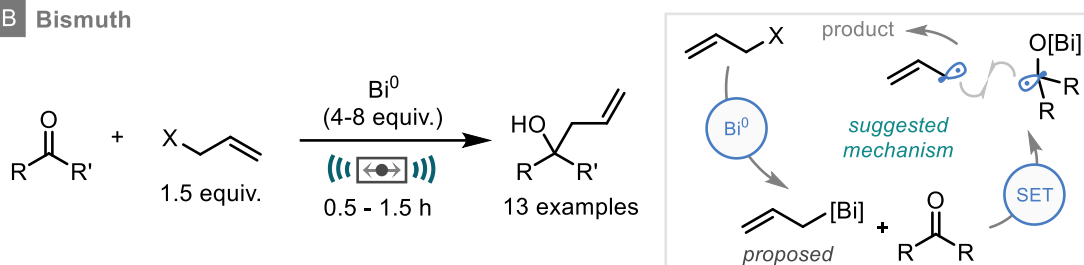
To overcome these limitations, automated ball-mills have been employed for the activation of zero-valent metals. Initial work on this was presented by Komatsu and co-workers in 1996 showing a Reformatsky functionalisation of [60]fullerene mediated by Zn(0) was possible using a ‘vibrating mill’ inside a nitrogen bag whereby the zinc is mechanically activated *in situ* for organozinc formation (Scheme 1.7).⁸⁸

1 - Introduction to Mechanochemistry as an Emerging Tool for Organic Synthesis

A Reformatsky reaction of [60] fullerene



B Bismuth



Scheme 1.7 Mechanochemical Zn(0) activation for Reformatsky addition to fullerenes

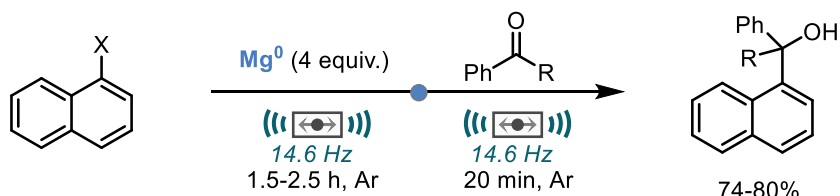
In 2003, Suzuki and co-workers also presented a mechanochemical Reformatsky reaction that bismuth(0) could display the same Reformatsky type reactivity with non-fullerene substrates (Scheme 1.7B).¹⁰⁸ It is suggested that this proceeds by formation of an allylbismuth species, followed by single electron transfer.

Magnesium remains heavily important in organic synthesis, with its primary use being in the formation and use of Grignard reagents. Despite this, the activation of magnesium, through removal of the outer MgO layer can also be capricious. Mechanical methods for its activation and use have been identified. Initial reports came from Harrowfield and co-workers that reported that in a glovebox environment, the milling of 1-halonaphthalenes with magnesium powder affords a fine black powder, which was then shown to react with acetophenone or benzophenone to give the Grignard addition products in good yields (74-80%, Scheme 1.8A). Magnesium has since been shown to insert into C-F bonds, which is significantly more challenging than other carbon-halide bonds. Hanusa and co-workers demonstrated this through the mixer mill reaction of 2-fluoronaphthalene (**30**) with 8 equivalents of magnesium in a glove-box (Scheme 1.8B). The proposed organomagnesium intermediate (**31**) could either be quenched with H₂O to give naphthalene (**32**) or treated with FeCl₃ in a second milling step to afford a low yield of the dimer product (22%, **33**).

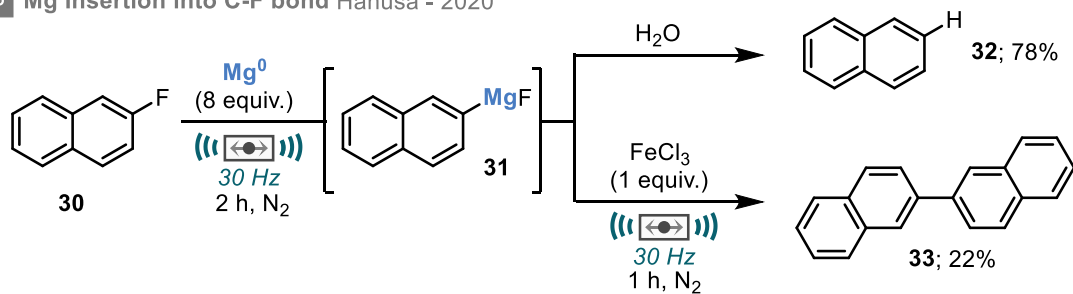
To demonstrate the powerful capabilities of ball-milling techniques, Ito and co-workers disclosed the facile synthesis of Grignard reagents without the requirement for an inert atmosphere (Scheme 1.8C).⁴¹ The simple mechanochemical mixing of magnesium

turnings and an aryl or alkyl bromide proceeds efficiently using THF as a LAG agent. This lack of air sensitivity allows the opening of the jar in air to add a carbonyl derivative to the reaction mixture, where a further hour of milling under air affords the Grignard addition product. Whilst liquid halides proceeded excellently, the use of some solid halides required mounting of a heat gun. The heat gun was set at 110 °C with the internal temperature reaching 70 °C as measured by thermographic imaging.

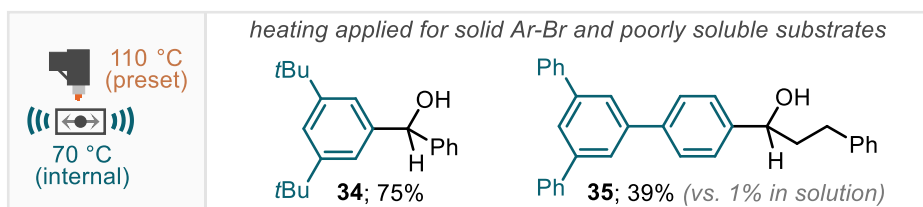
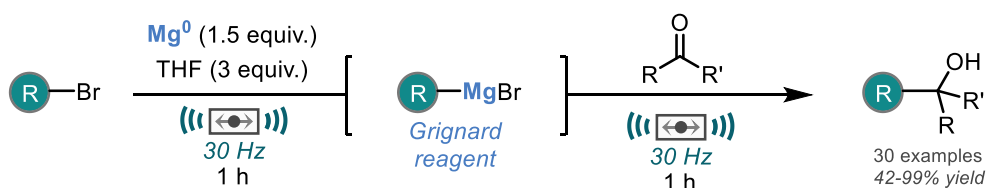
A Mechanochemically induced Grignard reaction Harrowfield - 2001



B Mg Insertion into C-F bond Hanusa - 2020



C Mechanochemical Grignard formation in air Ito - 2021



Scheme 1.8 Mechanochemical activation of magnesium

To further showcase the benefits of running reactions under ball-milling conditions, substrates which show only trace reactivity in solution due to poor solubility in THF solvent, were amenable to these heated mechanochemical conditions, including large phenyl-terphenyl bromide **35**. This essentially allows access to Grignard reagents previously unattainable by solution methods. The authors also demonstrate the use of the formed Grignard reagents by reaction with Weinreb amides, esters, nitriles and chlorosilanes. The utilisation of ball-milling as a method to activate magnesium metal is

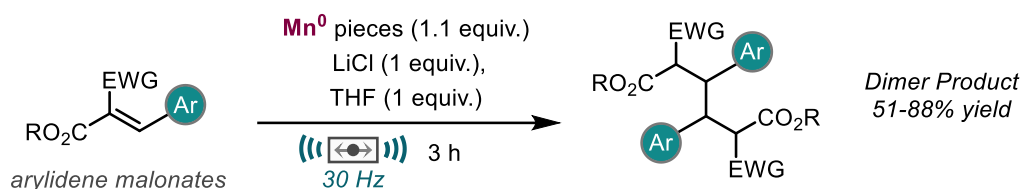
a promising area and is currently receiving much attention with Bolm and Wu also providing contributions for Grignard reactivity with CO₂ and Minisci C-H alkylation respectively.^{109,110}

As discussed earlier (Scheme 1.5), Guan, Mack and co-workers circumvented the need for air sensitive Ni(0) catalysts by using nickel pellets for the cyclotetramerization of alkynes, demonstrating successful activation of metallic nickel.⁸⁶

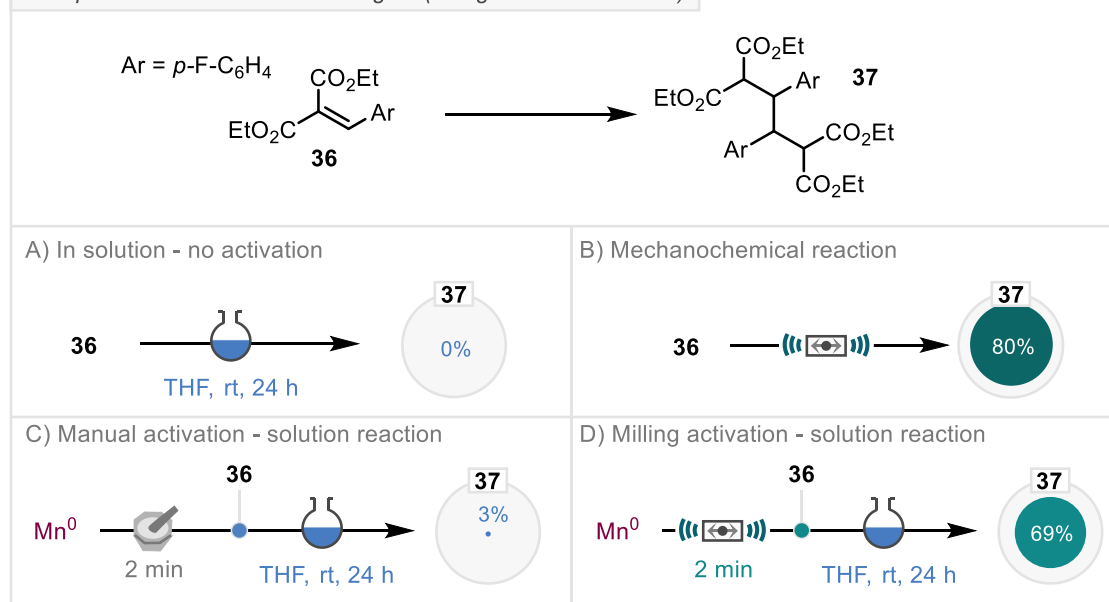
Browne and co-workers have recently developed mechanochemical methods for the activation of zinc without the need for inert set-ups (discussed in more detail in Chapter 3). Initially, they established a LAG approach for organozinc formation from a wide range of organohalides, subsequently demonstrating its use in a Pd-PEPPSI catalysed Negishi cross-coupling.¹¹¹ Adapting these conditions, they then discovered robust protocols for the formation of zinc enolates for Reformatsky addition, as well as the Barbier type allylation of carbonyl compounds.^{112,113}

Recently, the activation of manganese metal has also been established. Browne and co-workers in searching for conditions for organomanganese formation, discovered a method for the reductive dimerization of arylidene malonates using manganese pieces (Scheme 1.9).¹¹⁴ It was found that LiCl and THF as additives were essential for this reactivity to occur. A selection of benzylidene malonate derivatives were subjected to the reaction conditions, showing variation on the aryl ring, as well as exploring different electron withdrawing groups. Notably when the cyano-substituted substrate was employed in the reaction conditions, the dimer was formed with exquisite diastereoselectivity, only producing a single diastereomer.

Mechanochemical reactivity of manganese (Browne)



Comparison between methodologies (using conditions above)



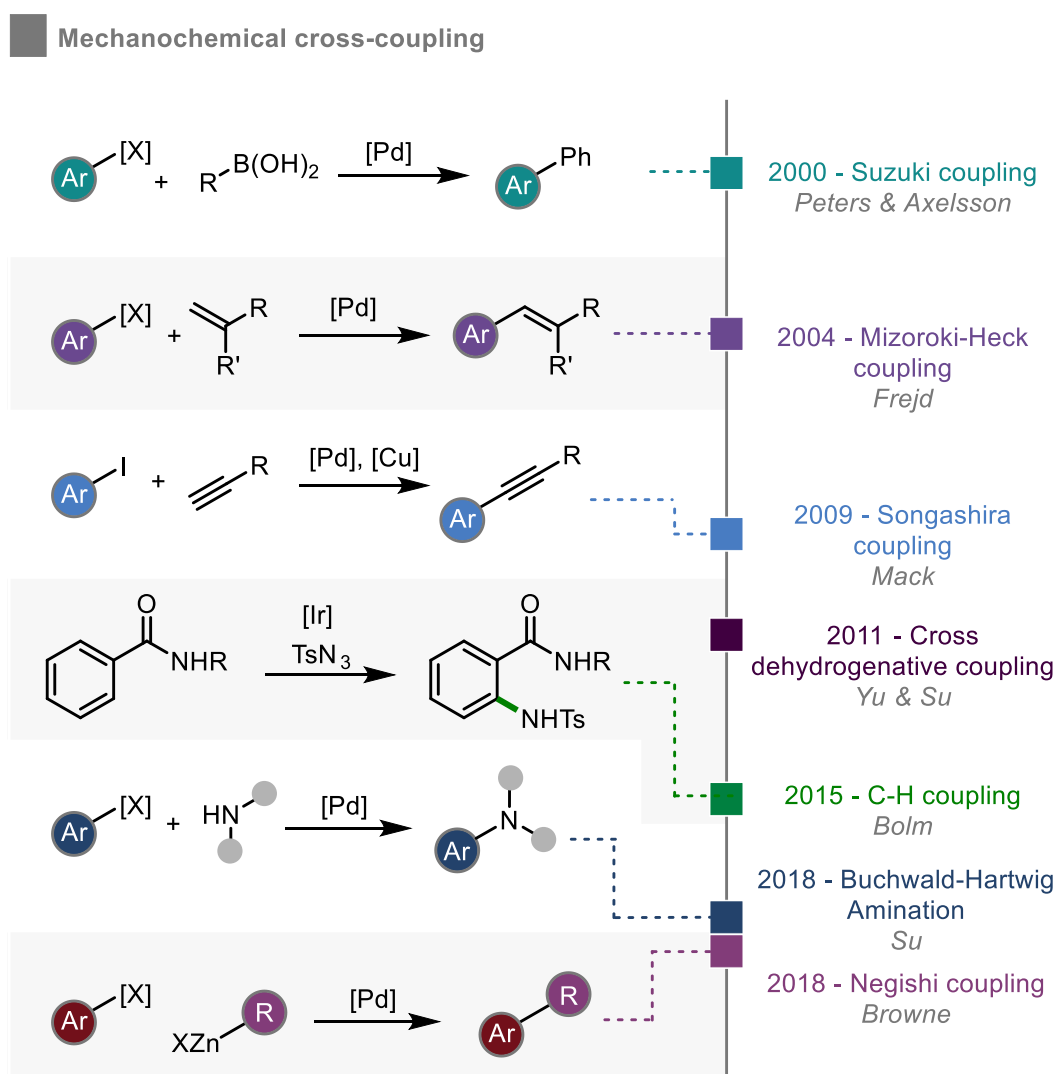
Scheme 1.9 Mechanochemical activation of manganese

Interestingly, without any mechanical activation of the metal, the solution phase reaction in THF at room temperature over 24 hours resulted in no product and complete starting material retention (A) compared to the 3-hour milled reaction which afforded 80% of dimer product (B). To assess if it is the full reaction that requires mechanochemical treatment, a pre-activation step was added. It was found that pre-activation by manual grinding for 2 minutes using a mortar and pestle, and then transferring the finely ground metal to the solution reaction gave only 3% product (C). Pre-milling Mn for 2 minutes at 30 Hz before addition to the reaction at room temperature for 24 hours gave excellent yields of 69% (D) These yields are comparable to those achieved in the mill for 3 hours highlighting the opportunities that mechanical pre-activation in a mill can offer in unlocking the reactivity of materials even in subsequent solution reactions.

1.5 Emergence of Mechanochemistry in Cross-coupling

Cross-coupling remains a powerful and crucial strategy in the synthesis of C-C and C-X bonds and has been widely applied across a number of areas including natural product synthesis, medicinal chemistry, and material science.^{115–118} Whilst the benefits of solution

based methods have been well established, the sustainable benefit (and in many cases enhanced reactivity) that arises from performing these reactions in the absence of (bulk) solvent adds value to these popular reactions. To this end, many of the commonly encountered cross-coupling reactions have been investigated under mechanochemical conditions.^{71,73,119} Scheme 1.10 summarizes the first known reports for cornerstone cross-coupling reactions.



Scheme 1.10 Mechanochemical cross-coupling

The first cross-coupling to be performed under milling conditions was the Suzuki-Miyaura coupling reaction. In 2000, Peters, Axelsson, and co-workers reported successful Pd-catalysed coupling of a small range of aryl halides with phenyl boronic acid using K_2CO_3 as a base, and sodium chloride as a grinding auxiliary.¹²⁰ The Suzuki reaction has since gone on to be the most explored of the coupling reactions under ball-milling conditions,

with various groups improving the reaction through careful ligand design, the use of LAG, or adaptation for coupling of insoluble materials.^{40,121–129}

Following this, the Mizoroki-Heck coupling was explored by Frejd and co-workers in 2004.¹³⁰ The reaction was performed in a planetary mill and coupled aryl halides with protected amino acrylates using Pd(OAc)₂. The same group then expanded this work for the coupling of haloanilines.¹³¹ Different approaches have been taken to improve the reaction, particularly for unactivated alkene substrates, in addition to protocols to enable oxidative Heck-coupling pathways.^{132–134}

The Pd-catalysed Sonogashira coupling reaction of aryl iodides with either phenylacetylene or trimethylsilylacetylene was disclosed by Mack and co-workers in 2009.⁴⁵ The reaction was performed initially using copper iodide, however, it was found that the reaction provided comparable yields when the milling vessel and jar material were changed to copper. This work was closely followed by a faster, ligand / copper-free variation from Stolle and co-workers.¹³⁵ More recently, Ito and co-workers report solvent-free construction of large polycyclic conjugated systems using a mounted heat gun.¹³⁶

C-H coupling is a powerful strategy that allows for the synthesis of complex structures from readily available starting materials. Bolm and co-workers introduced this concept to ball-milling in 2015 through an Ir-catalysed C-H bond amidation of benzamides with sulfonyl azides.⁷⁷ However, a previous report outlining mechanochemical cross dehydrogenative coupling published in 2011 by Su and co-workers could also be considered as C-H coupling.⁸³

Despite being the leading reaction for the synthesis of arylamines, the Buchwald-Hartwig has only recently been adapted for use under ball-milling conditions. Su and co-workers reported the first example of solvent-free coupling in 2018 without the need for inert conditions employing Na₂SO₄ as a grinding auxiliary.⁹⁴ This was closely followed by a Pd-PEPPSI catalysed approach from Browne and co-workers and olefin-accelerated solid-state coupling from Ito and co-workers.^{50,90}

In the same year, Browne and co-workers also reported the first examples of facile synthesis of organozinc reagents, and their subsequent use in a Pd-PEPPSI catalysed Negishi coupling reaction.¹¹¹

Despite the clear advancements in mechanochemical cross-coupling, there still remains unexplored reactivity. For example, non C-N carbon-heteroatom coupling as well as cross-electrophile coupling.

1.6 Conclusions and Outlook

The application of ball milling has been shown to be a sustainable method for solvent minimised synthesis and has been highlighted as an important technology for the future of chemistry. However, recent development and advancements have also uncovered a variety of beneficial properties with respect to organic synthesis. These advantages include shorter reaction times, access to alternative products, and the facile activation of zero-valent metals. The ability to promote reactivity that is otherwise unattainable using traditional solution-based methods gives a good platform for the discovery of new reactivity. It has previously been a little difficult to predict exactly which reactions benefit from mechanical energy. However, the recent surge in interest for ball-milling in organic synthesis means that the area is currently in an exciting stage of identification and discovery with an increasing number of publications each year reporting across a broad range of synthetic methodologies.

The ultimate goal is to develop solvent free / minimised processes for use on an industrial scale. Indeed, there are research groups already assessing the chemical engineering challenges that are presented by this ambition. One such technology that has emerged and shows great promise is twin-screw extrusion. However, in most cases, twin-screw extrusion scale-up has only been shown for reactions that have already been established successfully under ball-milling conditions. The importance of ball-milling is therefore paramount.

Despite the advancements made so far, there is still clear potential for further application to more transformations. The more reactions and benefits seen using mechanochemistry will help in further understanding the technique and improve predictions of transformations using this enabling technology.

1.7 Thesis Aims and Objectives

The aims of the thesis are to further investigate the application of ball-milling to organic synthesis. The focus will be on identifying reactions that benefit from reaction under ball-milling conditions. This will likely be achieved by adaptation of conditions from solution-based methods. However, in some cases, different reactivity to that achieved in solution may be observed. These opportune differences will be probed in order to establish an understanding that can aid in future development of mechanochemical reactions. It is also important to compare the reactivity observed in solution to any developed milling protocols to give context to any differences observed.

The field of mechanochemical synthesis will be expanded by building upon the established benefits of the technique and their application to new reactions with a strong

focus on transition metal-catalysed cross-coupling reactions, starting with Pd-catalysed C-S coupling.

1.8 Bibliography

- 1 N. Hoffmann, *Chem. Rev.*, 2008, **108**, 1052–1103.
- 2 A. B. Beeler, *Chem. Rev.*, 2016, **116**, 9629–9630.
- 3 M. Yan, Y. Kawamata and P. S. Baran, *Chem. Rev.*, 2017, **117**, 13230–13319.
- 4 A. Wiebe, T. Gieshoff, S. Möhle, E. Rodrigo, M. Zirbes and S. R. Waldvogel, *Angew. Chem. Int. Ed.*, 2018, **57**, 5594–5619.
- 5 N. Shan, F. Toda and W. Jones, *Chem. Commun.*, 2002, 2372–2373.
- 6 L. Takacs, *Chem. Soc. Rev.*, 2013, **42**, 7649–7659.
- 7 J.-L. Do and T. Friščić, *ACS Cent. Sci.*, 2017, **3**, 13–19.
- 8 S. L. James, C. J. Adams, C. Bolm, D. Braga, P. Collier, T. Friščić, F. Grepioni, K. D. M. Harris, G. Hyett, W. Jones, A. Krebs, J. Mack, L. Maini, A. G. Orpen, I. P. Parkin, W. C. Shearouse, J. W. Steed and D. C. Waddell, *Chem. Soc. Rev.*, 2011, **41**, 413–447.
- 9 A. Stolle, T. Szuppa, S. E. S. Leonhardt and B. Ondruschka, *Chem. Soc. Rev.*, 2011, **40**, 2317–2329.
- 10 J. L. Howard, Q. Cao and D. L. Browne, *Chem. Sci.*, 2018, **9**, 3080–3094.
- 11 J. G. Hernández and C. Bolm, *J. Org. Chem.*, 2017, **82**, 4007–4019.
- 12 J. Andersen and J. Mack, *Green Chem.*, 2018, **20**, 1435–1443.
- 13 K. Horie, M. Barón, R. B. Fox, J. He, M. Hess, J. Kahovec, T. Kitayama, P. Kubisa, E. Maréchal, W. Mormann, R. F. T. Stepto, D. Tabak, J. Vohlidal, E. S. Wilks and W. J. Work, *Pure Appl. Chem.*, 2004, **76**, 889–906.
- 14 D. J. C. Constable, P. J. Dunn, J. D. Hayler, G. R. Humphrey, J. Johnnie L. Leazer, R. J. Linderman, K. Lorenz, J. Manley, B. A. Pearlman, A. Wells, A. Zaks and T. Y. Zhang, *Green Chem.*, 2007, **9**, 411–420.
- 15 M. C. Bryan, P. J. Dunn, D. Entwistle, F. Gallou, S. G. Koenig, J. D. Hayler, M. R. Hickey, S. Hughes, M. E. Kopach, G. Moine, P. Richardson, F. Roschangar, A. Steven and F. J. Weiberth, *Green Chem.*, 2018, **20**, 5082–5103.
- 16 F. Gomollón-Bel, *Chem. Int.*, 2019, **41**, 12–17.
- 17 K. J. Ardila-Fierro and J. G. Hernández, *ChemSusChem*, 2021, **14**, 2145–2162.
- 18 D. Tan and F. García, *Chem. Soc. Rev.*, 2019, **48**, 2274–2292.
- 19 L. Takacs, *J. Therm. Anal. Calorim.*, 2007, **90**, 81–84.
- 20 A. R. Ling and J. L. Baker, *J. Chem. Soc. Trans.*, 1893, **63**, 1314–1327.
- 21 D. Margetić and V. Štrukil, in *Mechanochemical Organic Synthesis*, eds. D. Margetić and V. Štrukil, Elsevier, Boston, 2016, pp. 1–54.
- 22 A. A. L. Michalchuk, I. A. Tumanov and E. V. Boldyreva, *CrystEngComm*, 2019, **21**, 2174–2179.
- 23 G. R. Kumar, K. Jayasankar, S. K. Das, T. Dash, A. Dash, B. K. Jena and B. K. Mishra, *RSC Adv.*, 2016, **6**, 20067–20073.
- 24 F. Schneider, A. Stolle, B. Ondruschka and H. Hopf, *Org. Process Res. Dev.*, 2009, **13**, 44–48.
- 25 P. Staleva, J. G. Hernández and C. Bolm, *Chem. – Eur. J.*, 2019, **25**, 9202–9205.
- 26 C. F. Burmeister and A. Kwade, *Chem. Soc. Rev.*, 2013, **42**, 7660–7667.
- 27 A. C. Jones, W. I. Nicholson, J. A. Leitch and D. L. Browne, *Org. Lett.*, 2021, **23**, 6337–6341.
- 28 M. T. J. Williams, L. C. Morrill and D. L. Browne, *ACS Sustain. Chem. Eng.*, 2020, **8**, 17876–17881.
- 29 A. Stolle, R. Schmidt and K. Jacob, *Faraday Discuss.*, 2014, **170**, 267–286.
- 30 D. E. Crawford, *Beilstein J. Org. Chem.*, 2017, **13**, 65–75.
- 31 D. E. Crawford and J. Casaban, *Adv. Mater.*, 2016, **28**, 5747–5754.
- 32 D. E. Crawford, C. K. G. Miskimmin, A. B. Albadarin, G. Walker and S. L. James, *Green Chem.*, 2017, **19**, 1507–1518.

- 33 B. D. Egleston, M. C. Brand, F. Greenwell, M. E. Briggs, S. L. James, A. I. Cooper, D. E. Crawford and R. L. Greenaway, *Chem. Sci.*, 2020, **11**, 6582–6589.
- 34 D. Crawford, J. Casaban, R. Haydon, N. Giri, T. McNally and S. L. James, *Chem. Sci.*, 2015, **6**, 1645–1649.
- 35 D. E. Crawford, S. L. James and T. McNally, *ACS Sustain. Chem. Eng.*, 2018, **6**, 193–201.
- 36 Q. Cao, D. E. Crawford, C. Shi and S. L. James, *Angew. Chem.*, 2020, **132**, 4508–4513.
- 37 B. M. Sharma, R. S. Atapalkar and A. A. Kulkarni, *Green Chem.*, 2019, **21**, 5639–5646.
- 38 N. Cindro, M. Tireli, B. Karadeniz, T. Mrla and K. Užarević, *ACS Sustain. Chem. Eng.*, 2019, **7**, 16301–16309.
- 39 J. Andersen and J. Mack, *Angew. Chem. Int. Ed Engl.*, 2018, **57**, 13062–13065.
- 40 T. Seo, N. Toyoshima, K. Kubota and H. Ito, *J. Am. Chem. Soc.*, 2021, **143**, 6165–6175.
- 41 R. Takahashi, A. Hu, P. Gao, Y. Gao, Y. Pang, T. Seo, J. Jiang, S. Maeda, H. Takaya, K. Kubota and H. Ito, *Nat. Commun.*, 2021, **12**, 6691.
- 42 F. Fischer, N. Fendel, S. Greiser, K. Rademann and F. Emmerling, *Org. Process Res. Dev.*, 2017, **21**, 655–659.
- 43 R. Schmidt, C. F. Burmeister, M. Baláž, A. Kwade and A. Stolle, *Org. Process Res. Dev.*, 2015, **19**, 427–436.
- 44 H. Kulla, F. Fischer, S. Benemann, K. Rademann and F. Emmerling, *CrystEngComm*, 2017, **19**, 3902–3907.
- 45 D. A. Fulmer, W. C. Shearouse, S. T. Medonza and J. Mack, *Green Chem.*, 2009, **11**, 1821–1825.
- 46 W. Pickhardt, S. Grätz and L. Borchardt, *Chem. – Eur. J.*, 2020, **26**, 12903–12911.
- 47 C. G. Vogt, S. Grätz, S. Lukin, I. Halasz, M. Etter, J. D. Evans and L. Borchardt, *Angew. Chem. Int. Ed.*, 2019, **58**, 18942–18947.
- 48 E. Losev, S. Arkhipov, D. Kolybalov, A. Mineev, A. Ogienko, E. Boldyreva and V. Boldyrev, *CrystEngComm*, DOI:10.1039/D1CE01703A.
- 49 M. Arhangelskis, D.-K. Bučar, S. Bordignon, M. R. Chierotti, S. A. Stratford, D. Voinovich, W. Jones and D. Hasa, *Chem. Sci.*, 2021, **12**, 3264–3269.
- 50 Q. Cao, W. I. Nicholson, A. C. Jones and D. L. Browne, *Org. Biomol. Chem.*, 2019, **17**, 1722–1726.
- 51 J.-L. Do, C. Mottillo, D. Tan, V. Štrukil and T. Friščić, *J. Am. Chem. Soc.*, 2015, **137**, 2476–2479.
- 52 J. Bonnamour, T.-X. Métro, J. Martinez and F. Lamaty, *Green Chem.*, 2013, **15**, 1116–1120.
- 53 J. L. Howard, Y. Sagatov and D. L. Browne, *Tetrahedron*, 2018, **74**, 3118–3123.
- 54 P. Ying, J. Yu and W. Su, *Adv. Synth. Catal.*, 2021, **363**, 1246–1271.
- 55 D. Hasa, G. Schneider Rauber, D. Voinovich and W. Jones, *Angew. Chem. Int. Ed.*, 2015, **54**, 7371–7375.
- 56 J. L. Howard, Y. Sagatov, L. Repousseau, C. Schotten and D. L. Browne, *Green Chem.*, 2017, **19**, 2798–2802.
- 57 Z.-J. Jiang, Z.-H. Li, J.-B. Yu and W.-K. Su, *J. Org. Chem.*, 2016, **81**, 10049–10055.
- 58 J. L. Howard, M. C. Brand and D. L. Browne, *Angew. Chem. Int. Ed.*, 2018, **57**, 16104–16108.
- 59 S. Mashkouri and M. Reza Naimi-Jamal, *Molecules*, 2009, **14**, 474–479.
- 60 S. Lukin, M. Tireli, I. Lončarić, D. Barišić, P. Šket, D. Vrsaljko, M. di Michiel, J. Plavec, K. Užarević and I. Halasz, *Chem. Commun.*, 2018, **54**, 13216–13219.
- 61 H. Kulla, S. Haferkamp, I. Akhmetova, M. Röllig, C. Maierhofer, K. Rademann and F. Emmerling, *Angew. Chem. Int. Ed.*, 2018, **57**, 5930–5933.

- 62 B. P. Hutchings, D. E. Crawford, L. Gao, P. Hu and S. L. James, *Angew. Chem. Int. Ed.*, 2017, **56**, 15252–15256.
- 63 E. Colacino, V. Isoni, D. Crawford and F. García, *Trends Chem.*, 2021, **3**, 335–339.
- 64 C. Gomes, C. S. Vinagreiro, L. Damas, G. Aquino, J. Quaresma, C. Chaves, J. Pimenta, J. Campos, M. Pereira and M. Pineiro, *ACS Omega*, 2020, **5**, 10868–10877.
- 65 G.-W. Wang, *Chem. Soc. Rev.*, 2013, **42**, 7668–7700.
- 66 A. Stolle and B. Ranu, *Ball Milling Towards Green Synthesis: Applications, Projects, Challenges*, Royal Society of Chemistry, 2014.
- 67 A. Beillard, T.-X. Métro, X. Bantreil, J. Martinez and F. Lamaty, *Chem. Sci.*, 2017, **8**, 1086–1089.
- 68 S. De, F. Joó, H. Horváth, A. Udvardy and C. E. Czégényi, *J. Organomet. Chem.*, 2020, **918**, 121308.
- 69 A. Beillard, X. Bantreil, T.-X. Métro, J. Martinez and F. Lamaty, *Green Chem.*, 2018, **20**, 964–968.
- 70 G. Pisanò and C. S. J. Cazin, *ACS Sustain. Chem. Eng.*, 2021, **9**, 9625–9631.
- 71 A. Porcheddu, E. Colacino, L. De Luca and F. Delogu, *ACS Catal.*, 2020, **10**, 8344–8394.
- 72 Z.-J. Jiang, Z.-H. Li, J.-B. Yu and W.-K. Su, *J. Org. Chem.*, 2016, **81**, 10049–10055.
- 73 K. Kubota and H. Ito, *Trends Chem.*, 2020, **2**, 1066–1081.
- 74 S. Zhao, Y. Li, C. Liu and Y. Zhao, *Tetrahedron Lett.*, 2018, **59**, 317–324.
- 75 M. T. J. Williams, L. C. Morrill and D. L. Browne, *ChemSusChem*, 2022, **15**, e202102157.
- 76 C. M. Zinser, F. Nahra, M. Brill, R. E. Meadows, D. B. Cordes, A. M. Z. Slawin, S. P. Nolan and C. S. J. Cazin, *Chem. Commun.*, 2017, **53**, 7990–7993.
- 77 G. N. Hermann, P. Becker and C. Bolm, *Angew. Chem. Int. Ed.*, 2016, **55**, 3781–3784.
- 78 D. Lee, Y. Kim and S. Chang, *J. Org. Chem.*, 2013, **78**, 11102–11109.
- 79 Y. Fort, M. C. Berthe and P. Caubere, *Tetrahedron*, 1992, **48**, 6371–6384.
- 80 J. Mack and M. Shumba, *Green Chem.*, 2007, **9**, 328–330.
- 81 L. Chen, D. Leslie, M. G. Coleman and J. Mack, *Chem. Sci.*, 2018, **9**, 4650–4661.
- 82 D. Tan, C. Mottillo, A. D. Katsenis, V. Štrukil and T. Friščić, *Angew. Chem. Int. Ed.*, 2014, **53**, 9321–9324.
- 83 W. Su, J. Yu, Z. Li and Z. Jiang, *J. Org. Chem.*, 2011, **76**, 9144–9150.
- 84 J. G. Hernández, N. A. J. Macdonald, C. Mottillo, I. S. Butler and T. Friščić, *Green Chem.*, 2014, **16**, 1087–1092.
- 85 K.-Y. Jia, J.-B. Yu, Z.-J. Jiang and W.-K. Su, *J. Org. Chem.*, 2016, **81**, 6049–6055.
- 86 R. A. Haley, A. R. Zellner, J. A. Krause, H. Guan and J. Mack, *ACS Sustain. Chem. Eng.*, 2016, **4**, 2464–2469.
- 87 S. K. Rodrigo, I. V. Powell, M. G. Coleman, J. A. Krause and H. Guan, *Org. Biomol. Chem.*, 2013, **11**, 7653–7657.
- 88 G.-W. Wang, Y. Murata, K. Komatsu and T. S. M. Wan, *Chem. Commun.*, 1996, 2059–2060.
- 89 J. V. Davis, O. Guio, B. Captain and C. D. Hoff, *ACS Omega*, 2021, **6**, 18248–18252.
- 90 K. Kubota, T. Seo, K. Koide, Y. Hasegawa and H. Ito, *Nat. Commun.*, 2019, **10**, 111.
- 91 S. Wu, W. Shi and G. Zou, *New J. Chem.*, 2021, **45**, 11269–11274.
- 92 X.-B. Lan, Y. Li, Y.-F. Li, D.-S. Shen, Z. Ke and F.-S. Liu, *J. Org. Chem.*, 2017, **82**, 2914–2925.

- 93 F.-D. Huang, C. Xu, D.-D. Lu, D.-S. Shen, T. Li and F.-S. Liu, *J. Org. Chem.*, 2018, **83**, 9144–9155.
- 94 Q.-L. Shao, Z.-J. Jiang and W.-K. Su, *Tetrahedron Lett.*, 2018, **59**, 2277–2280.
- 95 K. Kubota, R. Takahashi, M. Uesugi and H. Ito, *ACS Sustain. Chem. Eng.*, 2020, **8**, 16577–16582.
- 96 K. Kubota, R. Takahashi and H. Ito, *Chem. Sci.*, 2019, **10**, 5837–5842.
- 97 Paul. Knochel and R. D. Singer, *Chem. Rev.*, 1993, **93**, 2117–2188.
- 98 S. C. Berk, M. C. P. Yeh, N. Jeong and P. Knochel, *Organometallics*, 1990, **9**, 3053–3064.
- 99 F. Langer, L. Schwink, A. Devasagayaraj, P.-Y. Chavant and P. Knochel, *J. Org. Chem.*, 1996, **61**, 8229–8243.
- 100 G. Picotin and P. Miginiac, *J. Org. Chem.*, 1987, **52**, 4796–4798.
- 101 M. Kimura and M. Seki, *Tetrahedron Lett.*, 2004, **45**, 1635–1637.
- 102 P. Knochel and J. F. Normant, *Tetrahedron Lett.*, 1984, **25**, 1475–1478.
- 103 M. S. Newman, *J. Am. Chem. Soc.*, 1942, **64**, 2131–2133.
- 104 R. Ikegami, A. Koresawa, T. Shibata and K. Takagi, *J. Org. Chem.*, 2003, **68**, 2195–2199.
- 105 S. Huo, *Org. Lett.*, 2003, **5**, 423–425.
- 106 K. V. Baker, J. M. Brown, N. Hughes, A. J. Skarnulis and A. Sexton, *J. Org. Chem.*, 1991, **56**, 698–703.
- 107 K. Tanaka, S. Kishigami and F. Toda, *J. Org. Chem.*, 1991, **56**, 4333–4334.
- 108 S. Wada, N. Hayashi and H. Suzuki, *Org. Biomol. Chem.*, 2003, **1**, 2160–2163.
- 109 V. S. Pfennig, R. C. Vilella, J. Nikodemus and C. Bolm, *Angew. Chem. Int. Ed.*, 2022, **61**, e202116514.
- 110 C. Wu, T. Ying, X. Yang, W. Su, A. V. Dushkin and J. Yu, *Org. Lett.*, 2021, **23**, 6423–6428.
- 111 Q. Cao, J. L. Howard, E. Wheatley and D. L. Browne, *Angew. Chem. Int. Ed.*, 2018, **57**, 11339–11343.
- 112 Q. Cao, R. T. Stark, I. A. Fallis and D. L. Browne, *ChemSusChem*, 2019, **12**, 2554–2557.
- 113 J. Yin, R. T. Stark, I. A. Fallis and D. L. Browne, *J. Org. Chem.*, 2020, **85**, 2347–2354.
- 114 W. I. Nicholson, J. L. Howard, G. Magri, A. C. Seastram, A. Khan, R. R. A. Bolt, L. C. Morrill, E. Richards and D. L. Browne, *Angew. Chem. Int. Ed.*, 2021, **60**, 23128–23133.
- 115 C. C. C. Johansson Seechurn, M. O. Kitching, T. J. Colacot and V. Snieckus, *Angew. Chem. Int. Ed.*, 2012, **51**, 5062–5085.
- 116 M. J. Buskes and M.-J. Blanco, *Molecules*, 2020, **25**, 3493–3514.
- 117 P. Ruiz-Castillo and S. L. Buchwald, *Chem. Rev.*, 2016, **116**, 12564–12649.
- 118 S. Xu, E. H. Kim, A. Wei and E. Negishi, *Sci. Technol. Adv. Mater.*, 2014, **15**, 044201.
- 119 X. Yang, C. Wu, W. Su and J. Yu, *Eur. J. Org. Chem.*, 2022, e202101440.
- 120 S. F. Nielsen, D. Peters and O. Axelsson, *Synth. Commun.*, 2000, **30**, 3501–3509.
- 121 L. M. Klingensmith and N. E. Leadbeater, *Tetrahedron Lett.*, 2003, **44**, 765–768.
- 122 F. Schneider and B. Ondruschka, *ChemSusChem*, 2008, **1**, 622–625.
- 123 F. Schneider, A. Stolle, B. Ondruschka and H. Hopf, *Org. Process Res. Dev.*, 2009, **13**, 44–48.
- 124 F. Schneider, T. Szuppa, A. Stolle, B. Ondruschka and H. Hopf, *Green Chem.*, 2009, **11**, 1894–1899.
- 125 F. Bernhardt, R. Trozki, T. Szuppa, A. Stolle and B. Ondruschka, *Beilstein J. Org. Chem.*, 2010, **6**, 7, DOI: 10.3762/bjoc.6.7.
- 126 G. Cravotto, D. Garella, S. Tagliapietra, A. Stolle, S. Schüßler, S. E. S. Leonhardt and B. Ondruschka, *New J. Chem.*, 2012, **36**, 1304–1307.

- 127 T. Seo, T. Ishiyama, K. Kubota and H. Ito, *Chem. Sci.*, 2019, **10**, 8202–8210.
- 128 G. Bárti, D. Csókás, T. Yong, S. M. Tam, R. R. S. Shi, R. D. Webster, I. Pápai, F. García and M. C. Stuparu, *Angew. Chem. Int. Ed.*, 2020, **59**, 21620–21626.
- 129 R. Takahashi, T. Seo, K. Kubota and H. Ito, *ACS Catal.*, 2021, **11**, 14803–14810.
- 130 E. Tullberg, D. Peters and T. Frejd, *J. Organomet. Chem.*, 2004, **689**, 3778–3781.
- 131 E. Tullberg, F. Schacher, D. Peters and T. Frejd, *Synthesis*, 2006, **2006**, 1183–1189.
- 132 V. Declerck, E. Colacino, X. Bantreil, J. Martinez and F. Lamaty, *Chem. Commun.*, 2012, **48**, 11778–11780.
- 133 J. Yu, H. Shou, W. Yu, H. Chen and W. Su, *Adv. Synth. Catal.*, 2019, **361**, 5133–5139.
- 134 W. Shi, J. Yu, Z. Jiang, Q. Shao and W. Su, *Beilstein J. Org. Chem.*, 2017, **13**, 1661–1668.
- 135 R. Thorwirth, A. Stolle and B. Ondruschka, *Green Chem.*, 2010, **12**, 985–991.
- 136 Y. Gao, C. Feng, T. Seo, K. Kubota and H. Ito, *Chem. Sci.*, 2022, **13**, 430–438.

2 A Robust Pd-PEPPSI catalysed Carbon-Sulfur Coupling by Ball-milling

2.1 Introduction	29
2.1.1 Aryl C-S Bond Formation	29
2.1.2 Development and Utilisation of Pd-PEPPSI Pre-catalysts	34
2.1.3 Carbon-heteroatom Coupling by Ball-milling	38
2.1.4 Project Overview, Aims and Objectives	41
2.2 Results and Discussion	42
2.2.1 Initial Findings	42
2.2.2 Optimisation	42
2.2.3 Reaction Scope and Limitations	47
2.2.4 Exploring Thioether / Disulfide Reactivity	54
2.2.5 Coupling from Disulfides	56
2.2.6 Phase Transition Induced Reactivity	57
2.2.7 Comparison to Solution	61
2.3 Conclusions and Future Outlook.....	63
2.4 Bibliography	64

2.1 Introduction

Carbon-heteroatom coupling has broad utility across the production of many biologically active compounds including pharmaceuticals, natural products, and agrochemicals. The alkylation or arylation of heteroatoms comprises 23% of all steps in the production of pharmaceuticals.¹ Therefore, C-S coupling and the formation of aryl thioethers remains an important challenge for synthesis for many bio-active compounds (Figure 2.1).

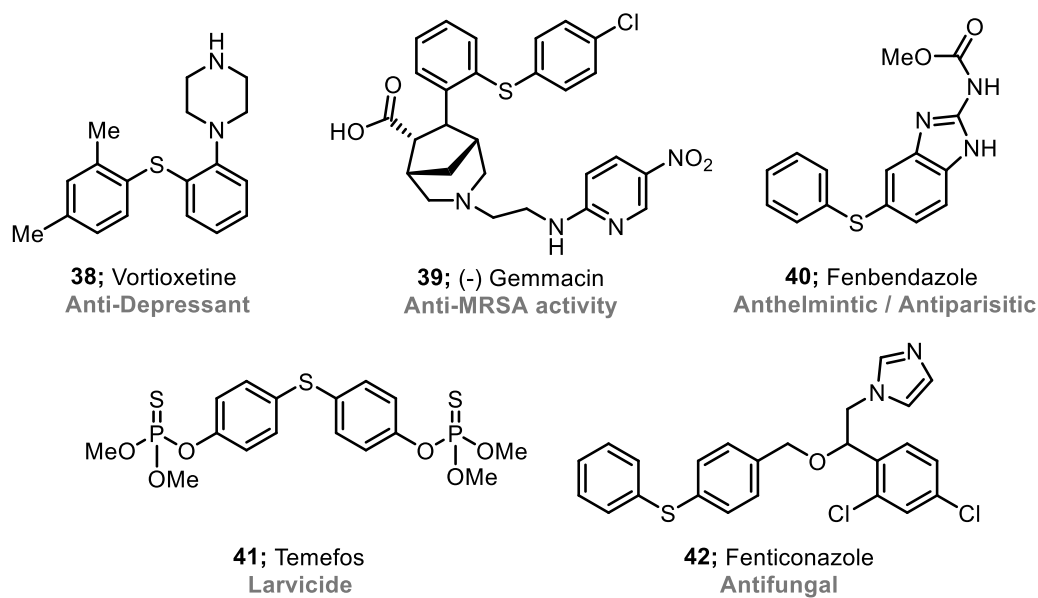
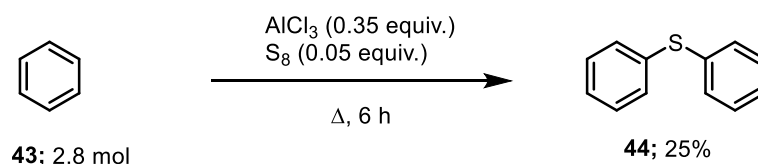


Figure 2.1 Pharmaceutical and bioactive molecules containing aryl thioether groups.

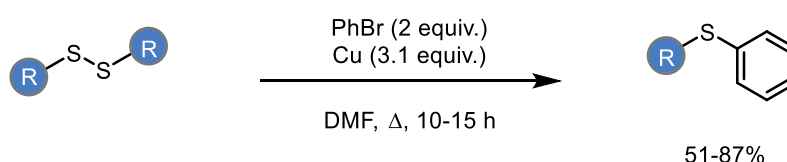
2.1.1 Aryl C-S Bond Formation

The synthesis of aryl C-S bonds is an important process in the synthesis of organic building blocks and has been achieved by numerous methods utilising a wide range of techniques and approaches. Classical methods typically involve the use of elemental sulfur to give diphenyl sulfide,² the reduction of disulfides with copper,³ and thiolation of aryl halides with various metal thiolate salts (**45**) (Scheme 2.1).^{4,5} Each of these approaches presents limitations. For example, the use of harsh reaction conditions or the use of stoichiometric metals.

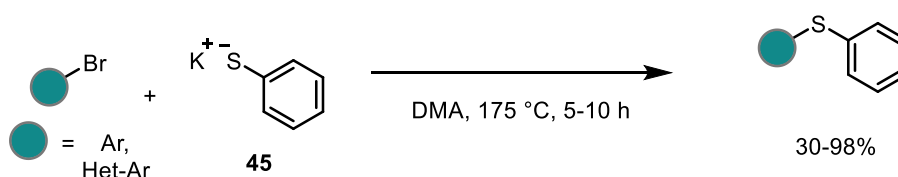
A Elemental sulfur (Dougherty and Hammond) - 1935



B Reaction of disulfides (Campbell) - 1962



C Halide displacement with thiolate salt (Campbell) - 1964

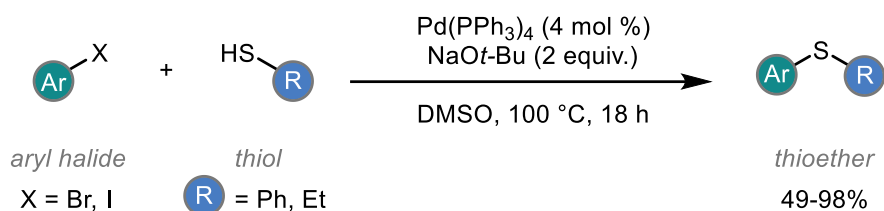


Scheme 2.1 Classical methods to forge aryl C-S bonds

Transition metal-catalysed processes have emerged as a popular approach for carbon-heteroatom bond formation, due to its simplicity and generality. Transition metal-catalysed formation of C-N bonds has been explored extensively, with the Buchwald-Hartwig reaction becoming the primary method for synthesis of aryl amines.⁶ However, synthesis of C-S bond via metal-catalysed processes has received much less attention, possibly due to the tendency for catalyst poisoning that arises with the use of organosulfur compounds.

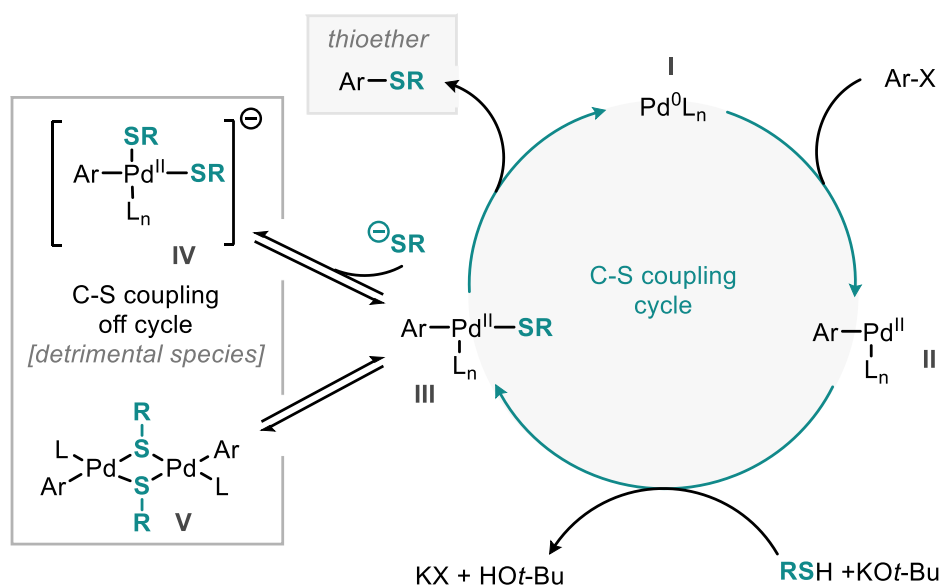
A common approach taken for aryl C-S bond formation is the coupling reaction between readily available aryl halides and thiols using a variety of different transition metal catalyst systems.⁷⁻¹³ As with other coupling reactions, catalyst systems based on palladium have been most explored and developed due to the versatility and applicability demonstrated by Pd-catalysed cross coupling reactions.^{14,15} The first example of a Pd-catalysed C-S coupling was shown by Migita and co-workers demonstrating successful coupling of a small range aryl halides with potassium thiolate salts (Scheme 2.2).¹⁶ In this work, the authors present evidence for an oxidative addition pathway using palladium, which differs from previously established substitution pathways that are typically observed when using thiolate salts.

2 - A Robust Pd-PEPPSI catalysed Carbon-Sulfur Coupling by Ball-milling



Scheme 2.2 Initial Pd-catalysed C-S by Migita and co-workers

After inception of this methodology, development of C-S coupling by Pd-catalysis has been explored for improvement to the applicability of the process. Improvements to the reaction conditions have also been documented by optimising methods for shorter reaction times, lower temperatures, or milder reagents.¹⁷⁻²⁵ From extensive development, as well as mechanistic insight presented by Hartwig and co-workers,^{26,27} a mechanism has been elucidated for carbon-sulfur coupling which has now become the widely accepted mechanism for this coupling (Scheme 2.3).



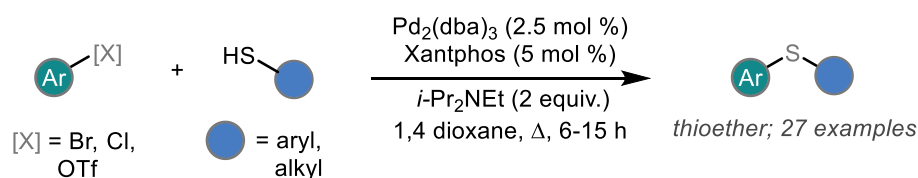
Scheme 2.3 Catalytic cycle for Pd-catalysed C-S coupling

The understood mechanism proceeds akin to many other palladium catalysed cross-coupling reactions (Suzuki, Stille, Buchwald-Hartwig, etc...). Initially, the aryl halide undergoes oxidative addition with a Pd⁰ species to give a Pd^{II} species **II**. This is followed by nucleophilic addition of a thiolate to the palladium centre. This process mimics what would be described as a transmetalation in other related cross-coupling reactions. The thiolate is likely generated through deprotonation of the thiol coupling partner. Potassium tert-butoxide is a common choice of base for this deprotonation. The palladium thiolate species **III** then undergoes reductive elimination to afford the thioether cross coupled product.

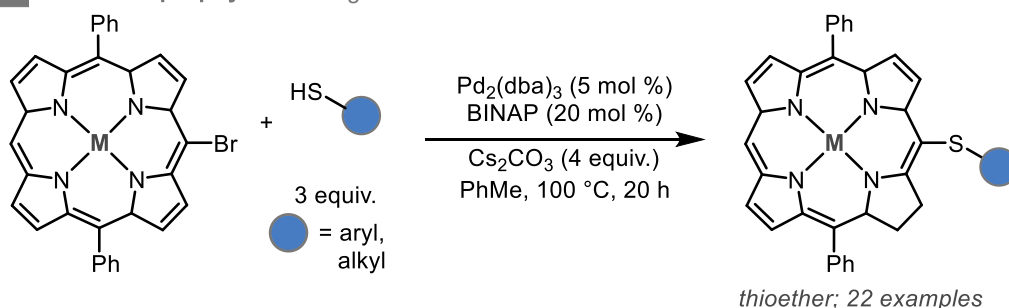
Whilst the catalytic cycle follows a similar mechanistic pathway as a Buchwald-Hartwig coupling, the use of sulfur containing nucleophiles presents significant challenges in palladium catalysis. Sulfur has a well-established tendency to poison transition metals, and this is particularly prevalent in Pd-catalysis. Due to these unwanted interactions between palladium and sulfur, off-cycle species such as **IV** and **V** can be formed during C-S coupling reactions.²⁶⁻²⁸ The most commonly proposed detrimental off-cycle species are formed from the active palladium thiolate species (Scheme 2.3, **III**), whereby another thiolate anion can bind to form the anionic Pd (II) species **IV**. Another option for deactivation is dimerisation to form a thiolate-bridged palladium dimer **V**. Both deactivating pathways are reversible processes, with the extent of deactivation varying with many factors including the exact thiol used, as well as the palladium catalyst system in place. For successful cross-coupling, these detrimental pathways must be minimised to promote reactivity along the catalytic cycle.

2 - A Robust Pd-PEPPSI catalysed Carbon-Sulfur Coupling by Ball-milling

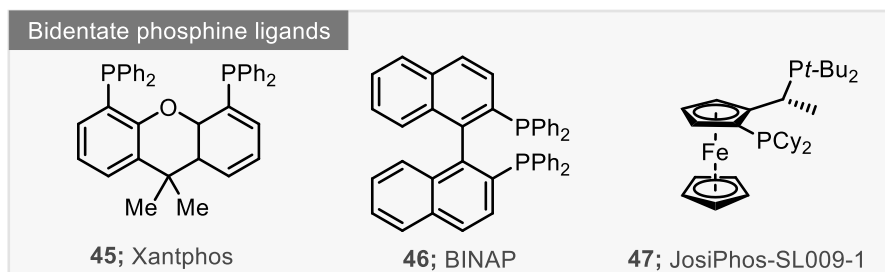
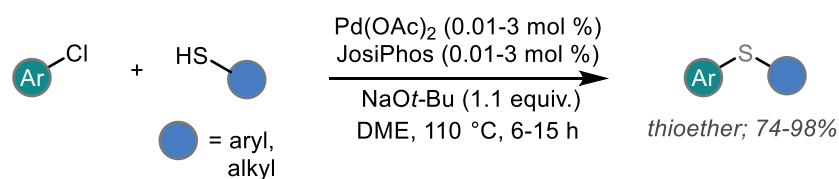
A Xantphos for general C-S coupling Itoh - 2004



B BINAP for porphyrins Zhang - 2004



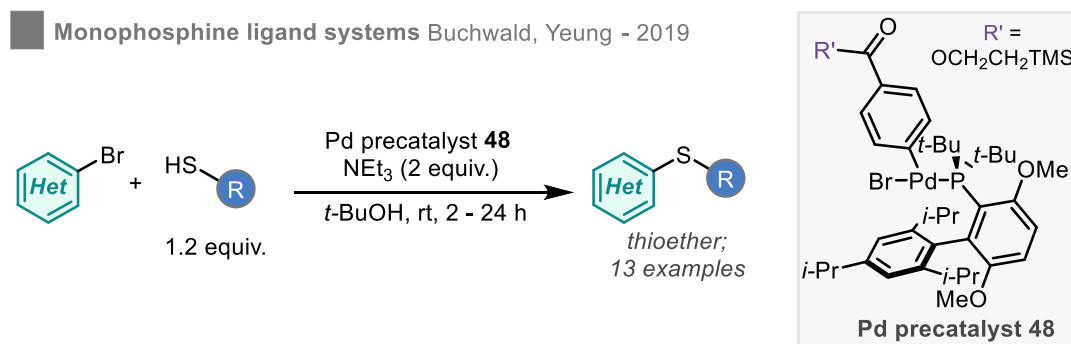
C JosiPhos for aryl chlorides Hartwig - 2006



Scheme 2.4 Development of bidentate phosphine ligands for Pd-catalysed C-S coupling

To overcome this common problem associated with C-S coupling, many different approaches have been taken to target minimisation of disruptive pathways and hence promote reductive elimination to give the desired thioether products. In most cases this involves careful consideration of the catalyst and ligand system used. In particular, it has been shown that the use of bidentate phosphine ligands has allowed for development and application towards complex coupling manifolds. Some examples of this include the Xantphos (**45**) for the coupling of a range of aryl halides and thiols (Scheme 2.4A),²⁹ BINAP (**46**) for the construction of sulfanyl porphyrins (Scheme 2.4B),³⁰ and JosiPhos derived ligands (**47**) for the powerful coupling of often challenging chloroarene substrates (Scheme 2.4C).²⁷ These approaches allow for effective coupling, however, still generally require manipulation under inert atmospheres, long reaction times and elevated temperatures in some cases. Developing upon this work, Buchwald, Yeung and co-

workers have more recently demonstrated some success for the use of monophosphine ligands at lower temperatures using soluble bases (Scheme 2.5).³¹



Scheme 2.5 Monophosphine ligands for milder coupling conditions

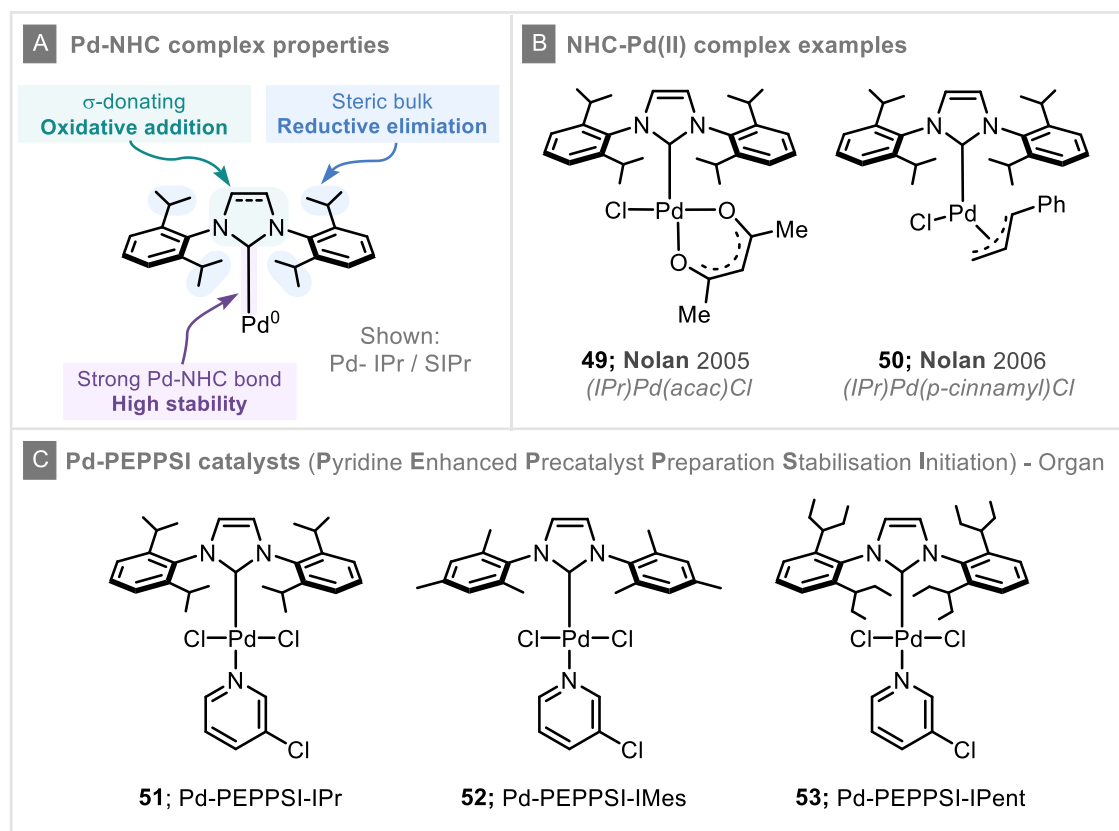
The use of phosphine-based ligands has become a convenient and well documented approach across all Pd-catalysed coupling reactions. They exhibit excellent σ -donation to palladium, although this imparted electron density is relieved a little through back-bonding to the P-R σ^* -orbital.³² They also pose the potential risk of dissociation from the metal centre, likely due to their stability in their uncoordinated state. This issue is particularly common in phosphine ligands with large cone angles.³³ Dissociation (even temporarily) from the metal centre can have serious effects on the catalytic cycle and as a result can lead to many unwanted side-reactions. A modern, elegant solution to this has been through the development of Pd-NHC complexes, especially Pd-PEPPSI (Pyridine Enhanced Pre-catalyst Preparation Stabilisation Initiation) pre-catalysts.^{33,34}

2.1.2 Development and Utilisation of Pd-PEPPSI Pre-catalysts

In a bid to target the known issues with Pd-phosphine based catalyst, whilst also seeking to improve upon established systems, a range of Pd-NHC pre-catalysts have been explored throughout the last 15 years for various cross-coupling reactions. A wide range of NHC ligands are easily prepared and their subsequent coordination to palladium has shown to be facile. The use of NHCs derived from imidazolium salts has emerged as an excellent option for cross-coupling reactions. These NHC ligands, when complexed to palladium, exhibit many desirable properties for use in a typical palladium catalytic cycle which has been achieved through careful design of their structure (Scheme 2.6A). Firstly, substitution on both nitrogen atoms of the imidazolium carbene allows for the introduction of steric bulk without having a detrimental effect on the electronics on the palladium centre. This concept of 'flexible steric bulk' aids in promoting reductive elimination. Secondly, σ -donation of the NHCs to palladium combined with little to no π -back donation increase the electron density around Pd^0 , facilitating oxidative addition. Finally,

2 - A Robust Pd-PEPPSI catalysed Carbon-Sulfur Coupling by Ball-milling

the strong Pd-C bond to the NHC, and the instability of the carbene in its free state disfavours any ligand dissociation leading to high stability and activity.

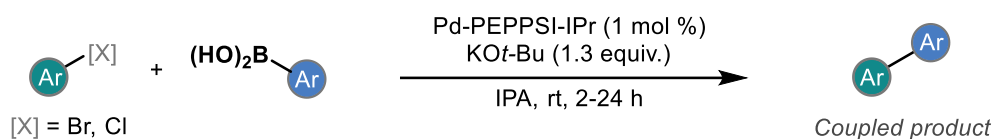


Scheme 2.6 Examples of NHC-Pd(II) complexes

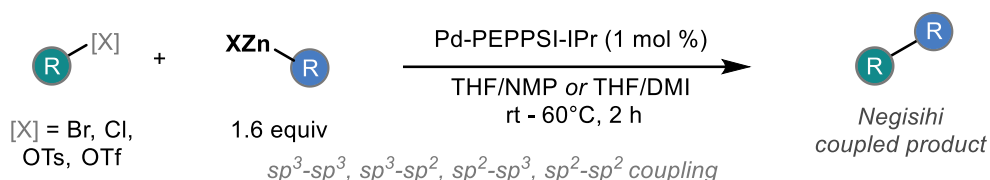
Ideally, discrete NHC-Pd(0) complexes would be used in the reaction as this represents the active species on the catalytic cycle and efforts have been made for the synthesis of such complexes, mainly by synthesis of palladium NHC dimer complexes.^{35,36} However, NHC-Pd(0) complexes typically suffer from poor stability to air and moisture. As a result of this, synthesis of these complexes can prove challenging. To this end, a number of NHC-Pd(II) pre-catalyst complexes have been developed and are shown to be more stable to moisture and air with the benefit of facile preparation on multigram scale.^{37–46} The use of NHC-Pd(II) complexes in catalysis leads to an additional requirement for ‘activation’ to the active Pd(0) species. For this, additional ligands on the Pd-complex must be labile enough to allow for initial reduction to the active species whilst also exhibiting low rebinding rates so as not to poison any active palladium intermediate species. To this end, many NHC-Pd(II) pre-catalysts have been designed with this objective in mind. Nolan and co-workers discovered useful complexes with acetylacetonate as the labile ‘throw-away’ ligand such as (IPr)Pd(acac)Cl (Figure 2.6B, **49**) and studied their use in various cross-coupling reactions.⁴⁷ Following this work, the same group explored the design of NHC-Pd(allyl) complexes and subsequently NHC-Pd(*p*-

cinnamyl) complexes.^{38,48} These powerful pre-catalysts have been shown to have broad applicability with (IPr)Pd(p-cinnamyl)Cl (Scheme 2.6B, **50**) demonstrating high activity in cross coupling reactions.^{38,49}

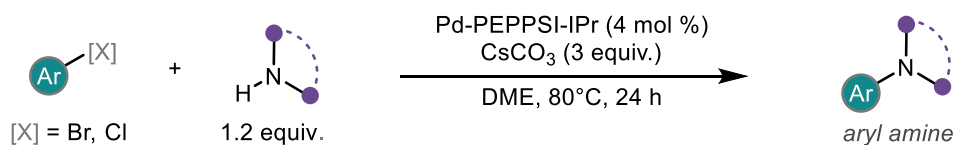
A Pd-PEPPSI catalysed Suzuki-Miyaura coupling Organ - 2006



B Pd-PEPPSI catalysed Negishi coupling Organ - 2006



C Pd-PEPPSI catalysed Buchwald-Hartwig coupling Organ - 2007



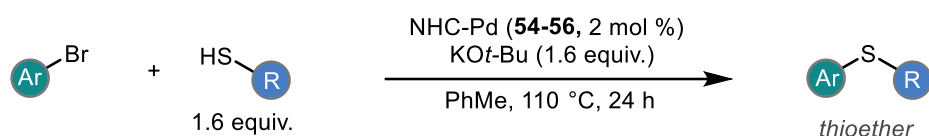
Scheme 2.7 Pd-PEPPSI catalysed cross coupling

Nolan's pre-catalysts demonstrate excellent activity for transition-metal catalysed cross-coupling, however the stability was low under ambient conditions often requiring storage under strictly inert conditions and commonly in a glove box. Organ and co-workers set out to originate a family of air and moisture stable NHC-Pd(II) pre-catalysts. The key feature for design was the incorporation of a pyridine ligand, more specifically, 3-halo pyridines which had previously been shown to increase stability and activity of ruthenium cross-metathesis catalysts.⁵⁰ Organ's work developing palladium pre-catalysts bearing (3-halo)pyridine as the 'throw-away' ligand to promote catalyst activation and an NHC ligand led to the invention of Pd-PEPPSI (**P**yridine **E**nhance **P**recatalyst **P**reparation **S**tabilisation **I**nitiation) pre-catalysts; a family of NHC-Pd(II) complexes exhibiting remarkable stability and high activity for coupling reactions (Scheme 2.6C).^{33,37}

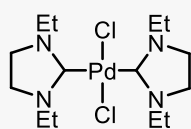
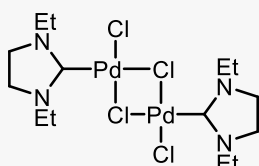
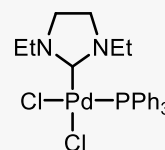
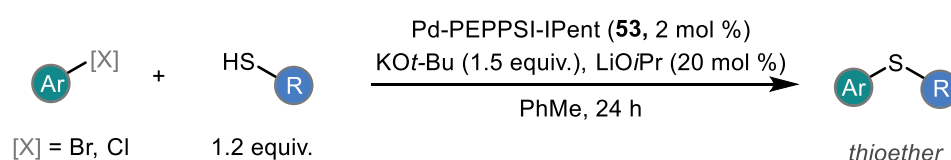
Commonly encountered Pd-PEPPSI catalysts are those with various aryl substitution patterns on the imidazolium core. These include Pd-PEPPSI-IPr (**51**),^{37,51-56} Pd-PEPPSI-IMes (**52**),^{37,57} and Pd-PEPPSI-IPent (**53**).^{55,58-62} Pd-PEPPSI catalysed cross-coupling has been shown to be effective for a number of different popular couplings including, but not limited to Suzuki Miyaura coupling (Scheme 2.7A),³⁷ Negishi coupling (Scheme 2.7B),⁶³ and Buchwald-Hartwig couplings (Scheme 2.7C).⁵⁴

Following the success of NHC-Pd complexes and Pd-PEPPSI pre-catalysts for C-N coupling reactions, the methodology has since been extended to include the more challenging C-S coupling reactions. Initial work of NHC-Pd was described by Liu and co-workers and tests a range of palladium pre-catalysts (**54-56**) bearing and ethyl-substituted imidazolium (SIEt) as the NHC ligand with (SIEt)Pd(PPh₃)Cl (**56**) proving to be the most active in coupling aryl halides with various thiols. In the procedure, KO*t*-Bu is used as the base and reaction carried out at 110 °C in toluene (Scheme 2.8A).⁶⁴ It was found that alkyl thiols performed poorly under the reactions and aryl chloride did not undergo coupling at all.

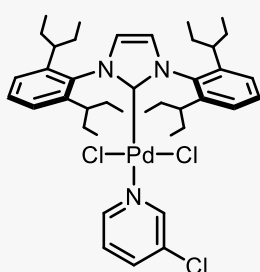
To address these shortcomings and develop a more general procedure for C-S coupling, Organ and co-workers explored the use Pd-PEPPSI pre-catalysts aiming for milder conditions. In this study, the authors reported excellent activity using Pd-PEPPSI-IPent (**53**) in conjunction with KO*t*-Bu as a base at relatively low temperatures (<40 °C) for the successful coupling of (hetero)aryl chlorides with alkyl and aryl thiols (Scheme 2.8B).⁶⁵ In this study, the use of an 'activation step' is required whereby Pd-PEPPSI-IPent (**53**) is pre-heated to 80 °C with LiO*i*-Pr (20 mol%) before addition of the thiol coupling partner. This step is a requirement due to the somewhat unclear reduction pathway for Pd^{II} reduction to Pd⁰ in sulfination reactions in comparison to other coupling reactions whereby excess organometallic reagent is an obvious source of reductant.²² Exploring the mechanistic aspects of catalyst activation further, Organ and co-workers proceeded to show that under the reductive conditions of LiO*i*-Pr, the 3-chloropyridine ligand is reduced to pyridine. This is subsequently overcome by modification of Pd-PEPPSI-IPent and assessment of its catalytic ability. It was found that a suitable structure was that of Pd-PEPPSI-IPent^{Cl}(*o*-picoline) (**57**) whereby the 3-chloropyridine ligand is exchanged for *o*-picoline and chlorines are implemented onto the NHC backbone. This modification facilitated reduction from Pd^{II} to Pd⁰ and as result required a much lower activation temperature.⁶⁶ Key to this study was the understanding that a combination of KO*t*-Bu and LiO*i*-Pr leads to the formation of KO*i*-Pr *in situ* which aides in pre-catalyst activation.

A NHC-Pd Sulfination Liu - 2010

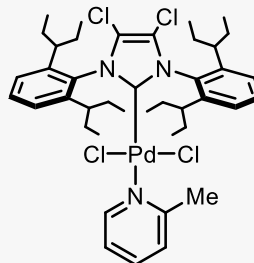
Catalysts explored

**54****55****56; (SIEt)Pd(PPh₃)Cl****B** Pd-PEPPSI catalysed C-S coupling

Organ - 2011

53
Pd-PEPPSI-IPentPre-activation
of catalyst
80 °C, 30 min

Organ - 2013

57
Pd-PEPPSI-IPent^{Cl}
(o-picoline)No activation
required**Scheme 2.8** Pd-NHC catalysed C-S coupling**2.1.3 Carbon-heteroatom Coupling by Ball-milling**

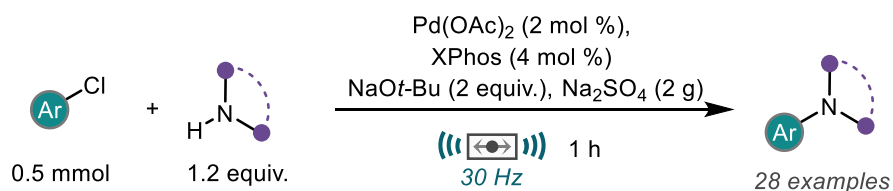
The construction of C-C bonds by mechanochemical methods has been greatly developed over the past 20 years. During this time the benefits of mechanochemistry has been applied to various important cross-coupling reactions.^{67,68} The first protocol of mechanochemical cross-coupling was demonstrated through the Suzuki-Miyaura coupling of a small range of aryl bromides and arylboronic acids by Peters and co-workers.⁶⁹ From this pioneering work, a number of different protocols have been reported detailing improvements to the conditions so as to expand the scope of the reaction, reduce reaction times and catalyst loadings, and open up reaction possibilities previously not accessible by solutions methods.⁷⁰⁻⁷⁸ Whilst the Suzuki coupling has received much of the attention for mechanochemical Pd-catalysed cross-coupling, methods have also been developed for successful use in the Negishi,⁷⁹ (Mizoroki-)Heck,⁸⁰⁻⁸⁵ and Sonogashira coupling reactions.⁸⁶⁻⁸⁸ A key concept underpinning these discoveries is that mechanochemistry has the ability to carry out sensitive organometallic chemistry

2 - A Robust Pd-PEPPSI catalysed Carbon-Sulfur Coupling by Ball-milling

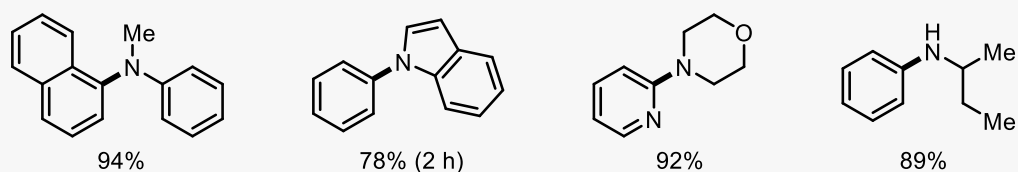
(including oxidative addition of aryl halides using palladium) without the need for glove-box / Schlenk-line techniques.⁸⁹

In contrast to the extensive work exploring C-C coupling by ball-milling, carbon-heteroatom cross-coupling remains relatively underexplored. Aryl C-N bonds represent a core fragment in many important molecules and the formation of these bonds is an important tool in the pharmaceutical sector. One of the most well-established and effective methods for the construction of aryl C-N bonds is through the Pd-catalysed coupling of aryl halides with amines. i.e. the Buchwald-Hartwig amination.^{6,90,91}

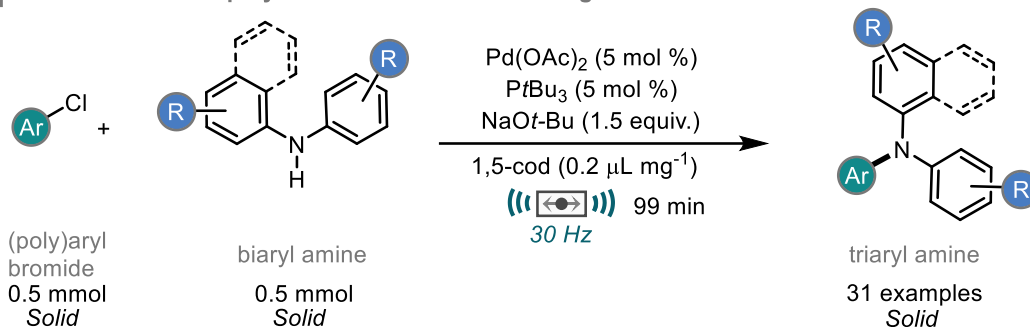
A Pd-Phosphine Buchwald-Hartwig amination Su - 2018



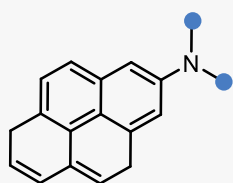
Selected examples



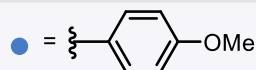
B Olefin accelerated polyaromatic Buchwald-Hartwig amination Ito - 2019



gram-scale solid-state C-N coupling

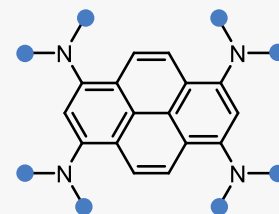


58; 88% (0.5 mmol)
2.57 g, 92% (7 mmol)



59; 89%
vs solution
Higher yield
faster reaction
no inert protection

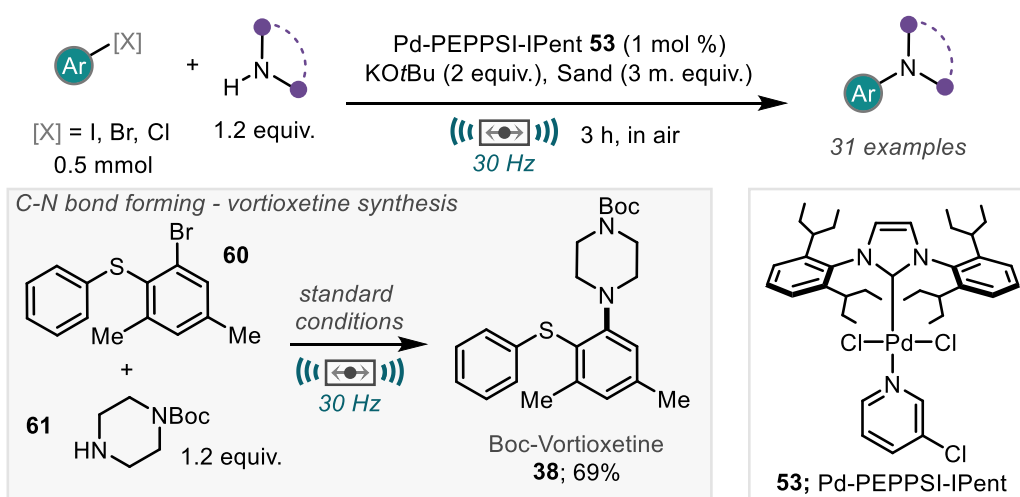
hole-transporting material



Scheme 2.9 Pd-phosphine catalysed Buchwald-Hartwig amination by ball-milling

A mechanochemical approach to the Buchwald-Hartwig amination has recently been discovered by multiple groups, assessing the capabilities and advantages of solvent free C-N coupling by ball-milling. Su and co-workers were the first to report such a protocol in 2018, whereby a Pd(OAc)₂ / XPhos system was found to successfully couple aryl chlorides with a range of amines (Scheme 2.9A).⁹² In this study, the use of Na₂SO₄ was found to be crucial for achieving high yields. The authors state that the use of the additive helps produce a powder-like reaction mixture. In 2019, Ito and co-workers also made use of a Pd / phosphine catalyst system for impressive solid-state C-N coupling (Scheme 2.9B).⁹³ Key to the success of this work was the inclusion of 1,5-cyclooctadiene as an additive to aid in the dispersion of palladium catalyst in all-solid media and therefore drastically accelerate the solid-state reaction allowing for the synthesis of polyaromatic triarylamine compounds including hole-transport material **59**. These large polyaromatic compounds can suffer from issues in solution-based methods regarding their insolubility in common reaction solvents demonstrating mechanochemistry as an excellent alternative, particularly with the successful scale up to multi-gram scale as is shown. This work was expanded by Ito and co-workers more recently to allow for the coupling of previously incompatible carbazoles *via* a high-temperature ball-milling process.⁹⁴

A Ball-milling Pd-PEPPSI catalysed Buchwald-Hartwig amination Browne - 2019



Scheme 2.10 Pd-PEPPSI catalysed Buchwald-Hartwig amination by ball-milling

Concurrent to these reports, Browne and co-workers developed a Pd-PEPPSI-IPent catalysed protocol for the construction of a range of aryl amines in good to excellent yield without the need for protection from air or moisture using sand as a grinding auxiliary (Scheme 2.10).⁹⁵ The authors propose that the reaction rate for product formation is much faster when compared to analogous solution-based examples. The larger difference in rates of product formation versus catalyst deactivation results in a reliable,

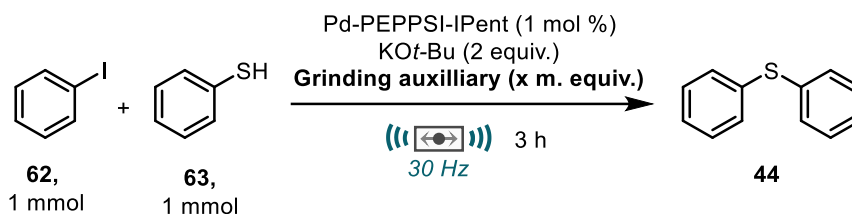
robust technique for aryl amine synthesis, which is exemplified in this by the achievement of good yield for the key C-N bond forming step in the synthesis of Vortioxetine (**38**).

2.1.4 Project Overview, Aims and Objectives

Ball-milling, an established enabling technology, has been effectively applied to well-established cross-coupling reactions for the construction of C-C bonds. This methodology has more recently been extended to the synthesis of aryl C-N bonds through multiple variations of a Buchwald-Hartwig amination demonstrating the benefits of solvent-free / solid-state synthesis. This gives a strong foundation for development in carbon-heteroatom coupling under a mechanochemical manifold. Transition metal-catalysed C-S coupling to furnish aryl thioethers has not yet been explored by ball-milling. It is thought the use of ball-milling in conjunction with Pd-PEPPSI pre-catalysts could alleviate some of the typical issues (stability, sensitivity, and catalyst poisoning) seen when using sulfur-based compounds for palladium catalysis as well as providing unique benefits / reactivity.

2 - A Robust Pd-PEPPSI catalysed Carbon-Sulfur Coupling by Ball-milling

Table 2.1 Optimisation of grinding auxiliary

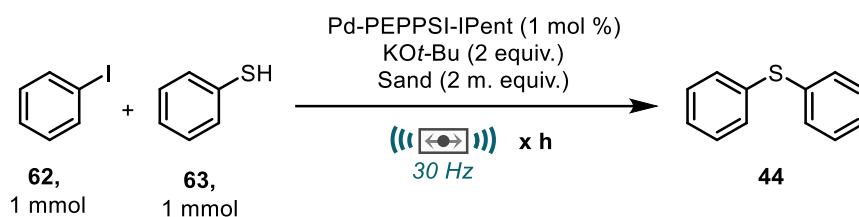


Entry	Grinding Auxiliary	Mass equiv.	Yield 44 (%) ^a
1	-	-	0
2	Sand	1	45
3	Sand	2	94
4	Sand	3	76
5	NaCl	2	0
6	MgSO ₄	2	0
7	Celite	2	85
8	SiO ₂	2	0

^a Yield determined by ¹H NMR spectroscopy using mesitylene as an internal standard.

Interestingly, in the absence of grinding auxiliary, the reaction does not proceed and returns quantitative amounts of starting materials. This is possibly due to the liquid starting materials not having a surface to react upon or poor energy transfer. Increasing the mass equivalents of sand appeared to give a linear increase in yield up to a maximum of 94% achieved with 2 mass equivalents (Table 2.1, entry 3). This excellent yield is a result of good mixing and could be visually confirmed upon opening the jars with the mixture being spread evenly across the whole jar. The lower yield of 76% observed with 3 mass equivalents arises from poorer mixing and 'gumming' of the materials whereby the sticky mixture is localised on the milling ball.

To explore the role of the grinding auxiliary, a small range of commonly encountered additives were screened using 2 mass equivalents (Table 2.1, entries 5-8). Celite was the only other grinding agent that provided any product. Highly absorbent silica and magnesium sulfate both performed poorly as they prevented efficient mixing of the materials. Two equivalents of sand proved to be optimal for promoting efficient mixing / mass-transfer, thus was taken forward in the optimisation.

Table 2.2 Reaction time optimisation

Entry	Time	Yield 44 (%) ^a
1	0.5	25
2	1	25-77
3	1.5	96 (92)^b
4	2	95
5	3	94

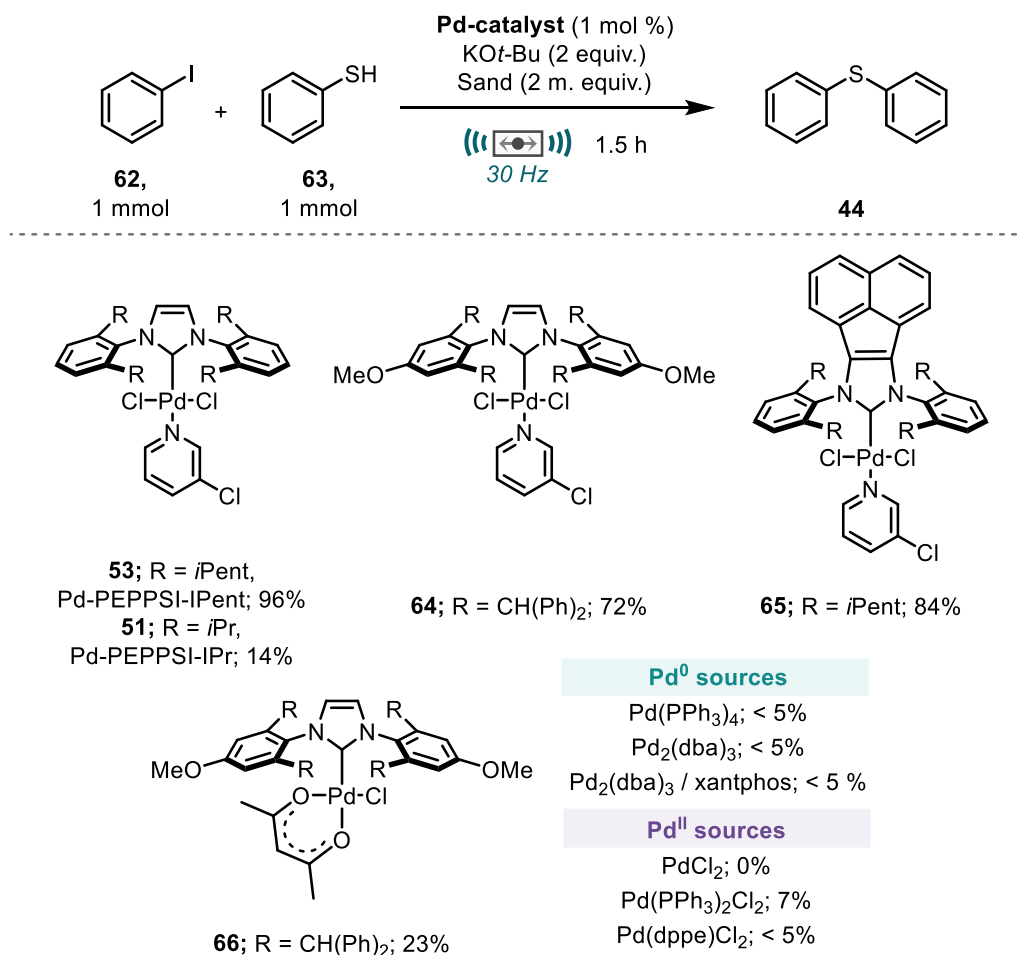
^aYield determined by ¹H NMR spectroscopy using mesitylene as an internal standard. ^b Isolated yield.

With an excellent yield already achieved, the reaction time was probed to determine the point at which the reaction was completed (Table 2.2). Unfortunately, aliquots cannot be taken from the milling vessel during reaction, thereby preventing the monitoring of a single reaction. Therefore, multiple identical reactions were set up and run for different time periods (0.5 – 3 h). The yield remained excellent at a reduced reaction time of 1.5 h (Table 2.1, entry 3). A further shortened reaction time of just 0.5 h returned a poor yield of product (25%). Curiously, a reaction time of 1 h, provided a wide range of results across 3 different reactions (25-77%) suggesting a key event in the reaction sequence may be taking place around this time point. A reaction time of 1.5 hours was continued for the optimisation due to its consistent excellent yield across 3 runs.

The catalyst system was explored next. Firstly, a range of Pd-PEPPSI type catalysts were subjected to the standard conditions (Scheme 2.12). Pd-PEPPSI-IPent (**53**) proved to be significantly more effective than the more widely utilised Pd-PEPPSI-IPr (**51**) in this coupling giving 94% and 14% product, respectively. This remarkable difference in yield could be explained by the subtle change in steric bulk, with the *iso*-pentyl groups aiding the reductive elimination step of the catalytic cycle significantly. Another popular PEPPSI pre-catalyst with increased steric bulk (**64**) also demonstrated good yield (72%), again demonstrating the importance of large steric bulk on the catalyst for reductive elimination. Adding a naphthyl backbone to the imidazole functionality (**65**) and thereby slightly increasing the electron density around palladium provided excellent yield (84%) with the remainder of starting material **62** returned suggesting effective but slightly slower rate of coupling when compared to Pd-PEPPSI-IPent (**53**). Replacement of the stabilising pyridyl group and one chloride ligand with bidentate acetylacetonate (**66**), the yield was

2 - A Robust Pd-PEPPSI catalysed Carbon-Sulfur Coupling by Ball-milling

significantly reduced in comparison to its PEPPSI counterpart **64**, showing the need for pyridine as a labile stabilising ligand. Other common Pd⁰ catalysts such as Pd(PPh₃)₄ and those based on Pd₂(dba)₃ gave only trace product. Simple Pd^{II} pre-catalysts also did not fare well in the reaction with Pd(PPh₃)Cl₂ affording the best result of just 7% NMR yield. These simple (pre)-catalysts being ineffective in the system detail the necessity for the highly active and privileged Pd-PEPPSI pre-catalysts. Due to its superior activity, Pd-PEPPSI-IPent (**53**) was taken forward for the remainder of optimisation.



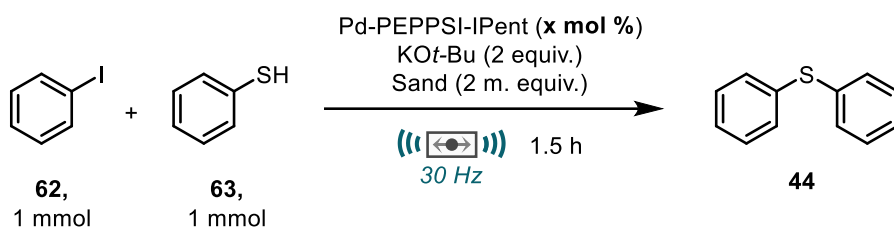
Yields determined by ¹H NMR spectroscopy using mesitylene as an internal standard.

Scheme 2.12 Catalyst screen

Due to the expense of the pre-catalyst at the time of investigation (the cost of which has significantly reduced recently) and the general cost of palladium, achieving a comparable yield with a lower pre-catalyst loading would be highly desirable. Pleasingly, it was shown that loading could be halved to 0.5 mol % with no detrimental effect on yield (Table 2.3, entry 3). However, it was found that this was the limit for decreasing pre-catalyst loading,

as the reaction with 0.25 mol % pre-catalyst provided a significant reduction in yield with just 11% of desired product being formed (Table 2.3, entry 4).

Table 2.3 Investigation of catalyst loading



Entry	Pre-catalyst loading (x mol %)	Yield 44 (%) ^a
1	2	96
2	1	96 (92) ^b
3	0.5	95 (92) ^b
4	0.25	11

^aYield determined by ¹H NMR spectroscopy using mesitylene as an internal standard. ^b Isolated yield.

Proceeding with 0.5 mol % Pd-PEPPSI-IPent as the pre-catalyst, the base was next explored (Table 2.4). With 2 equivalents of KO*t*-Bu being the current optimal base in the reaction, the loading was increased and decreased to observe any effects on reactivity. Interestingly, increasing the loading of base to 3 equivalents resulted in almost complete return of starting materials and only a small amount of product observed. This is likely due to the increased mass going into the milling vessel and thereby restriction of efficient mixing. This rationale can be reinforced by the aesthetics of the reaction mixture after milling, with the entire grey mixture being localised on the milling ball, which was also shown to reduce yield in Table 2.1 when increased grinding auxiliary also resulted in ‘gumming’ of the mixture. Lower loadings of KO*t*-Bu gave significantly lower yields (Table 2.4, entries 3-4). Variation from KO*t*-Bu as the base resulted in reduced yield in all cases. NaO*t*-Bu performed poorly in the reaction (13%) perhaps due to the stronger Na-O bond in comparison to the K-O bond. Without the use of solvent, the release of the active form of the base will be more difficult and therefore may be less effective for deprotonation. Weaker inorganic bases were found to be worse in the reaction indicating the need for the significantly stronger base KO*t*-Bu. Organic bases (DIPEA, DBU) also gave reduced yields however did afford a reasonable amount of product. The optimal choice of KO*t*-Bu aligns with literature where it is the most common base used for this transformation. It is worth noting that KO*t*-Bu was used without purification from commercial bottle. Using freshly sublimed KO*t*-Bu saw no change in yield.

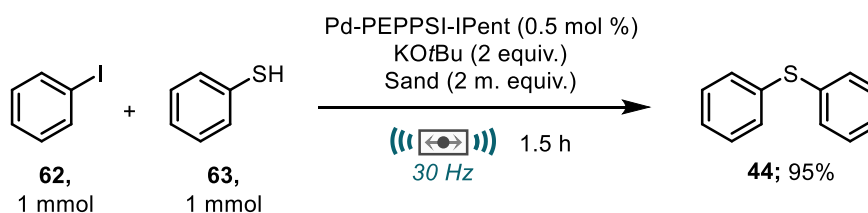
Table 2.4 Base optimisation

Entry	Base	Equiv.	Yield 44 (%) ^a
1	KO <i>t</i> -Bu	3	5
2	KO <i>t</i> -Bu	2	95 (92) ^b
3	KO <i>t</i> -Bu	1.5	49
4	KO <i>t</i> -Bu	1	32
5	NaO <i>t</i> -Bu	2	13
6	KOH	2	11
7	Cs ₂ CO ₃	2	6
8	DIPEA	2	23
9	DBU	2	28

^a Yield determined by ¹H NMR spectroscopy using mesitylene as an internal standard.

^b Isolated yield

After investigation of the parameters, the optimal conditions were identified (Scheme 2.13) and were taken forward to explore the scope of the reaction.

**Scheme 2.13** Optimal conditions

2.2.3 Reaction Scope and Limitations

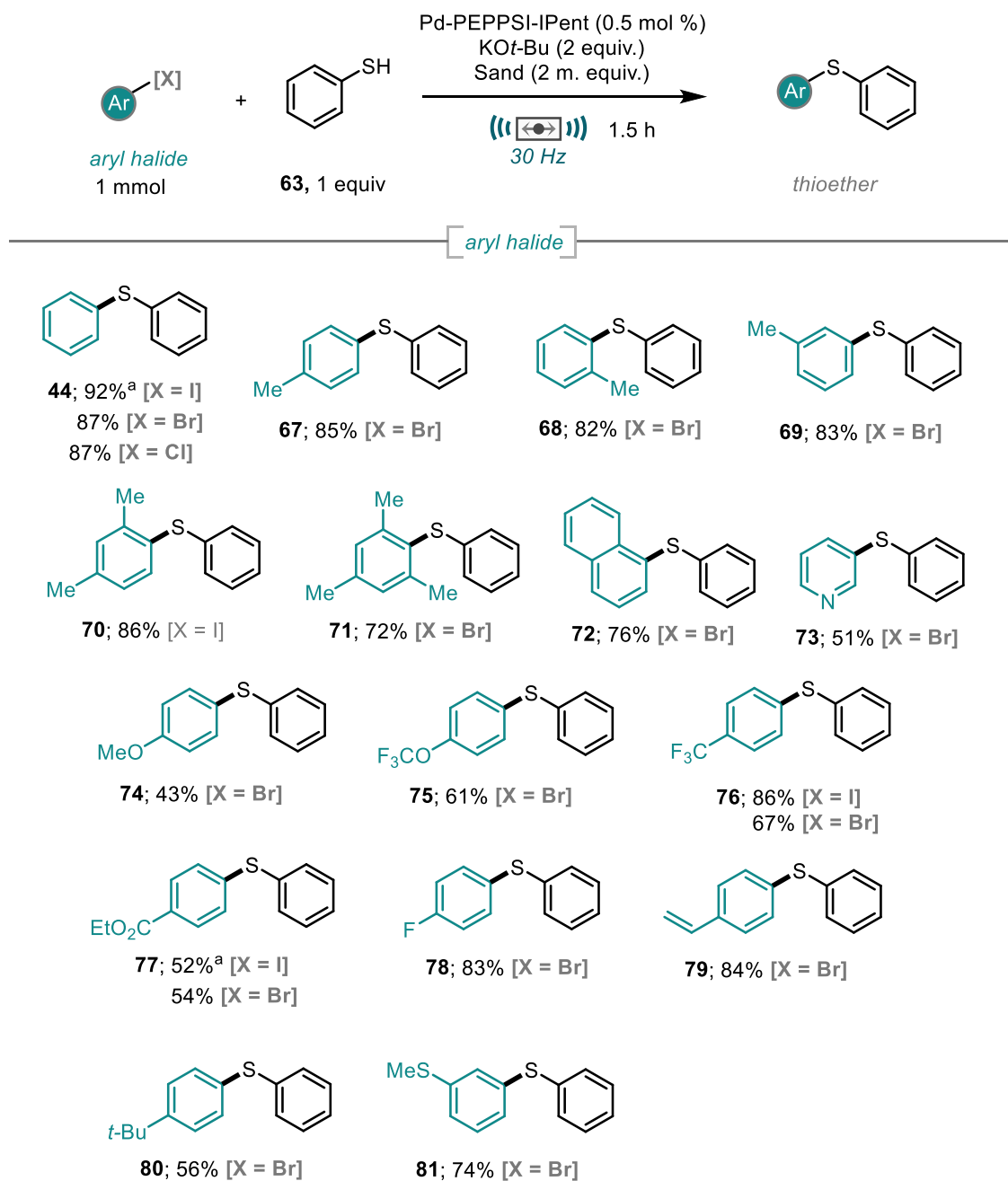
The reaction scope was first explored by application of the optimised conditions to a range of aryl halides (Scheme 2.14). It is worth noting that for all reactions, no precaution was taken to remove air or moisture from reaction vessel or materials. It was quickly discovered that many substrates required greater than the 1.5 hour reaction time. Therefore, reactions were run for 3 hours as standard procedure. The reaction showed excellent tolerance for aryl bromides as well as the significantly more challenging aryl chlorides with both bromobenzene and chlorobenzene coupling effectively with thiophenol to give diphenyl sulfide (**44**) with minimal difference in yield compared to iodobenzene. This increases the potential of the scope considering the increased availability of bromo and chloroarenes.

Functionality was demonstrated at all positions around the aryl ring through the reaction of the different isomers of bromotoluene as well as 2,4-dimethyl bromobenzene; all of which produced excellent yields (82-88%, **67**, **68**, **69**, **70**). Interestingly, 2-bromotoluene showed very little reduction in yield compared to 4-bromotoluene suggesting tolerance for sterics on the aryl halide coupling partner. This steric tolerance was shown further using more demanding substrates such as mesityl bromide and 1-bromonaphthalene (**71** and **72**).

As is often predicted when performing cross-coupling reactions, electron rich aryl halides were less successful in the reaction as shown by the modest yield achieved by attempted coupling of 4-bromoanisole (42%, **74**). This is due to the significantly reduced rate of oxidative addition for Pd-catalysis when inserting into electron rich systems. As expected, aryl halides bearing electron withdrawing functionality generally performed well, providing good to excellent yields in the case of inductively withdrawing groups (-OCF₃, CF₃, **75** and **76**) and moderate yield for mesomerically electron withdrawing groups (**77**). For electron withdrawing aryl halides, there is a possibility that the thioether products could be obtained *via* an S_NAr pathway which would bypass the need for the palladium catalyst. To test this, electron deficient aryl halides (**75**, **76**, and **77**) were also run without any Pd-PEPPSI-IPent present. In all cases, no thioether product was observed suggesting reactivity proceeds only by Pd-catalysed cross coupling.

Interestingly, despite pyridine being a well-known palladium poison,³³ 3-bromopyridine could be coupled in good yield (52%, **73**). This shows that should 3-bromopyridine undergo ligand exchange with 3-chloropyridine already present in the pre-catalyst, activation and subsequent activity of the catalyst still proceeds. Due to the nature of the solid-state reaction and not having any solvent to facilitate ligand exchange, it is unclear if this exchange takes place.

2 - A Robust Pd-PEPPSI catalysed Carbon-Sulfur Coupling by Ball-milling



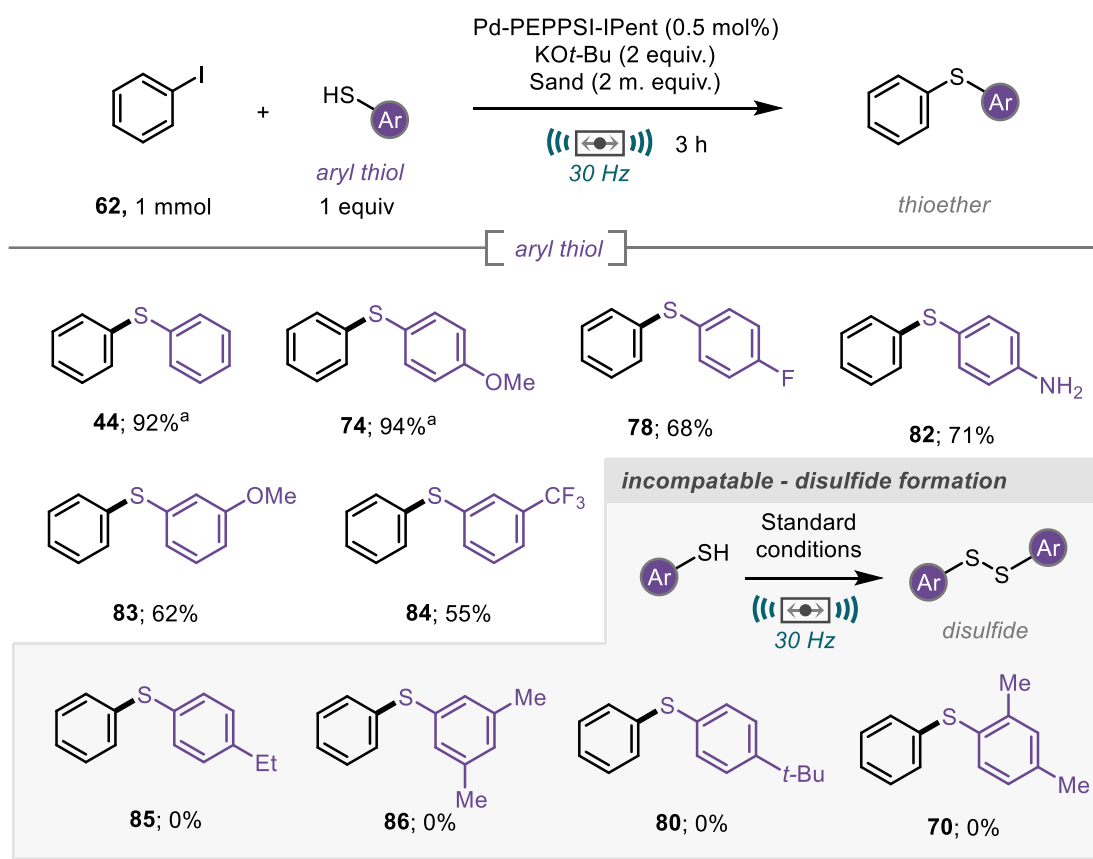
Isolated yields reported. ^a Reaction time: 1.5 h

Scheme 2.14 Aryl halide scope.

The coupling of 4-bromostyrene also occurred in excellent yield (84%, **79**) under the reaction conditions showing no self-Heck reaction. Substrates bearing sites with acidic protons such as free phenols and carboxylic acids were unsuccessful in the reaction. This is due to initial deprotonation at these sites with KO t -Bu. Increasing the equivalents of base could not overcome this issue suggesting that the reaction cannot proceed using the corresponding potassium salts.

Having explored the scope of aryl halide coupling partner, attention turned to exploring the capabilities of the thiol coupling partner.

Initially, a range of aryl thiols were subjected to the reaction conditions (Scheme 2.15). Initial results showed good to excellent conversion to the desired coupled products (55% - 94%). The electron rich 4-methoxythiophenol could be coupled in 94% using a shorter reaction time of 1.5 h, presumably due to its increased nucleophilicity (74%). Free anilines were able to undergo coupling without substantial poisoning of the Pd-catalyst, as shown by reaction using 4-aminothiophenol to give **82** in 71%. This example also showed complete selectivity for C-S coupling over Buchwald-Hartwig coupling.



Isolated yields reported. ^a Reaction time: 1.5 h

Scheme 2.15 Initial aryl thiol scope

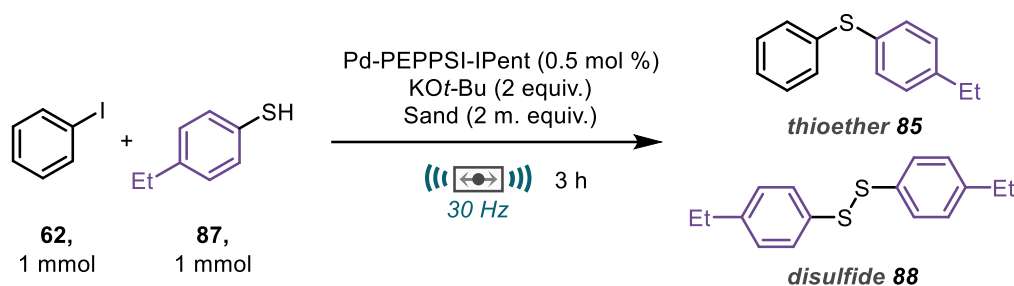
For some examples, no desired thioether product was obtained. Instead, significant quantities of disulfide product were observed (>75% in all cases). Despite being a somewhat unusual pathway considering the absence of any obvious oxidant, this aerobic oxidation of thiols has previously been explored using a planetary mill and by manual grinding.^{97,98} It was thought the addition of a reductant into the reaction could aid in promoting the desired coupling reaction by minimising the amount of disulfide produced

2 - A Robust Pd-PEPPSI catalysed Carbon-Sulfur Coupling by Ball-milling

or by returning any disulfide formed back to the thiol. Previous literature demonstrates the use of zinc metal as a reductant for this purpose.¹²

The reaction chosen to study the effects of a reductant was that of iodobenzene (**62**) and 4-ethylthiophenol (**87**). Under the standard mechanochemical reaction conditions, no thioether product **85** was achieved and 84% of disulfide **88** was observed (Table 2.5, entry 1).

Table 2.5 Minimisation of unwanted disulfide



Entry	Variation from above	Yield 85 (%) ^a	Yield 88 (%) ^{ab}
1	None	0	84
2	Reductant: Zn mesh (2 equiv.)	72	0
3	Reductant: Zn mesh (1.5 equiv.)	7	0
4	Reductant: Zn mesh (2.5 equiv.)	93(89)^c	0
5	Reductant: Zn mesh (3 equiv.)	93	0
6	Reductant: Mn pieces (2 equiv.)	0	0
7	Reductant: Mn powder (2 equiv.)	0	0

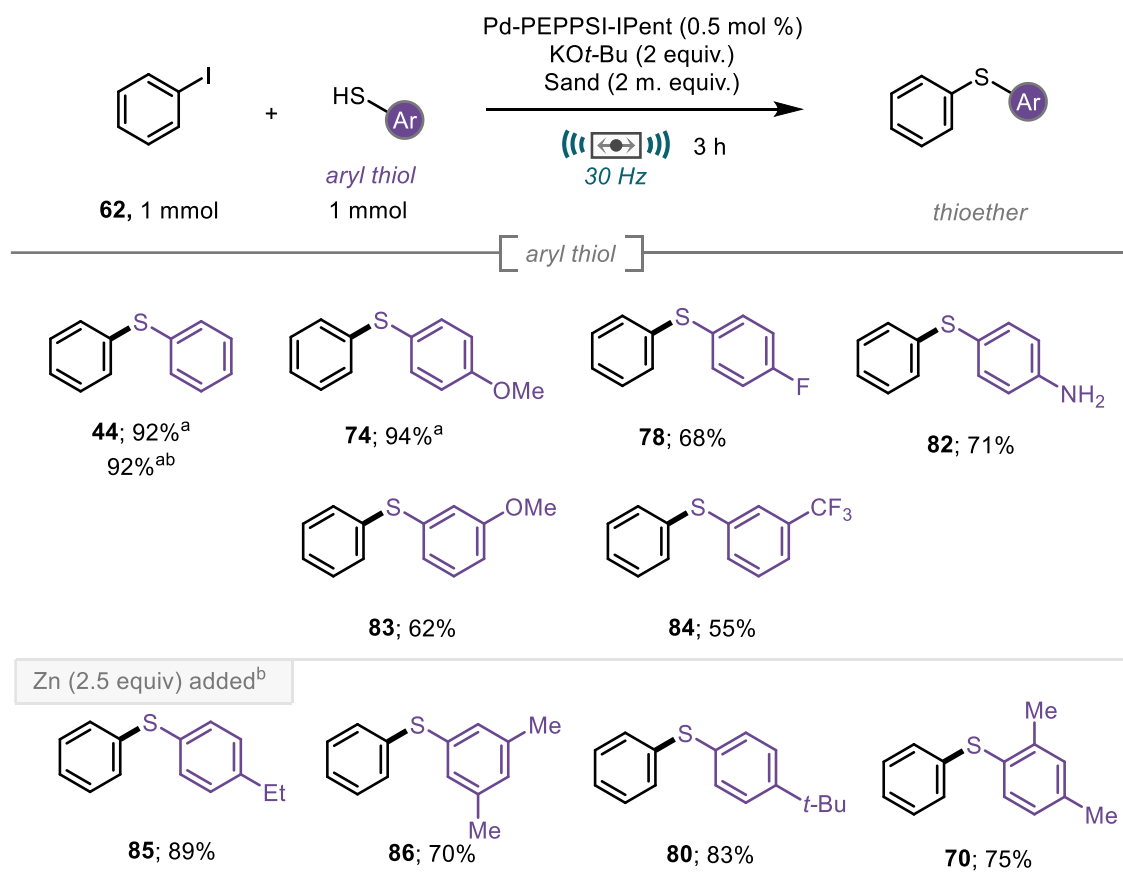
^a Yield determined by ¹H NMR spectroscopy using mesitylene as an internal standard.

^b Yield calculated with respect to product (maximum 0.5 mmol) ^c Isolated yield.

With the addition of 2 equivalents of 'zinc flake (325 mesh)', reactivity was switched to afford the desired thioether **85** as the exclusive product (Table 2.2, entry 2). It is worth noting that the zinc used was not pre-activated or pre-treated in any way (often achieved by use of chemical additives). Having successfully averted any formation of disulfide **88**, a small optimisation was carried out to determine the loading of reductant required to give the best yield. Dropping the loading of zinc to 1.5 equivalents resulted in a large reduction in product yield with only 7% observed (Table 2.5, entry 3). Increasing the zinc loading to 2.5 equivalents resulted in an increase to 89% isolated yield (Table 2.5, entry 4). This was deemed to be the optimal loading after observing no increase in yield using 3 equivalents of zinc (Table 2.5, entry 5). Manganese metal was also investigated as an alternative reductant to zinc with both manganese pieces and powder tested under the reaction conditions. No product (**85**) or disulfide (**88**) was observed in either case (Table

2.5 entries 6-7), showing that manganese has a detrimental effect on the reaction whether it be by interacting with the palladium-coupling cycle or by altering the texture of the mixture and causing inefficient mixing.

With these findings, the substrates that previously gave no product and large amounts of disulfide (**85**, **86**, **80**, **70**) were resubjected to the standard conditions, this time with the addition of zinc allowing for an expanded scope to be demonstrated (Scheme 2.16).



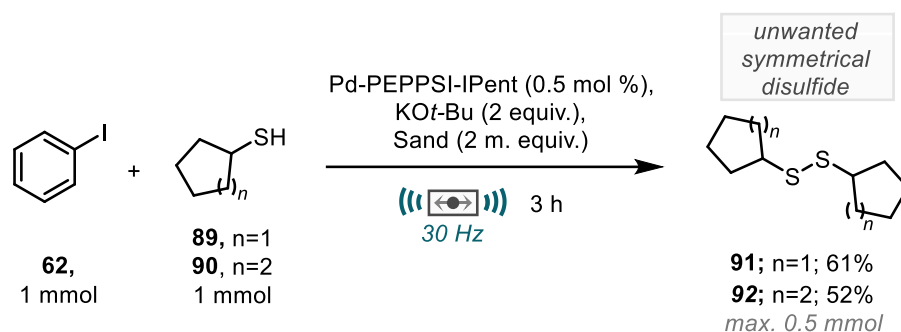
Isolated yields reported. ^a reaction time: 1.5 h ^b standard conditions + Zn flake (325 mesh, 2.5 equiv.)

Scheme 2.16 Expanded aryl thiol scope

A remarkable switch in selectivity to thioether product was achieved for all four previously incompatible examples with good to excellent yields now possible (70-89%, Scheme 2.16). The addition of zinc did not affect the yield of previously successful examples, this was demonstrated by reaction with and without zinc giving identical results for the formation of **44**.

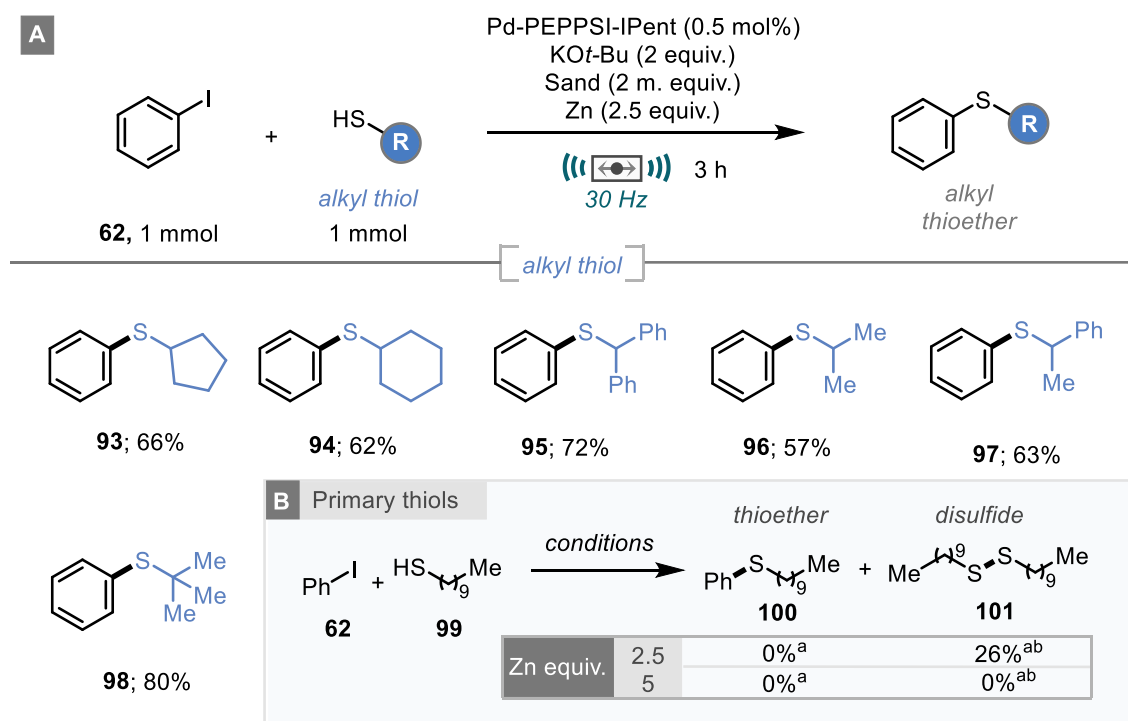
The coupling of alkyl thiols was next to be investigated. This is generally regarded as a more challenging process.^{65,99}

2 - A Robust Pd-PEPPSI catalysed Carbon-Sulfur Coupling by Ball-milling



Scheme 2.17 Initial alkyl thiol coupling attempt

Initial results showed that using the standard conditions identified in Scheme 2.13 resulted in a significant amount of disulfide formation (52-61%, **91** and **92**) when using cyclopentanethiol (**89**) and cyclohexanethiol (**90**) as the thiol coupling partner (Scheme 2.17). This issue could be resolved by using the same approach taken previously with the aryl thiol substrates. With the addition of 2.5 equivalents of zinc into the reaction, a small range of alkyl thiols could be successfully coupled in moderate to excellent yield (57-80%, Scheme 2.18A). The reaction could tolerate secondary and tertiary thiols including a mixture of cyclic and acyclic systems.



Isolated yields reported. ^a Yield determined by ¹H NMR spectroscopy using mesitylene as an internal standard. ^b Yield calculated with respect to product (maximum 0.5 mmol)

Scheme 2.18 Scope of alkyl thiols

Primary alkyl thiols were unsuccessful for mechanochemical coupling (Scheme 2.18B). Attempted coupling of iodobenzene (**62**) with decanethiol (**99**) produced no desired

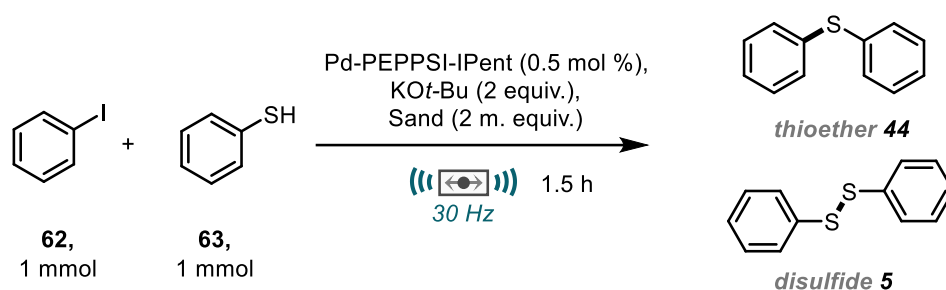
thioether (**100**) under the reaction conditions and instead furnished 26% disulfide (**101**) even with the inclusion of 2.5 equivalents of zinc as a reductant. Increasing zinc loading to 5 equivalents did prevent disulfide formation, however, did not improve the product yield. Therefore, the scope of alkyl thiols is limited to secondary and tertiary thiols.

2.2.4 Exploring Thioether / Disulfide Reactivity

The formation of disulfides from the coupling reaction raises some interesting questions; how does the oxidation occur? At what point in the reaction does this happen? It would be logical to assume that disulfide formation occurs as the preferred pathway when the cross-coupling reaction is slower, i.e., in the case of alkyl thiols and selected aryl thiols.

To explore the disulfide formation, the parent coupling reaction was subjected to multiple control reactions, each time with one reagent omitted from the mixture to assess the role of each component and the effect it has on the selectivity of thioether vs disulfide (Table 2.6).

Table 2.6 Investigation of disulfide formation



Entry	Variation from above	Yield 44 (%) ^a	Yield 5 (%) ^{ab}
1	none	96 (92) ^c	0
2	No Pd-PEPPSI IPent	0	>95
3	No KOtBu	0	>95
4	No Sand	0	>95%
5	No 62	0	>95%

^aYield determined by ¹H NMR spectroscopy using mesitylene as an internal standard.

^bYield calculated with respect to product (maximum 0.5 mmol) ^c Isolated yield.

The findings show that all components are necessary for the desired cross-coupling and without them, expectedly, no coupling product (**44**) is observed. However, it was found that quantitative diphenyl disulfide **5** was observed in every case when any component was removed (Table 2.6, entries 2-5). This shows that there is not a direct interaction between the thiol partner and any other individual reagent that results in disulfide formation. Curiously, this suggest that the thiol starting material is being oxidised by a different mechanism. A possible option is aerobic oxidation, a concept previously discussed by Ranu and co-workers for disulfide synthesis by ball-milling.⁹⁸

2 - A Robust Pd-PEPPSI catalysed Carbon-Sulfur Coupling by Ball-milling

To explore this concept under our conditions, thiophenol was ball-milled by itself for 3 hours in a stainless-steel jar with stainless-steel milling ball under an air atmosphere. From this reaction quantitative diphenyl disulfide was received confirming that the thiol does not require any other reagent for oxidation (Table 2.7, entry 1). To assess the speed of this reaction, lower reaction times were tested using different reactions for each time period. Quantitative conversion from thiophenol to diphenyl disulfide could be achieved after just 0.5 h (Table 2.7, entry 3). This fast reaction helps to explain that why, when no productive cross-coupling occurs, the reaction instead gives disulfide. A shorter reaction time of just 15 minutes still produced a significant amount of disulfide **5** (80%) but also returned a small amount of thiophenol (Table 2.7, entry 4) implying the aerobic oxidation reaction is completed between 15 and 30 minutes. To ensure that the oxidation reaction was not a result of interaction of the thiol with contaminants from previously milled reactions, the protocol used for 0.5 h (Table 2.7, entry 3) was repeated using new milling jars, new milling balls and a new bottle of thiophenol. The outcome from this was consistent with the previous result with quantitative disulfide observed.

Table 2.7 Mechanochemical thiol oxidation

Reaction scheme: Thiophenol (**63**, 1 mmol) $\xrightarrow{((\leftarrow\bullet\rightarrow))) \times \text{h}, 30 \text{ Hz}}$ Diphenyl disulfide (**5**, max. 0.5 mmol)

Entry	Time	Yield 5 (%) ^a
1	3 h	>95%
2	1 h	>95%
3	0.5 h	>95%
4	0.25 h	80% (+20% 63)
5	0.5, variation: + Zn (2.5 equiv.)	0% (100% 63)

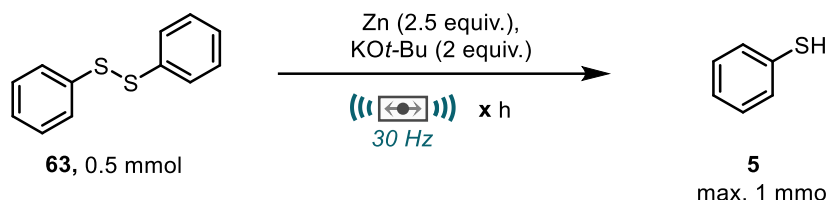
^a Yield determined by ¹H NMR spectroscopy using mesitylene as an internal standard. Yield calculated with respect to product (maximum 0.5 mmol)

The above studies give a plausible route for the formation of disulfides in the mechanochemical coupling reaction.

Next to be investigated was the role that zinc plays in preventing disulfide formation in the outcome of the reaction. To probe this, reduction of disulfide under ball-milling conditions was attempted using only zinc metal with a 3-hour reaction time so as to mirror that of the coupling protocol. From this reaction, disulfide starting material **5** was returned in quantitative amounts. However, it was discovered that in combination with the reaction base, KO^t-Bu, zinc metal could successfully reduce diphenyl disulfide (**5**) to thiophenol

(**63**) giving >95% in 3 hours after a weak acidic quench (Table 2.8, entry 1). To ensure that reduction was not occurring during workup, diphenyl disulfide was subjected to just the workup phase, where no thiol was observed indicating reduction indeed occurs in the mechanochemical reaction.

Table 2.8 Mechanochemical disulfide reduction



Entry	Time	Yield 63 (%) ^a
1	3 h	>95%
2	1 h	>95%
3	0.5 h	82%
4	0.25 h	48%

^aYield determined by ¹H NMR spectroscopy using mesitylene as an internal standard. Yield calculated with respect to product (maximum 1 mmol)

Assessing the time required for reduction showed that complete conversion to thiol was achieved at 1 hour (Table 2.8 entry 2) with lower times showing reduced conversion.

From these results, a rationale can be made for the role of zinc. It is likely that in cases where disulfide formation occurs due to slower coupling, the addition of zinc helps by reducing any unwanted disulfide formed during the reaction as exhibited by the results in table 2.8. It is also possible that zinc prevents disulfide formation in the first instance as no disulfide was observed upon milling thiophenol with zinc (Table 2.7, entry 5). However, this result could also be a result of disulfide formation and fast subsequent reduction back to the thiol. It is also possible that the rate of disulfide formation is enhanced in the absence of all other reagents.

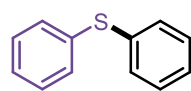
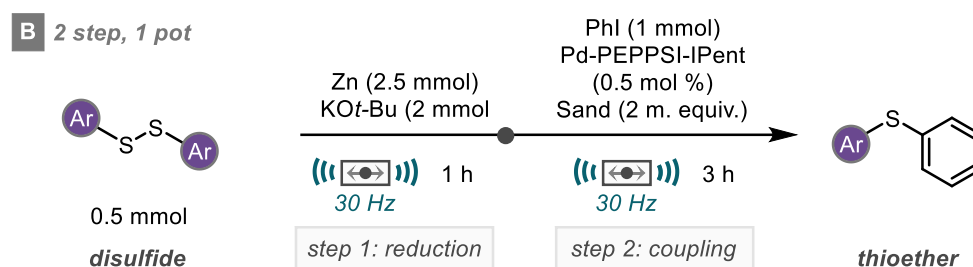
2.2.5 Coupling from Disulfides

Disulfides are typically less hazardous and malodorous than their thiol counterparts. Therefore, coupling from disulfides is beneficial and desirable. Since the careful control of mechanochemical thioether / disulfide reactivity has been established (Section 2.2.4), the coupling of disulfides with aryl halides was a promising avenue to explore. The reaction proposed involved a 2 step, 1 pot methodology including preliminary reduction of a disulfide with zinc and KOt-Bu, followed by Pd-cross coupling with iodobenzene to provide the desired thioether all within one milling jar.

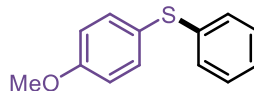
2 - A Robust Pd-PEPPSI catalysed Carbon-Sulfur Coupling by Ball-milling

For the initial reduction step, a reaction time of 1 hour was used to ensure complete reduction. It is likely that the result of this step will not be the corresponding thiol but rather the potassium or zinc thiolate salt. Upon completion of the 1-hour reduction, the jar was opened (in air) and all other reagents needed for mechanochemical cross-coupling (iodobenzene, Pd-PEPPSI-IPent and sand) were added. The milling vessel was then closed and placed back on the mill and subjected to 3 hours of milling as per the standard conditions for coupling.

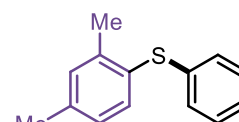
Using this methodology, application to a small range of disulfides was demonstrated to give the desired thioether products (Scheme 2.19A) in either comparable or slightly reduced yields (70-80%) when compared to the standard thiol coupling reaction.



44; 80%

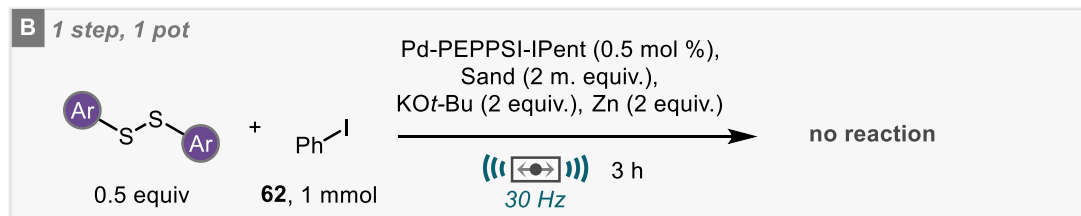


74; 71%



70; 70%

Isolated yields reported



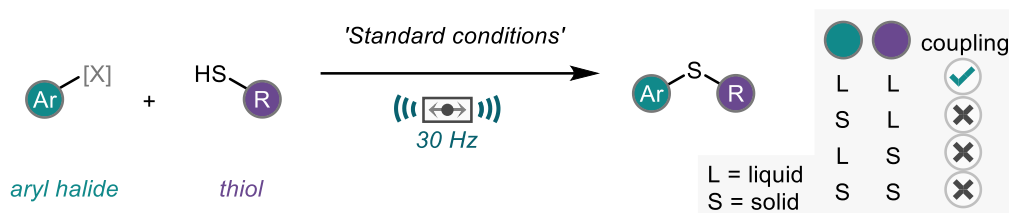
Scheme 2.19 Coupling from disulfide starting materials

The reaction was also attempted using a 1 step, 1 pot process whereby all reagents were placed in the jar at the start of the reaction and milled for 3 hours. No thioether product was observed when carrying out the reaction this way, conveying the need for separate reduction and coupling steps for successful reactivity (Scheme 2.19B).

2.2.6 Phase Transition Induced Reactivity

The physical state of reactants can play a crucial role in the outcome of mechanochemical conditions due to mixing properties and how materials interact with

each other. During investigations into the mechanochemical thiol coupling reaction, it was discovered that coupling was only achieved when both starting materials were liquid and if either the aryl halide or thiol was solid, no reaction was possible and instead starting materials returned (Scheme 2.20).



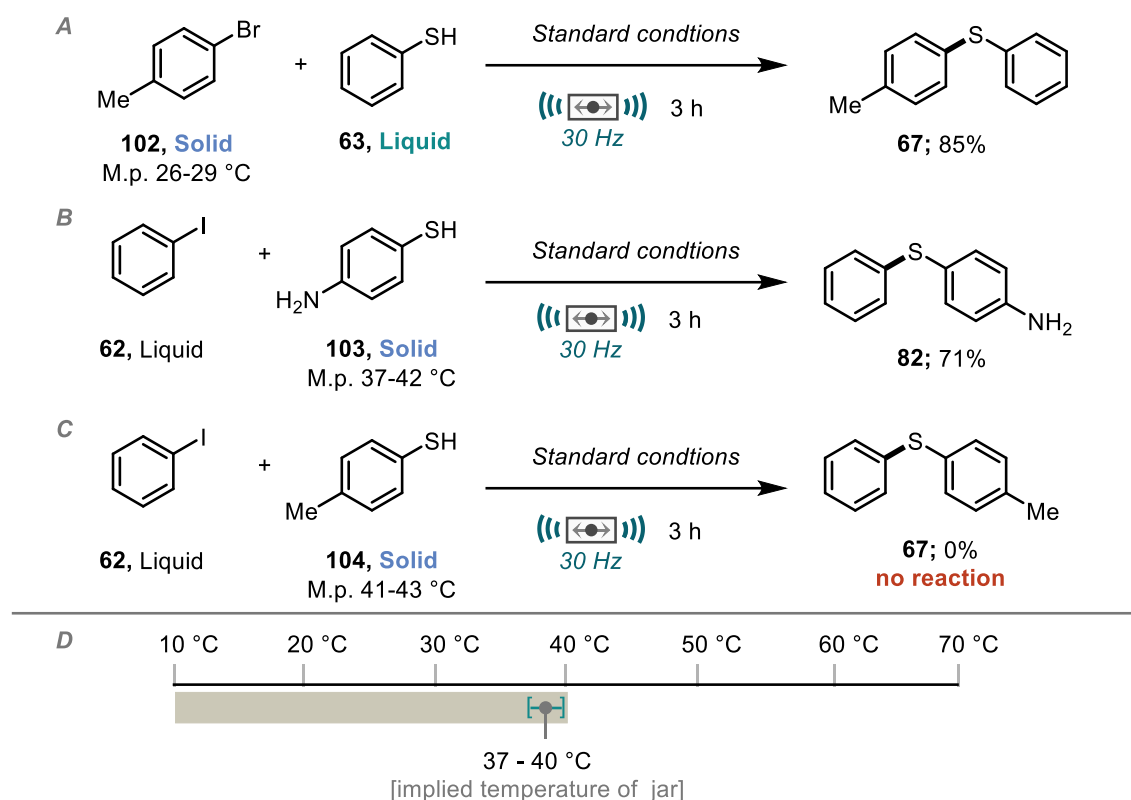
Scheme 2.20 Effect of physical state on reactivity.

Interestingly, there were a couple of notable exceptions to this. The reaction of thiophenol (**63**) with the solid 4-methylbromobenzene (**102**), which has a low melting point of 26-29 °C proceeded to give the thioether product (**67**) in excellent yield as was typical with the standard liquid-liquid coupling (Scheme 2.21A). This was also shown to be the case when coupling iodobenzene with the solid 4-aminothiophenol (**103**), which has an increased melting point of 37-42 °C (Scheme 2.21B). However, when the coupling of iodobenzene with 4-methylthiophenol (**104**) was attempted, no reaction was observed (Scheme 2.21C). This substrate with a slightly higher melting point (41-43 °C) proved to be the cut off for reaction with many other higher melting point substrates (>45 °C) failing in the reaction.

Mechanochemical reactions produce heat as a by-product from every collision inside the milling jar since not all kinetic energy from the ball is imparted into the reaction materials at the point of impact. Depending on the nature of the reaction and milling parameters, the jar can often be warm / hot to the touch just after reaction completion. This heat generated by this process can be described as the 'latent heat' of the reaction. In this case, it is proposed that solids with melting points just above room temperature are brought into a 'melt-phase' and are thereby able to react as if they were liquid and undergo coupling readily. Since the cut off point for possible coupling is observed with 4-methylthiophenol (**104**) it is implied that the temperature inside the jar as a result of 'latent heat' is around 40 °C (Scheme 2.21D). This phase-transition induced reactivity is an interesting prospect and may arise because of improved mixing or even due to changes in the crystal lattice structures. At the time of discovery, Ito and co-workers explored this concept for the selective mono-arylation of aryl bromides by Pd-catalysed Suzuki-Miyaura coupling.¹⁰⁰

2 - A Robust Pd-PEPPSI catalysed Carbon-Sulfur Coupling by Ball-milling

Standard conditions = Pd-PEPPSI IPent (0.5 mol %), KO^t-Bu (2 equiv.), Sand (2 m. equiv.)



Scheme 2.21 Reactivity of solid substrates

To test the 'phase-transition induced reactivity' hypothesis for the thiol coupling reaction, a 'simple insulation' approach was taken whereby the milling jar was insulated with cotton wool and aluminium foil to retain the latent heat of milling within the reaction milling vessel (Figure 2.2). The results of this showed a profound change in reactivity. For 4-methylthiophenol (**104**), a substrate that previously gave no desired product; 'simple insulation' of the jar gave 84% yield suggesting that the elevated temperature in the milling jar allowed the substrate to melt and therefore undergo coupling (Scheme 2.22).

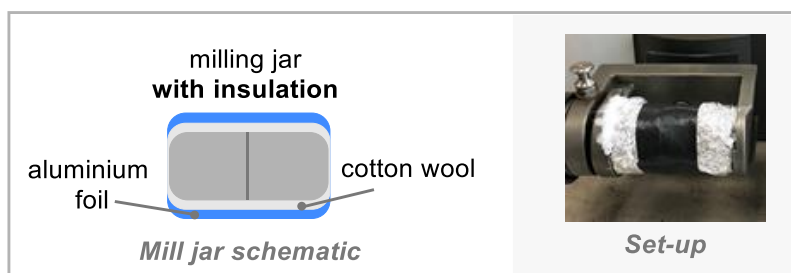
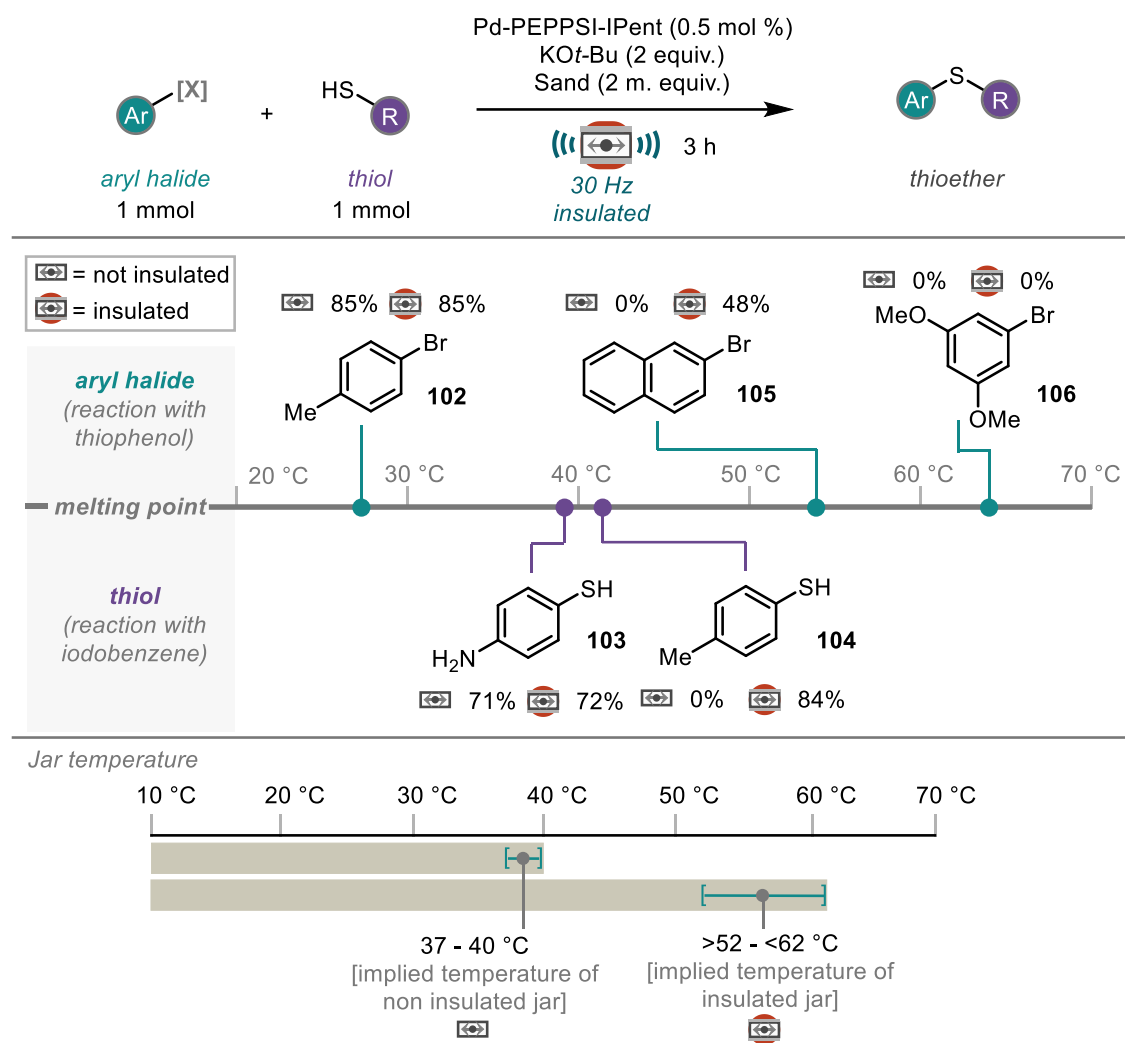


Figure 2.2 Insulated milling jar

Investigation of this 'on-off' reactivity by insulating the milling jar was extended to solid substrates with melting points greater than $>40\text{ }^{\circ}\text{C}$ (Scheme 2.22). 2-Bromonaphthalene (**105**), which melts at a higher temperature (between $52\text{-}55\text{ }^{\circ}\text{C}$), previously afforded no cross-coupled product in the non-insulated jar. However, by 'simple insulation' of the jar, 48% desired product was achieved, again demonstrating the profound change in reactivity. This methodology was extended further to attempt the coupling of 1-bromo-3,5-dimethoxybromobenzene (**106**), which melts at $62\text{-}66\text{ }^{\circ}\text{C}$. No coupling product was observed from this reaction even with insulation. This could suggest that the substrate is not melting even with the 'latent heat' produced. Taken together, this allows us to indirectly determine the temperature inside the jar using the differing conditions. Without insulation, as previously discussed, the implied temperature is $37\text{-}40\text{ }^{\circ}\text{C}$ whereas with insulation, the implied temperature is in the region of $52\text{-}62\text{ }^{\circ}\text{C}$. It is worth noting for low yielding liquid-liquid coupling (e.g. 4-methoxybromobenzene with thiophenol, 43%), no improvement was seen with insulation. To explore this with increased accuracy would require thermally controlled equipment, which has previously been developed by Užarević and co-workers amongst others.¹⁰¹

2 - A Robust Pd-PEPPSI catalysed Carbon-Sulfur Coupling by Ball-milling



Scheme 2.22 Phase transition induced reactivity

2.2.7 Comparison to Solution

The final aspect to be explored was a comparison of the mechanochemical thiol coupling reaction to the reaction in analogous solution conditions. The reaction to be tested was that of 4-fluorobromobenzene with thiophenol. For these reactions, the conditions were carried out using 1,4-dioxane as solvent due to it being the most common solvent used for this type of coupling.^{65,66} The conditions remained the same as those used under mechanochemical conditions with the exception that sand was omitted from the mixture. For reaction under air, no precaution was taken to remove air / moisture from the reaction and solvent was taken from a non-dried bottle. For reaction under N₂, solvent was taken from a dried, sealed bottle.

The yield under air, as determined by ^{19}F , reached a maximum of 4% after 1 hour which did not increase over a 24-hour period. The reaction under an inert atmosphere, gave a maximum of 5% which was observed after 2 hours with no further increase. The mechanochemical reaction provided 83% of thioether after 2 hours, clearly demonstrating the advantages and unique characteristics offered by ball-milling for this coupling reaction. The reaction not working in solution-phase, even under an inert atmosphere again demonstrates the necessity for catalyst pre-activation.

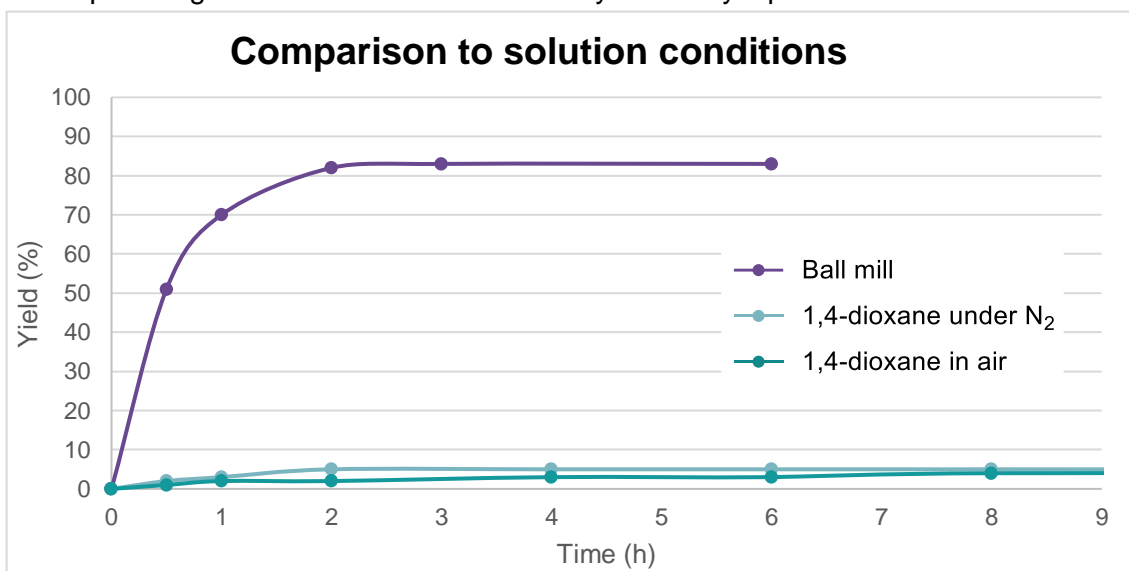


Figure 2.3 Comparison to solution conditions

For reported solution examples, pre-activation of the catalyst is often required.⁶⁶ For the mechanochemical reaction, no pre-activation step is required for successful coupling. It is important to consider the form of the base in the reaction, with differing basicity and nucleophilicity possible in the absence of solvent. The results shown in Figure 2.3 also hint that the Pd-catalyst may be more stable under ball-milling conditions. This could be because of increased turnover frequency or by the regeneration of catalytically active species from inactive / off-cycle species.

2.3 Conclusions and Future Outlook

In conclusion, the first mechanochemical metal-catalysed carbon-sulfur coupling reaction has been demonstrated expanding the growing area of organometallic coupling reactions enabled by ball-milling. The developed protocol requires no exclusion of air / moisture and does not need a catalyst pre-activation step. The protocol was explored for a broad range to give good to excellent yields when using different aryl halides and various aryl and alkyl thiols. For the latter, the key to successful coupling was the inclusion of zinc metal to minimise the production of disulfide.

The interconversion between thiols and disulfides was discussed with results showing that thiols will undergo oxidation to the corresponding disulfide when milled alone. Disulfides could be reduced with the use of zinc metal and KO t -Bu allowing for careful control of the sulfinated compounds in the reactions. This control could then be exemplified by the successful and desirable 2 step, 1 pot coupling from disulfide starting materials to afford the thioether products in a process that circumvents the use of malodorous thiols.

The concept of phase-transition induced reactivity was displayed for substrates where the melting point was just above room temperature. By the use of 'simple insulation', the latent heat within the jar could be retained to raise the temperature enough to melt substrates and hence undergo the coupling reaction. Given that a thermocouple-controlled system, would allow for more accurate temperature control and measurement,¹⁰¹ the importance of the physical state for ball-milling reaction as well as the melt-phase theory is an under-developed area. However, development is increasing as demonstrated by recent work by Ito and co-workers exploring *in situ* crystallisation to promote reactivity in a mechanochemical setting.¹⁰⁰

Having identified conditions and demonstrated tolerance for reaction on a 1 mmol scale, the protocol would have the potential to be scaled up. This first option would be to increase the jar size to accommodate the increase in scale. It is important to consider the parameters present when scaling up like this, for example the jar size and ball size. Another option would be to adapt the process for continuous procession by twin-screw extrusion (TSE). TSE is a recent development and has thus far not been explored in great depth for the scale-up coupling reactions with only limited examples reported.¹⁰²

2.4 Bibliography

- 1 S. D. Roughley and A. M. Jordan, *J. Med. Chem.*, 2011, **54**, 3451–3479.
- 2 G. Dougherty and P. D. Hammond, *J. Am. Chem. Soc.*, 1935, **57**, 117–118.
- 3 J. R. Campbell, *J. Org. Chem.*, 1962, **27**, 2207–2209.
- 4 R. Adams, W. Reifschneider and D. Nair, *Croat. Chem. Acta*, 1957, **29**, 277–285.
- 5 J. R. Campbell, *J. Org. Chem.*, 1964, **29**, 1830–1833.
- 6 P. A. Forero-Cortés and A. M. Haydl, *Org. Process Res. Dev.*, 2019, **23**, 1478–1483.
- 7 A. Correa, M. Carril and C. Bolm, *Angew. Chem.*, 2008, **120**, 2922–2925.
- 8 Y.-C. Wong, T. T. Jayanth and C.-H. Cheng, *Org. Lett.*, 2006, **8**, 5613–5616.
- 9 V. P. Reddy, K. Swapna, A. V. Kumar and K. R. Rao, *J. Org. Chem.*, 2009, **74**, 3189–3191.
- 10 Y. Zhang, K. C. Ngeow and J. Y. Ying, *Org. Lett.*, 2007, **9**, 3495–3498.
- 11 M. Carril, R. SanMartin, E. Domínguez and I. Tellitu, *Chem. – Eur. J.*, 2007, **13**, 5100–5105.
- 12 K. D. Jones, D. J. Power, D. Bierer, K. M. Gericke and S. G. Stewart, *Org. Lett.*, 2018, **20**, 208–211.
- 13 A. Ghorbani-Choghamarani, Z. Moradi and G. Azadi, *J. Sulfur Chem.*, 2018, **39**, 237–251.
- 14 Norio. Miyaura and Akira. Suzuki, *Chem. Rev.*, 1995, **95**, 2457–2483.
- 15 C. C. C. Johansson Seechurn, M. O. Kitching, T. J. Colacot and V. Snieckus, *Angew. Chem. Int. Ed.*, 2012, **51**, 5062–5085.
- 16 M. Kosugi, T. Shimizu and T. Migita, *Chem. Lett.*, 1978, **7**, 13–14.
- 17 M. Murata and S. L. Buchwald, *Tetrahedron*, 2004, **60**, 7397–7403.
- 18 J.-Y. Lee and P. H. Lee, *J. Org. Chem.*, 2008, **73**, 7413–7416.
- 19 Z. Qiao, J. Wei and X. Jiang, *Org. Lett.*, 2014, **16**, 1212–1215.
- 20 J. Mao, T. Jia, G. Frensch and P. J. Walsh, *Org. Lett.*, 2014, **16**, 5304–5307.
- 21 G. Teverovskiy, D. S. Surry and S. L. Buchwald, *Angew. Chem. Int. Ed.*, 2011, **50**, 7312–7314.
- 22 E. Alvaro and J. F. Hartwig, *J. Am. Chem. Soc.*, 2009, **131**, 7858–7868.
- 23 M. A. Fernández-Rodríguez and J. F. Hartwig, *J. Org. Chem.*, 2009, **74**, 1663–1672.
- 24 T. Scattolin, E. Senol, G. Yin, Q. Guo and F. Schoenebeck, *Angew. Chem. Int. Ed.*, 2018, **57**, 12425–12429.
- 25 M. A. Fernández-Rodríguez, Q. Shen and J. F. Hartwig, *Chem. – Eur. J.*, 2006, **12**, 7782–7796.
- 26 J. Louie and J. F. Hartwig, *J. Am. Chem. Soc.*, 1995, **117**, 11598–11599.
- 27 M. A. Fernández-Rodríguez, Q. Shen and J. F. Hartwig, *Chem. – Eur. J.*, 2006, **12**, 7782–7796.
- 28 C. H. Bartholomew, P. K. Agrawal and J. R. Katzer, in *Advances in Catalysis*, eds. D. D. Eley, H. Pines and P. B. Weisz, Academic Press, 1982, vol. 31, pp. 135–242.
- 29 T. Itoh and T. Mase, *Org. Lett.*, 2004, **6**, 4587–4590.
- 30 G.-Y. Gao, A. J. Colvin, Y. Chen and X. P. Zhang, *J. Org. Chem.*, 2004, **69**, 8886–8892.
- 31 J. Xu, R. Y. Liu, C. S. Yeung and S. L. Buchwald, *ACS Catal.*, 2019, **9**, 6461–6466.
- 32 P. B. Dias, M. E. M. de Piedade and J. A. M. Simões, *Coord. Chem. Rev.*, 1994, **135–136**, 737–807.
- 33 M. G. Organ, G. A. Chass, D.-C. Fang, A. C. Hopkinson and C. Valente, *Synthesis*, 2008, 2776–2797.
- 34 E. A. B. Kantchev, C. J. O'Brien and M. G. Organ, *Angew. Chem. Int. Ed.*, 2007, **46**, 2768–2813.

- 35 L. R. Titcomb, S. Caddick, F. G. N. Cloke, D. J. Wilson and D. McKerrecher, *Chem. Commun.*, 2001, 1388–1389.
- 36 C. W. K. Gstöttmayr, V. P. W. Böhm, E. Herdtweck, M. Grosche and W. A. Herrmann, *Angew. Chem. Int. Ed.*, 2002, **41**, 1363–1365.
- 37 O'Brien Christopher J., Kantchev Eric Assen B., Valente Cory, Hadei Niloufar, Chass Gregory A., Lough Alan, Hopkinson Alan C., and Organ Michael G., *Chem. – Eur. J.*, 2006, **12**, 4743–4748.
- 38 N. Marion, O. Navarro, J. Mei, E. D. Stevens, N. M. Scott and S. P. Nolan, *J. Am. Chem. Soc.*, 2006, **128**, 4101–4111.
- 39 W. A. Herrmann, J. Fischer, K. Öfele and G. R. J. Artus, *J. Organomet. Chem.*, 1997, **530**, 259–262.
- 40 V. César, S. Bellemin-Laponnaz and L. H. Gade, *Organometallics*, 2002, **21**, 5204–5208.
- 41 A. C. Frisch, A. Zapf, O. Briel, B. Kayser, N. Shaikh and M. Beller, *J. Mol. Catal. Chem.*, 2004, **214**, 231–239.
- 42 A. C. Frisch, F. Rataboul, A. Zapf and M. Beller, *J. Organomet. Chem.*, 2003, **687**, 403–409.
- 43 S. K. Schneider, W. A. Herrmann and E. Herdtweck, *J. Mol. Catal. Chem.*, 2006, **245**, 248–254.
- 44 N. M. Scott and S. P. Nolan, *Eur. J. Inorg. Chem.*, 2005, **2005**, 1815–1828.
- 45 H. Lebel, M. K. Janes, A. B. Charette and S. P. Nolan, *J. Am. Chem. Soc.*, 2004, **126**, 5046–5047.
- 46 O. Navarro, R. A. Kelly and S. P. Nolan, *J. Am. Chem. Soc.*, 2003, **125**, 16194–16195.
- 47 O. Navarro, N. Marion, N. M. Scott, J. González, D. Amoroso, A. Bell and S. P. Nolan, *Tetrahedron*, 2005, **61**, 9716–9722.
- 48 O. Navarro, H. Kaur, P. Mahjoor and S. P. Nolan, *J. Org. Chem.*, 2004, **69**, 3173–3180.
- 49 O. Navarro, N. Marion, J. Mei and S. P. Nolan, *Chem. – Eur. J.*, 2006, **12**, 5142–5148.
- 50 J. A. Love, J. P. Morgan, T. M. Trnka and R. H. Grubbs, *Angew. Chem. Int. Ed.*, 2002, **41**, 4035–4037.
- 51 I. Larrosa, C. Somoza, A. Banquy and S. M. Goldup, *Org. Lett.*, 2011, **13**, 146–149.
- 52 P. Lei, G. Meng, Y. Ling, J. An and M. Szostak, *J. Org. Chem.*, 2017, **82**, 6638–6646.
- 53 M. G. Organ, M. Abdel-Hadi, S. Avola, N. Hadei, J. Nasielski, C. J. O'Brien and C. Valente, *Chem. – Eur. J.*, 2007, **13**, 150–157.
- 54 M. G. Organ, M. Abdel-Hadi, S. Avola, I. Dubovyk, N. Hadei, E. A. B. Kantchev, C. J. O'Brien, M. Sayah and C. Valente, *Chem. – Eur. J.*, 2008, **14**, 2443–2452.
- 55 C. Valente, M. E. Belowich, N. Hadei and M. G. Organ, *Eur. J. Org. Chem.*, 2010, 4343–4354.
- 56 S. Shi, P. Lei and M. Szostak, *Organometallics*, 2017, **36**, 3784–3789.
- 57 J.-X. Xu, F. Zhao and X.-F. Wu, *Org. Biomol. Chem.*, 2020, **18**, 9796–9799.
- 58 M. G. Organ, S. Çalimsiz, M. Sayah, K. H. Hoi and A. J. Lough, *Angew. Chem. Int. Ed.*, 2009, **48**, 2383–2387.
- 59 A. Khadra, S. Mayer and M. G. Organ, *Chem. – Eur. J.*, 2017, **23**, 3206–3212.
- 60 M. K. Kolli, N. M. Shaik, G. Chandrasekar, S. Chidara and R. B. Korupolu, *New J. Chem.*, 2017, **41**, 8187–8195.
- 61 S. Sharif, R. P. Rucker, N. Chandrasoma, D. Mitchell, M. J. Rodriguez, R. D. J. Froese and M. G. Organ, *Angew. Chem. Int. Ed.*, 2015, **54**, 9507–9511.
- 62 M. Dowlut, D. Mallik and M. G. Organ, *Chem. – Eur. J.*, 2010, **16**, 4279–4283.
- 63 M. G. Organ, S. Avola, I. Dubovyk, N. Hadei, E. A. B. Kantchev, C. J. O'Brien and C. Valente, *Chem. – Eur. J.*, 2006, **12**, 4749–4755.
- 64 C.-F. Fu, Y.-H. Liu, S.-M. Peng and S.-T. Liu, *Tetrahedron*, 2010, **66**, 2119–2122.

- 65 M. Sayah and M. G. Organ, *Chem. – Eur. J.*, 2011, **17**, 11719–11722.
66 M. Sayah and M. G. Organ, *Chem. – Eur. J.*, 2013, **19**, 16196–16199.
67 K. Kubota and H. Ito, *Trends Chem.*, 2020, **2**, 1066–1081.
68 A. Porcheddu, E. Colacino, L. De Luca and F. Delogu, *ACS Catal.*, 2020, **10**, 8344–8394.
69 S. F. Nielsen, D. Peters and O. Axelsson, *Synth. Commun.*, 2000, **30**, 3501–3509.
70 L. M. Klingensmith and N. E. Leadbeater, *Tetrahedron Lett.*, 2003, **44**, 765–768.
71 F. Schneider and B. Ondruschka, *ChemSusChem*, 2008, **1**, 622–625.
72 F. Schneider, T. Szuppa, A. Stolle, B. Ondruschka and H. Hopf, *Green Chem.*, 2009, **11**, 1894–1899.
73 F. Schneider, A. Stolle, B. Ondruschka and H. Hopf, *Org. Process Res. Dev.*, 2009, **13**, 44–48.
74 F. Bernhardt, R. Trotzki, T. Szuppa, A. Stolle and B. Ondruschka, *Beilstein J. Org. Chem.*, 2010, **6**, 7.
75 G. Cravotto, D. Garella, S. Tagliapietra, A. Stolle, S. Schüßler, S. E. S. Leonhardt and B. Ondruschka, *New J. Chem.*, 2012, **36**, 1304–1307.
76 Z.-J. Jiang, Z.-H. Li, J.-B. Yu and W.-K. Su, *J. Org. Chem.*, 2016, **81**, 10049–10055.
77 T. Seo, T. Ishiyama, K. Kubota and H. Ito, *Chem. Sci.*, 2019, **10**, 8202–8210.
78 T. Seo, K. Kubota and H. Ito, *J. Am. Chem. Soc.*, 2020, **142**, 9884–9889.
79 Q. Cao, J. L. Howard, E. Wheatley and D. L. Browne, *Angew. Chem. Int. Ed.*, 2018, **57**, 11339–11343.
80 E. Tullberg, D. Peters and T. Frejd, *J. Organomet. Chem.*, 2004, **689**, 3778–3781.
81 E. Tullberg, F. Schacher, D. Peters and T. Frejd, *Synthesis*, 2006, **2006**, 1183–1189.
82 X. Zhu, J. Liu, T. Chen and W. Su, *Appl. Organomet. Chem.*, 2012, **26**, 145–147.
83 V. Declerck, E. Colacino, X. Bantreil, J. Martinez and F. Lamaty, *Chem. Commun.*, 2012, **48**, 11778–11780.
84 J. Yu, Z. Hong, X. Yang, Y. Jiang, Z. Jiang and W. Su, *Beilstein J. Org. Chem.*, 2018, **14**, 786–795.
85 J. Yu, H. Shou, W. Yu, H. Chen and W. Su, *Adv. Synth. Catal.*, 2019, **361**, 5133–5139.
86 D. A. Fulmer, W. C. Shearouse, S. T. Medonza and J. Mack, *Green Chem.*, 2009, **11**, 1821–1825.
87 R. Thorwirth, A. Stolle and B. Ondruschka, *Green Chem.*, 2010, **12**, 985–991.
88 Y. Gao, C. Feng, T. Seo, K. Kubota and H. Ito, *Chem. Sci.*, 2022, **13**, 430–438
89 K. Kubota, R. Takahashi and H. Ito, *Chem. Sci.*, 2019, **10**, 5837–5842.
90 R. Dorel, C. P. Grugel and A. M. Haydl, *Angew. Chem. Int. Ed.*, 2019, **58**, 17118–17129.
91 P. Ruiz-Castillo and S. L. Buchwald, *Chem. Rev.*, 2016, **116**, 12564–12649.
92 Q.-L. Shao, Z.-J. Jiang and W.-K. Su, *Tetrahedron Lett.*, 2018, **59**, 2277–2280.
93 K. Kubota, T. Seo, K. Koide, Y. Hasegawa and H. Ito, *Nat. Commun.*, 2019, **10**, 111.
94 K. Kubota, T. Endo, M. Uesugi, Y. Hayashi and H. Ito, *ChemSusChem*, DOI:10.1002/cssc.202102132.
95 Q. Cao, W. I. Nicholson, A. C. Jones and D. L. Browne, *Org. Biomol. Chem.*, 2019, **17**, 1722–1726.
96 K. Kubota, R. Takahashi, M. Uesugi and H. Ito, *ACS Sustain. Chem. Eng.*, 2020, **8**, 16577–16582.
97 A. Parmar and H. Kumar, *Synth. Commun.*, 2007, **37**, 2301–2308.
98 T. Chatterjee and B. C. Ranu, *RSC Adv.*, 2013, **3**, 10680–10686.
99 J. F. Hartwig, *Inorg. Chem.*, 2007, **46**, 1936–1947.
100 T. Seo, K. Kubota and H. Ito, *J. Am. Chem. Soc.*, 2020, **142**, 9884–9889.

2 - A Robust Pd-PEPPSI catalysed Carbon-Sulfur Coupling by Ball-milling

- 101 N. Cindro, M. Tireli, B. Karadeniz, T. Mrla and K. Užarević, *ACS Sustain. Chem. Eng.*, 2019, **7**, 16301–16309.
- 102 B. M. Sharma, R. S. Atapalkar and A. A. Kulkarni, *Green Chem.*, 2019, **21**, 5639–5646.

3 Cross-electrophile Coupling of Alkyl and Aryl Halides under Ball-milling Conditions

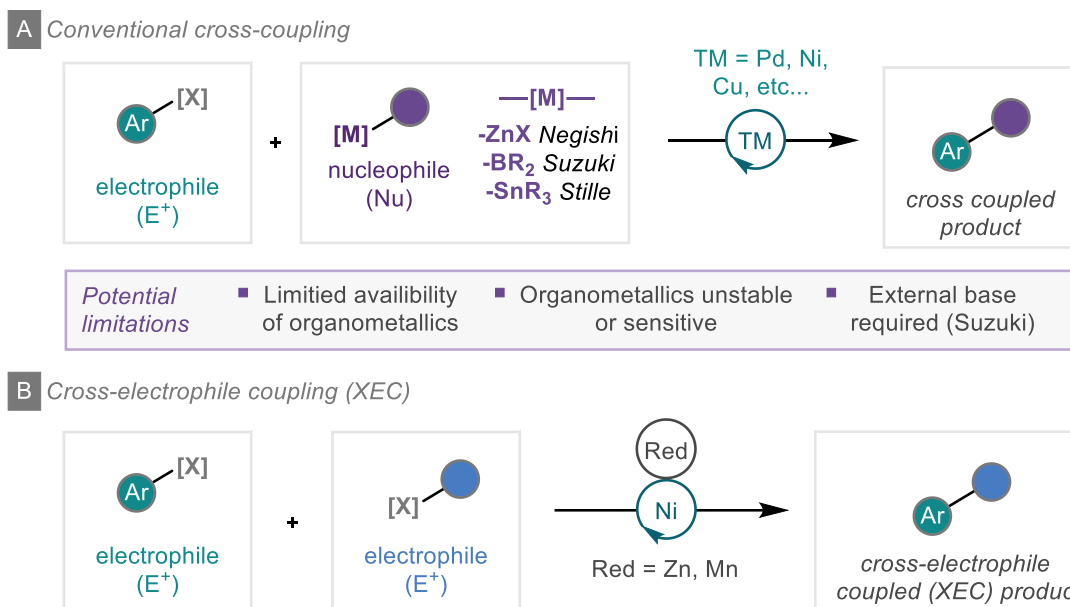
3.1 Introduction	69
3.1.1 Ni-catalysed Cross-electrophile Coupling	69
3.1.2 Selectivity and Mechanistic Implications	72
3.1.3 Typical Zinc Activation in Solution	75
3.1.4 Mechanical Activation of Zinc	76
3.1.5 Overview, Project Aims and Objectives	79
3.2 Results and Discussion	81
3.2.1 Initial Findings	81
3.2.2 Optimisation	81
3.2.3 Aryl (Pseudo)Halide Scope	90
3.2.4 Initial Alkyl Halide Scope and Re-optimisation for Alkyl Bromides	92
3.2.5 Alkyl Halide Scope	95
3.2.6 Toleration of Different Reductant Forms	97
3.2.7 Mechanistic Insight	98
3.2.8 Scale-up	101
3.3 Conclusions and Future Work	103
3.4 Comparisons to Other Ball-milling Cross-electrophile Coupling Reactions	104
3.5 Bibliography	105

3.1 Introduction

Mechanochemical techniques have been shown to exhibit unique advantages for many transition-metal catalysed cross-coupling reactions.¹⁻³ These include reduced reaction times, reduced temperatures, reduced catalyst loadings, and negating the need for an inert atmosphere or glovebox manipulation.⁴⁻⁸ Thus far, its use for reductive coupling has not been explored.

3.1.1 Ni-catalysed Cross-electrophile Coupling

Owing to its powerful C-C bond forming capabilities, transition metal catalysed cross-coupling has become an important tool for synthetic organic chemists across a number of disciplines.⁹ The Nobel prize winning Pd-catalysed reactions developed by Richard Heck,¹⁰⁻¹⁶ Ei-ichi Negishi,^{17,18} and Akira Suzuki^{19,20} revolutionised cross-coupling and improved upon classical metal-mediated approaches.²¹⁻²³ These methods make use of an electrophilic coupling partner (typically an organohalide) and a carbon nucleophile, which is commonly introduced as an organometallic reagent, e.g., the coupling of organoboron species in the Suzuki coupling, or organozinc intermediates for the Negishi coupling (Scheme 3.1A). Herein lies the potential limitation of conventional transition metal catalysed cross-coupling. The commercial availability of organometallic reagents is typically several factors lower than the materials they are derived from. The stability of organometallic reagents also varies significantly and can often be highly sensitive to air or moisture, meaning they are normally synthesised just prior to, or at the point of use. Taking the Negishi coupling as an example, the organozinc reagent required for transmetalation is commonly prepared from an electrophilic alkyl halide. To avoid this step and the preparation of potentially limiting organometallic reagents, the ability to couple directly from the alkyl halide would be highly beneficial. Cross-electrophile coupling has emerged as an elegant solution to this with much of the initial discovery being reported by Weix and co-workers, focussing on the nickel-catalysed coupling of two electrophilic components such as an aryl halide with an alkyl halide in the presence of a metal reductant (Scheme 3.1B).²⁴⁻²⁶ The choice of reductant is of great importance. The common choice for reductive coupling is zinc or manganese metal due to their moderate reduction potentials (-0.76 V and -1.16 V, respectively).



Scheme 3.1 A) Conventional transition-metal catalysed cross-coupling. B) Cross-electrophile coupling

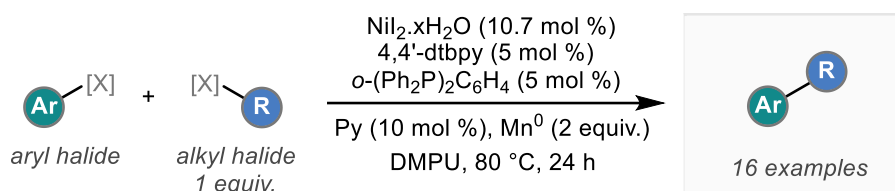
The initial report by Weix and co-workers in 2010 describes the first example of a nickel-catalysed reductive coupling of aryl (sp^2) halides with alkyl (sp^3) halides (Scheme 3.2A).²⁴ In this study, a small range of organohalides are coupled using a nickel bipyridyl type catalytic system with additional phosphine ligands, pyridine as an additive and manganese as the metal reductant. The authors give evidence against the formation of any organomanganese intermediates that could undergo transmetalation. Firstly, it is understood that organomanganese reagents are typically difficult to synthesis from alkyl halides.²⁷ To support this, the reaction of manganese and 1-iodooctane showed very little consumption of alkyl iodide after 24 hours at 80° C and full return of starting material at 60° C. When considering that coupling reactions with 1-iodooctane are typically complete within this 24-hour period, it is unlikely that organomanganese intermediates are being formed. To further support this claim, the use of a non-metallic reductant (TDAE, 1,1,2,2-tetrakis(dimethylamino)ethylene) still allowed for the formation of 57% coupled product. Concurrently to this discovery, Gosmini and co-workers developed a cobalt-catalysed protocol for the alkylation of electronically activated haloarenes using manganese as the reductant (Scheme 3.2B).²⁸

Building upon this seminal work on nickel catalysed reductive coupling, Weix and co-workers adapted their previous protocol to greatly expand the scope to include heteroaryl bromides, a small range of aryl chlorides, and to allow for a much greater range of alkyl bromides to be coupled (Scheme 3.2C).²⁵ The reductant used in this adapted

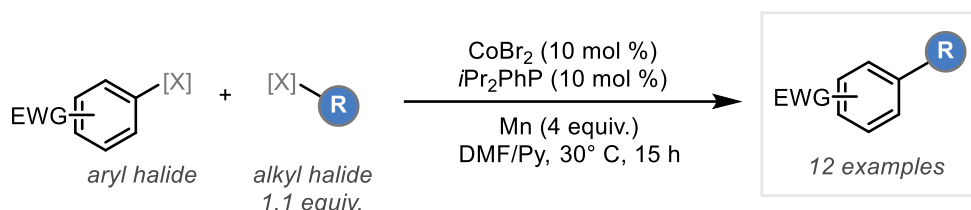
3 - Cross-electrophile Coupling of Alkyl and Aryl Halides under Ball-milling Conditions

methodology is zinc and key to enhanced reactivity of alkyl bromides is the inclusion of sodium iodide as an additive. Whilst the role of the iodide salt is somewhat unclear, a few different possibilities exist in that the iodide salt may aid in the initial reduction of the nickel catalyst, encourage the formation of more reactive nickel species, expedite beneficial ligand exchange reactions, and/or form a small amount of the corresponding alkyl iodide *in situ* and hence enhance reactivity.

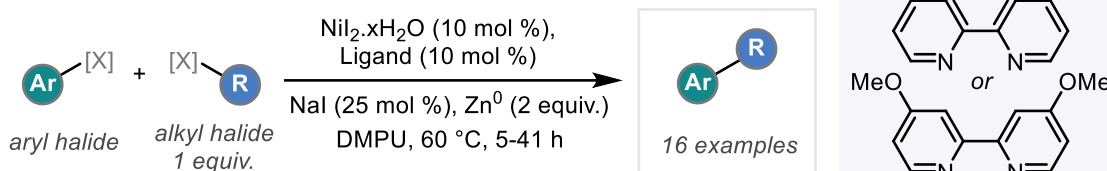
A Ni-catalysed aryl / alkyl halide reductive coupling Weix - 2010



B Co-catalysed reductive coupling of electron poor aryl bromides Gosmini - 2010



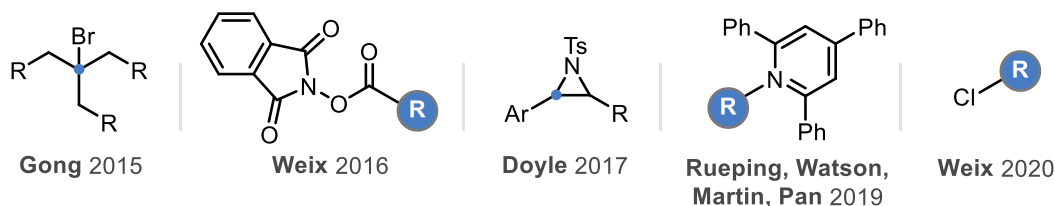
C Improved Ni-catalysed reductive coupling Weix - 2012



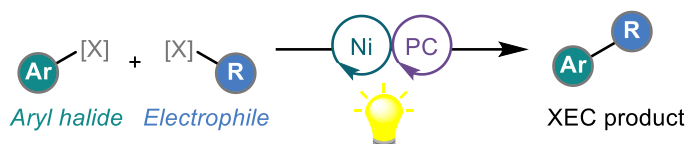
Scheme 3.2 Pioneering development of transition-metal catalysed cross-electrophile coupling

Following this initial exploration, extensive work has been carried out using nickel catalysis in a bid to enable coupling of different and more challenging electrophiles, particularly with respect to the alkyl (sp^3) partner.²⁹⁻⁴⁵ Selected examples of protocols that have been developed are the coupling of challenging alkyl halides (tertiary alkyl bromides and primary alkyl chlorides),^{46,47} enantioselective ring-opening coupling of aziridines,⁴⁸ decarboxylative reductive coupling of phthalimide redox active esters,⁴⁹ and reductive coupling from highly stable alkyipyridinium salts (Scheme 3.3A).⁵⁰⁻⁵³

A Alkyl electrophiles used in cross-electrophile coupling Selected examples



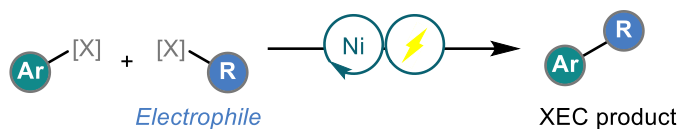
B Photoredox dual catalysis cross-electrophile coupling



Selected electrophiles

alkyl halides Macmillan, Lei - 2016
Katritzky salts Molander - 2019
aziridines Doyle - 2020
NHPI esters Molander - 2021

C Electrochemical cross-electrophile coupling



Selected electrophiles

alkyl halides Hansen - 2017
NHPI esters Bio - 2018
Loren - 2019

Scheme 3.3 Advancements in cross-electrophile coupling

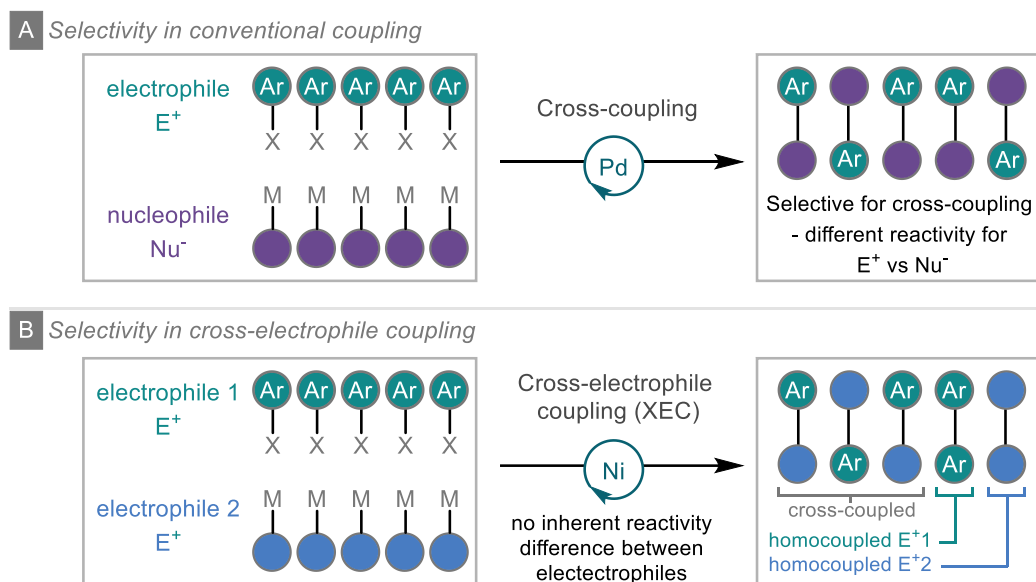
To minimise the metallic waste generated from the use of stoichiometric metal reductants, photoredox methods have been developed (Scheme 3.3B). Initial nickel-iridium dual catalytic systems were described for the cross-electrophile coupling of aryl and alkyl halides in 2016 within separate reports by MacMillan and Lei.^{54,55} The process for advancement for photocatalytic / nickel reductive coupling follows a similar trend to that observed under standard methods, with much of the work increasing the scope of the reaction and exploring different electrophiles.⁵⁶⁻⁶² The focus of which being on the same functionalities as before, such as ring opening of aziridines or epoxides,^{63,64} decarboxylative coupling of *N*-hydroxyphthalimide esters,⁶⁵ and coupling from Katritzky salts.⁶⁶ In addition to photoredox methods, cross-electrophile coupling has also been achieved by the use of electrochemical set-ups (Scheme 3.3C).⁶⁷⁻⁷²

3.1.2 Selectivity and Mechanistic Implications

Cross-electrophile coupling processes negates the use of organometallic reagents, instead relying on two different electrophile coupling partners. This creates a complex challenge with respect to selectivity. Under conventional cross-coupling manifolds (Negishi, Suzuki, etc.), the inherent reactivity difference between the electrophilic haloarene component and the carbon-nucleophilic organometallic intermediate ensures that excellent selectivity for cross-coupling is achieved (Scheme 3.4A). By removing the

3 - Cross-electrophile Coupling of Alkyl and Aryl Halides under Ball-milling Conditions

nucleophilic aspect from the reaction, the inherent reactivity difference is also removed. Therefore, controlling the selectivity when reacting two electrophiles with potentially similar reactivity presents an interesting challenge. Whilst cross-coupling is still possible, homocoupling pathways of each electrophilic partner become increasingly preferable when compared to conventional coupling manifolds (Scheme 3.4B).



Scheme 3.4 *Selectivity challenges of cross-electrophile coupling*

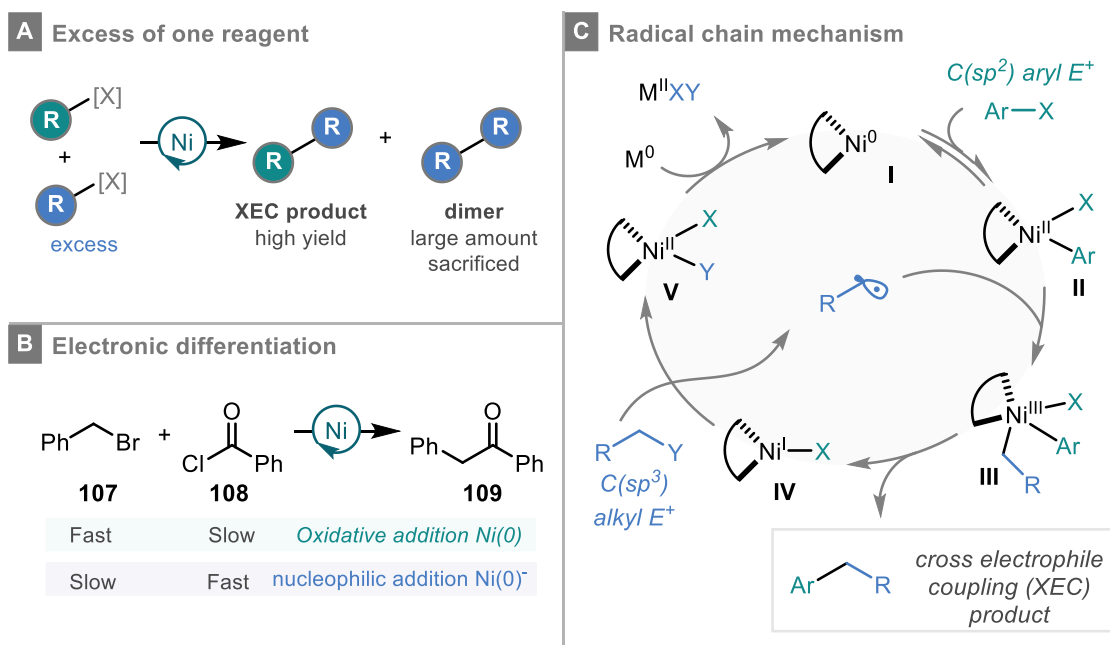
To understand the selectivity and mechanistic aspects of cross-electrophile coupling, several arguments have been put forward to control and rationalise the outcome of selectivity.

The first concept for increasing selectivity towards a cross-coupled product is to have one of the electrophilic starting materials in excess. This approach has been demonstrated in cobalt and nickel-catalysed cross-Ullman couplings, as well as for a Nickel-catalysed cross-Wurtz coupling.^{73–76} In these cases, whereby the starting materials are structurally similar and therefore little differentiation can be made between them, the use of a large excess of one of the halide coupling partners results in higher yields of cross-coupling at the cost of larger quantities of unwanted homocoupled dimer products (Scheme 3.5A).

Other methods to control the selectivity involve the differentiation of the two starting materials, either through steric or electronic factors. For electronic control, the reaction relies on the difference in preference of low-valent nickel species for different electrophiles so can be seen in the reductive acylation reaction of benzyl bromide (**107**)

and benzoyl chloride (**108**). Mechanistic studies show that benzyl bromide undergoes fast oxidative addition to Ni(0)bpy, and then after reduction with a metal, the nucleophilic attack of the resulting anionic Ni(0) complex to the acid chloride is fastest enabling good selectivity (Scheme 3.5B).⁷⁷ For cases where substrates have a much closer reactivity than that of acid chlorides vs. alkyl halides, steric factors can become influential in determining selectivity.⁷⁸

Weix's pioneering work introduces a more generalised strategy whereby substrates are differentiated based on homolytic vs. heterolytic reactivity. Extensive mechanistic studies on their original reductive coupling reaction of aryl halides with alkyl halides reveal that the rate of oxidative addition is much faster for the aryl halide component than the alkyl halide, whilst the radical formation shows the reverse trend with alkyl halides more readily undergoing single electron reduction.⁷⁹ The combination of these two factors gives rise to excellent selectivity via a proposed radical chain mechanism, for which the radical addition step has previously been shown to result in cross-coupling from pre-made oxidative addition Ni(II) complexes.^{80,81} This radical chain mechanism is further solidified from radical clock studies and subsequent mechanistic studies on similar systems.^{82–85}



Scheme 3.5 Methods for controlling selectivity (A and B) and the accepted radical chain mechanism (C)

From these important studies, the radical chain mechanism (Scheme 3.5C) has become the commonly accepted mechanism for this type of coupling. It proceeds by selective

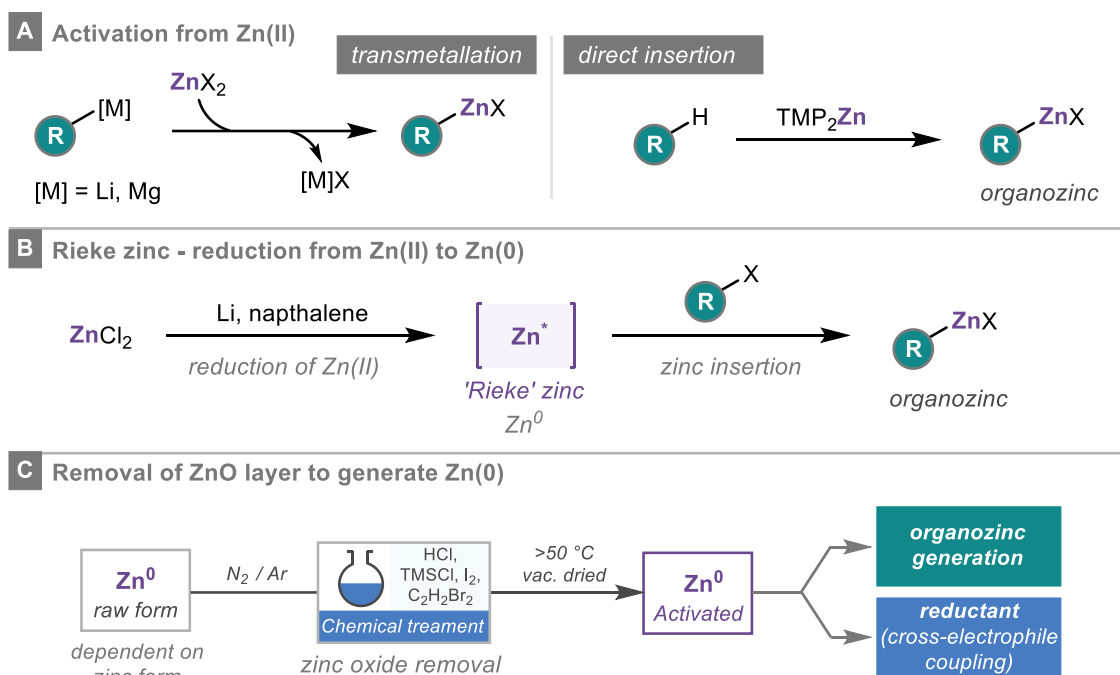
oxidative addition of an aryl halide to the active Ni(0) catalyst **I**. Reaction of the resulting Ni(II) species **II** with an alkyl radical gives rise to a diorganic Ni(III) complex **III**. Reductive elimination of the cross-coupled product generates a highly reactive Ni(I) species **IV** that reacts with the alkyl halide to give a Ni(II) dihalide species **V**, along with the regenerated alkyl radical. Finally, the Ni(II) complex can be reduced by the metal reductant (zinc or manganese) to turn over the catalytic cycle and regenerate the active Ni(0) intermediate **I**.

3.1.3 Typical Zinc Activation in Solution

One of the crucial features of cross-electrophile coupling reactions is the inclusion of a reductant to turn over the catalytic cycle and often to activate the pre-catalytic species. The reductant is typically a zero-valent metal. Zinc(0) metal is a common choice and has been employed for a wide range of reductive coupling reactions. It also finds a use across many other important reactions in organic synthesis including the Clemmenson reduction,⁸⁶ Reformatsky reaction,⁸⁷ Simmons-Smith reaction,⁸⁸ and Negishi cross-coupling.¹⁷

Regardless of its role in the reaction i.e., as a reductant or to generate organozinc intermediates, zinc must be activated immediately prior to use. Several options are available for this activation. Firstly, for organozinc generation, zinc(II) sources can be used for the metalation of C-H bonds either by transmetalation with organolithium/magnesium species,⁸⁹⁻⁹¹ or by direct insertion using zinc-amide bases (Scheme 3.6A).⁹²⁻⁹⁶ Alternatively insertion of zinc(0) into organohalides is possible and is classically achieved by the formation of 'rieke' zinc from the reduction of ZnCl₂ using alkali metals and naphthalene, followed by subsequent oxidative addition to an organohalide (Scheme 3.6B).⁹⁷⁻¹⁰²

More recently, methods have been developed to directly activate zinc metal by the removal of the zinc oxide surface layer by chemical reaction or entrainment. Typical processes for this use chemical additives such as HCl, iodine, 1,2-dibromoethane or trimethylchlorosilane (TMSCl) to generate the activated zinc (Scheme 3.6C). This approach, starting with zinc metal is the commonly used approach for nickel-catalysed cross-electrophile coupling. However, methods derived from zinc metal generally require inert / glovebox conditions and are highly dependent on the physical form of metal used.

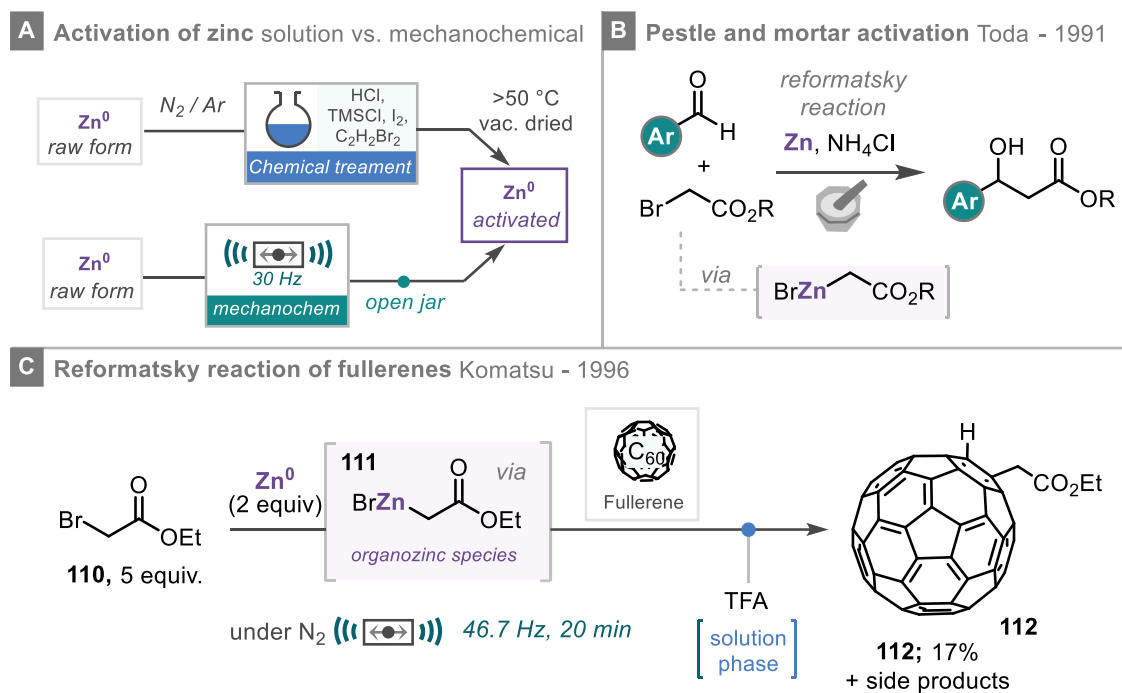


Scheme 3.6 Activation methods for zinc

3.1.4 Mechanical Activation of Zinc

As discussed, solution methods for the activation of zinc can exhibit capricious tendencies, requires inert atmospheres and/or chemical additives, and must be used immediately. As discussed briefly in Chapter 1 of this thesis, mechanochemistry has emerged as a useful tool for the activation of zero-valent metals. This concept of mechanical activation is highly applicable for the activation of zinc metal. In this simple approach, the 'raw-form' of the metal (as is commercially available) is activated by ball-milling (Scheme 3.7A). Since there is no requirement for any special treatment (such as chemical additives), the activation process can take place *in situ* during a mechanochemical reaction. This methodology therefore presents opportunity for more consistent zinc activation. Also, due to the fine metal powder received upon milling, there is very little dependency on the initial form of zinc used.

3 - Cross-electrophile Coupling of Alkyl and Aryl Halides under Ball-milling Conditions



Scheme 3.7 Early examples of mechanochemical activation of zinc for Reformatsky reactions

A preliminary report in 1991 by Toda and co-workers disclosed the use of a pestle and mortar for the mechanochemical activation of zinc. By manual grinding of a carbonyl derivative with an alkyl halide and zinc powder (5 equiv.), the authors demonstrated this concept to a set of Reformatsky additions and Barbier-type reaction systems (Scheme 3.7B). Despite this, the use of manual grinding can lead to reproducibility issues, and no further utility was reported using this method of often inconsistent mechanical activation.¹⁰³ Following this, translation to ball-milling apparatus was reported by Komatsu and co-workers for the Reformatsky-type addition of bromoacetates to [60]fullerene via the generation and subsequent reaction of organozinc intermediates (Scheme 3.7C). In this protocol, a vibrating ball-mill operating at 2800 cycles per minute (46.7 Hz) was employed. Ethyl bromoacetate (**110**), zinc dust, and [60] fullerene were all loaded into a milling capsule along with a stainless-steel milling ball. This reaction set-up is all carried out in a nitrogen bag. Following ‘agitation’ using a vibrating mill for 20 minutes, the mixture is quenched with TFA and 1,2-dichlorobenzene to produce the alkylated product **112** in 17% yield.

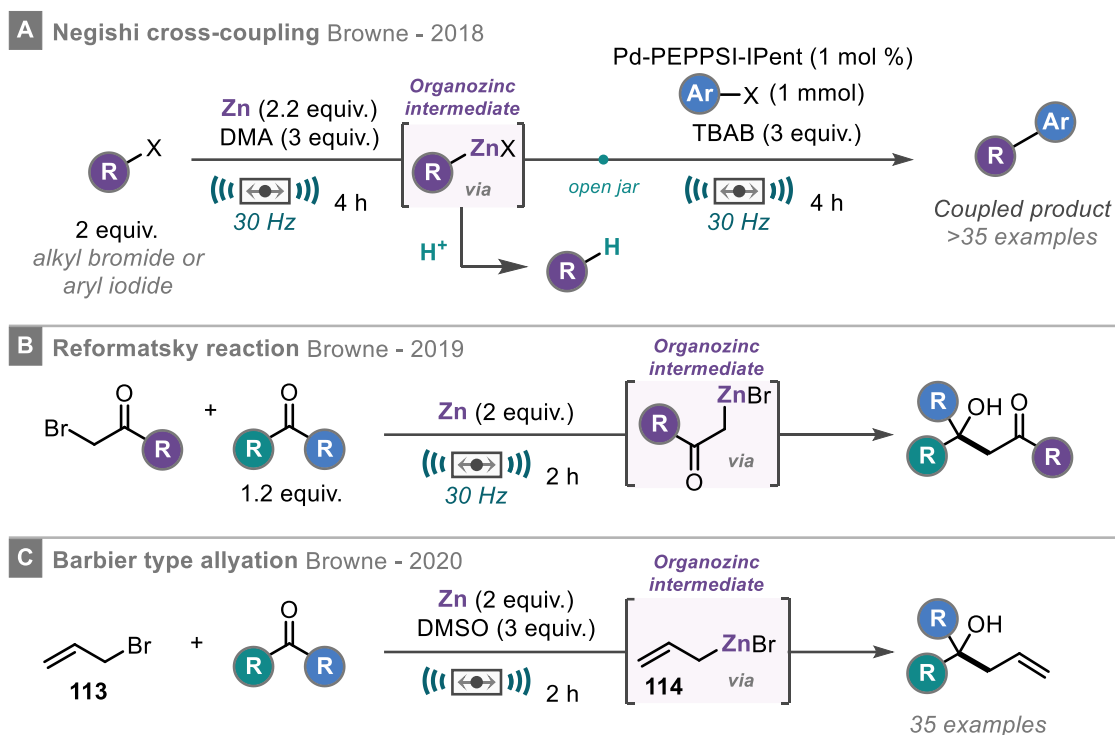
Browne and co-workers have continued to explore the activation of zinc by way of ball-milling. To this end, a simple procedure was developed for the preparation and subsequent use of organozinc intermediates in a Pd-catalysed Negishi Cross-coupling (Scheme 3.8A).¹⁰⁴ In this work, the synthesis of a sp^2 and sp^3 organozinc intermediates

is disclosed by simply milling the organohalide with zinc metal and *N,N*-dimethylacetamide for 4 hours. The yield of organozinc formed was monitored by acidic quench and quantification of the dehalogenated / hydrolysed product. The results showed excellent organozinc generation regardless of zinc form used. For the completion of the Negishi cross-coupling, the jar could be opened (in air) after the initial milling period and all other coupling reagents added to the jar. The Pd-PEPPSI-IPent catalysed Negishi cross-coupling could then be run for a further 4 hours demonstrating a (bulk) solvent-free approach to organozinc generation and subsequent utilisation. Furthermore, for this protocol, no caution is taken to remove any air or moisture from the system.

Building upon this discovery, Browne and co-workers reported other examples of useful C-C bond forming reactions that make use of this facile method for organozinc formation through the development of a Reformatsky addition to aldehydes and ketones (Scheme 3.8B) and a Barbier-type allylation reaction to form homoallylic alcohols (Scheme 3.8C).^{105,106}

For the mechanochemical Reformatsky reaction, the key step is again the formation of the organozinc intermediate, which can also be represented as a zinc enolate, by the insertion of zinc into an α -haloester. In this work, the initial organozinc formation and following interception of a carbonyl derivative all takes place within 2 hours of milling which is a notably shorter reaction time than previously observed with Negishi coupling. This is in part due to the higher susceptibility of α -halo esters to form organometallic reagents. A single, unoptimised example of this reactivity has previously been reported for use in a planetary mill by König and co-workers.¹⁰⁷

3 - Cross-electrophile Coupling of Alkyl and Aryl Halides under Ball-milling Conditions



Scheme 3.8 Mechanochemical activation for C-C bond forming reactions

In a similar fashion, Browne and co-workers harness this simple method for the Barbier-type allylation of ketones, aldehydes, and imines. After successful mechanical activation of zinc, the allyl organozinc reagent is formed and subsequently used for the synthesis of a library of homoallyl alcohols. In this case, DMSO is used as the LAG instead of DMA, which since the role of DMA has previously been discussed to stabilise organozinc materials, suggests that DMSO (a much less hazardous and environmentally benign alternative) can also act in this way. Again, the reaction time is shortened in comparison to the Negishi reaction due to the ease of zinc insertion into allyl bromide.

Alongside its use in generating organozinc generation, mechanochemically activated zinc has also been shown to be capable of reducing unwanted disulfide side-products in a mechanochemical Pd-catalysed C-S coupling reaction (Results shown in Chapter 2 of this thesis).¹⁰⁸

3.1.5 Overview, Project Aims and Objectives

Ball-milling has emerged as a useful tool in the activation of zero-valent metals and has shown applications to organozinc formation. Ni-catalysed cross-electrophile coupling has undergone rapid development since its breakthrough in 2010, however has not yet been explored under ball-milling conditions. Key to successful catalytic turnover for cross-electrophile coupling is the inclusion of a reductant, which is often zinc. Using

conventional solution methods, the zinc metal must be activated immediately prior to use and using strictly inert conditions. The aim of this project is to explore whether mechanochemical activation of zinc could be used as an alternative method allowing the cross-electrophile coupling reaction to occur within one reaction vessel under ambient conditions and assess if this organometallic reaction displays similar unique benefits as previously observed for transition metal-coupling by ball-milling.

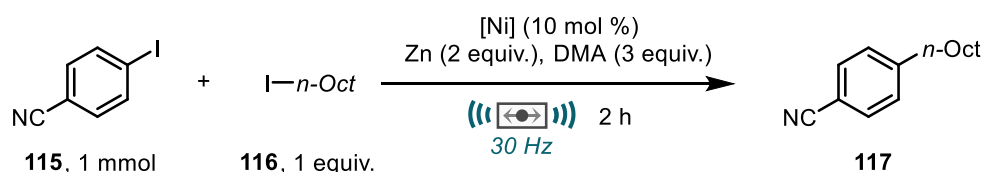
3.2 Results and Discussion

Initial work on this project was carried out as a collaborative study with Yerbol Sagatov, (MPhil / PhD student) and Tom Linford Wood, who was an MRes placement student working under the supervision of Dr William Nicholson (PhD student in the group at the time). Their contributions are clearly indicated throughout the optimisation section.

3.2.1 Initial Findings

Studies commenced by evaluating the reaction of 4-iodobenzonitrile (**115**) and 1-iodooctane (**116**) as the two electrophile coupling partners (Table 3.1). The reaction was to be carried out on a 1 mmol scale using a 15 mL stainless steel milling jar and a 3 g stainless steel milling ball. Initial screening focussed on the use of common air-stable nickel(II) pre-catalysts. 2 equivalents of zinc (granular) was used as the reductant and 3 equivalents DMA was used as a liquid additive due to its established capability of stabilising activated zinc under mechanochemical conditions.¹⁰⁴ Promisingly, reactivity was observed with NiCl₂(PCy₃)₂ furnishing 17% of desired cross-electrophile coupled product **117** (Table 3.1, entry 1). This was improved to 50% with the use of NiCl₂(PPh₃)₂ (Table 3.1, entry 2). The use of bidentate phosphine ligands provided moderate but slightly diminished yields from that observed with NiCl₂(PPh₃)₂ (Table 3.1 entries 3-4).

Table 3.1 Initial results obtained by Yerbol Sagatov and Tom-Linford Wood.



Entry	[Ni] catalyst	Yield 117 (%) ^a
1	NiCl ₂ (PCy ₃) ₂	17
2	NiCl ₂ (PPh ₃) ₂	50 (47) ^b
3	NiCl ₂ (dppe)	43
4	NiCl ₂ (dppp)	42

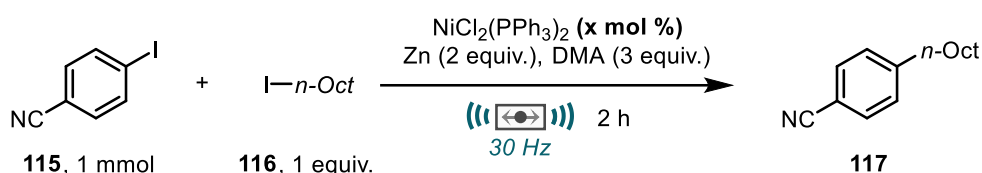
^a Yield determined by ¹H NMR spectroscopy using mesitylene as an internal standard. ^b Isolated yield.

3.2.2 Optimisation

With promising results obtained in the initial discovery, optimisation studies were carried out to explore the effect of each parameter and component on the reaction yield. To

probe the reaction initially the loading of pre-catalyst $\text{NiCl}_2(\text{PPh}_3)_2$ was altered (Table 3.2). Firstly, it was confirmed that the reaction was unsuccessful when no catalyst was used, and instead returned quantitative amounts of both starting coupling partners (Table 3.2, entry 1). From the initial conditions (Table 3.2, Entry 5), a sharp decrease in yield to 13% was observed when the pre-catalyst loading was halved to 5 mol % thus displaying far inferior catalytic activity (Table 3.2, entry 3). Doubling the pre-catalyst loading to 20 mol % did not provide any increase in the yield of cross-coupled product (Table 3.2 entry 6). Therefore, 10 mol % of $\text{NiCl}_2(\text{PPh}_3)_2$ was shown to be optimal.

Table 3.2 Optimisation of catalyst loading. Results obtained by Yerbol Sagatov.



Entry	Pre-catalyst loading (mol %)	Yield 117 (%) ^a
1	0	0
2	2	2
3	5	13
4	8	43
5	10	50(47)^b
6	20	49

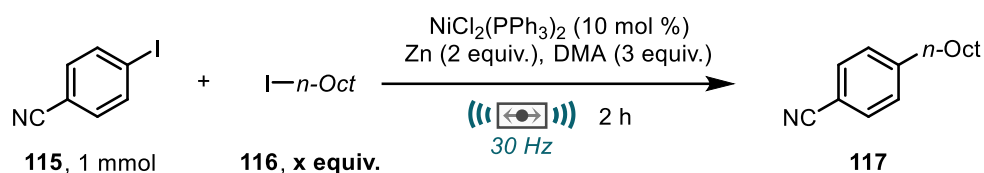
^a Yield determined by ^1H NMR spectroscopy using mesitylene as an internal standard. ^b Isolated yield.

As the reaction is likely limited by the radical generation from the alkyl halide component, the stoichiometry of this coupling partner is important for successful reactivity. To explore this, the ratio of the two starting materials was changed. Raising the amount of 1-iodooctane (**116**) to 1.2 equivalents resulted in an increased yield of 67% (Table 3.3, entry 2). This gives credence to the above statement on the alkyl radical generation being a crucial step in the catalytic cycle. This effect is amplified when 1.5 equivalents of 1-iodooctane is used, giving an excellent yield of 85% (Table 3.3, entry 3). Addition of more alkyl halide proved somewhat detrimental after this point with 1.75 and 2 equivalents of 1-iodooctane giving lower yields in the reaction, possibly due to liquid content in the jar

3 - Cross-electrophile Coupling of Alkyl and Aryl Halides under Ball-milling Conditions

and therefore slightly more inefficient mixing (Table 3.3 entries 4-5). 1.5 Equivalents of alkyl halide coupling partner was therefore found to be optimal for the reaction.

Table 3.3 Optimisation of alkyl halide loading. Results obtained by Yerbol Sagatov.

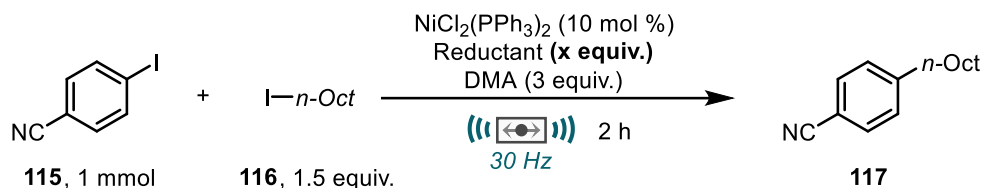


Entry	Alkyl halide	Yield 17 (%) ^a
1	1	50(47) ^b
2	1.2	67
3	1.5	85
4	1.75	75
5	2	76

^a Yield determined by ¹H NMR spectroscopy using mesitylene as an internal standard. ^b Isolated yield.

Next to be investigated was the reductant used in the reaction. For this, the amount of zinc was varied first to establish the optimal loading for efficient coupling. The zinc form used in the reaction was Zn granular (20-30 mesh). During this study, it was found that a reduced loading of zinc gave reduced yields of **117** for reactions with 1 and 1.5 equivalents of zinc, however, good conversion to product was still observed for both reactions (67% and 77%, respectively, Table 3.4, entries 2-3). Increasing the amount of zinc resulted in no increase in yield when using 3 or 4 equivalents of zinc (Table 3.4 entries 5-6), instead giving similar yields to that previously observed at 2 equivalents (Table 3.4, entry 4). In the absence of zinc, no cross-coupled product was observed, and the reaction returned both organohalide partners in quantitative amounts. The lack of product achieved demonstrates the importance of reductant in the catalytic turnover. In addition to this, the coupling reaction should still be able to undergo one catalytic cycle without zinc producing up to 10% cross-electrophile coupled product assuming successful pre-catalyst activation. The observation of 0% desired product strongly indicates that Zn(0) also has an important role in the initial reduction of Ni(II) to the active Ni(0) species, most likely releasing ZnCl₂ in the process.

Table 3.4 Investigation of reductant. Entries 2-6 obtained by Yerbol Sagatov.



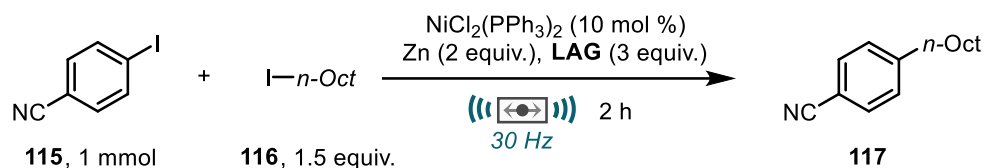
Entry	Reductant	Reductant equiv.	Yield 117 (%) ^a
1	Zn	0	0
2	Zn	1	67
3	Zn	1.5	77
4	Zn	2	85
5	Zn	3	85
6	Zn	4	76
7	Mn (pieces)	2	78
8	Mn (powder)	2	64

^a Yield determined by ¹H NMR spectroscopy using mesitylene as an internal standard.

Another reductant commonly employed in cross-electrophile coupling manifolds is manganese. This was also explored for the ball-milling reaction using manganese pieces and manganese powder (2 equivalents in each case). Whilst good reactivity was observed in both cases, the yield achieved using manganese was slightly lower than using zinc as the reductant (64-78%, Table 3.4, entries 7-8). Zinc was therefore carried forward for optimisation studies.

The role of *N,N*-dimethylacetamide (DMA) as a liquid additive has previously been established to aid in stabilisation of activated zinc species under mechanochemical conditions.¹⁰⁴ Dimethylsulfoxide (DMSO) has also been shown to be a suitable LAG for organozinc generation by ball-milling for a Barbier-type allylation of alcohols.¹⁰⁶ The common attribute for these two solvents is moderate Lewis basicity as determined by a high Gutmann donor number (DN) with DMA having a DN of 27.8 Kcal mol⁻¹ and DMSO being slightly higher at 29.8 Kcal mol⁻¹.¹⁰⁹ To assess the effect of the liquid additive in the mechanochemical cross electrophile coupling reaction, a range of common solvents with varying Gutmann donor numbers were screened (Table 3.5).

3 - Cross-electrophile Coupling of Alkyl and Aryl Halides under Ball-milling Conditions

Table 3.5 Screening of liquid additives

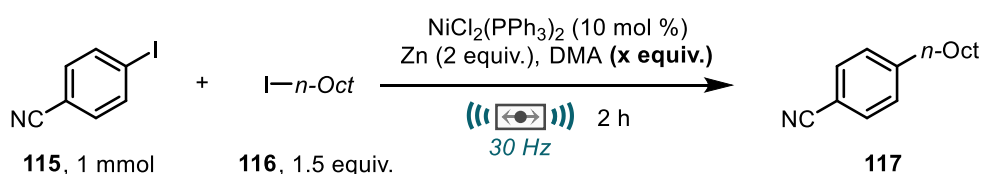
Entry	LAG	LAG DN ^a	Yield 117 (%) ^b
1	None	N/A	4
2	Hexane	0	trace
3	CHCl ₃	4	trace
4	CH ₃ CN	14.1	13
5	EtOAc	17.1	7
6	THF	20	13
7	DMF	26.6	72
8	DMA	27.8	85
9	DMSO	29.8	67
10	DMPU	33	80
11	Pyridine	33.1	28

^a Gutmann donor number from reported literature.¹⁰⁹ ^b Yield determined by ¹H NMR spectroscopy using mesitylene as an internal standard.

Firstly, it was confirmed that reaction without any additive resulted in the formation of only a small amount of **117** (4%, Table 3.5 entry 1). Screening solvents with low donor numbers (<4, Table 3.5, entries 2-3) showed that little to no reactivity occurs, with only trace amounts of **117** observed. Moving to LAGs with moderate donor numbers (14-20) resulted in increased product yield but remained low (<=13%, Table 3.5, entries 4-6). The low yields experienced from low to moderate DN solvents suggest destabilisation of the activated zinc. As anticipated, high DN solvents (>25) provided greatly increased yields when used as LAGs in the reaction, with DMF, DMA, DMSO and DMPU all giving good to excellent yields (67-85%, Table 3.5, entries 7-10). Pyridine, despite having a high DN of 33.1, performed poorly in the reaction (28%, Table 3.5, entry 11). This is likely due to competing coordination between pyridine and 1,10-phenanthroline to the nickel catalyst. This results in disruption to the catalytic cycle and possibly poisoning of the catalyst. DMA provided the highest yield of **117** so was deemed to be optimal (Table 3.5, entry 8).

Having established that DMA was the best choice as an additive, a screen to determine the optimal amount was carried out (Table 3.6). It was found that lowering the amount of DMA had detrimental effect on the product yield (Table 3.6, entries 1-3). Increasing the quantity of DMA to 4 or 5 equivalents resulted in a steady decrease in yield, possibly due to some decreased efficiency in mixing (Table 3.6, entries 5-6). It was found that 3 equivalents of DMA showed the best conversion for this transformation (Table 3.6, entry 4).

Table 3.6 Optimisation of liquid additive quantity



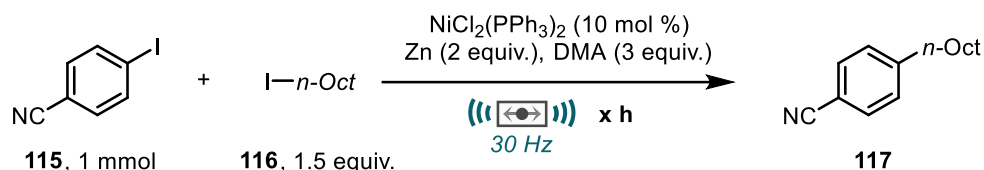
Entry	DMA equiv.	Yield 117 (%) ^a
1	0.5	27
2	1	28
3	2	61
4	3	85
5	4	79
6	5	67

^a Yield determined by ¹H NMR spectroscopy using mesitylene as an internal standard.

It was also determined that the 2-hour reaction period was sufficient for the highest reactivity (Table 3.7, entry 2). Decreased reaction times gave lower yields and increased reaction times provided no improvement to the yield of **117** observed (Table 3.7). It is worth noting that the 2-hour reaction period under mechanochemical conditions is significantly reduced from reaction times used in solution (typically above 12 hours).

3 - Cross-electrophile Coupling of Alkyl and Aryl Halides under Ball-milling Conditions

Table 3.7 Reaction time optimisation



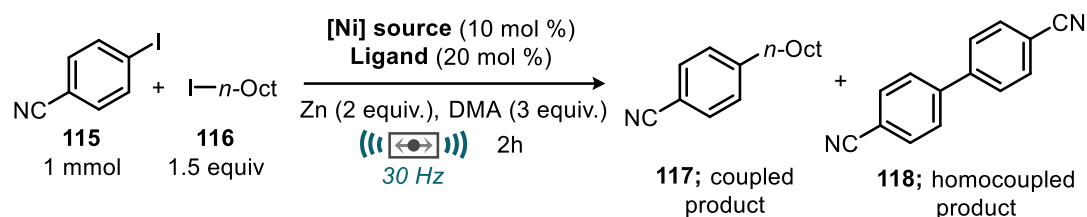
Entry	Time (h)	Yield 117 (%) ^a
1	1	79
2	2	85(80)^b
3	3	61
4	4	67

^a Yield determined by ¹H NMR spectroscopy using mesitylene as an internal standard.

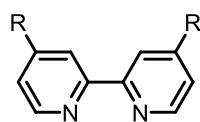
^b Isolated yield

To improve the yield further, the catalyst system was revisited. Initially, the focus was on the use of simple Nickel-phosphine based pre-catalysts. However, it was thought that a switch to nickel sources in conjunction with exogenous bipyridyl type ligands could further improve the yield. To probe these systems, 10 mol % of the nickel source and 20 mol % of bidentate ligand was used to ensure successful coordination. Initial results showed that inexpensive $\text{NiCl}_2 \cdot 6\text{H}_2\text{O}$ as the nickel source and 2,2'-bipyridine showed good conversion to the coupled product **117** (63%, Table 3.8, entry 2), however a small amount of unwanted homocoupled biaryl product **118** was also observed (10%). Upon screening other bipyridine ligands (Table 3.8, entries 3-4), it was discovered that 4,4'-di-*tert*-butyl-2,2'-bipyridine was effective in the coupling reaction giving rise to similar yields of **117** (83%) to that exhibited with the phosphine-based ligands with only trace amounts of biaryl formation (Table 3.8 entry 4). Screening other common bidentate nitrogen ligands, it was found that 1,10 phenanthroline gave an improved yield of 91% **117**, with trace homocoupled product **118** observed (Table 3.8, entry 5). Tridentate terpyridine ligands (**L6**, **L7**) whilst still showing moderate yields of cross-electrophile coupling, also gave greatly increased yields of **118** by homocoupling (Table 3.8, entries 7-8). Reaction with no added ligand provided no product and instead returned both halide starting materials (Table 3.8, entry 9). From the screening of different ligands, it was determined that 1,10-phenanthroline was the optimal choice.

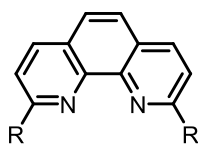
Table 3.8 Catalytic system screen



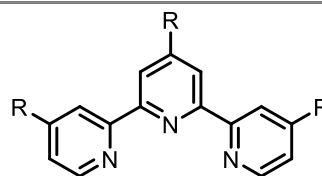
Entry	[Ni] source	Ligand	Yield 117 (%) ^a	Yield 118 (%) ^a
1	NiCl ₂ (PPh ₃) ₂	-	85(80) ^b	trace
2	NiCl ₂ •6H ₂ O	L1	64	10
3	NiCl ₂ •6H ₂ O	L2	83	trace
4	NiCl ₂ •6H ₂ O	L3	51	12
5	NiCl₂•6H₂O	L4	91(85)^b	trace
6	NiCl ₂ •6H ₂ O	L5	27	4
7	NiCl ₂ •6H ₂ O	L6	47	23
8	NiCl ₂ •6H ₂ O	L7	52	42
9	NiCl ₂ •6H ₂ O	-	0	0
10	NiCl ₂ (anhyd.)	L4	31	trace
11	NiCl ₂ •dme	L4	78	2
12	NiBr ₂ •dme	L4	42	9
13	NiI ₂	L4	11	4



L1; R = H
L2; R = *t*Bu
L3; R = OMe



L4; R = H
L5; R = Me



L6; R = H
L7; R = Me

^a Yield determined by ¹H NMR spectroscopy using mesitylene as an internal standard. ^b

Isolated yield

Taking 1,10-phenanthroline (**L4**) as the optimal ligand, a small range of different nickel sources were screened in combination with it to assess reactivity (Table 3.8, entries 10-13). The hydration of NiCl₂ seems to have an important effect on the reaction as a greatly reduced yield of **117** is seen when using anhydrous NiCl₂ (31%, table 3.8, entry 10). The reaction using NiCl₂•dme produced an excellent yield of 78%, however this is still lower than the optimal NiCl₂•6H₂O (Table 3.8, entry 11). Different nickel halide salts performed

3 - Cross-electrophile Coupling of Alkyl and Aryl Halides under Ball-milling Conditions

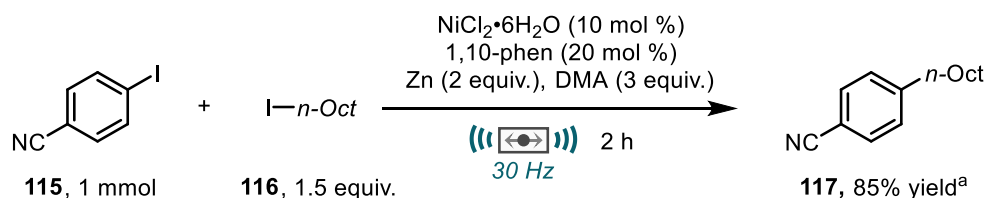
worse in the reaction which could mean activation of nickel chloride is faster / easier than bromide or iodide counterparts (Table 3.8, entries 12-13). Therefore, it was determined that the optimal catalytic system was $\text{NiCl}_2 \cdot 6\text{H}_2\text{O}$ as the nickel source and 1,10-phenanthroline as the added ligand.

Table 3.9 Investigation of catalyst to ligand ratio.

Entry	Cat. loading (mol %)	Ligand loading (mol %)	Yield 117 (%) ^a
1	10	20	91(85) ^b
2	5	20	61
3	10	10	72
4	10	15	81

^a Yield determined by ^1H NMR spectroscopy using mesitylene as an internal standard. ^b Isolated yield

Finally, the ratio of catalyst to ligand was explored. A reduction in the amount of $\text{NiCl}_2 \cdot 6\text{H}_2\text{O}$ provided a diminished yield of 61% (Table 3.9, entry 2). Similarly reducing the ratio between catalyst and ligand to less than 1:2 by decreasing ligand loading also provided slightly reduced yields (Table 3.9, entries 3-4).

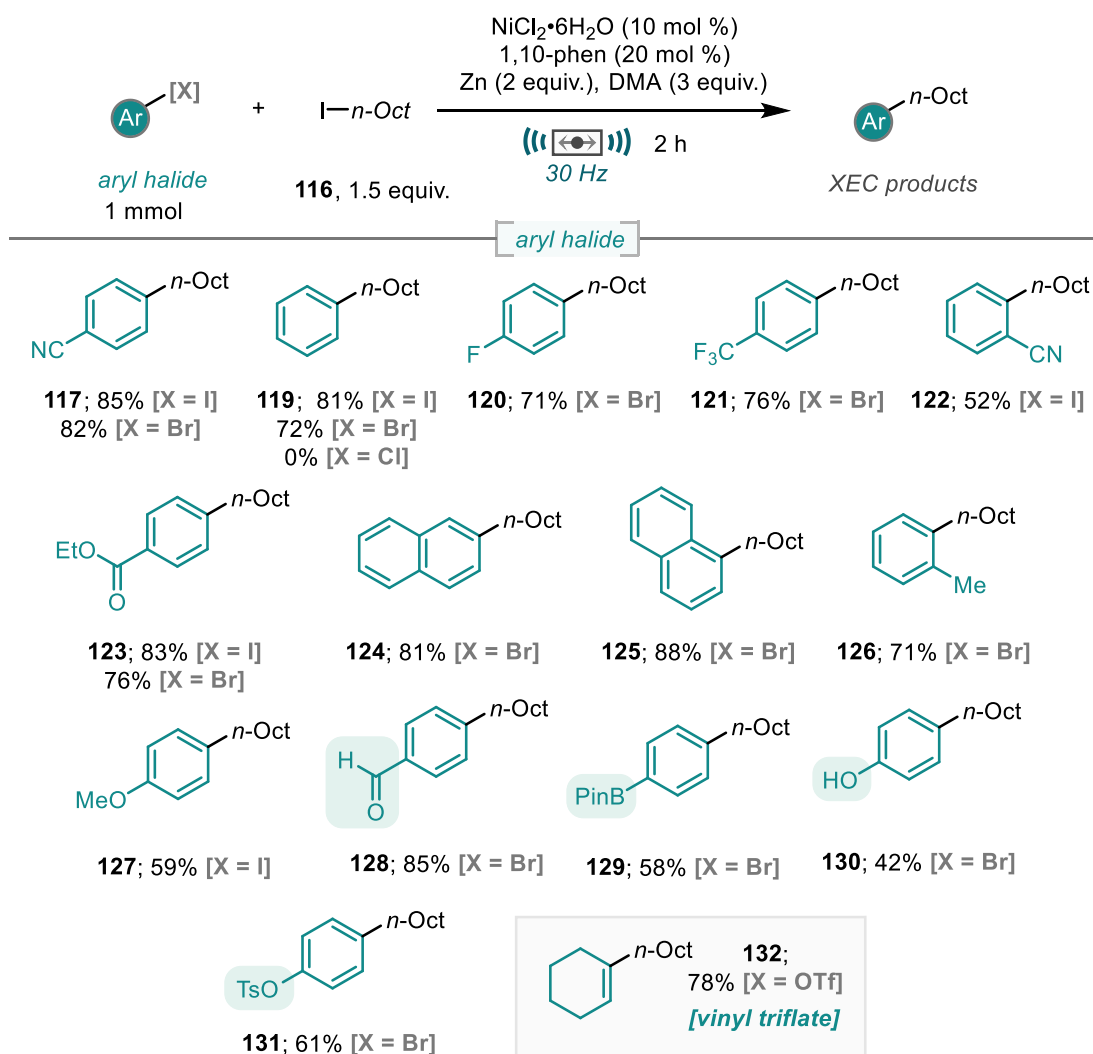


Scheme 3.9 Optimised conditions. ^a Isolated yield.

After investigating the different parameters and conditions, optimal conditions were identified (Scheme 3.9). This was determined to be 1.5 equivalents of alkyl halide, $\text{NiCl}_2 \cdot 6\text{H}_2\text{O}$ (10 mol %), 1,10-phenanthroline (20 mol %), zinc (granular, 2 equiv.) and DMA (3 equiv.).

3.2.3 Aryl (Pseudo)Halide Scope

With optimised conditions identified, the tolerance of the reaction to different coupling partners was explored. First to be investigated was the aryl (sp^2) halide coupling partner. For this, a range of aryl halide coupling partners were subjected to the reaction conditions with 1-iodooctane (**116**) as the alkyl (sp^3) halide coupling partner (Scheme 3.10). No precaution was taken to remove air or moisture from the reaction in any case.



Isolated yields reported.

Scheme 3.10 Scope of aryl (sp^2) (pseudo)halides

Initial results demonstrated that the catalytic system was capable of oxidative insertion into aryl bromides as well as aryl iodides. The ability of this is only slightly lower, as exhibited by reaction of 4-bromobenzonitrile and 4-iodobenzonitrile giving a 3% discrepancy in the yield of **117** achieved. This effect is more obvious in the reaction of

3 - Cross-electrophile Coupling of Alkyl and Aryl Halides under Ball-milling Conditions

iodobenzene vs bromobenzene to give octylbenzene **119** with a 9% difference in yield observed. The catalytic system is shown to be incapable of insertion into the aryl C-Cl bond of chlorobenzene, an insertion that can often be challenging by nickel catalysis. The reaction here returned both starting materials untouched.

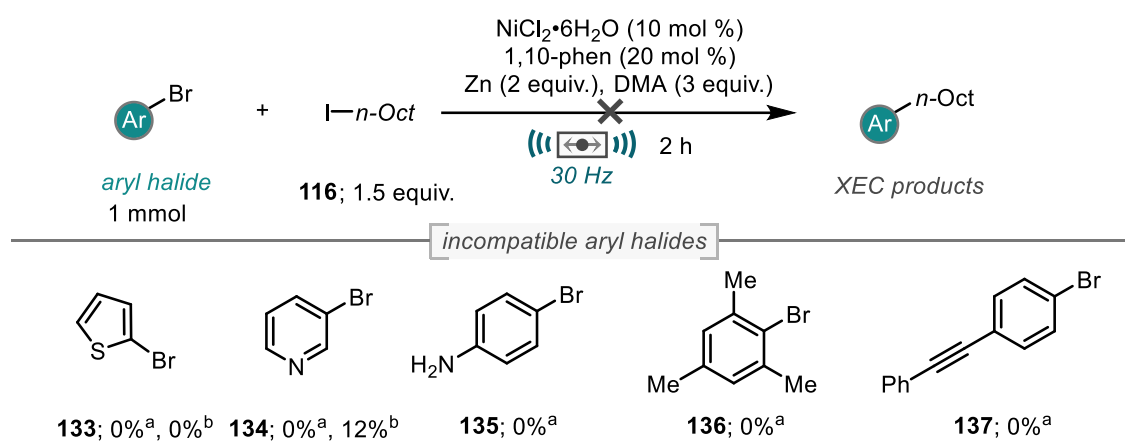
The reaction showed good tolerance to the electronics of the haloarenes. Electron poor aryl halides proceeded in excellent yields and showed tolerance to functionality such as nitrile and ester groups (Scheme 3.10; **117**, **121**, **122**, and **123**). Reactions with unactivated, electron neutral aryl halides also performed well under the reaction conditions signifying good oxidative addition into these systems (Scheme 3.10; **119**, **120**, **124**, **125**, and **126**). In addition, sterically hindered *ortho*-substituted haloarenes were shown to efficiently couple with negligible suppression of product yield (Scheme 3.10; **125** and **125**). Electronically deactivated systems proceeded in the cross-electrophile coupling; however, a somewhat reduced yield was observed as exemplified through the reaction of 4-bromoanisole giving 59% of **127**, which represents a 20-30% decrease from the neutral and activated systems. This is likely due to the slower rate of oxidative addition into electron rich systems.

Moving to explore the tolerance to sensitive and useful functional groups, it was found that substrates with highly electrophilic sites, such as aldehydes, selectively underwent the cross-coupling pathway and showed no undesirable reactivity at the carbonyl site (Scheme 3.10, **128**). Free phenols were also tolerated, albeit in moderate yield (Scheme 3.10, **130**), showcasing the well-established benefit of cross electrophile coupling in that no exogenous base is required. This allows the coupling of haloarenes bearing acidic sites which is not possible with other coupling that typically require base to aid with the catalytic cycle; for example, the necessity of base for the generation of a 4-coordinate anionic boronate species in the Suzuki-Miyaura coupling. For the mechanochemical reaction substrates bearing other reaction sites for cross-coupling, such as boronate esters or tosylates, coupling was exclusively selective for reaction at the halide site (Scheme 3.10; **128** and **131**). This allows for the formation of products retaining useful synthetic handles for orthogonal derivatisation. In addition, coupling of pseudohalides is possible as demonstrated as the coupling of a vinyl triflate to give excellent product yield (78%, Scheme 3.10, **132**).

Throughout the scope, some substrates were shown to be incompatible (Scheme 3.11) Firstly, heteroaromatic halides proved unable to undergo coupling with both 2-bromothiophene and 3-bromopyridine giving no product (Scheme 3.11; **133** and **134**). In the case of 3-bromopyridine, an increase to 12% NMR yield was shown when the workup

was changed from the standard acidic workup (1M HCl) to a neutral aqueous workup. It is possible that these heterocyclic substrates are competing with the ligand for coordination to the nickel centre. Another possibility is that even after successful oxidative addition, protodemetalation can occur releasing thiophene or pyridine. There is evidence for this as the starting material was consumed during reaction in both cases; 27% in the case of 2-bromothiophene and 45% in the case of 3-bromopyridine. 4-bromoaniline (**135**) also showed no coupling and instead was returned from the reaction, albeit not quite in quantitative amounts (89% haloarene returned).

Other substrates to be unsuccessful were the sterically challenging 2-bromomesitylene (**136**) and an aryl bromide containing alkyne functionality (**137**), both of which returned quantitative amounts of starting material.



Yields determined by ^1H NMR using mesitylene as an internal standard.

^a 1M HCl workup (standard procedure) ^b H_2O workup

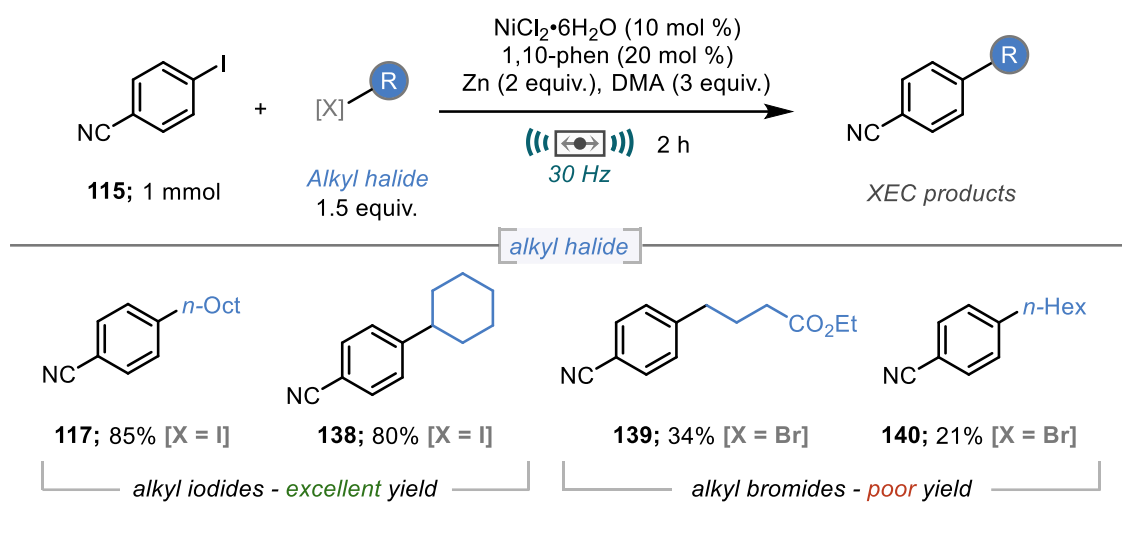
Scheme 3.11 Incompatible substrates

3.2.4 Initial Alkyl Halide Scope and Re-optimisation for Alkyl Bromides

With good tolerance shown for the aryl (sp^2) coupling partner, attention next turned to assessment of the alkyl (sp^3) halide coupling partner. This is typically perceived as the more complicated and difficult coupling partner due to issues with homocoupling.^{26,47,79} For this scope study, the parent aryl bromide, 4-iodobenzonitrile **115**, was attempted to be coupled with a range of alkyl halides using the optimised conditions (Scheme 3.12).

Initial studies using the optimised conditions showed that alkyl iodides performed well in the reaction (80-85%, Scheme 3.12; **117** and **138**). However, alkyl bromides produced dramatically reduced yields as seen when using ethyl 4-bromobutyrate or 1-bromohexane as the alkyl halide partner, giving just 34% and 21% coupled products **139** and **140** respectively.

3 - Cross-electrophile Coupling of Alkyl and Aryl Halides under Ball-milling Conditions



Isolated yields reported

Scheme 3.12 Initial alkyl halide scope

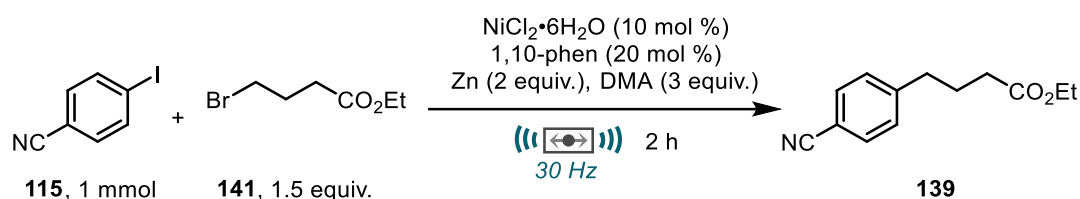
Alkyl bromides are generally more desirable for cross-coupling than alkyl iodides due to greatly increased commercial availability and stability. Therefore, it was established that whilst the current optimised conditions were a good choice for coupling alkyl iodides, a different / adapted approach would be needed for the successful coupling of alkyl bromides. Ethyl 4-bromobutyrate (**141**) served as the model substrate for the identification of suitable set of conditions for alkyl bromide coupling.

The starting point for re-optimisation was the previously described optimised conditions that resulted in a 34% yield of ethyl 4-(4-cyanophenyl)butanoate (**139**) and returning 60% of 4-iodobenzonitrile **115** (Table 3.10, entry 1). Firstly, a longer reaction time of 4 hours was attempted for longer as there was still a significant amount of unreacted starting material left after the initial 2-hour period. However, the increase in reaction time showed no significant change in distribution between product and remaining starting material and still produced just 35% of **139** (Table 3.10, entry 10). Early reports on cross electrophile coupling discuss the use of additives to promote reactivity; these are typically iodide salts with sodium iodide being a popular choice.^{25,26,79} The role of these salts is somewhat unclear, although Weix and co-workers describe the possibility of catalyst stabilisation as well as an *in situ* Finkelstein type reaction to convert some of the alkyl bromide to alkyl iodide and hence accelerate the reaction rate.

For the mechanochemical reaction, various iodide salts were screened (Table 3.10, entries 3-5). The addition of 2 equivalents of sodium iodide to the standard conditions resulted in a remarkable increase in the yield of **139** from 34% to 80%. Other iodide

sources gave improved yield, however the effect of this was lower. Using potassium iodide gave an increase to 46% yield (Table 3.10, entry 4), and tert-butyl ammonium iodide gave only a slight increase to 37% (Table 3.10, entry 5). Having established that sodium iodide was the best additive, the quantity added to the reaction was varied. (Table 3.10, entries 6-9). Halving the loading of sodium iodide to 1 equivalent did not lower the yield and produced 81% of the desired product. However, further reductions in sodium iodide quantity resulted in significant decrease in yield to the point that 0.25 equivalents of sodium iodide gave a similar yield than without any additive (36%, Table 3.10, entry 9).

Table 3.10 Re-optimisation for aryl bromides



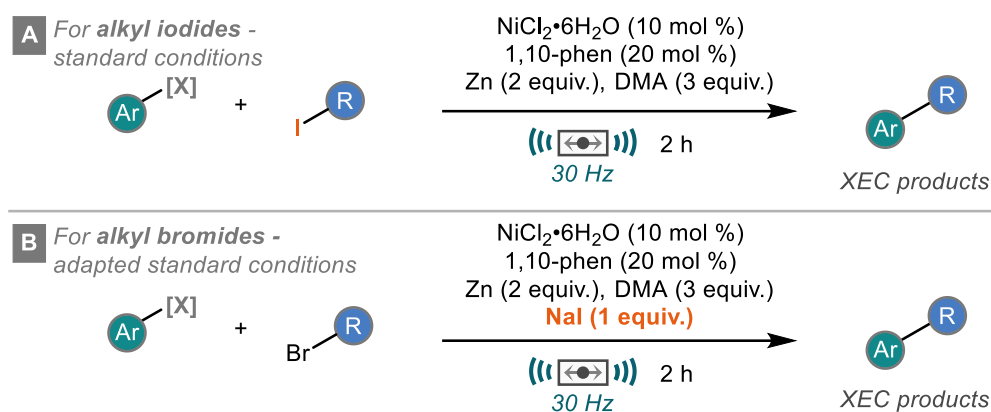
Entry	Variation from conditions	Yield 139 (%) ^a	115 remaining (%) ^a
1	none	34	60 ^b
2	Time: 4 h	35	56
3	Additive: NaI (2 equiv.)	80	6
4	Additive: KI (2 equiv.)	46	51
5	Additive: TBAI (2 equiv.)	37	55
6	Additive: NaI (1 equiv.)	81	3
7	Additive: NaI (0.75 equiv.)	61	27
8	Additive: NaI (0.5 equiv.)	46	49
9	Additive: NaI (0.25 equiv.)	36	61

^a Yield determined by ¹H NMR spectroscopy using mesitylene as an internal standard. ^b

Isolated yield.

These findings allow for two slightly different procedures; one for alkyl iodides and one for alkyl halides. For alkyl iodides, the original optimised conditions are suitable (Scheme 3.13A). For alkyl bromides, a small modification to the standard conditions can be applied, being the addition of 1 equivalent sodium iodide (Scheme 3.13B).

3 - Cross-electrophile Coupling of Alkyl and Aryl Halides under Ball-milling Conditions



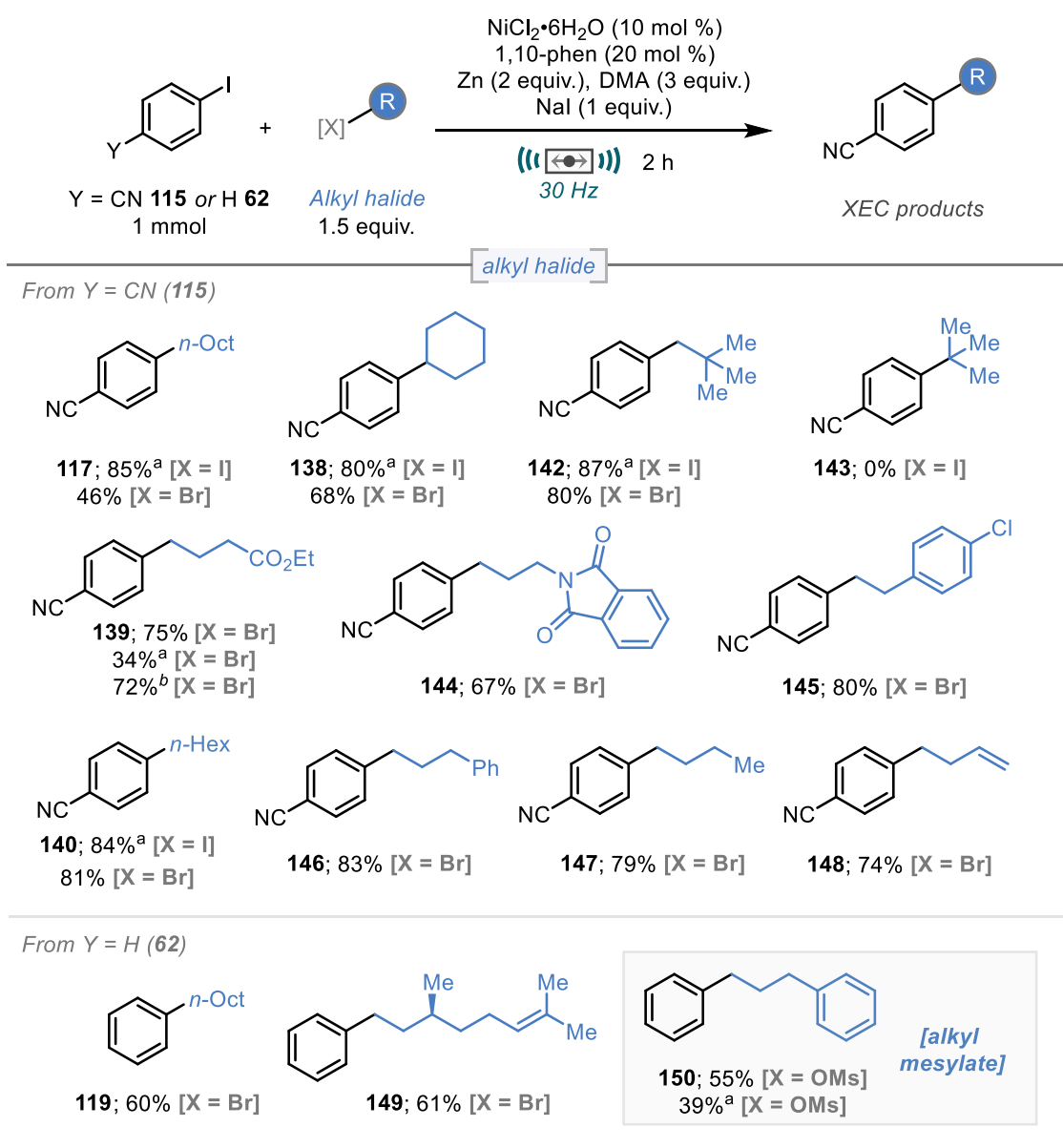
Scheme 3.13 Modified reaction conditions for alkyl bromides

3.2.5 Alkyl Halide Scope

Having established that the coupling of alkyl iodides gives high product yields using the standard reaction conditions and that the coupling of alkyl bromides occurs in greatly improved yields with the inclusion of sodium iodide, the scope of the reaction was revisited (Scheme 3.14). This would give an indication on whether the use of sodium iodide gives consistently improved yields across a variety of alkyl bromides. 4-Iodobenzonitrile was used as the aryl halide partner in most cases.

As expected, cross-electrophile coupling of alkyl iodides proceeded in excellent yield (>80%) without the use sodium iodide (Scheme 3.14; **117**, **138**, **140** and **142**). Due to enhanced stability, primary alkyl halides make up much of the scope explored. These generally performed very well in the reaction. Secondary halides also couple effectively as shown by the reaction of iodocyclohexane and bromocyclohexane giving **138** in 80% and 68%, respectively. Secondary alkyl halides appear to be the limit for the sp^3 component as the methodology could not be extended to tertiary alkyl halides with *tert*-butyl iodide giving 0% desired product (Scheme 3.14, **143**). Pleasingly, *tert*-amyl bromide, a substrate that has previously been shown to be difficult to couple underwent mechanochemical coupling in good yield (68%, Scheme 3.14, **142**). As shown previously in re-optimisation, alkyl chains bearing carboxylic esters could be coupled in good yield (75%, Scheme 3.14, **139**). The yield of **139** was only slightly reduced to 72% when using 4-bromobenzonitrile as the aryl halide component instead its iodoarene analogue. In addition to ester functionality, the reaction was also compatible with phthalimides, which are considered as protected amines. (67%, **144**). Also possible is the reaction of halides bearing alkene functionality (74%, **148**) as well as a selection of unfunctionalised skeletal alkyl chains (**140**, **146** and **147**). As discussed in the aryl (sp^2) halide scope (Scheme

3.14), the mechanochemical reaction showed no oxidative addition into chloroarenes, therefore reaction of alkyl halides functionalised with a distal chloroarene moiety coupled selectively leaving the aryl chloride untouched as a useful synthetic intermediate for further reactivity if desired (Scheme 3.14, **145**).



Isolated yields reported. ^a No NaI added. ^b 4-Bromobenzonitrile used as aryl halide.

Scheme 3.14 Full scope of alkyl (sp^3) halides

For longer chain alkyl bromides, homocoupling of the aryl halides dominated reactivity leading to reduced yields, as observed in the coupling of 4-iodobenzonitrile (**115**) with 1-bromooctane. It is thought that the rate of insertion into the highly activated C-I bond of 4-iodobenzonitrile and subsequent homocoupling is much faster than the desired

3 - Cross-electrophile Coupling of Alkyl and Aryl Halides under Ball-milling Conditions

catalytic cycle pathway. To investigate this further, 1-bromooctane was coupled with a more electron neutral haloarene, iodobenzene (**62**) in an attempt to disfavour the homocoupling pathway and therefore limit biaryl formation. As predicted, the desired coupling reaction was improved, furnishing octylbenzene in a moderate 60% yield (Scheme 3.14, **119**). Iodobenzene also showed good reactivity with enantioenriched (*S*)-(+)-citronellyl bromide affording 61% product (Scheme 3.14, **149**).

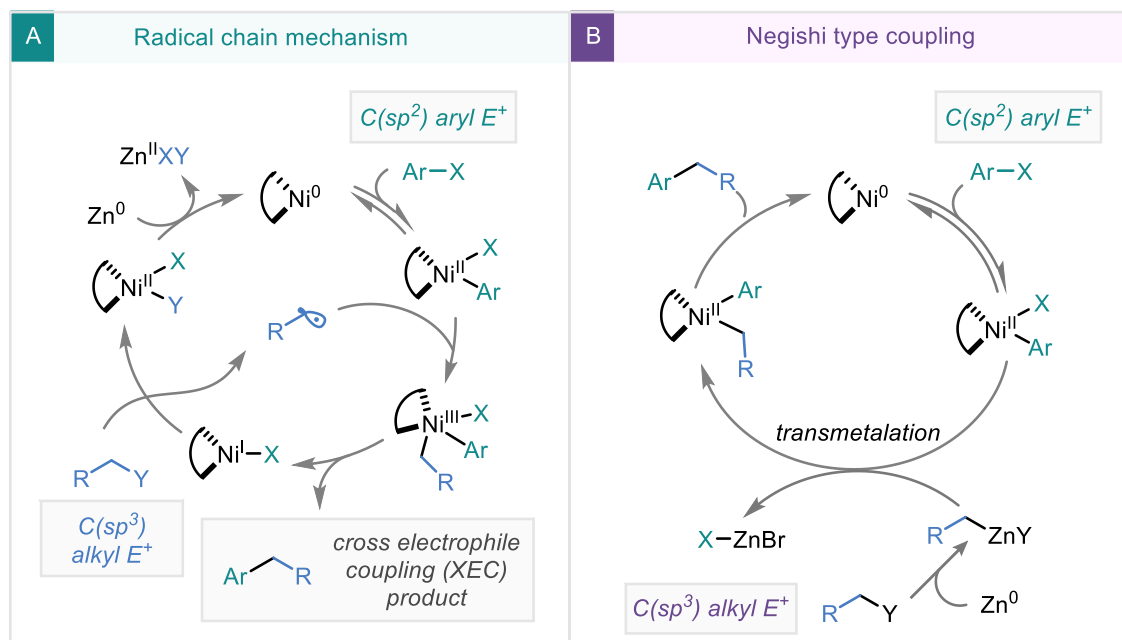
To assess if the reaction was limited to just alkyl halides, the reaction of a pseudohalide was examined. For this, an alkyl mesylate, 3-phenylpropyl methanesulfonate, was coupled with iodobenzene using the same methodology employed for alkyl bromide coupling, meaning the inclusion of sodium iodide. 55% Cross-electrophile coupling was observed showing the application of the reaction to both halides and pseudohalides (Scheme 3.14, **150**). Since it is possible that one of the roles of sodium iodide could be to form the alkyl iodide from the alkyl sulfonate *in situ*, the reaction was also run in the absence of additive. This gave a reduced yield of 39% suggesting that the alkyl mesylate is capable by itself for the radical generation required for the catalytic cycle and is simply enhanced by the addition of sodium iodide. Alkyl sulfonates have previously been explored for nickel-catalysed cross-electrophile coupling by Shu and co-workers.¹¹⁰

Unfortunately, the coupling of alkyl chlorides was unsuccessful under the reaction conditions, even with the use of sodium iodide, as shown by the reaction of ethyl 4-chlorobutyrate giving quantitative recovery of starting material and 0% of coupled product **139**.

3.2.6 Tolerance of Different Reductant Forms

The reductant plays an important role in cross-electrophile coupling. It serves to turn over the catalytic cycle as well as reducing the Ni(II) pre-catalyst to the active Ni(0) catalytic species. The most common reductants used for cross-electrophile coupling are zinc and manganese due to their moderate reduction potential (-0.76 V and -1.16 V, respectively). Under traditional solution conditions, activation of these metals can be capricious and greatly depend on the form of the metals used. To assess if this trait is also seen in a mechanochemical reaction, a variety of zinc(0) and manganese(0) sources were screened in the reaction without prior treatment / activation. All reductant forms were purchased from commercial sources.

3 - Cross-electrophile Coupling of Alkyl and Aryl Halides under Ball-milling Conditions

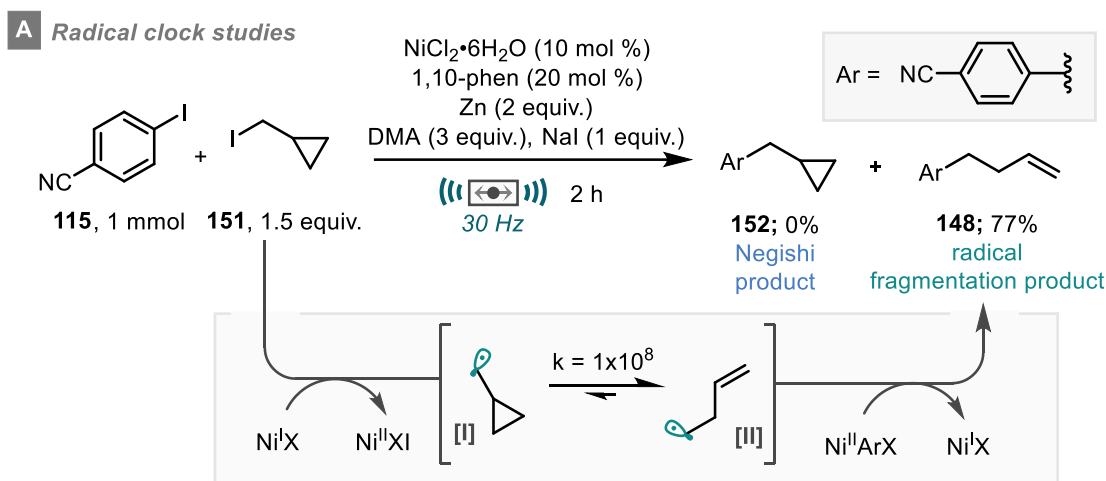


Scheme 3.16 Possible mechanistic pathways. A) Radical chain B) Negishi type.

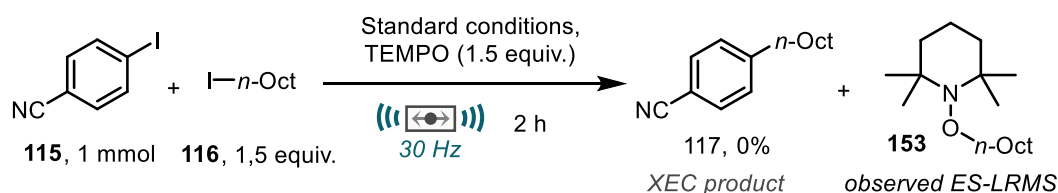
Mechanochemical methods have thus far proved to be a powerful tool for the activation of zero valent methods. A previous report by Browne and co-workers detailed an *in situ* generation of organozinc intermediates from alkyl halides followed by subsequent Pd-catalysed Negishi coupling. It is still a possibility that the cross-electrophile coupling reaction by ball milling is proceeding via this organozinc formation.

To probe the formation of radical intermediates, a common radical clock experiment was carried out (Scheme 3.17). For this, cyclopropylmethyl iodide (**151**) was used as the alkyl halide coupling partner and 4-iodobenzonitrile as the aryl halide partner. Following the previously understood single-electron radical chain process (Scheme 3.16A) would result in the well-established cyclopropylmethyl radical fragmentation of **I** to **III**, giving the ring opened homoallylarene product (**148**, Scheme 3.17A). However, under a 2 electron Negishi-type coupling (as described in Scheme 3.16B), the insertion of zinc and subsequent cross-coupling would lead to the ring-closed product (**152**, Scheme 3.17). From the mechanochemical reaction using the standard conditions, the ring fragmentation product **148** was received in an excellent 77% yield with none of the ring closed Negishi-type product observed at all (Scheme 3.17A). This gives a strong indication that the mechanochemical reaction proceeds via a single-electron pathway and operates akin to the previously established mechanism seen in solution-phase transformations. The radical clock experiment was also carried out using cyclopropyl bromide under the modified reaction conditions (i.e. addition of sodium iodide) to ensure the reaction of alkyl bromides proceeded in a similar fashion to their corresponding iodide

analogues. Indeed, the ring opened product fragmentation was again isolated in 57% yield demonstrating a single electron pathway.



B Radical trapping studies - TEMPO



Scheme 3.17A Probing of radical intermediates

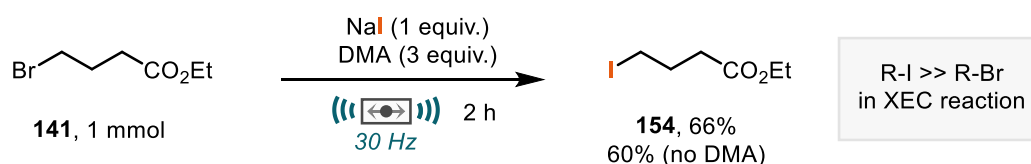
The addition of a radical inhibitor (TEMPO) into the parent reaction completely suppressed any cross-coupled product formation (Scheme 3.17B). Attempts to isolate the alkyl-TEMPO adduct **153** that would arise from successful trapping of the generated alkyl radical proved unsuccessful, possibly due to the poor stability of the N-O bond under the reductive conditions used in the reaction. The adduct was observed by mass spectrometry (electrospray ionisation). Whilst the radical trapping results do not give conclusive evidence by itself, the complete suppression of yield alongside the spectrometric observation of the adduct supports the findings from the radical clock experiment.

Also of particular interest is the role of sodium iodide in greatly improving the reactivity of alkyl bromides. Weix's initial reports describe the role of sodium iodide as being unclear. However, they do propose a few different possibilities suggesting that the iodide may aid in the initial reduction of the nickel catalyst, encourage the formation of more reactive nickel species, expedite beneficial ligand exchange reactions, and/or form a

3 - Cross-electrophile Coupling of Alkyl and Aryl Halides under Ball-milling Conditions

small amount of the corresponding alkyl iodide *in situ* and hence enhance reactivity.²⁵ Although many of these are difficult to probe under the mechanochemical conditions due to lack of *in situ* spectroscopic conditions, the formation of alkyl iodides from alkyl bromides can be investigated by the removal of any coupling partners / catalysts.

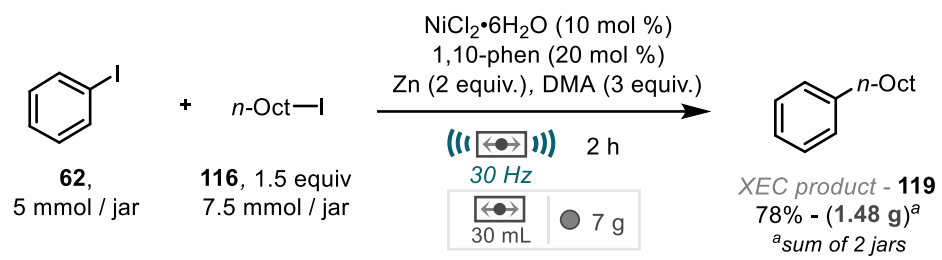
To probe this possible Finkelstein type reactivity under ball-milling conditions, ethyl 4-bromobutyrate (**141**) was placed in a milling jar with sodium iodide and DMA. The mixture was then milled for 2 hours upon which the ethyl 4-iodobutyrate (**151**) could be isolated in 66% yield (Scheme 3.18). This was repeated with the omission of the LAG and the yield remained similar (60%). Therefore, described is an efficient process for the solvent-free, mechanochemical conversion of alkyl bromides to alkyl iodides using sodium iodide. This *in situ* transformation is the likely source of the greatly increased yields when using sodium iodide with alkyl bromides, as the rate of coupling for alkyl iodides is inherently faster. However, improvement due to other factors cannot be ruled out.



Scheme 3.18 Mechanochemical Finkelstein type reactivity of alkyl bromides

3.2.8 Scale-up

Scaling-up mechanochemical reactions presents many complications, mainly that the energy provided by the mixer mill does not scale directly when altering the jar size. Pleasingly, it was found that translation to a larger scale was possible by doubling the reaction vessel volume to a 30 mL milling jar and a 7.2 g milling ball, which is a little over double the mass of that used in the optimised conditions (3 g) to maintain a somewhat consistent filling ratio. Two 5 mmol reactions, each coupling iodobenzene (**62**) with 1-iodooctane (**116**) were run simultaneously, combined, and worked up / isolated together to afford 1.48 g of octylbenzene **119** which represents a 78% yield for cross-electrophile coupling (Scheme 3.19). This value is slightly diminished in comparison to the smaller test-scale reaction (81% Scheme 3.10). This small discrepancy would likely be overcome by careful optimisation at the desired scale. However, it is promising that the initial translation to larger scale was achieved smoothly, and the conditions gave a strong foundation should the reaction want to be adapted for different large-scale reactor techniques such as for use in rotary drum reactors and twin-screw extrusion.



Scheme 3.19 Scale up. Results by Dr Jamie Leitch.

3.3 Conclusions and Future Work

To conclude, ball-milling has successfully been applied for a nickel-catalysed cross-electrophile coupling reaction of aryl halides and alkyl halides. This work showcases the benefit of utilising mechanochemical methods for the activation of zinc. Previously, only the formation of organozinc intermediates has been explored using this facile method for zinc activation. This work represents the first example of mechanochemically activating zinc for use as a reductant and one of the first reports for cross-electrophile coupling in a ball-milling manifold that were reported in quick succession (The other reported method is discussed in section 3.4).

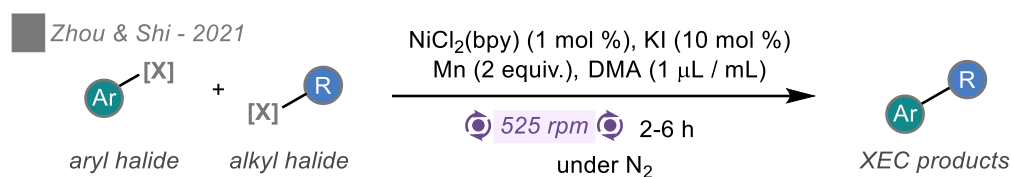
The developed protocol requires no exclusion of air or moisture from the reaction set-up. This tolerance to water is particularly beneficial in the use of inexpensive, readily available $\text{NiCl}_2 \cdot 6\text{H}_2\text{O}$ as the nickel source. The developed method could be directly applied to a range of aryl halides bearing various (sensitive) functionality. However, whilst the initial optimised method was applicable to a range of alkyl iodides, the coupling of alkyl bromides resulted in poor yields under standard conditions. This issue was overcome by the addition of sodium iodide to the reaction mixture. Further studies suggest this promoted an *in situ* Finkelstein reaction to convert alkyl bromides to alkyl iodides within the mechanochemical reaction. This showed a profound increase in yield for the previously poorly performing alkyl bromides. This strategy could then be applied to a range of primary and secondary alkyl bromides. However, tertiary alkyl bromides and alkyl chlorides remains a limitation.

Tolerance to five different zinc forms as well as two different forms of manganese was shown. This demonstrates the powerful capability of ball-milling techniques as solution-phase methods are often dependent on zinc form whereas ball-milling renders all zinc forms equally reactive by grinding into a reactive powder. Mechanistic aspects of the reaction were explored by radical clock and radical trapping experiments. The results of which indicate that a process akin to the well-established radical chain mechanism that has been extensively explored previously. Also shown was an initial scale-up to gram scale cross-coupling.

The protocol does not come without limitations. The main limitations shown are an inability to couple heteroaryl halides, as well as limited reaction seen when attempting to couple aryl or alkyl chlorides. Ongoing work within the research group is targeting the reaction of heteroaromatic halides by the screening of different ligand / catalyst systems. There is also a possibility for the use of alternative electrophiles by ball-milling enabled reductive coupling (explored in Chapter 4).

3.4 Comparisons to Other Ball-milling Cross-electrophile Coupling Reactions

Imminently prior to the publication of this work, the first example of a mechanochemical cross-electrophile coupling was reported by way of a manganese-mediated reaction using a planetary mill by Zhou, Shi, and co-workers (Scheme 3.20). This work presents many of the features and benefits already discussed within this thesis including the use of iodide additive for increased reactivity. The reaction requires the use of a nitrogen atmosphere, but also allows for use of just 1 mol % nickel catalyst. The publication once again displays the facile activation of zero-valent metals, in this case manganese, for use in organic synthesis.¹¹¹



Scheme 3.20. Manganese mediated cross-electrophile coupling by ball-milling

3.5 Bibliography

- 1 K. Kubota and H. Ito, *Trends Chem.*, 2020, **2**, 1066–1081.
- 2 A. Porcheddu, E. Colacino, L. De Luca and F. Delogu, *ACS Catal.*, 2020, **10**, 8344–8394.
- 3 F. Effaty, X. Ottenwaelder and T. Friščić, *Curr. Opin. Green Sustain. Chem.*, 2021, **32**, 100524.
- 4 J. L. Howard, Q. Cao and D. L. Browne, *Chem. Sci.*, 2018, **9**, 3080–3094.
- 5 A. Stolle and B. Ranu, *Ball Milling Towards Green Synthesis: Applications, Projects, Challenges*, Royal Society of Chemistry, 2014.
- 6 J.-L. Do and T. Friščić, *ACS Cent. Sci.*, 2017, **3**, 13–19.
- 7 S. L. James, C. J. Adams, C. Bolm, D. Braga, P. Collier, T. Friščić, F. Grepioni, K. D. M. Harris, G. Hyett, W. Jones, A. Krebs, J. Mack, L. Maini, A. G. Orpen, I. P. Parkin, W. C. Shearouse, J. W. Steed and D. C. Waddell, *Chem. Soc. Rev.*, 2011, **41**, 413–447.
- 8 G.-W. Wang, *Chem. Soc. Rev.*, 2013, **42**, 7668–7700.
- 9 C. C. C. Johansson Seechurn, M. O. Kitching, T. J. Colacot and V. Snieckus, *Angew. Chem. Int. Ed.*, 2012, **51**, 5062–5085.
- 10 R. F. Heck, *J. Am. Chem. Soc.*, 1968, **90**, 5518–5526.
- 11 R. F. Heck, *J. Am. Chem. Soc.*, 1968, **90**, 5526–5531.
- 12 R. F. Heck, *J. Am. Chem. Soc.*, 1968, **90**, 5542–5546.
- 13 R. F. Heck, *J. Am. Chem. Soc.*, 1968, **90**, 5531–5534.
- 14 R. F. Heck, *J. Am. Chem. Soc.*, 1968, **90**, 5535–5538.
- 15 R. F. Heck, *J. Am. Chem. Soc.*, 1968, **90**, 5546–5548.
- 16 R. F. Heck and J. P. Nolley, *J. Org. Chem.*, 1972, **37**, 2320–2322.
- 17 E. Negishi, A. O. King and N. Okukado, *J. Org. Chem.*, 1977, **42**, 1821–1823.
- 18 A. O. King, N. Okukado and E. Negishi, *J. Chem. Soc. Chem. Commun.*, 1977, 683–684.
- 19 N. Miyaura, K. Yamada and A. Suzuki, *Tetrahedron Lett.*, 1979, **20**, 3437–3440.
- 20 N. Miyaura and A. Suzuki, *J. Chem. Soc. Chem. Commun.*, 1979, 866–867.
- 21 C. Glaser, *Berichte Dtsch. Chem. Ges.*, 1869, **2**, 422–424.
- 22 F. Ullmann and J. Bielecki, *Berichte Dtsch. Chem. Ges.*, 1901, **34**, 2174–2185.
- 23 A. Wurtz, *Justus Liebigs Ann. Chem.*, 1855, **96**, 364–375.
- 24 D. A. Everson, R. Shrestha and D. J. Weix, *J. Am. Chem. Soc.*, 2010, **132**, 920–921.
- 25 D. A. Everson, B. A. Jones and D. J. Weix, *J. Am. Chem. Soc.*, 2012, **134**, 6146–6159.
- 26 D. A. Everson and D. J. Weix, *J. Org. Chem.*, 2014, **79**, 4793–4798.
- 27 G. Cahiez, C. Duplais and J. Buendia, *Chem. Rev.*, 2009, **109**, 1434–1476.
- 28 M. Amatore and C. Gosmini, *Chem. – Eur. J.*, 2010, **16**, 5848–5852.
- 29 L. Yi, T. Ji, K.-Q. Chen, X.-Y. Chen and M. Rueping, *CCS Chem.*, , DOI:10.31635/ccschem.021.202101196.
- 30 X. Lu, J. Yi, Z.-Q. Zhang, J.-J. Dai, J.-H. Liu, B. Xiao, Y. Fu and L. Liu, *Chem. – Eur. J.*, 2014, **20**, 15339–15343.
- 31 Y. Zhao and D. J. Weix, *J. Am. Chem. Soc.*, 2014, **136**, 48–51.
- 32 G. A. Molander, S. R. Wisniewski and K. M. Traister, *Org. Lett.*, 2014, **16**, 3692–3695.
- 33 A. H. Cherney and S. E. Reisman, *J. Am. Chem. Soc.*, 2014, **136**, 14365–14368.
- 34 G. A. Molander, K. M. Traister and B. T. O'Neill, *J. Org. Chem.*, 2014, **79**, 5771–5780.
- 35 X. Li, Z. Feng, Z.-X. Jiang and X. Zhang, *Org. Lett.*, 2015, **17**, 5570–5573.
- 36 N. T. Kadunce and S. E. Reisman, *J. Am. Chem. Soc.*, 2015, **137**, 10480–10483.
- 37 J. Wang, J. Zhao and H. Gong, *Chem. Commun.*, 2017, **53**, 10180–10183.
- 38 K. M. M. Huihui, R. Shrestha and D. J. Weix, *Org. Lett.*, 2017, **19**, 340–343.

- 39 C. Xu, W.-H. Guo, X. He, Y.-L. Guo, X.-Y. Zhang and X. Zhang, *Nat. Commun.*, 2018, **9**, 1170.
- 40 C. Heinz, J. P. Lutz, E. M. Simmons, M. M. Miller, W. R. Ewing and A. G. Doyle, *J. Am. Chem. Soc.*, 2018, **140**, 2292–2300.
- 41 Y. Ye, H. Chen, J. L. Sessler and H. Gong, *J. Am. Chem. Soc.*, 2019, **141**, 820–824.
- 42 K. J. Garcia, M. M. Gilbert and D. J. Weix, *J. Am. Chem. Soc.*, 2019, **141**, 1823–1827.
- 43 J. M. E. Hughes and P. S. Fier, *Org. Lett.*, 2019, **21**, 5650–5654.
- 44 L. Su, G. Ma, Y. Song and H. Gong, *Org. Lett.*, 2021, **23**, 2493–2497.
- 45 Y. Fang, T. Rogge, L. Ackermann, S.-Y. Wang and S.-J. Ji, *Nat. Commun.*, 2018, **9**, 2240.
- 46 X. Wang, S. Wang, W. Xue and H. Gong, *J. Am. Chem. Soc.*, 2015, **137**, 11562–11565.
- 47 S. Kim, M. J. Goldfogel, M. M. Gilbert and D. J. Weix, *J. Am. Chem. Soc.*, 2020, **142**, 9902–9907.
- 48 B. P. Woods, M. Orlandi, C.-Y. Huang, M. S. Sigman and A. G. Doyle, *J. Am. Chem. Soc.*, 2017, **139**, 5688–5691.
- 49 K. M. M. Huihui, J. A. Caputo, Z. Melchor, A. M. Olivares, A. M. Spiewak, K. A. Johnson, T. A. DiBenedetto, S. Kim, L. K. G. Ackerman and D. J. Weix, *J. Am. Chem. Soc.*, 2016, **138**, 5016–5019.
- 50 H. Yue, C. Zhu, L. Shen, Q. Geng, K. J. Hock, T. Yuan, L. Cavallo and M. Rueping, *Chem. Sci.*, 2019, **10**, 4430–4435.
- 51 J. Liao, C. H. Basch, M. E. Hoerner, M. R. Talley, B. P. Boscoe, J. W. Tucker, M. R. Garnsey and M. P. Watson, *Org. Lett.*, 2019, **21**, 2941–2946.
- 52 R. Martin-Montero, V. R. Yatham, H. Yin, J. Davies and R. Martin, *Org. Lett.*, 2019, **21**, 2947–2951.
- 53 S. Ni, C.-X. Li, Y. Mao, J. Han, Y. Wang, H. Yan and Y. Pan, *Sci. Adv.*, , DOI:10.1126/sciadv.aaw9516.
- 54 P. Zhang, C. “Chip” Le and D. W. C. MacMillan, *J. Am. Chem. Soc.*, 2016, **138**, 8084–8087.
- 55 Z. Duan, W. Li and A. Lei, *Org. Lett.*, 2016, **18**, 4012–4015.
- 56 A. Paul, M. D. Smith and A. K. Vannucci, *J. Org. Chem.*, 2017, **82**, 1996–2003.
- 57 V. Bacauanu, S. Cardinal, M. Yamauchi, M. Kondo, D. F. Fernández, R. Remy and D. W. C. MacMillan, *Angew. Chem. Int. Ed Engl.*, 2018, **57**, 12543–12548.
- 58 T. Q. Chen and D. W. C. MacMillan, *Angew. Chem. Int. Ed.*, 2019, **58**, 14584–14588.
- 59 A. Pomberger, Y. Mo, K. Y. Nandiwale, V. L. Schultz, R. Duvadie, R. I. Robinson, E. I. Altinoglu and K. F. Jensen, *Org. Process Res. Dev.*, 2019, **23**, 2699–2706.
- 60 Z. G. Brill, C. B. Ritts, U. F. Mansoor and N. Sciammetta, *Org. Lett.*, 2020, **22**, 410–416.
- 61 S. H. Lau, M. A. Borden, T. J. Steiman, L. S. Wang, M. Parasram and A. G. Doyle, *J. Am. Chem. Soc.*, 2021, **143**, 15873–15881.
- 62 H. A. Sakai, W. Liu, C. “Chip” Le and D. W. C. MacMillan, *J. Am. Chem. Soc.*, 2020, **142**, 11691–11697.
- 63 T. J. Steiman, J. Liu, A. Mengiste and A. G. Doyle, *J. Am. Chem. Soc.*, 2020, **142**, 7598–7605.
- 64 M. Parasram, B. J. Shields, O. Ahmad, T. Knauber and A. G. Doyle, *ACS Catal.*, 2020, **10**, 5821–5827.
- 65 L. M. Kammer, S. O. Badir, R.-M. Hu and G. A. Molander, *Chem. Sci.*, 2021, **12**, 5450–5457.
- 66 J. Yi, S. O. Badir, L. M. Kammer, M. Ribagorda and G. A. Molander, *Org. Lett.*, 2019, **21**, 3346–3351.
- 67 R. J. Perkins, D. J. Pedro and E. C. Hansen, *Org. Lett.*, 2017, **19**, 3755–3758.

- 68 H. Li, C. P. Breen, H. Seo, T. F. Jamison, Y.-Q. Fang and M. M. Bio, *Org. Lett.*, 2018, **20**, 1338–1341.
- 69 T. Koyanagi, A. Herath, A. Chong, M. Ratnikov, A. Valiere, J. Chang, V. Molteni and J. Loren, *Org. Lett.*, 2019, **21**, 816–820.
- 70 B. L. Truesdell, T. B. Hamby and C. S. Sevov, *J. Am. Chem. Soc.*, 2020, **142**, 5884–5893.
- 71 G. S. Kumar, A. Peshkov, A. Brzozowska, P. Nikolaienko, C. Zhu and M. Rueping, *Angew. Chem. Int. Ed.*, 2020, **59**, 6513–6519.
- 72 K.-J. Jiao, D. Liu, H.-X. Ma, H. Qiu, P. Fang and T.-S. Mei, *Angew. Chem. Int. Ed.*, 2020, **59**, 6520–6524.
- 73 M. Amatore and C. Gosmini, *Angew. Chem. Int. Ed.*, 2008, **47**, 2089–2092.
- 74 X. Yu, T. Yang, S. Wang, H. Xu and H. Gong, *Org. Lett.*, 2011, **13**, 2138–2141.
- 75 Q. Qian, Z. Zang, S. Wang, Y. Chen, K. Lin and H. Gong, *Synlett*, 2013, **24**, 619–624.
- 76 H. Xu, C. Zhao, Q. Qian, W. Deng and H. Gong, *Chem. Sci.*, 2013, **4**, 4022–4029.
- 77 C. Amatore, A. Jutand, J. Périchon and Y. Rollin, *Monatshefte Für Chem. Chem. Mon.*, 2000, **131**, 1293–1304.
- 78 R. Shrestha, S. C. M. Dorn and D. J. Weix, *J. Am. Chem. Soc.*, 2013, **135**, 751–762.
- 79 S. Biswas and D. J. Weix, *J. Am. Chem. Soc.*, 2013, **135**, 16192–16197.
- 80 L. S. Hegedus and L. L. Miller, *J. Am. Chem. Soc.*, 1975, **97**, 459–460.
- 81 J. Breitenfeld, J. Ruiz, M. D. Wodrich and X. Hu, *J. Am. Chem. Soc.*, 2013, **135**, 12004–12012.
- 82 R. J. Kinney, W. D. Jones and R. G. Bergman, *J. Am. Chem. Soc.*, 1978, **100**, 7902–7915.
- 83 S. Wang, Q. Qian and H. Gong, *Org. Lett.*, 2012, **14**, 3352–3355.
- 84 Y. Dai, F. Wu, Z. Zang, H. You and H. Gong, *Chem. – Eur. J.*, 2012, **18**, 808–812.
- 85 C.-S. Yan, Y. Peng, X.-B. Xu and Y.-W. Wang, *Chem. – Eur. J.*, 2012, **18**, 6039–6048.
- 86 E. Clemmensen, *Berichte Dtsch. Chem. Ges.*, 1914, **47**, 51–63.
- 87 S. Reformatsky, *Berichte Dtsch. Chem. Ges.*, 1887, **20**, 1210–1211.
- 88 H. E. Simmons and R. D. Smith, *J. Am. Chem. Soc.*, 1958, **80**, 5323–5324.
- 89 K. R. Campos, A. Klapars, J. H. Waldman, P. G. Dormer and C. Chen, *J. Am. Chem. Soc.*, 2006, **128**, 3538–3539.
- 90 L. Jin, C. Liu, J. Liu, F. Hu, Y. Lan, A. S. Batsanov, J. A. K. Howard, T. B. Marder and A. Lei, *J. Am. Chem. Soc.*, 2009, **131**, 16656–16657.
- 91 E. Hevia, J. Z. Chua, P. García-Álvarez, A. R. Kennedy and M. D. McCall, *Proc. Natl. Acad. Sci.*, 2010, **107**, 5294–5299.
- 92 S. H. Wunderlich and P. Knochel, *Angew. Chem.*, 2007, **119**, 7829–7832.
- 93 C. I. Stathakis, S. M. Manolikakes and P. Knochel, *Org. Lett.*, 2013, **15**, 1302–1305.
- 94 S. M. Manolikakes, M. Ellwart, C. I. Stathakis and P. Knochel, *Chem. – Eur. J.*, 2014, **20**, 12289–12297.
- 95 D. Haas, D. Sustac-Roman, S. Schwarz and P. Knochel, *Org. Lett.*, 2016, **18**, 6380–6383.
- 96 Y.-H. Chen, C. P. Tüllmann, M. Ellwart and P. Knochel, *Angew. Chem. Int. Ed.*, 2017, **56**, 9236–9239.
- 97 R. D. Rieke, S. J. Uhm and P. M. Hudnall, *J. Chem. Soc. Chem. Commun.*, 1973, 2269–2270.
- 98 R. D. Rieke, P. T.-J. Li, T. P. Burns and S. T. Uhm, *J. Org. Chem.*, 1981, **46**, 4323–4324.
- 99 L. Zhu, R. M. Wehmeyer and R. D. Rieke, *J. Org. Chem.*, 1991, **56**, 1445–1453.
- 100 M. V. Hanson and R. D. Rieke, *J. Am. Chem. Soc.*, 1995, **117**, 10775–10776.

- 101 R. D. Rieke, M. V. Hanson, J. D. Brown and Q. J. Niu, *J. Org. Chem.*, 1996, **61**, 2726–2730.
- 102 A. Guijarro, D. M. Rosenberg and R. D. Rieke, *J. Am. Chem. Soc.*, 1999, **121**, 4155–4167.
- 103 K. Tanaka, S. Kishigami and F. Toda, *J. Org. Chem.*, 1991, **56**, 4333–4334.
- 104 Q. Cao, J. L. Howard, E. Wheatley and D. L. Browne, *Angew. Chem. Int. Ed.*, 2018, **57**, 11339–11343.
- 105 Q. Cao, R. T. Stark, I. A. Fallis and D. L. Browne, *ChemSusChem*, 2019, **12**, 2554–2557.
- 106 J. Yin, R. T. Stark, I. A. Fallis and D. L. Browne, *J. Org. Chem.*, 2020, **85**, 2347–2354.
- 107 C. Falenczyk, B. Pöllöth, P. Hilgers and B. König, *Synth. Commun.*, 2015, **45**, 348–354.
- 108 A. C. Jones, W. I. Nicholson, H. R. Smallman and D. L. Browne, *Org. Lett.*, 2020, **22**, 7433–7438.
- 109 V. Gutmann, *Coord. Chem. Rev.*, 1976, **18**, 225–255.
- 110 J. Duan, Y.-F. Du, X. Pang and X.-Z. Shu, *Chem. Sci.*, 2019, **10**, 8706–8712.
- 111 S. Wu, W. Shi and G. Zou, *New J. Chem.*, 2021, **45**, 11269–11274.

4 Mechanochemical Reductive Coupling of Activated Amides with Alkyl Halides

4.1 Introduction	110
4.1.1 Definitions for Non-planar Amides	110
4.1.2 Twisted / Activated Amides – Structure and Reactivity	111
4.1.3 Acyclic Twisted Amides for Use in Synthesis	113
4.1.4 Activated Amides for Reductive Cross-coupling	116
4.1.5 Twisted Amides Under Ball-milling Conditions	118
4.1.6 Outlook and Aims	118
4.2 Results and Discussion	120
4.2.1 Initial Findings	120
4.2.2 Optimisation of Reaction Conditions	120
4.2.3 Alkyl Halide Scope	127
4.2.4 Amide Backbone Scope	129
4.2.5 Assessment of Activated / Twisted Amides	131
4.2.6 Mechanistic Considerations	133
4.2.7 Scale-up	135
4.2.8 Alternative Reactivity	136
4.4 Conclusions and Future Direction	138
4.5 Bibliography	140

4.1 Introduction

In chapter 3 of this thesis, the cross-electrophile coupling reaction of aryl halides and alkyl halides was explored under ball-milling conditions. The reaction displayed some unique benefits that arise from using this technology including shorter reaction times compared to solution methods the lack of requirements for inert reaction set-ups, and most interestingly the facile mechanical activation of zero-valent metals *in situ*. To expand the capabilities of this methodology, various reductive coupling reactions comprising of different electrophiles could be explored. The selective construction of ketones remains an important reaction, particularly for late-stage functionalisation of pharmaceutical / bioactive molecules. Their formation generally relies on the use of highly basic organometallic reagents (e.g., RLi and RMgX) which can present limitations.¹ A recent approach towards acylation is through the use of twisted amides, which exhibit profound activity compared to typical planar amides.² Whilst their use for transition metal coupling with organometallic nucleophiles has been well documented, reductive coupling methods have thus far been underexplored.

4.1.1 Definitions for Non-planar Amides

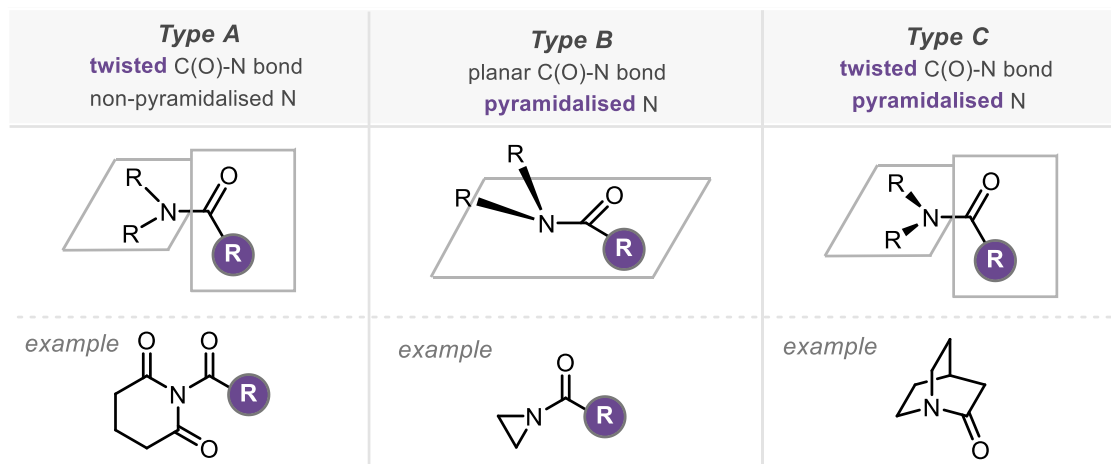
Amide bond distortion is typically defined according to Winkler-Dunitz distortion parameters.³ The twist angle (τ) represents the degree of rotation about the N-C(O) bond and pyramidalisation parameters (χ_N and χ_C) describe pyramidalisation at nitrogen and carbon. The twist angle is 0° for planar amides (e.g., formamide) and 90° for a fully perpendicular bond. Pyramidalisation parameters (χ) are 0° for planar amides and 60° for full pyramidalised bonds. Due to carbon pyramidalisation (χ_C) being 0° or close to 0° irrespective of geometry, it is usually discounted, and the primary descriptors are therefore twist angle (τ) and nitrogen pyramidalisation (χ_N).

Twisted amides can be grouped into 3 main types using a classification first introduced by Yamada (Scheme 4.1).^{2,4-6} These can be defined as:

- **Type A** – These contain a twisted C(O)-N bond ($\tau > 0^\circ$) and a non-pyramidalised nitrogen ($\chi_N \approx 0^\circ$). E.g., *N*-acyl glutarimides.
- **Type B** – These contain a planar C(O)-N bond ($\tau > 0^\circ$) and a pyramidalised nitrogen ($\chi_N > 0^\circ$). These typically arise from conformationally locked small ring systems E.g., *N*-acyl aziridines.

4 - Mechanochemical Reductive Coupling of Activated Amides with Alkyl Halides

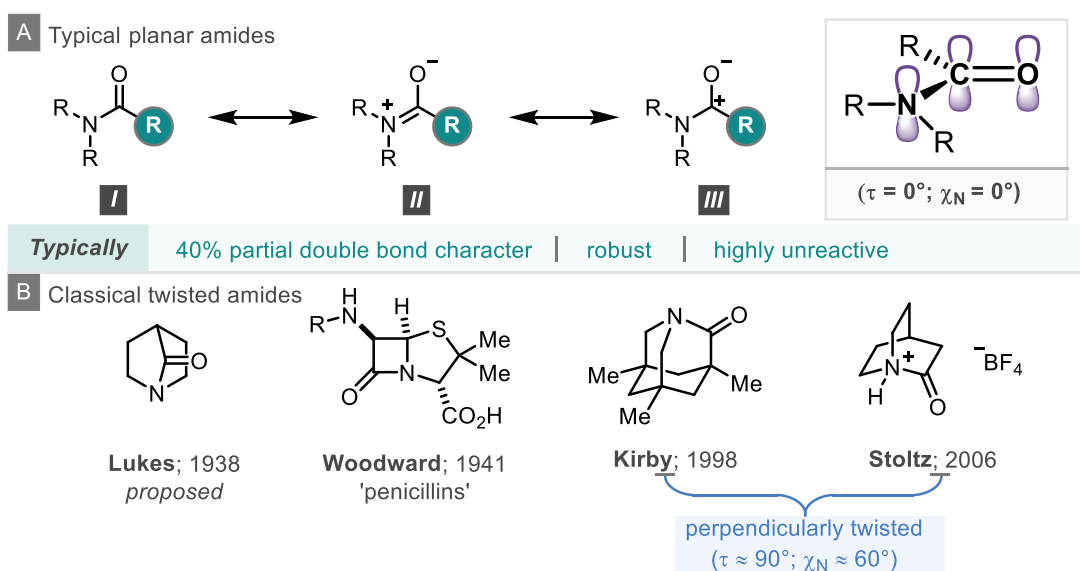
- **Type C** – These contain both a twisted C(O)-N bond ($\tau > 0^\circ$) and a pyramidalised nitrogen ($\chi_N > 0^\circ$). These systems are typically observed with conformationally restricted bridged-lactam structures.



Scheme 4.1 Classification of twisted amides

4.1.2 Twisted / Activated Amides – Structure and Reactivity

The C-N amide bond is typically regarded as being among the least reactive bonds in organic synthesis owing to ‘amidic resonance’ (Scheme 4.2A).^{7,8} Simple amides contain planar bonds of approximately 40% partial double bond character.⁹ This conjugation from the lone pair on nitrogen to the π^* orbital of the C-O bond results in a highly unreactive, robust functional group. As a result, selective organic synthesis by amide C-N cleavage remains difficult.

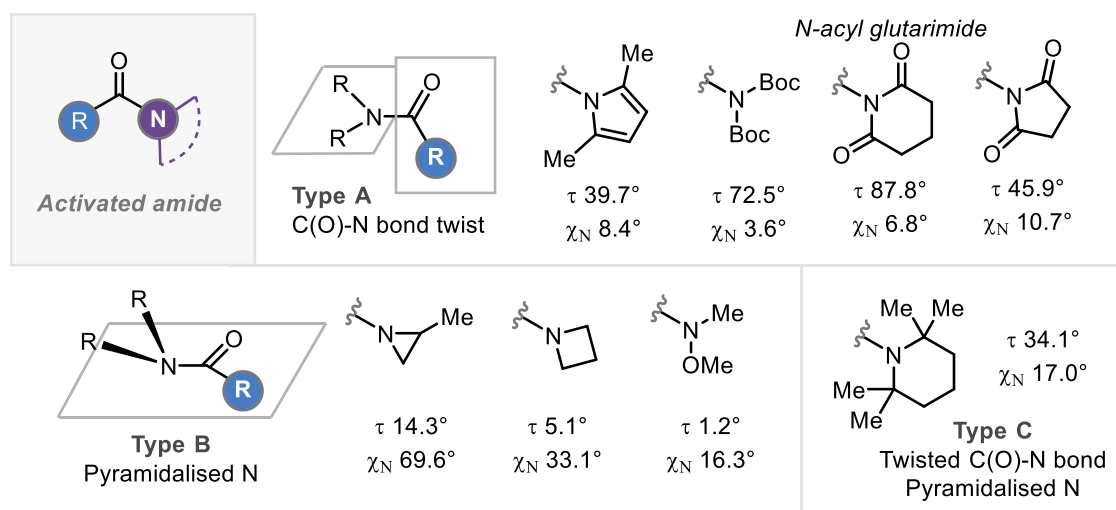


Scheme 4.2 A) Amidic resonance. B) Classical twisted amides

The chemical and structural properties of amides can be greatly affected by distortion of the amide bond. This concept has been recognised for almost a century with early studies discussing distortion as the key feature for reactivity. For example, Lukes and co-workers proposed a bridge lactam structure that was potentially distorted in 1938. This was followed by studies from Woodward and co-workers in 1941 that showed that the key factor for reactivity of β -lactam antibiotics (penicillins) was the strain of the amide bond (Scheme 4.2B). Following this, a range of different nonplanar bridged lactam structures were identified, and their properties have been explored.^{10–15} The boundaries of distorted amides was pushed to its limits by Kirby and co-workers in 1998 through the disclosure of 1-aza-2-adamantanone, which was shown to contain an almost perfectly perpendicular amide bond ($\tau = 85.8^\circ$, $\chi_N = 61.7^\circ$).^{16–18} The highly twisted amide showed remarkable properties, in that its reactivity could almost be considered the same as a ketone, leading to its unofficial definition as an amino-ketone. In 2006, Stoltz and co-workers pushed the limits of this further and disclosed the synthesis and full x-ray characterisation of 2-quinuclidinium tetrafluoroborate, which has become the archetypal twisted amide due to its near-perfect amide twist ($\tau = 85.8^\circ$, $\chi_N = 61.7^\circ$, Scheme 4.2B).¹⁹ These highly twisted, highly pyramidalised amides are considered type C non-planar amides by Yamada's definitions (*vide supra*, Section 4.1.1)

Despite their impressive structural features, conformationally restricted bridged lactams have limited use for synthetic transformations. With this in mind, there has been a recent impetus for the identification and design of acyclic amides that exhibit ground-state destabilisation through distortion of the amide bond. This has facilitated the development of many strategies for the introduction of acyl functionalities in organic synthesis either by direct nucleophilic addition or by cross-coupling after the N-C(O) bond undergoes oxidative addition to a low-valent metal.^{2,20–24} Whilst a plethora of possibilities exist, popular choices are acyclic amides that can be synthesised through simple methods (often an amide coupling directly from a carboxylic acid). There are a number of type A acyclic twisted amides that are twisted out of the plane (high τ value) either by steric influence or electronic resonance into adjacent acyl groups, or a combination of both effects (Scheme 4.3A). Acyclic type B twisted amides have also been shown to be synthetically useful. These are typically amides that are pyramidalised as a result of conformational effects (Scheme 4.3B).

4 - Mechanochemical Reductive Coupling of Activated Amides with Alkyl Halides

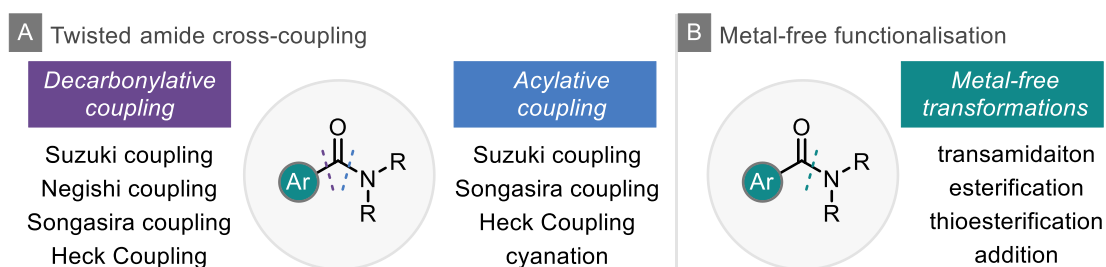


Scheme 4.3 Examples of acyclic twisted amides

N-Acyl glutarimides have emerged as a popular choice, particularly in twisted amide coupling, for several reasons, including its near perpendicular twist ($\tau = 87.8$), its stability to a range of conditions negating any decomposition pathways, and excellent activation of the N-C bond due to delocalisation of the nitrogen lone pair into the glutarimide carbonyls.

4.1.3 Acyclic Twisted Amides for Use in Synthesis

Since their inception, twisted amides have been explored extensively for a range of cross-coupling reactions (Scheme 4.4A).^{2,21,25,26} This understanding of amide bond distortion as well as development of milder conditions has also recently allowed for metal-free protocols for functionalisation (Scheme 4.4B).²⁵



Scheme 4.4 Applications of twisted amides in organic synthesis

Acyl cross coupling is a useful method for the introduction of the acyl group in synthesis. Until recently, amides were not considered useful for this transformation due to the difficulty of N-C(O) oxidative addition resulting from amidic resonance. Ground-state

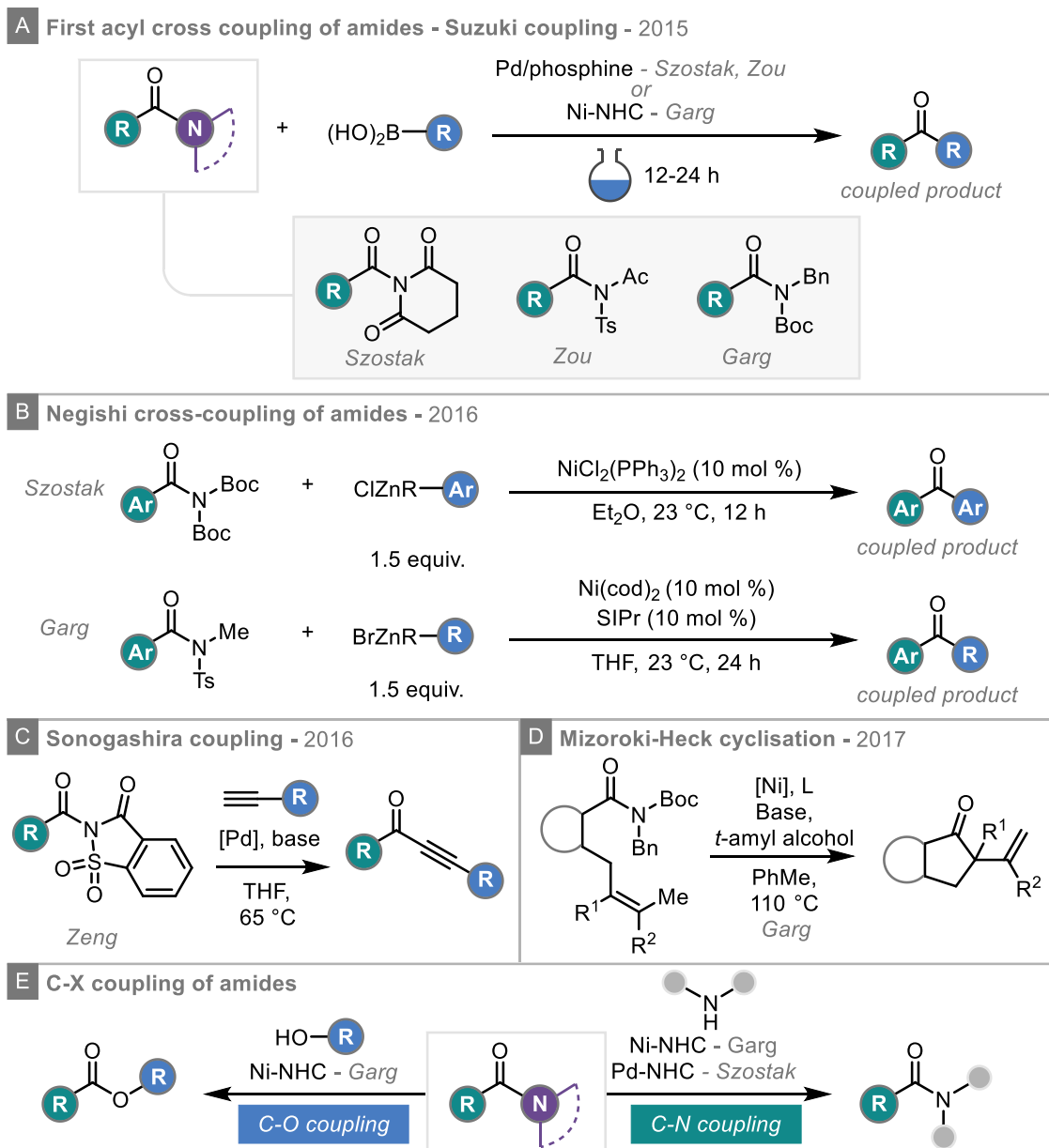
destabilisation through twisted amides presents opportunities for their use in well-established transition-metal cross coupling reactions.

C-C Bond formation remains a key reaction in organic synthesis and a useful method for this construction is through the Suzuki-Miyaura cross-coupling. The first examples of selective acyl-cross coupling of amides with organoboranes were reported in quick succession by Szostak, Zou and Garg in 2015 (Scheme 4.5A).²⁷⁻²⁹ Each of the reports achieves selective N-C(O) bond oxidative addition through destabilisation of the amide bond in different twisted amides and makes use of either Pd/phosphine or Ni/NHC catalysis. This pioneering work led to a multitude of reports addressing various aspects of the reaction to access a wider range of applications, increase the scope of amide electrophiles and discover milder conditions. A particularly interesting variation of twisted amide Suzuki coupling is a base-free protocol developed by Amgoune.³⁰ In this study the use of twisted amides for orthogonal functionalisation is explored by robustness in a ruthenium-photoredox reaction followed by successful palladium coupling.

Ketone synthesis by palladium or nickel catalysed Negishi cross couplings have also been described with initial work disclosed in separate reports by Szostak and Garg (Scheme 4.5B).^{31,32} Both reports showed excellent scope for coupling of amides with aryl or alkyl organozinc reagents under exceptionally mild room temperature conditions. In addition, other C-C bond forming reactions have been demonstrated by way of a Sonogashira coupling for the construction of ynones (Scheme 4.5C) and intramolecular Heck coupling for the synthesis of cyclic ketones. (Scheme 4.5D).^{33,34}

Acyl cross-coupling has also been demonstrated for C-O and C-N coupling (Scheme 4.5E). In fact, the nickel-catalysed esterification process developed by Garg and co-workers represents one of the first reported couplings of amides.³⁵ This process was then modified for the inclusion of alkyl amide substrates and lower catalyst loadings.^{36,37} The esterification approach was then shown to be successful using other first row transition metals as catalysts (cobalt and manganese).^{38,39} Similarly to esterification, mild C-N acyl coupling for transamidation of amides has also been developed, with this work again led by Garg and Szostak. As with previous coupling reactions, Garg opted for a Ni-NHC approach,^{40,41} whilst Szostak employed a Pd-NHC system.⁴²⁻⁴⁴ Since these initial reports, methods for metal-free esterification and transamidation of amides have been established.⁴⁵⁻⁴⁹

4 - Mechanochemical Reductive Coupling of Activated Amides with Alkyl Halides



Scheme 4.5 Acyl cross-coupling of twisted amides

Whilst acyl cross-coupling has clearly been at the forefront for amide functionalisations, a recent surge in interest has led to the discovery of decarbonylative coupling protocols. These typically proceed by initial oxidative addition of the destabilised N-C bond and subsequent CO de-insertion. These systems have been shown to be widely applicable to several transition-metal (predominantly nickel) catalysed cross-coupling reactions including Suzuki-Miyaura,^{50,51} Mizoroki-Heck,⁵² and Sonogashira couplings,^{53,54} in addition to decarbonylative amidation, borylation, and cyanation reactions.⁵⁵⁻⁵⁸

4.1.4 Activated Amides for Reductive Cross-coupling

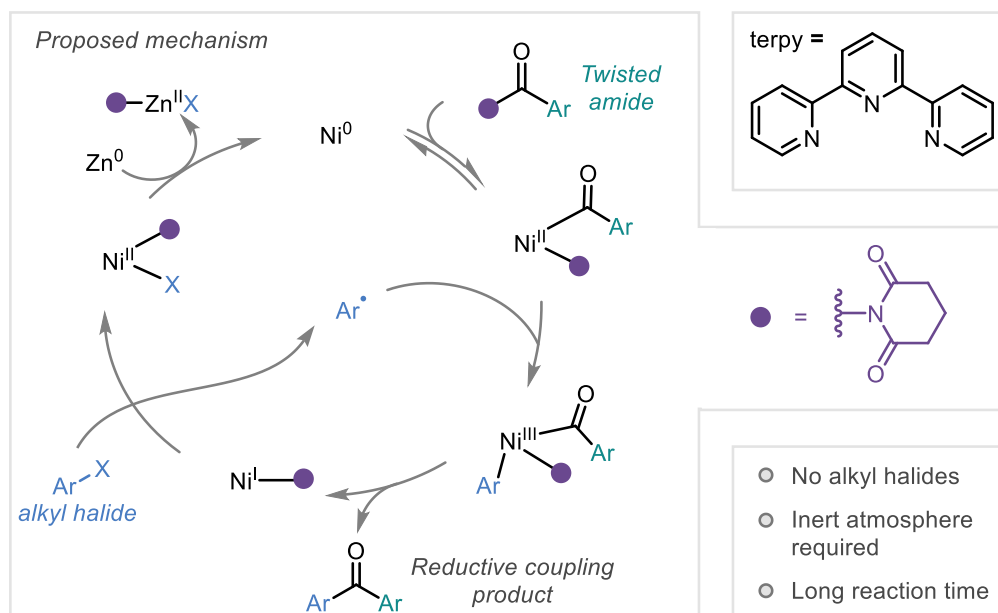
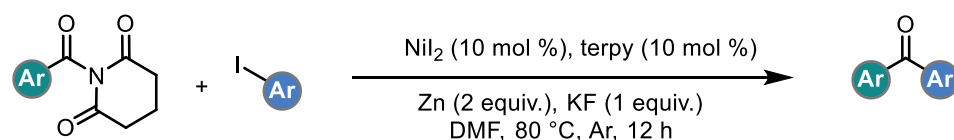
As discussed in the previous section, conventional cross-coupling of twisted amides have been explored extensively since 2015 for both acyl coupling and decarbonylative coupling manifolds. However, their use in open-shell radical processes is underexplored.

An early photoredox example from Molander and co-workers takes advantage of the activated N-C bond in *N*-acyl succinimides for a nickel-catalysed coupling with alkyl radicals generated from single electron oxidation of alkyl trifluoroborates, aided by iridium photocatalysis.⁵⁹ This initial facile oxidative addition of activated amides to a nickel catalyst and subsequent radical transmetalation is akin to that observed with the well-defined radical chain mechanism that is operational for many reductive coupling transformations, the most notable of which is nickel-catalysed cross-electrophile coupling, a concept first pioneered by Weix and co-workers.^{60–64}

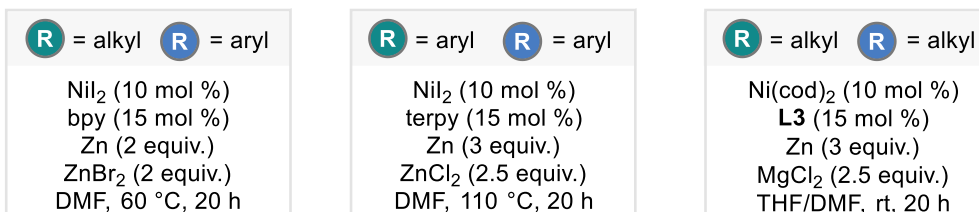
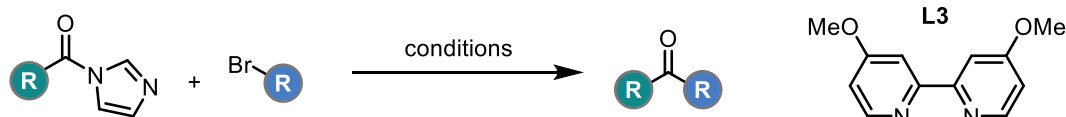
Reductive coupling methods have also been developed whereby a stoichiometric reductant is used to complete the catalytic cycle. The first report of reductive cross-coupling enabled by C-N activation was presented by Han and co-workers and describes the coupling of almost perfectly twisted *N*-acyl glutarimides with aryl iodides to afford diaryl ketones (Scheme 4.6A).⁶⁵ Following radical probe studies, the Ni/Zn mediated reaction was proposed to proceed by the same radical chain mechanism initially proposed by Weix.⁶² Oxidative addition of the twisted amide occurs, followed by radical addition to give a Ni(III) species. Reductive elimination of the dialkyl ketone can then occur, and the resulting Ni(I) species is then used for single electron reduction of the aryl iodide, giving the aryl radical required for addition. Zinc then regenerates the active Ni(0) catalyst following reduction of the Ni(II) species. This initial report shows only coupling of aryl iodides, and the protocol required strictly inert conditions using DMF in solvent quantities.

4 - Mechanochemical Reductive Coupling of Activated Amides with Alkyl Halides

A Reductive coupling of amides with aryl iodides Han - 2017



B Reductive coupling of amides with aryl bromides Li - 2020



- Natural products demonstrated
- Glovebox conditions
- ZnCl₂ requires melting

Scheme 4.6 Ni-catalysed reductive coupling of activated amides

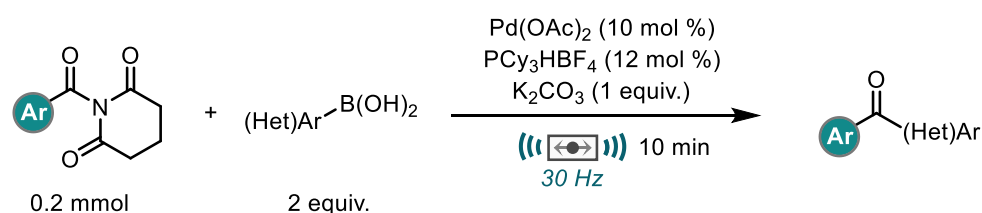
A later report by Li and co-workers greatly expanded the scope of the reaction using easy-to-prepare acyl imidazoles as the activated amide component (Scheme 4.6B).⁶⁶ These amides behave differently to the previous twisted amides discussed thus far in this chapter (*N*-acyl glutarimides / succinimides etc.) in that C-N bond activation is achieved through single-electron reduction of the amide instead of ground-state distortion. Due to this, the mechanism is a bit more contentious, although evidence was given for the intermediacy of acyl radicals. The described protocol showed excellent

tolerance, with aryl or alkyl amides shown to couple to aryl or alkyl bromides and aryl amides shown to couple with aryl bromides. Late-stage application to natural product derivatisation was also demonstrated showing the excellent capabilities of this procedure. However, there are some limitations with the protocol. Due to the use of zinc and air sensitive nickel catalysts in some cases, glovebox manipulation is required for the reaction. DMF is also used in solvent quantities, which could present issues with restrictions for its use currently being assessed. In addition, ZnCl_2 must be melted prior to use to remove any water from the salt.

Improved methods have been shown for radical coupling amides through photoredox / nickel dual catalysis using silyl radicals as well as deaminative coupling with Katritzky salts derived from primary amines.^{67,68}

4.1.5 Twisted Amides Under Ball-milling Conditions

Simultaneously to the experimental work reported further in this chapter (Section 4.2), Szostak and co-workers reported the first example of the use of twisted amides under mechanochemical conditions.⁶⁹ In this report, the authors disclosed a Pd-catalysed Suzuki cross-coupling of *N*-acyl glutarimides with a range of (hetero)aryl boronic acids for the solvent-free construction of diaryl ketones (Scheme 4.7). The described protocol allowed for effective coupling using 10 mol % $\text{Pd}(\text{OAc})_2$ after just 10 minutes and could be applied for the derivatisation of carboxylic acid drug molecules. Also shown is the use of hammering as an alternative, inexpensive method for mechanochemical reactivity.



Scheme 4.7 Suzuki coupling of *N*-acyl glutarimides under ball-milling conditions

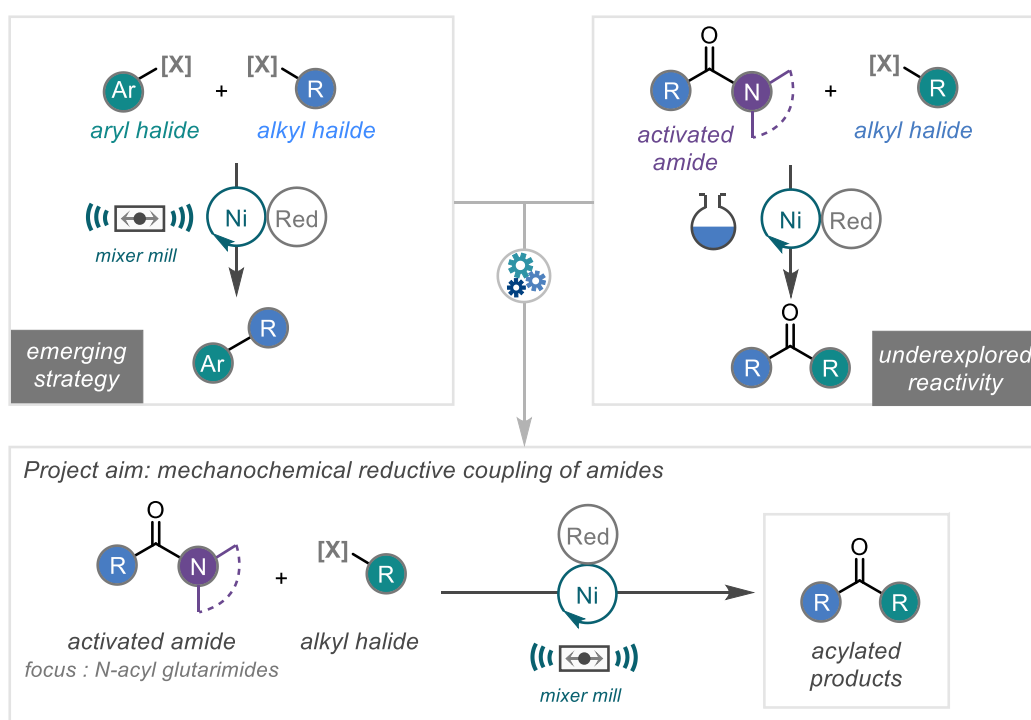
4.1.6 Outlook and Aims

Reductive coupling of amides is still in its infancy and it is possible this is due a number of reasons, including potential selectivity issues that arise from cross-electrophile coupling,⁶⁴ the requirement of inert / glovebox set ups, and the necessity to activate zero-valent metals such as zinc and manganese. Initial reports (and previous work in this thesis, Chapter 3) have identified ball-milling as an emerging strategy for the facile *in situ* mechanical activation of zinc and manganese for use in transition-metal catalysed

4 - Mechanochemical Reductive Coupling of Activated Amides with Alkyl Halides

reductive coupling manifolds, negating the need for inert set-ups or capricious chemical activation methods.^{70,71}

The aim of this project is to explore the reductive coupling reaction of twisted amides with alkyl halides for the formation of ketone products (Scheme 4.8). This represents a more complicated / underexplored reaction in comparison to previous successfully mechanochemical cross-electrophile coupling reactions and would broaden the utility of twisted amides for coupling in solvent-free / minimised environments.

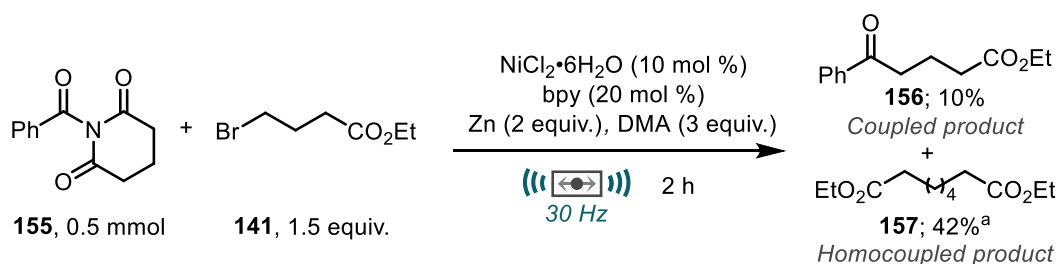


Scheme 4.8 Overview and project aims

4.2 Results and Discussion

4.2.1 Initial Findings

A good starting point for testing the nickel-catalysed reductive acylation reaction was to slightly modify conditions previously found to be successful for mechanochemical nickel-catalysed reductive coupling of aryl halides and alkyl halides.⁷⁰ The application of these conditions to the reductive acylation reaction was probed using *N*-benzoyl glutarimide (**155**, 0.5 mmol) as the activated amide and ethyl 4-bromobutyrate (**141**, 1.5 equiv.) as the alkyl halide component. An alkyl bromide was chosen due to the increased availability and stability of alkyl bromides in comparison to the analogous alkyl iodides. The reaction was carried out on a 0.5 mmol scale in a 15 mL stainless steel milling jar with a 3 g stainless steel milling ball and with no precaution taken to remove air or moisture from the reaction. The 2-hour ball-milling reductive reaction of these two electrophiles with NiCl₂•6H₂O (10 mol %), 2,2'-bipyridine (bpy, 20 mol %), zinc (2 equiv.), and DMA (3 equiv.) proceeded to afford 10% of desired coupled product **156** (Scheme 4.9). A significant quantity of alkyl homocoupled product (**157**, 42%) was also observed. This could be a result of slow oxidative addition into the twisted amide and hence homocoupling due to either radical combination or due to greater amounts of organozinc generation.



Yields determined by ¹H NMR spectroscopy using mesitylene as an internal standard. ^a Yield with respect to alkyl halide starting material **141**

Scheme 4.9 Initial reductive acylation result

With an initial set of conditions giving a promising, but low yield of desired product, optimisation studies commenced to improve the yield and decrease the quantity of unwanted homocoupling in the reaction.

4.2.2 Optimisation of Reaction Conditions

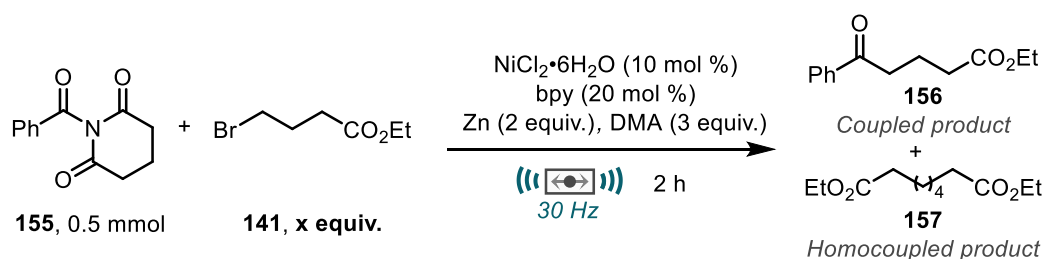
First to be investigated was the stoichiometry of the two starting materials. Since the reaction could be dependent upon the oxidative addition of the twisted amide, the amount of alkyl radical available for coupling should influence the outcome of the reaction. A

4 - Mechanochemical Reductive Coupling of Activated Amides with Alkyl Halides

larger amount of available alkyl halide for radical generation would likely result in higher coupled product yields.

To explore this, 0.5 mmol of *N*-acyl glutarimide (**155**) was subjected to the reaction conditions identified in the initial discovery phase (Scheme 4.9). However, varying amounts of alkyl halide was added as the coupling partner. An increase to 2 equivalents of **141** resulted in a desirable increase in yield to 32% of cross-coupled product **156** and proceeded to give a beneficial decrease in homocoupled product **157** (Table 4.1, entry 2). Whilst the increase in yield of desired product **156** can be explained by an increase in the amount of alkyl halide allowing for more efficient alkyl radical generation, the decrease in homocoupled product is somewhat counterintuitive, as it would be expected that an increase in alkyl halide loading would give equal or greater amounts of homocoupled product. Increasing the amount of alkyl bromide further up to 3 equivalents did not affect the coupled product yield and showed small increases in homocoupling activity (Table 4.1, entries 3-4).

Table 4.1 Investigation of alkyl halide stoichiometry



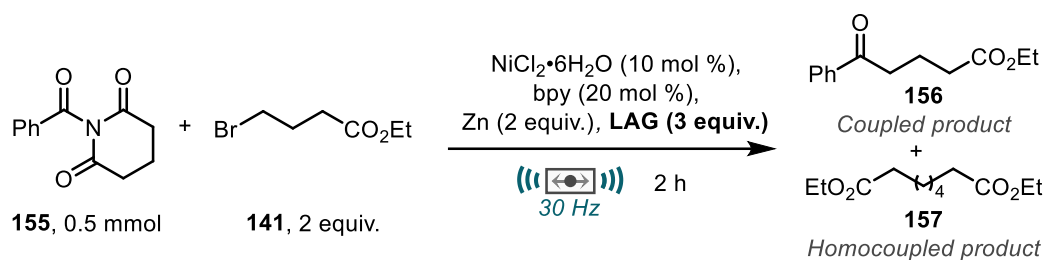
Entry	141 equiv.	Zn equiv.	Yield 156 (%) ^a	Yield 157 (%) ^{ab}
1	1.5	2	10	42
2	2	2	32	24
3	2.5	2	31	30
4	3	2	32	34
5	3	3	30	28

^a Yield determined by ¹H NMR spectroscopy using mesitylene as an internal standard. ^b Yield calculated with respect to starting material **141**.

To assess if increased loadings of zinc influenced the homocoupling pathway, the reaction with 3 equivalents of alkyl bromide was also run with an increased loading of reductant. No significant difference in yield or product distribution was observed with increased zinc loading (Table 4.1, entry 5).

Additives can often significantly affect the outcome of mechanochemical reactions. *N,N*-dimethylacetamide (DMA) has now been used on multiple occasions to aid with mechanical activation of zero-valent metals such as zinc or manganese.^{70–72} However, other additives such as THF and DMSO have also been shown to be successful, and in some favourable cases, no additive is required at all.^{73–75} To determine the necessity and/or choice of liquid additive for the coupling reaction, a range of common activators and solvents were screened as potential additives (Table 4.2).

Table 4.2 Investigation of liquid additive



Entry	LAG	Yield 156 (%) ^a	Yield 157 (%) ^{ab}
1	DMA	32	24
2	DMA (5 equiv.)	34	26
3	DMSO	25	25
4	DMF	8	17
5	NMP	5	14
6	THF	0	0
7	CH_2Cl_2	0	0
8	MeCN	0	0
9	PhMe	0	0

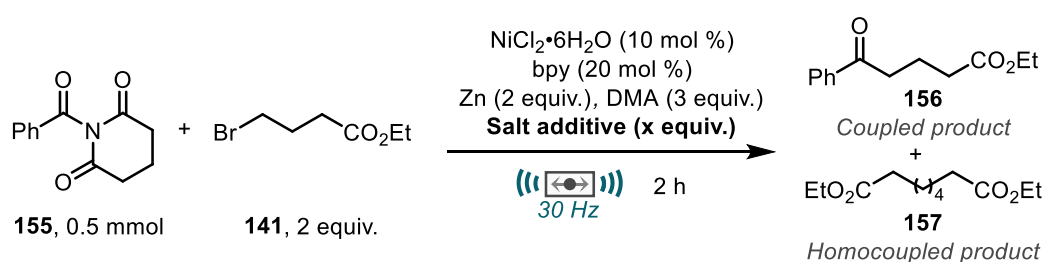
^a Yield determined by ¹H NMR spectroscopy using mesitylene as an internal standard. ^b Yield calculated with respect to starting material **141**.

Consistent with previous studies, solvents with high Gutmann donor numbers (>25) were the only additives shown to enable reactivity (Table 4.2, entries 1-4) whilst other additives showed no reactivity for either reductive coupling or homocoupling (Table 4.2, entries 5-9).⁷⁶ DMA proved to be the most successful in the reaction, however a higher loading (5 equivalents) did not perform any better in the reaction, therefore it was determined that 3 equivalents of DMA as LAG in the reaction.

4 - Mechanochemical Reductive Coupling of Activated Amides with Alkyl Halides

In many cases, the use of solid additives can aid in mechanochemical reactivity, either through the use of innocent solid materials such as sand to give a surface for liquid reagents to react on, or by using less innocent additives such as sodium chloride to actively promote reactivity.⁷⁷⁻⁸¹ It has also been shown that readily available non-toxic chloride, bromide and sulfate salts can accelerate transition-metal catalysed cross-coupling reactions.⁸² To this end, a small variety of simple salts was trialled for use in the mechanochemical reductive acylation reaction, using 2 equivalents of solid additive in each case (Table 4.3).

Table 4.3 Addition of salt additives



Entry	Salt additive	Salt equiv.	Yield 156 (%) ^a	Yield 157 (%) ^{ab}
1	LiBr	2	32	29
2	LiCl	2	19	0
3	NaCl	2	55	32
4	NaBr	2	36	36
5	Na ₂ SO ₄	2	30	27
6	K ₂ SO ₄	2	29	28
7	NaCl	1	54	31
8	NaCl	0.5	43	28

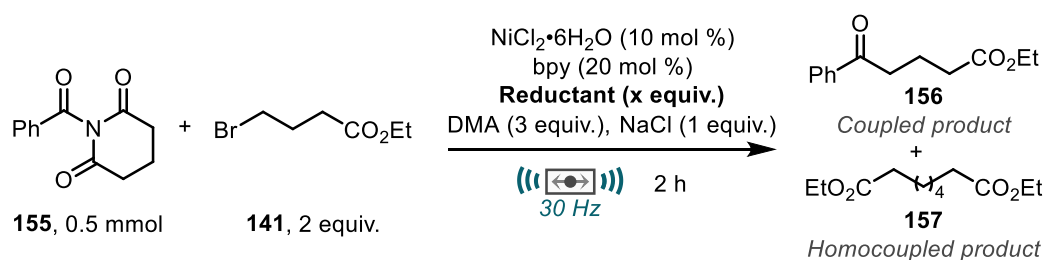
^a Yield determined by ¹H NMR spectroscopy using mesitylene as an internal standard. ^b Yield calculated with respect to starting material **141**.

The addition of lithium salts showed no improvement to the reaction yield (Table 4.3, entries 1-2). Intriguingly, lithium bromide reduced the yield of coupled product to 19%, however it also managed to completely suppress the homocoupling pathway. The rationale for this is unclear. The addition of sodium chloride furnished the best yield of **156** thus far, giving an increased yield of 55% (Table 4.3, entry 3). The use of sodium bromide, sodium sulfate and potassium sulfate all showed very little deviation in yield and product distribution from that observed in the absence of salt additive (Table 4.3,

entries 4-6). The significant improvement to yield observed when using sodium chloride was explored further to establish the optimal amount of additive needed (Table 4.3, entries 7-8). Indeed, it was found that lowering the loading of additive to 1 equivalent allowed for the achievement of similar yield (54%, table 4.3, entry 7). However, lowering the amount of additive again to 0.5 equivalents saw a diminished product yield of 43% (Table 4.3, entry 7). From these studies, 1 equivalent of sodium chloride as an additive was optimal.

The significant quantities of homocoupled product formed (~30%) presents several issues. Firstly, it is assumed this homocoupling pathway will also be present and in some cases amplified when using other alkyl halides. Also, significant production of homocoupled diester product **157** resulted in challenging isolation. If the homocoupling pathway could be suppressed somewhat, it would give a more general set of conditions with which to explore the scope of the reaction. It is possible that homocoupling can occur by either radical combination of two identical alkyl radical fragments or by insertion of activated zinc into the alkyl halide partner to form an organozinc intermediate and then direct attack to another equivalent of alkyl halide starting material. Therefore, the reductant was changed from zinc to manganese since organomanganese reagents are somewhat more challenging to form, even by mechanical activation (Table 4.4).⁸³

Table 4.4 Reductant switch



Entry	Reductant	Red. equiv.	Yield 156 (%) ^a	Yield 157 (%) ^{ab}
1	Zn (flake)	2	54	31
2	Mn (powder)	2	54	2
3	Mn (pieces)	2	48	3
4	Mn (powder)	3	54	2

^a Yield determined by ¹H NMR spectroscopy using mesitylene as an internal standard. ^b Yield calculated with respect to starting material **141**.

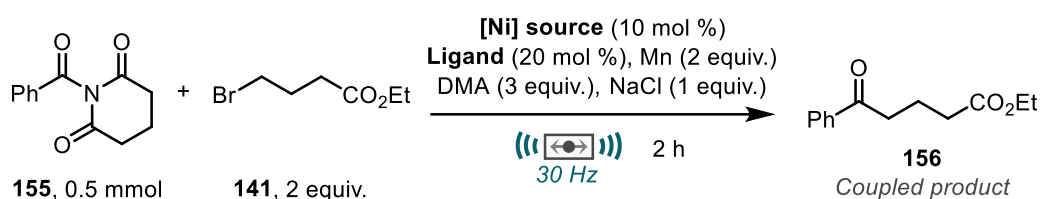
The switch from zinc to manganese powder for the coupling reaction gave an identical yield (54%) for the desired coupled product and almost completely suppressed formation

4 - Mechanochemical Reductive Coupling of Activated Amides with Alkyl Halides

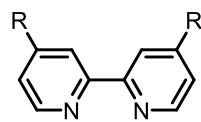
of the unwanted homocoupled product (Table 4.4, entry 2). This was also seen with manganese pieces although slightly lower coupled product was observed (Table 4.4, entry 3). Increasing the amount of manganese powder did not increase product yield (Table 4.4, entry 4). Due to the beneficial ability of suppressing homocoupling whilst maintaining product yield, manganese was chosen as the reductant for the remainder of the optimisation.

Having successfully minimised the formation of homocoupled product **157**, attention returned to increasing the yield of reductive coupled product **156** by assessment of the catalyst and ligand system (Table 4.5).

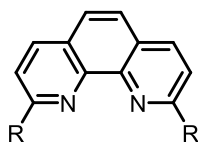
Table 4.5 Catalytic system screen



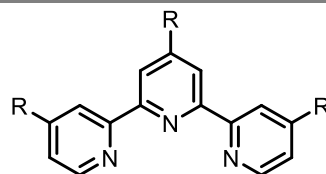
Entry	[Ni] source	Ligand	Yield 156 (%) ^a
1	NiCl ₂ •6H ₂ O	L1	54
2	NiCl ₂ •6H ₂ O	L2	46
3	NiCl ₂ •6H ₂ O	L3	62
4	NiCl ₂ •6H ₂ O	L4	76(72) ^b
5	NiCl ₂ •6H ₂ O	L5	70
6	NiCl ₂ •6H ₂ O	L6	14
7	NiCl ₂ •6H ₂ O	L7	trace
8	NiCl ₂ •6H ₂ O	-	0
9	NiCl ₂ •dme	L4	24
10	NiBr ₂ •dme	L4	31
11	NiI ₂	L4	42
12	NiCl ₂ (anhyd.)	L4	16



L1; R = H
L2; R = *t*-Bu
L3; R = OMe



L4; R = H
L5; R = Me



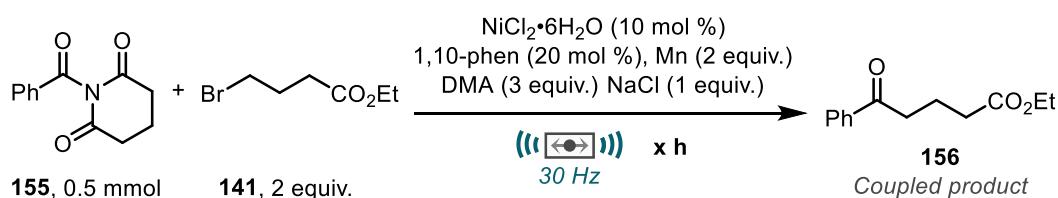
L6; R = H
L7; R = Me

^a Yield determined by ¹H NMR spectroscopy using mesitylene as an internal standard.

^b Isolated yield.

A range of commonly employed bidentate nitrogenic ligands were screened. It was found 4,4'-dimethoxybipyridine (**L3**) gave a slightly improved yield of 62% (Table 4.5, entry 3). However, greater improvement was seen using 1,10-phenanthroline (**L4**), affording 76% yield of **156** (Table 4.5, entry 4). This proved to be slightly higher than neocuproine (**L5**, table 4.5, entry 5). Terpyridine-type ligands were unsuccessful in the reaction (Table 4.5, entries 6-7). The absence of ligand also resulted in no coupling and instead returned quantitative amount of twisted amide **155** (Table 4.5, entry 8). Alternative nickel sources were also screened in combination with **L4**, as this ligand gave the best results (Table 4.5 entries 9-11). In all cases, the yield obtained was significantly reduced (24-42%) from that observed using NiCl₂·6H₂O (76%). Anhydrous NiCl₂ also gave very poor yield in comparison to the hexahydrate counterpart (16%, Table 4.5, entry 12). From the catalytic system studies, it was discovered that the most active combination was NiCl₂·6H₂O and 1,10-phenanthroline (**L4**).

Table 4.6 Reaction time optimisation



Entry	Time (h)	Yield 156 (%) ^a
1	1	79
2	2	85(80)^b
3	3	61
4	4	67

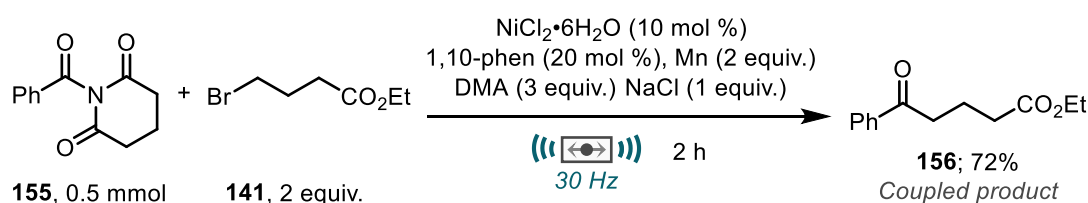
^a Yield determined by ¹H NMR spectroscopy using mesitylene as an internal standard.

^b Isolated yield.

4 - Mechanochemical Reductive Coupling of Activated Amides with Alkyl Halides

Finally, reducing the reaction time showed diminution of reaction yield (Table 4.6, entries 2-3) and increasing reaction time gave no improvement in the yield of acylated product **156** and instead showed decrease in product yield suggesting a potential decomposition pathway (Table 4.6, entry 4).

To conclude optimisation studies, after careful consideration of reaction parameters, the optimal conditions for mechanochemical reductive acylation was determined to be 2 equivalents of alkyl halide, NiCl₂·6H₂O (10 mol %), 1,10-phenanthroline (20 mol %), manganese powder (2 equiv.), DMA (3 equiv.) and sodium chloride (1 equiv.) affording the acylated product in 72% isolated yield after 2 hours for the parent reaction (Scheme 4.10).



Scheme 4.10 Optimised conditions. Isolated yield reported.

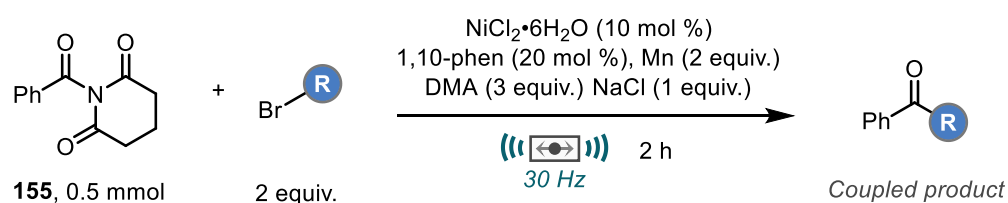
4.2.3 Alkyl Halide Scope

After the identification of optimal conditions for mechanochemical reductive coupling of twisted amides, attention was turned to the application of the reaction. First to be explored was the tolerance to various alkyl halide coupling partners (Scheme 4.11)

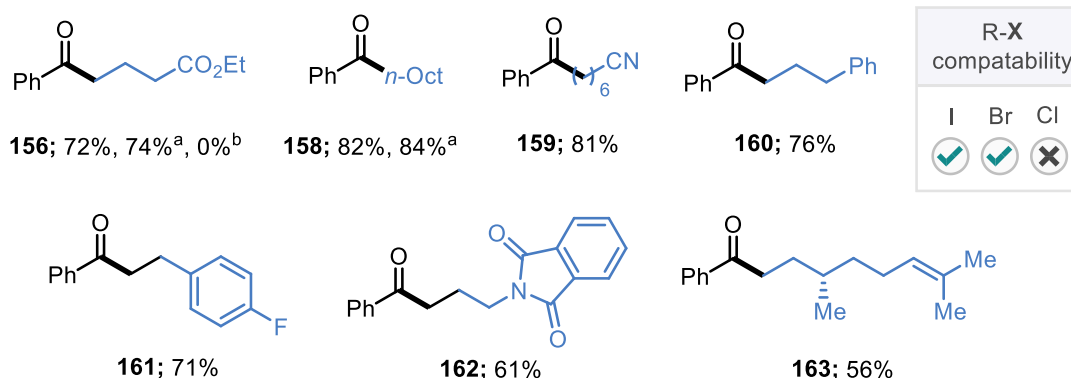
Firstly, it was found that the coupling of alkyl iodides was also possible as shown by the coupling of *N*-benzoyl glutarimide **141** with ethyl 4-iodobutyrate and 1-iodooctane to give cross-coupled products **156** and **258** respectively in excellent yields. The yield achieved from using alkyl iodides was very similar to that achieved using the corresponding alkyl bromides. Unfortunately, the reductive coupling of alkyl chloride fragments was not possible, and the reaction with ethyl 4-chlorobutyrate returned quantitative amounts of starting material showing that no coupling or homocoupling is occurring (**156**, Scheme 4.11).

A range of simple chain primary alkyl halides were coupled in excellent yield under the standard conditions (Scheme 4.11). Tolerance to functional groups was also shown by the coupling of alkyl halides containing a carboxylic ester (**156**, 72%), nitrile (**158**, 82%), protected amine / phthalimide (**162**, 61%), or alkene group (**163**, 56%).

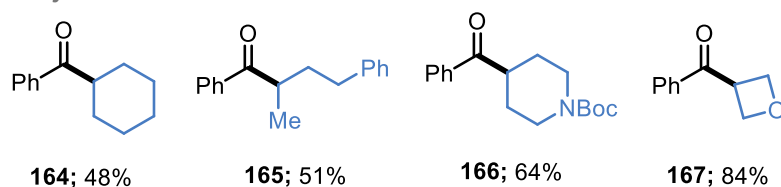
Application to secondary halides was also possible, however lower yields were typically observed. It was discovered that in all cases an extended reaction period of 3 hours provided improved results and that extending the time beyond this point did not improve the yield of acylated product. Therefore, secondary halides were all run for 3 hours. Otherwise unfunctionalised cyclic and acyclic alkyl halide fragments underwent reductive acylation to give moderate yields of coupled product (48-51%, **164** and **165**). *N*-Boc protected 4-bromopiperidine also proceeded to give good yield of cross-coupled product (64%, **166**). Pleasingly, oxetane fragments, which serve as a bioisostere for carbonyl functionality, could be introduced in excellent yield as shown by the coupling of 3-bromooxetane to give 84% of **167**.



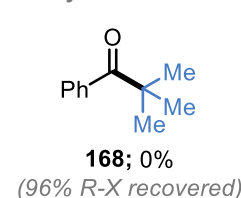
1° alkyl halides



2° alkyl halides^c



3° alkyl halides^c



Isolated yields reported. ^a Alkyl iodide used instead of alkyl bromide. ^b Alkyl chloride used instead of alkyl iodide. ^c 3 hour reaction time.

Scheme 4.11 Alkyl halide scope

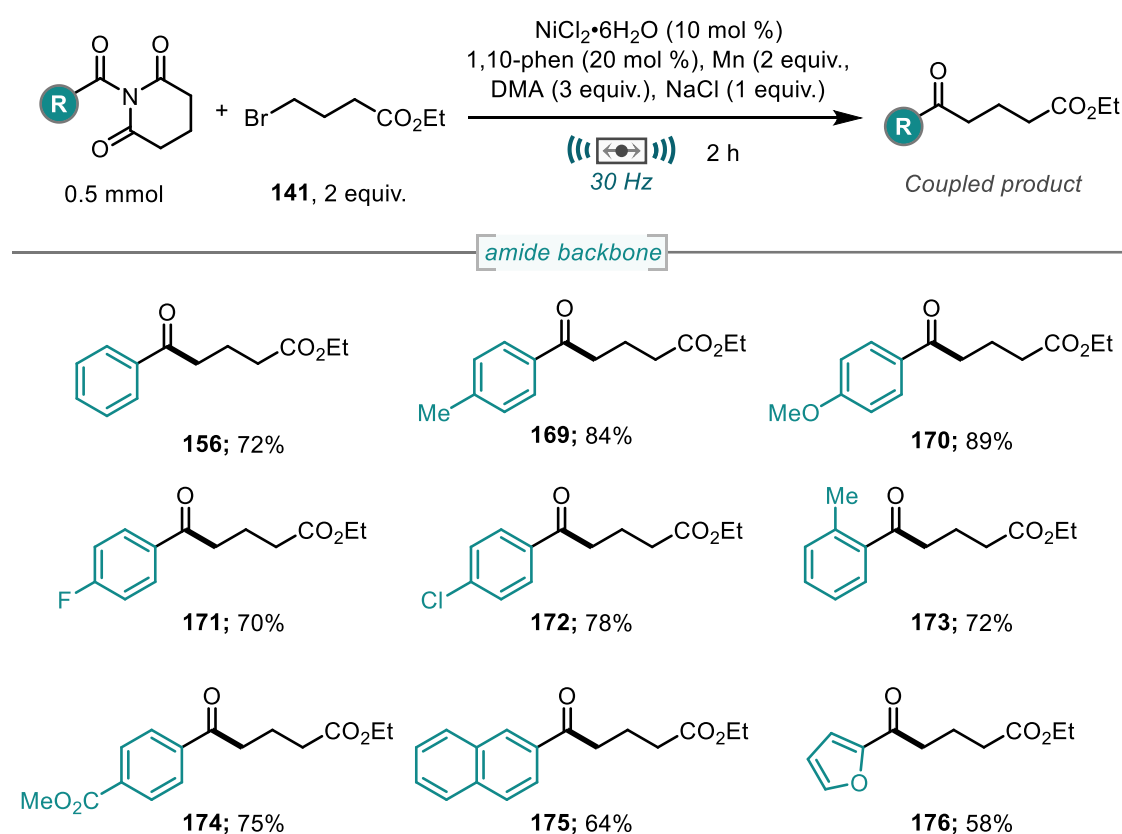
Unfortunately, challenging tertiary alkyl halides proved ineffective in the reaction, even with extended reaction times, as demonstrated by the 3-hour reaction of *N*-benzoyl glutarimide (**151**) with tert-butyl iodide affording no product (**168**). Since almost all (96%)

4 - Mechanochemical Reductive Coupling of Activated Amides with Alkyl Halides

of the tertiary iodide was isolated following unsuccessful coupling, it is assumed that the radical formation from tertiary halides is not possible under these reaction conditions.

4.2.4 Amide Backbone Scope

Having established tolerance and limitations with respect to the alkyl halide coupling partner, attention next turned to the twisted / activated amide component to assess various functionality upon the backbone of the amide (i.e., the group connected at C-C(O) rather than C(O)-N). Initially, aryl amide (benzamide) type-structures were investigated for the formation of aryl-alkyl ketones. For this, a range of *N*-benzoyl glutarimides bearing differing functionality around the ring were coupled using the standard conditions and ethyl-4-bromobutyrate (**141**) as the alkyl halide partner (Scheme 4.12).

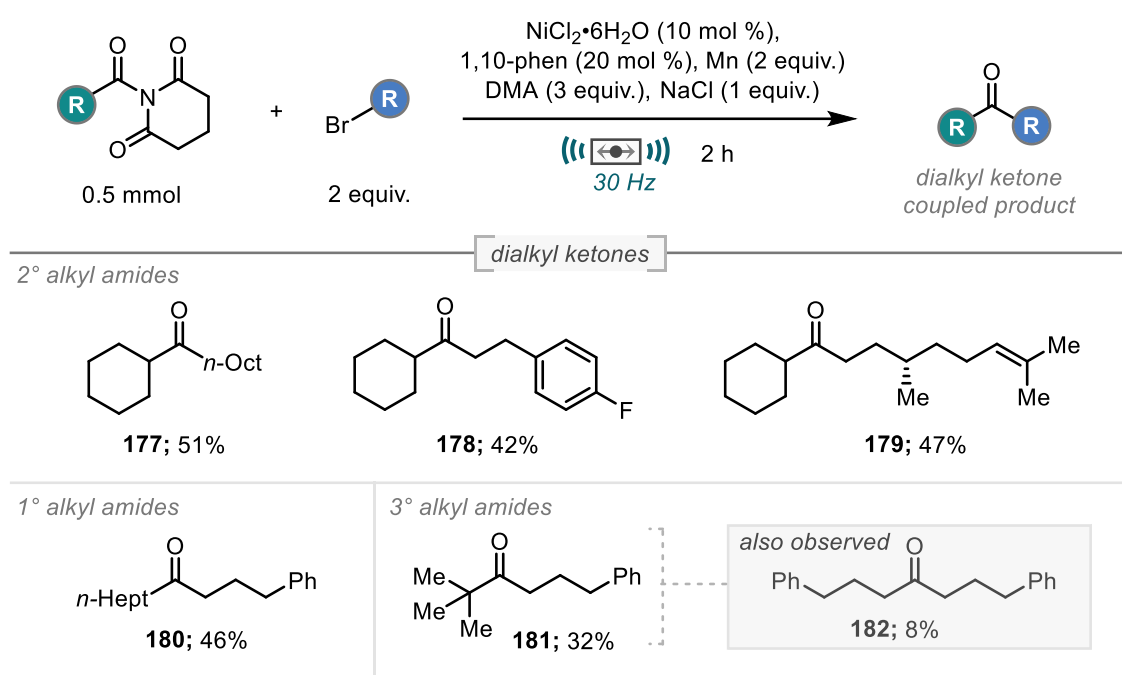


Isolated yields reported.

Scheme 4.12 Aryl group tolerance on *N*-acyl glutarimides

The nickel-catalysed mechanochemical methodology was shown to be tolerant to different electronic factors. Amides bearing electron-neutral aromatics performed well in the reaction (Scheme 4.12; 64-84%; **156**, **169**, **173**, and **175**). Electron-withdrawing

carboxylic ester functionality had little effect on the yield of the reaction (75%, **174**) and an electron-rich anisole derivative gave increased yield of 98% (Scheme 4.12, **170**). In addition, the sterically hindered *ortho*-substituted *N*-acyl glutarimide (**155**) was coupled successfully with no detrimental effect on reactivity. For a substrate containing an aryl chloride, which serves as another possible coupling site, complete selectivity was seen for amide coupling over chloroarene coupling (78%, **172**), leaving a synthetically useful handle (aryl chloride) for potential further derivatisation. Twisted amides derived from furan were also shown to achieve moderate yield in the reaction demonstrating tolerance for heteroaromatic functionality (58%, **176**).



Isolated yields reported.

Scheme 4.13 Alkyl twisted amide coupling for dialkyl ketones synthesis

The investigation into possible functionality on the amide coupling partner continued by exploring coupling reaction between alkyl twisted amides and alkyl halides to synthesis dialkyl ketones, which is a motif that appears regularly in pharmaceutical and bioactive molecules.^{84,85} Methods for their synthesis often rely on the reaction of organometallic reagents with alkyl acid chlorides.⁸⁴ A small range of alkyl amides were shown to couple successfully in the mechanochemical reductive coupling reaction (Scheme 4.13). An acyl glutarimide connected to a secondary alkyl fragment (cyclohexyl) successfully furnished dialkyl ketone products upon reaction with three different alkyl halide partners (including (*S*)-citronellyl bromide), albeit in reduced yields to that observed for aryl-alkyl ketone formation (42-51%). Amides connected to primary alkyl fragments also proved possible

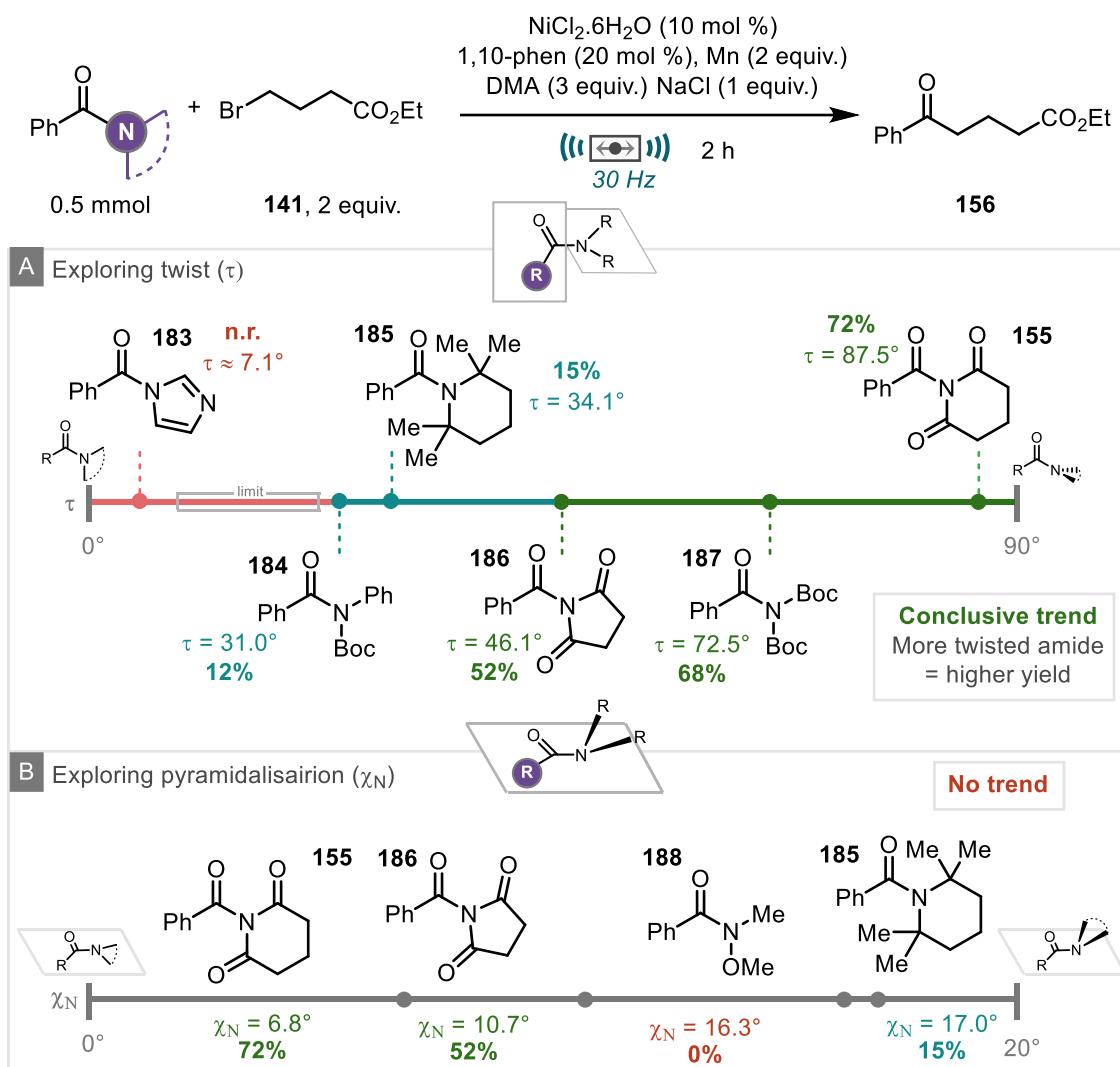
4 - Mechanochemical Reductive Coupling of Activated Amides with Alkyl Halides

as evidenced by the coupling reaction of the *n*-octanoic acid derived acyl glutarimide with 3-phenylbromopropane affording 46% of the dialkyl ketone product (Scheme 4.13, **180**). A twisted amide connected to a tertiary carbon centre (derived from pivalic acid) resulted in a lower yield of 32% cross-coupled product **181** when reacted with 3-phenylbromopropane and afforded a significant amount of alkyl halide homocoupled product. Curiously, a small quantity (~8%) of an additional side product was observed in this reaction. This symmetrical ketone product, 1,7-diphenylheptan-4-one (**182**), appears to be the homocoupled alkyl halide product, but with the insertion of a carbonyl group between the two identical alkyl chains. An altered mechanistic pathway, whereby CO extrusion / recombination is enabled, must be operational to achieve this symmetrical ketone product since the carbonyl fragment must originate from the twisted amide coupling partner.

4.2.5 Assessment of Activated / Twisted Amides

The final aspect of the reaction to be explored was the assessment of the twisted amide component. *N*-Benzoyl glutarimide exhibits an exceptionally high 'out of plane' twist (τ) value for the N-C(O) bond of 87.8°. It was anticipated that in line with previous studies, amides with lower twist values would be less active in the mechanochemical reaction.^{2,26,86,87}

Several different amides with varying twist values (τ) were subjected to the standard reaction conditions using the parent ethyl 4-bromobutyrate (**141**) as the alkyl halide partner (Scheme 4.14A). *N*-Benzoyl glutarimide **155**, with its near perpendicular twist (87.5°), afforded 72% of ketoester **156**. From this point, as anticipated, a clear trend emerged demonstrating that as the twist angle is reduced, so too is the yield of cross coupled product. Specifically, the results showed that *N*-benzoyl glutarimide **155** (72%, 87.5) gave the highest yield, and then the reaction gave decreasing yields through di-*tert*-butylcarbonate amide **187** (72.6°, 68%), *N*-acyl succinimide **186** (46.1°, 52%), TMP-amide **185** (34.1°, 15%) and *N*-Ph, Boc amide **184** (31°, 12%). *N*-Acyl imidazole **183** afforded no product for attempted coupling, suggesting oxidative insertion did not occur, mostly due to the planar structure of the amide. Whilst the twist for this amide is not exact, it is estimated to be around only 7° for the mesityl analogue.



Scheme 4.14 Assessment of twisted amides

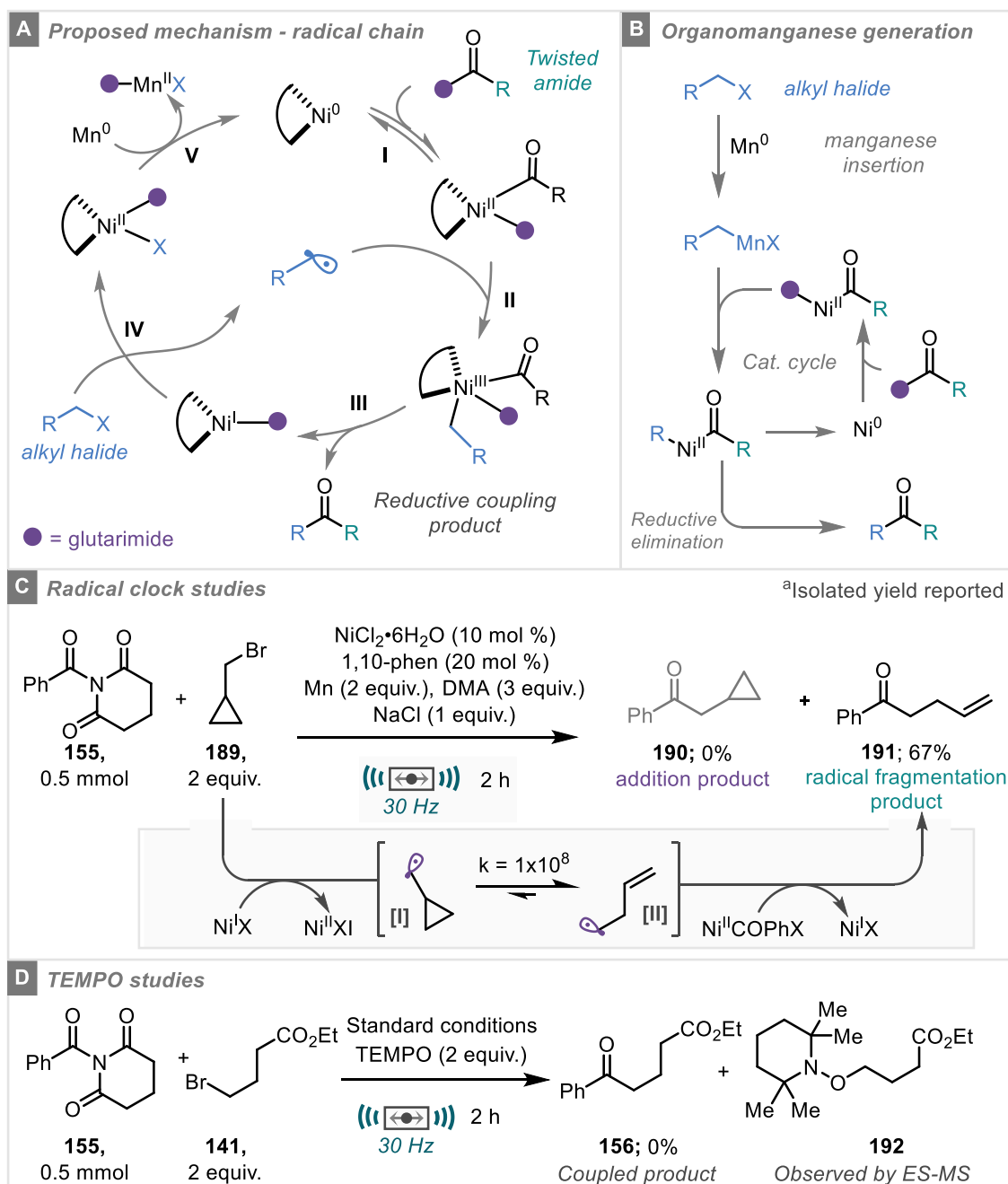
Having considered the twist angle (τ) of the N-C(O) bond and determined a strong correlation between the twist value and activity in the reaction, studies were carried out to assess any contribution of nitrogen pyramidalisation (χ_N) to the outcome of the reaction (Scheme 4.14B). *N*-b-Benzoyl glutarimide (**155**), in contrast to its exceptionally high twist value, has a low nitrogen pyramidalisation ($\chi_N = 6.8^\circ$). The resulting 72% product yield gave a starting point to compare other twisted amides to. From the results there is no clear correlation between χ_N and the reaction yield. Increased pyramidalisation of 10.7° for *N*-benzoyl succinimide (**186**) gave 52% and further pyramidalisation increase to 16.3° for Weinreb amide **188** gave no coupled product. However, TMP-amide **185**, which has a similar value of 17.0° affords 15% of desired product **156**.

To conclude the study on the effect of amide distortion on the reductive coupling reaction, no clear inference could be made for amides with differing nitrogen pyramidalisation.

However, the degree of twist of the N-C(O) bond proved to be crucial in the reaction with lower twist values giving reduced yield.

4.2.6 Mechanistic Considerations

The catalytic cycle for this transformation was expected to proceed via a radical chain pathway akin to Weix's original work and indeed previous mechanochemical cross-electrophile coupling reactions.^{60–62,70,71} This proceeds as follows; oxidative addition of twisted amide (Scheme 4.15A, **I**), followed by radical addition of the alkyl fragment (Scheme 4.15A, **II**), and subsequent reductive elimination of the unsymmetrical ketone (Scheme 4.15A, **III**). Manganese then turns over the catalytic cycle after the single electron reduction / activation of the alkyl halide coupling partner (Scheme 4.15A, **IV** and **V**). Previous reports have discussed the excellent capability of ball-milling the formation of organozinc reagents, which in the targeted reaction here would still give the desired product *via* Negishi type coupling of the twisted amide with an alkylzinc species.^{72,74,75} In this case however, manganese was used instead of as the reductant. The formation of organomanganese species is typically regarded as more challenging than organozinc intermediates, therefore their formation was unlikely in the mechanochemical reaction. Nevertheless, a pathway detailing an *in situ* organomanganese formation followed by transmetalation akin to a Negishi cross-coupling reaction was considered (Scheme 4.15B).



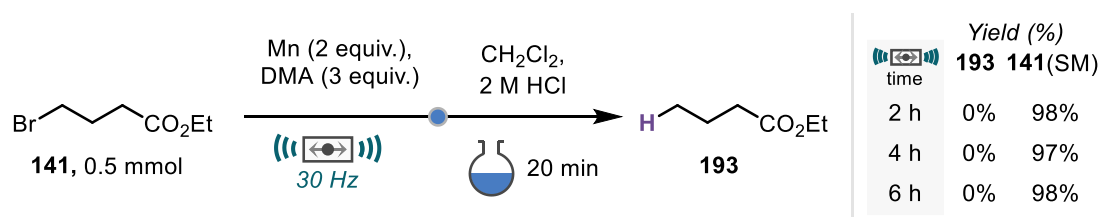
Scheme 4.15 Mechanistic studies

To probe the formation of radical intermediates, a commonly used alkyl radical clock experiment was carried out. The coupling reaction to be examined was between *N*-benzoyl glutarimide **155** and cyclopropylmethyl bromide **189**. Under the expected radical chain manifold, cyclopropylmethyl bromide would undergo a well-established radical fragmentation process (**[I]** to **[II]**), which after addition into the catalytic cycle would afford the homoallylketone product **191**. However, should the reaction proceed by a 2-electron process whereby an organomanganese intermediate is formed, this fragmentation would not take place and instead the ring closed product **190** would be observed. Under the

4 - Mechanochemical Reductive Coupling of Activated Amides with Alkyl Halides

standard mechanochemical reductive acylation conditions, the ring fragmented alkene product **191** was selectively formed and isolated in 67% yield (Scheme 4.15C). This strongly implies that the reaction proceeds by a radical process and operates similar to previous cross-electrophile coupling processes. Supporting evidence for this radical chain mechanism is shown through the observation of the TEMPO adduct **192** (by spectroscopic methods) upon addition of the radical inhibitor to the parent reaction. The adduct could not be isolated, likely due to poor stability of the N-O bond under the reductive conditions. In addition, a complete suppression in yield for coupled product **156** was observed (Scheme 4.15D)

The possible formation of organomanganese intermediates was further investigated by the application of adapted conditions previously shown to be effective for mechanochemical organozinc formation.⁷² Ethyl 4-bromobutyrate **141** was milled with manganese powder (2 equiv.) and DMA (3 equiv.) for 2-6 hours. Following the reaction period, the reaction was washed from the jar with CH₂Cl₂ and stirred with HCl (2 M) for 20 mins to hydrolyse any formed organomanganese species, allowing for crude quantification of organometallic generation via analysis of the protodehalogenated product **193**. However, 0% of this protonated product was observed in all cases, with almost complete starting material recovery observed in all cases (Scheme 4.16).

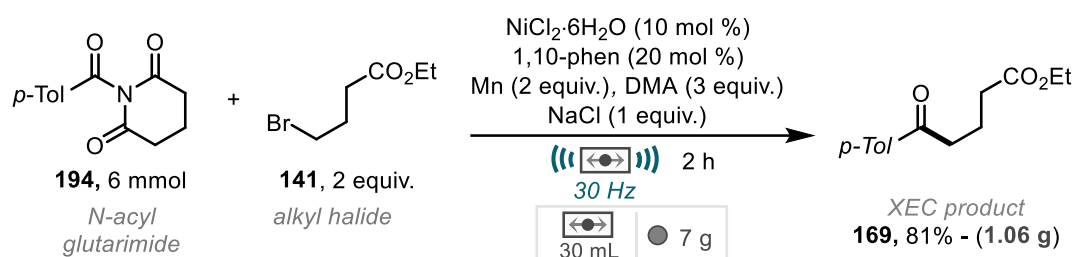


Scheme 4.16 Organomanganese generation

4.2.7 Scale-up

The optimisation and scope investigations were all carried out on a 0.5 mmol scale typically affording 50-150 mg of ketone material. Successful scale-up was possible by increasing the vessel size to a 25 mL stainless steel milling jar and using a 12 g milling ball. Twisted amide **155** (6 mmol) was coupled with ethyl 4-bromobutyrate **141** to afford 1.06 g (75%) of coupled ketoester product **156** (Scheme 4.16). This represents a slight decrease in yield from the same reaction on 0.5 mmol scale (84%, Scheme 4.12), which could be because of differing energies imparted onto the reactants by the different size balls, or a difference in filling ratio. However, this scale-up process demonstrates

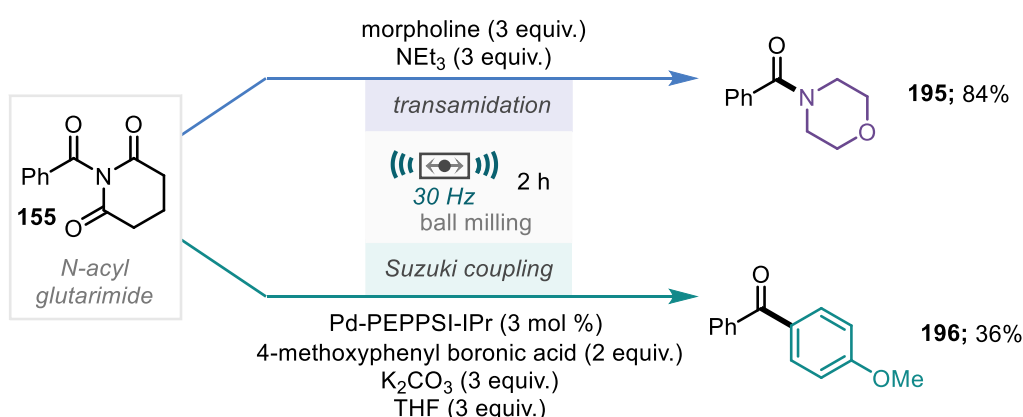
suitability to gram scale synthesis, although increasing the scale beyond this point would require careful consideration of the reaction vessel and equipment used.



Scheme 4.17 Scale up of mechanochemical twisted amide coupling

4.2.8 Alternative Reactivity

As discussed previously, *N*-acyl glutarimides have many uses outside of reductive coupling. To crudely assess the capability of these twisted amides and how they behave for alternative reaction modes under mechanochemical conditions, previously reported *N*-acyl glutarimide transformations were adapted for use under ball-milling conditions. Firstly, Szostak's conditions for transamidation were adapted for milling by removal of the reaction solvent (CH_2Cl_2).⁴⁹ Pleasingly, under these conditions, transamidation of *N*-benzoyl glutarimide **155** with morpholine proceeded excellently to give the morpholino amide **195** in 84% yield after 2 hours, which is comparable to the results achieved in solution after 24 hours (Scheme 4.18, top).



Scheme 4.18 Other reactivity of *N*-acyl glutarimides by ball-milling

A solvent minimised Pd-PEPPSI catalysed Suzuki cross-coupling was also demonstrated by adapting Szostak's conditions, using THF as a LAG instead of as the bulk solvent.⁴³ 4-Methoxyphenyl boronic acid could be coupled to give a 36% yield of **196** after 2 hours (Scheme 4.18, bottom). Simultaneously to this unreported experimental

4 - Mechanochemical Reductive Coupling of Activated Amides with Alkyl Halides

work, an optimised set of conditions was disclosed by Szostak, Zhang and co-workers using 10 mol % Pd(OAc)₂. This also represents the first published use of twisted amides in the ball-mill.⁶⁹

4.4 Conclusions and Future Direction

To conclude, this work has once again showcased the advantages of ball-milling for the activation of zero-valent metals (in this case manganese) for use in organic synthesis. The scope of Ni-catalysed reductive coupling under mechanochemical conditions has been expanded for the facile synthesis of ketones through the coupling of activated / twisted amides with alkyl halides. This negates the need for highly basic organometallics such as Grignard reagents. The ball-milling enabled reductive acylation proceeds with a much shorter reaction time than is typically seen using solution-based techniques. Coupling also occurs efficiently without the requirement for air-sensitive / glove-box techniques.

Through optimisation, it was found that inexpensive $\text{NiCl}_2 \cdot 6\text{H}_2\text{O}$ could be used as the nickel source and the addition of sodium iodide as an additive significantly improved reactivity. Key to maintaining selectivity for reductive coupling over alkyl homocoupling was the use of manganese as the reductant instead of zinc. The general method could be applied to a range of alkyl halides as well as a range of substituted *N*-acyl glutarimides including alkyl amides which allowed for the construction of unsymmetrical dialkyl ketones.

The degree of twist of the N-C(O) bond in the amide coupling partner was shown to be highly influential for the success of the reaction. Highly twisted amides such as *N*-acyl glutarimides performed excellently in the reaction, with decreasing twist angles giving decreasing yields. The effect of nitrogen pyramidalisation (χ_{N}) did not give a conclusive trend, suggesting that the 'out of plane' twist remains the crucial factor.

Evidence for the formation of alkyl radical intermediates was shown through radical clock and TEMPO studies leading to a proposed catalytic cycle akin to previous reports for cross-electrophile coupling. The formation of organomanganese intermediates was considered, however results showed little to no consumption of starting material and no formation of protodehalogenated product after hydrolysis after 6 hours. Application to gram-scale ketone synthesis was also demonstrated.

It is clear from this work and previous work on mechanochemical cross-electrophile coupling (Chapter 3 of this thesis) that whilst the system identified can be easily modified for different types of reductive coupling, alkyl chloride coupling remains a limitation. It is possible that a drastic change in catalyst / ligand system would allow for coupling of these challenging substrates.

4 - Mechanochemical Reductive Coupling of Activated Amides with Alkyl Halides

Having successfully shown coupling of twisted amides, which are derived from carboxylic acids, it would be interesting to consider a process whereby the amide could be made *in situ* under ball-milling conditions and subsequently coupled. The main obstacle with this is the use of amide coupling agents (SOCl₂, DCC, HOBT, etc.). Recently, methods for the direct amidation of esters have been reported using ball-milling conditions. As of now, weakly nucleophilic amines that often provide the basis for twisted amides (glutarimides, succinimides, etc.) have not been shown to be successful for direct amidation, however exciting work in this area could open possibilities for a 2 step-1-jar approach for the amidation and subsequent reductive coupling of carboxylic acids.

4.5 Bibliography

- 1 P. Knochel, I. Sapountzis and N. Gommermann, in *Metal-Catalyzed Cross-Coupling Reactions*, John Wiley & Sons, Ltd, 2004, pp. 671–698.
- 2 C. Liu and M. Szostak, *Chem. – Eur. J.*, 2017, **23**, 7157–7173.
- 3 F. K. Winkler and J. D. Dunitz, *J. Mol. Biol.*, 1971, **59**, 169–182.
- 4 S. Yamada, *Angew. Chem. Int. Ed. Engl.*, 1993, **32**, 1083–1085.
- 5 S. Yamada, *J. Org. Chem.*, 1996, **61**, 941–946.
- 6 S. Yamada, *Angew. Chem. Int. Ed. Engl.*, 1995, **34**, 1113–1115.
- 7 K. B. Wiberg, *Acc. Chem. Res.*, 1999, **32**, 922–929.
- 8 S. A. Glover and A. A. Rosser, *J. Org. Chem.*, 2012, **77**, 5492–5502.
- 9 Linus. Pauling, *J. Am. Chem. Soc.*, 1931, **53**, 1367–1400.
- 10 H. K. Hall and A. El-Shekeil, *Chem. Rev.*, 1983, **83**, 549–555.
- 11 S. A. Glover, in *Advances in Physical Organic Chemistry*, ed. J. P. Richard, Academic Press, 2007, vol. 42, pp. 35–123.
- 12 M. Szostak and J. Aubé, *Org. Biomol. Chem.*, 2010, **9**, 27–35.
- 13 M. Szostak and J. Aubé, *Chem. Rev.*, 2013, **113**, 5701–5765.
- 14 S. A. Glover and A. A. Rosser, *Molecules*, 2018, **23**, 2834.
- 15 R. Szostak and M. Szostak, *Molecules*, 2019, **24**, 274.
- 16 A. J. Kirby, I. V. Komarov, P. D. Wothers and N. Feeder, *Angew. Chem. Int. Ed.*, 1998, **37**, 785–786.
- 17 A. J. Kirby, I. V. Komarov and N. Feeder, *J. Am. Chem. Soc.*, 1998, **120**, 7101–7102.
- 18 A. J. Kirby, I. V. Komarov and N. Feeder, *J. Chem. Soc. Perkin Trans. 2*, 2001, 522–529.
- 19 K. Tani and B. M. Stoltz, *Nature*, 2006, **441**, 731–734.
- 20 S. A. Ruider and N. Maulide, *Angew. Chem. Int. Ed.*, 2015, **54**, 13856–13858.
- 21 G. Meng, S. Shi and M. Szostak, *Synlett*, 2016, **27**, 2530–2540.
- 22 J. E. Dander and N. K. Garg, *ACS Catal.*, 2017, **7**, 1413–1423.
- 23 D. Kaiser, A. Bauer, M. Lemmerer and N. Maulide, *Chem. Soc. Rev.*, 2018, **47**, 7899–7925.
- 24 S. Adachi, N. Kumagai and M. Shibasaki, *Tetrahedron Lett.*, 2018, **59**, 1147–1158.
- 25 G. Li, S. Ma and M. Szostak, *Trends Chem.*, 2020, **2**, 914–928.
- 26 G. Meng, J. Zhang and M. Szostak, *Chem. Rev.*, 2021, **121**, 12746–12783.
- 27 G. Meng and M. Szostak, *Org. Lett.*, 2015, **17**, 4364–4367.
- 28 X. Li and G. Zou, *Chem. Commun.*, 2015, **51**, 5089–5092.
- 29 N. A. Weires, E. L. Baker and N. K. Garg, *Nat. Chem.*, 2016, **8**, 75–79.
- 30 A. Reina, T. Krachko, K. Onida, D. Bouyssi, E. Jeanneau, N. Monteiro and A. Amgoune, *ACS Catal.*, 2020, **10**, 2189–2197.
- 31 B. J. Simmons, N. A. Weires, J. E. Dander and N. K. Garg, *ACS Catal.*, 2016, **6**, 3176–3179.
- 32 S. Shi and M. Szostak, *Org. Lett.*, 2016, **18**, 5872–5875.
- 33 M. Cui, H. Wu, J. Jian, H. Wang, C. Liu, S. Daniel and Z. Zeng, *Chem. Commun.*, 2016, **52**, 12076–12079.
- 34 J. M. Medina, J. Moreno, S. Racine, S. Du and N. K. Garg, *Angew. Chem. Int. Ed.*, 2017, **56**, 6567–6571.
- 35 L. Hie, N. F. Fine Nathel, T. K. Shah, E. L. Baker, X. Hong, Y.-F. Yang, P. Liu, K. N. Houk and N. K. Garg, *Nature*, 2015, **524**, 79–83.
- 36 L. Hie, E. L. Baker, S. M. Anthony, J.-N. Desrosiers, C. Senanayake and N. K. Garg, *Angew. Chem. Int. Ed.*, 2016, **55**, 15129–15132.
- 37 N. A. Weires, D. D. Caspi and N. K. Garg, *ACS Catal.*, 2017, **7**, 4381–4385.
- 38 Y. Bourne-Branchu, C. Gosmini and G. Danoun, *Chem. – Eur. J.*, 2017, **23**, 10043–10047.

4 - Mechanochemical Reductive Coupling of Activated Amides with Alkyl Halides

- 39 H. Nagae, T. Hirai, D. Kato, S. Soma, S. Akebi and K. Mashima, *Chem. Sci.*, 2019, **10**, 2860–2868.
- 40 E. L. Baker, M. M. Yamano, Y. Zhou, S. M. Anthony and N. K. Garg, *Nat. Commun.*, 2016, **7**, 11554.
- 41 J. E. Dander, E. L. Baker and N. K. Garg, *Chem. Sci.*, 2017, **8**, 6433–6438.
- 42 G. Meng, P. Lei and M. Szostak, *Org. Lett.*, 2017, **19**, 2158–2161.
- 43 S. Shi, P. Lei and M. Szostak, *Organometallics*, 2017, **36**, 3784–3789.
- 44 G. Li, T. Zhou, A. Poater, L. Cavallo, S. P. Nolan and M. Szostak, *Catal. Sci. Technol.*, 2020, **10**, 710–716.
- 45 G. Li, P. Lei and M. Szostak, *Org. Lett.*, 2018, **20**, 5622–5625.
- 46 D. Ye, Z. Liu, H. Chen, J. L. Sessler and C. Lei, *Org. Lett.*, 2019, **21**, 6888–6892.
- 47 G. Li, C.-L. Ji, X. Hong and M. Szostak, *J. Am. Chem. Soc.*, 2019, **141**, 11161–11172.
- 48 G. Li and M. Szostak, *Nat. Commun.*, 2018, **9**, 4165.
- 49 Y. Liu, M. Achtenhagen, R. Liu and M. Szostak, *Org. Biomol. Chem.*, 2018, **16**, 1322–1329.
- 50 Z. Luo, L. Xiong, T. Liu, Y. Zhang, S. Lu, Y. Chen, W. Guo, Y. Zhu and Z. Zeng, *J. Org. Chem.*, 2019, **84**, 10559–10568.
- 51 T. Zhou, C.-L. Ji, X. Hong and M. Szostak, *Chem. Sci.*, 2019, **10**, 9865–9871.
- 52 G. Meng and M. Szostak, *Angew. Chem. Int. Ed.*, 2015, **54**, 14518–14522.
- 53 L. Liu, D. Zhou, M. Liu, Y. Zhou and T. Chen, *Org. Lett.*, 2018, **20**, 2741–2744.
- 54 W. Srimontree, A. Chatupheeraphat, H.-H. Liao and M. Rueping, *Org. Lett.*, 2017, **19**, 3091–3094.
- 55 S.-C. Lee, L. Guo, H. Yue, H.-H. Liao and M. Rueping, *Synlett*, 2017, **28**, 2594–2598.
- 56 S. Shi and M. Szostak, *Org. Lett.*, 2017, **19**, 3095–3098.
- 57 F. Bie, X. Liu, Y. Shi, H. Cao, Y. Han, M. Szostak and C. Liu, *J. Org. Chem.*, 2020, **85**, 15676–15685.
- 58 A. Chatupheeraphat, H.-H. Liao, S.-C. Lee and M. Rueping, *Org. Lett.*, 2017, **19**, 4255–4258.
- 59 J. Amani, R. Alam, S. Badir and G. A. Molander, *Org. Lett.*, 2017, **19**, 2426–2429.
- 60 D. A. Everson, R. Shrestha and D. J. Weix, *J. Am. Chem. Soc.*, 2010, **132**, 920–921.
- 61 D. A. Everson, B. A. Jones and D. J. Weix, *J. Am. Chem. Soc.*, 2012, **134**, 6146–6159.
- 62 S. Biswas and D. J. Weix, *J. Am. Chem. Soc.*, 2013, **135**, 16192–16197.
- 63 D. J. Weix, *Acc. Chem. Res.*, 2015, **48**, 1767–1775.
- 64 D. A. Everson and D. J. Weix, *J. Org. Chem.*, 2014, **79**, 4793–4798.
- 65 S. Ni, W. Zhang, H. Mei, J. Han and Y. Pan, *Org. Lett.*, 2017, **19**, 2536–2539.
- 66 J. Zhuo, Y. Zhang, Z. Li and C. Li, *ACS Catal.*, 2020, **10**, 3895–3903.
- 67 T. Kerackian, A. Reina, D. Bouyssi, N. Monteiro and A. Amgoune, *Org. Lett.*, 2020, **22**, 2240–2245.
- 68 C.-G. Yu and Y. Matsuo, *Org. Lett.*, 2020, **22**, 950–955.
- 69 J. Zhang, P. Zhang, L. Shao, R. Wang, Y. Ma and M. Szostak, *Angew. Chem. Int. Ed.*, **n/a**, e202114146.
- 70 A. C. Jones, W. I. Nicholson, J. A. Leitch and D. L. Browne, *Org. Lett.*, 2021, **23**, 6337–6341.
- 71 S. Wu, W. Shi and G. Zou, *New J. Chem.*, 2021, **45**, 11269–11274.
- 72 Q. Cao, J. L. Howard, E. Wheatley and D. L. Browne, *Angew. Chem. Int. Ed.*, 2018, **57**, 11339–11343.
- 73 W. I. Nicholson, J. L. Howard, G. Magri, A. C. Seastram, A. Khan, R. R. A. Bolt, L. C. Morrill, E. Richards and D. L. Browne, *Angew. Chem. Int. Ed.*, 2021, **60**, 23128–23133.
- 74 J. Yin, R. T. Stark, I. A. Fallis and D. L. Browne, *J. Org. Chem.*, 2020, **85**, 2347–2354.

- 75 Q. Cao, R. T. Stark, I. A. Fallis and D. L. Browne, *ChemSusChem*, 2019, **12**, 2554–2557.
- 76 V. Gutmann, *Coord. Chem. Rev.*, 1976, **18**, 225–255.
- 77 R. Thorwirth, A. Stolle and B. Ondruschka, *Green Chem.*, 2010, **12**, 985–991.
- 78 R. Schmidt, R. Thorwirth, T. Szuppa, A. Stolle, B. Ondruschka and H. Hopf, *Chem. – Eur. J.*, 2011, **17**, 8129–8138.
- 79 J.-L. Do, C. Mottillo, D. Tan, V. Štrukil and T. Friščić, *J. Am. Chem. Soc.*, 2015, **137**, 2476–2479.
- 80 Q. Cao, W. I. Nicholson, A. C. Jones and D. L. Browne, *Org. Biomol. Chem.*, 2019, **17**, 1722–1726.
- 81 A. C. Jones, W. I. Nicholson, H. R. Smallman and D. L. Browne, *Org. Lett.*, 2020, **22**, 7433–7438.
- 82 B. Zhang, J. Song, H. Liu, J. Shi, J. Ma, H. Fan, W. Wang, P. Zhang and B. Han, *Green Chem.*, 2014, **16**, 1198–1201.
- 83 G. Cahiez, C. Duplais and J. Buendia, *Chem. Rev.*, 2009, **109**, 1434–1476.
- 84 R. K. Dieter, *Tetrahedron*, 1999, **55**, 4177–4236.
- 85 Y. Kakeno, M. Kusakabe, K. Nagao and H. Ohmiya, *ACS Catal.*, 2020, **10**, 8524–8529.
- 86 G. Meng and M. Szostak, *Eur. J. Org. Chem.*, 2018, 2352–2365.
- 87 Md. M. Rahman, C. Liu, E. Bisz, B. Dziuk, R. Lalancette, Q. Wang, H. Chen, R. Szostak and M. Szostak, *J. Org. Chem.*, 2020, **85**, 5475–5485.

5 Mechanochemical Fluorocyclisations Using a Hypervalent Fluoroiodane Reagent

5.1 Introduction	144
5.1.1 Fluorination in Organic Synthesis	144
5.1.2 Fluoroiodane Reagent Synthesis and General Application.....	146
5.1.3 Fluorocyclisation Using Fluoroiodane Reagent.....	148
5.1.4 Fluorocyclisation of β,γ -unsaturated Hydrazones and Oximes.....	149
5.1.5 Mechanochemical Fluorination	151
5.1.6 Outlook and Aims.....	153
5.2 Results and Discussion	155
5.2.1 Initial Assessment of Fluoroiodane Reagent - Mechanochemical Fluorolactonisation of Carboxylic Acids.....	155
5.2.2 Mechanochemical Amino Fluorocyclisation (Tetrahydropyridazines)....	159
5.2.3 Mechanochemical Oxy Fluorocyclisation (Dihydrooxazines)	163
5.2.4 Proposed Mechanism for Heterocycle Construction	167
5.3 Conclusions and Comparisons.....	170
5.4 Bibliography	172

5.1 Introduction

This project was carried out as part of collaboration with Dr Alison Stuart's research group at Leicester University. The project sought to identify fluorocyclisation conditions for use in both conventional solution-based set-ups and a solvent-minimised mechanochemical process. The identification of solution conditions was investigated at Leicester University by Dr William Riley and the results are not discussed in detail during this thesis, however insightful discussions between all parties during initial studies gave important points from which to build optimisation studies upon. Results obtained by Dr William Riley are clearly marked as such. Full optimisation studies for the solution-based method can be found in the recent report detailing this work.¹ The focus of this chapter will be on the identification and application of mechanochemical conditions for novel fluorinated heterocycle synthesis by fluorocyclisation.

As a result of the excellent activity of heterocycles *in vivo*, over 85% of small molecule pharmaceuticals approved by the FDA contain a nitrogen-based heterocycle as of 2019.² In addition, over 25% of approved drugs feature at least one fluorine heteroatoms. Due to this, the construction of fluorinated heterocycles is an important area of synthetic chemistry. An elegant approach is fluorocyclisation whereby a heteroatom can cyclise onto an alkene and simultaneously undergo fluorination. Whilst fluorocyclisation has been reported for the construction of fluoromethyl 5-membered dihydropyrazoles and isoxazoles, the selective construction of 5-fluoro tetrahydropyridazines and dihydrooxazines has not yet been explored (Figure 5.1).

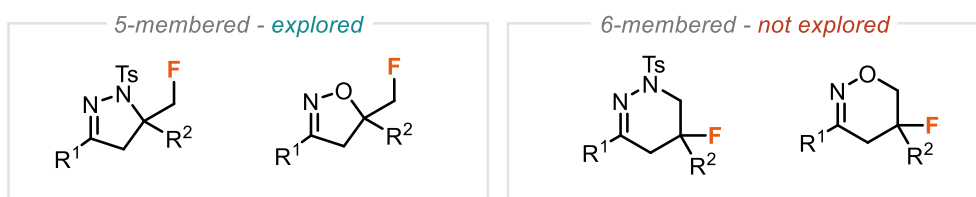


Figure 5.1 Fluorinated heterocycles

5.1.1 Fluorination in Organic Synthesis

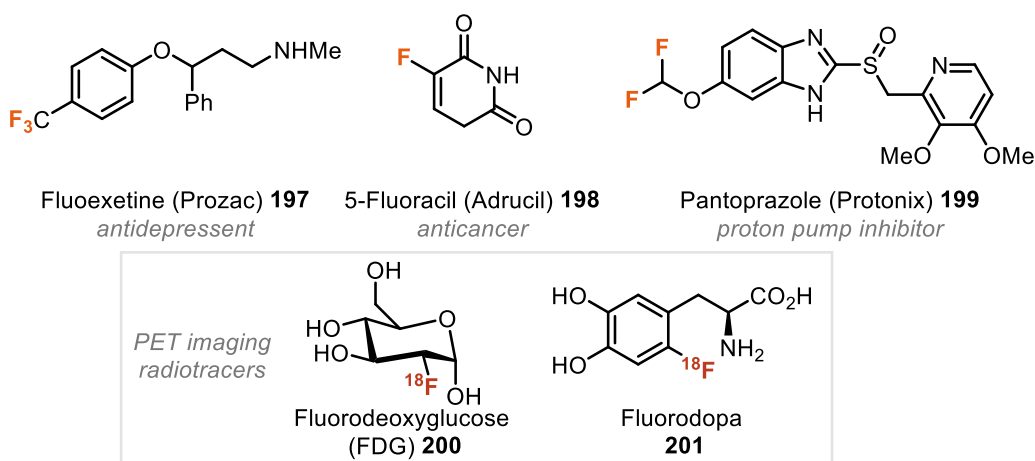
The C-F bond represents an important motif across several crucial disciplines within chemistry including pharmaceuticals and agrochemistry. Its unique properties have allowed for the careful tuning of drug molecules by improvement of metabolic stability, lipophilicity, and binding affinity upon fluorine incorporation.^{2,3} For this reason, many commonly encountered drug molecules contain at least one fluorine atom (Figure 5.2A). Additionally, fluorine can also act as a bioisostere for hydrogen and hydroxyl groups.

5 - Mechanochemical Fluorocyclisations Using a Hypervalent Fluoriodane Reagent

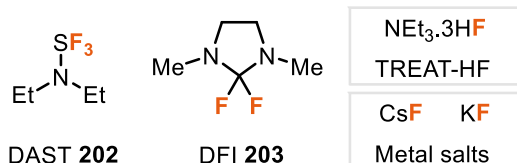
Synthetic methods for the introduction of fluorine have therefore become highly sought after, particularly given that ^{18}F has become a crucial radionuclide for positron emission tomography (PET) and has been applied to the diagnosis of cancer and Parkinsons disease amongst other illnesses.^{4,5}

Methods for introduction of fluorine are typically split into nucleophilic methods and electrophilic methods. Nucleophilic fluorinating reagents are typically readily available as they are typically derived from inexpensive HF (Figure 5.2B).⁶ Fluorination using HF requires special considerations in terms of safety measures of the equipment used, and carries a health risk due to its highly corrosive nature. Alkali metal fluoride salts are a common alternative, although suffer from reduced reactivity and often poor solubility. Deoxyfluorination is a common nucleophilic fluorine reaction, and one of the most powerful reagents for this transformation is highly reactive DAST (**202**).^{7,8} Despite its excellent reactivity, DAST presents safety issues due to *in situ* HF release in addition to explosive tendencies at temperatures greater than 50 °C owing to its rapid dismutation to SF_4 and $(\text{Et}_2\text{N})_2\text{SF}_2$. Therefore, much work has gone into developing (intrinsically) safer nucleophilic deoxyfluorination reagents such as DFI (**203**),⁹ PhenoFluor,¹⁰ and PyFluor.¹¹

A Commonly prescribed fluorinated pharmaceuticals



B Nucleophilic fluorinating reagents



C Electrophilic fluorinating reagents

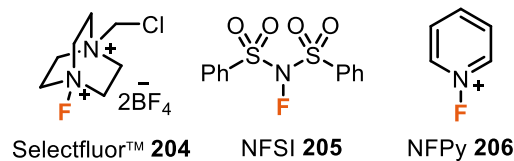


Figure 5.2 Fluorination in organic synthesis

To expand the scope of fluorination beyond attack of electron deficient systems with nucleophilic fluorine sources, a range of electrophilic fluorinating reagents have been developed (Figure 5.2C). The simplest takes the form of fluorine (F₂) gas, however, this suffers from many negative properties such that it is dangerous, extremely reactive, and a strong oxidant rendering unselective in many instances. The development of N-F fluoraza compounds has been an elegant solution with Selectfluor (**204**) subsequently commercialised as an easy to handle, bench stable solid for electrophilic fluorination, its synthesis does however still rely on the use of F₂ gas.^{12,13} Other N-F electrophilic reagents have also been developed such as NFSI (**205**),¹⁴ and *N*-fluoropyridinium salts (NFPy, **206**).¹⁵ However, Selectfluor still remains the most widely used electrophilic fluorinating reagent.^{16–19}

More recently, the use of hypervalent iodine fluorinating reagents have emerged as an effective method for fluorination (Figure 5.3). These are typically based on PIDA (Scheme 5.2, **207**) or Togni's trimethylation reagent (Figure 5.3, **208**), and can be split into linear and cyclic iodoarenes with the latter typically showing more desirable properties. For example, *p*-TollF₂ (Figure 5.3), whilst exhibiting excellent reactivity suffers from low stability and difficult preparation. Cyclic fluoroiodanes such as 1-fluoro-3,3-dimethyl-1,3-dihydro-1 λ^3 -benzo[*d*][1,2]iodaoxole (Figure 5.3, **210**) are typically easier to prepare and have good stability. Fluoroiodane reagent **210** will be the focus of the work described in this chapter.

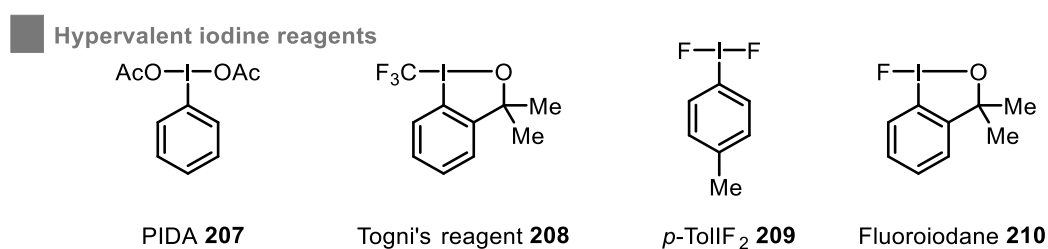


Figure 5.3 Hypervalent iodine reagents

5.1.2 Fluoroiodane Reagent Synthesis and General Application

1-Fluoro-3,3-dimethyl-1,3-dihydro-1 λ^3 -benzo[*d*][1,2]iodaoxole **210** (fluoroiodane) has recently emerged as an alternative fluorinating agent for many transformations demonstrating unique characteristics as well as divergent synthetic opportunities from that observed with aza-fluorinating agents.^{20,21}

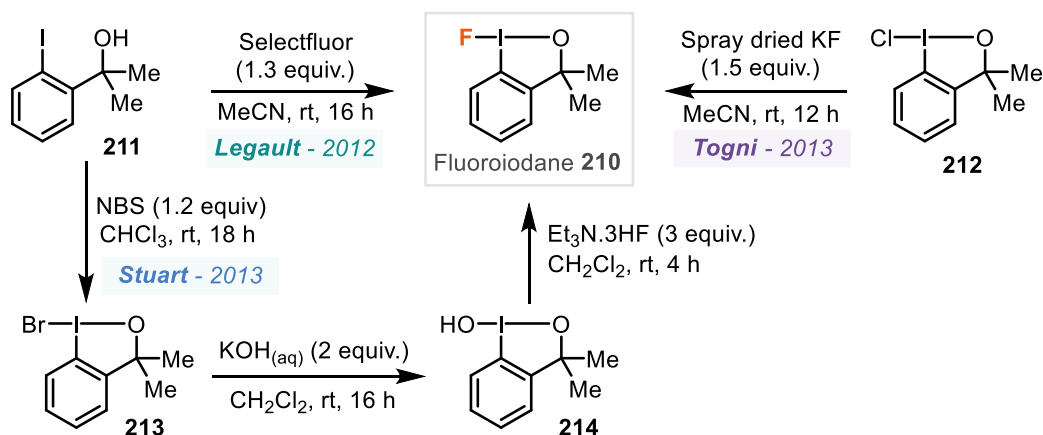
Its initial synthesis was achieved by Legault and co-workers by oxidative fluorination of 2-(2-iodophenyl)propan-2-ol (**211**) using Selectfluor as an electrophilic source of fluorine (Scheme 5.1A).²² The limitations of this approach are seen in the expensive nature of

5 - Mechanochemical Fluorocyclisations Using a Hypervalent Fluoroiodane Reagent

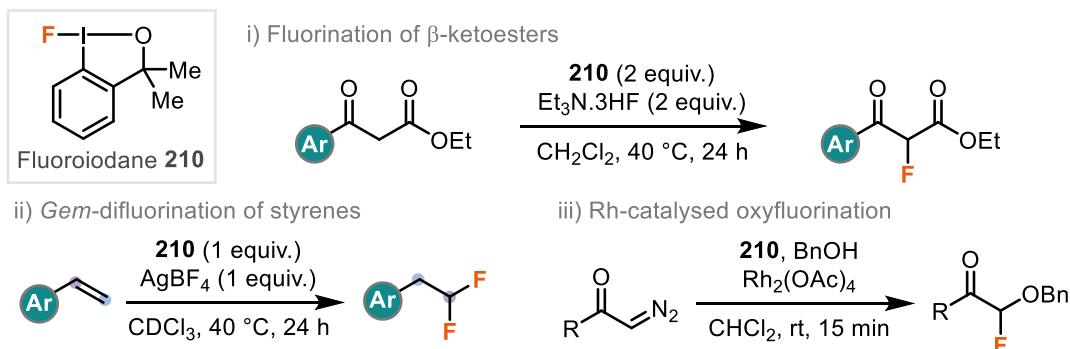
Selectfluor, particularly for large-scale synthesis. Togni and co-workers, in the preparation of a hypervalent iodine trifluoromethylation reagent, discuss the synthesis of the fluoroiodane **210** as a key intermediate in their protocol, and obtain it by nucleophilic fluorination of chloroiodane **212** with spray dried KF.²³

An alternative nucleophilic method was presented at the same time by Stuart and co-workers following a 3-step synthesis from iodoalcohol **211**, giving fluoroiodane **210** in good yields (56% overall yield). The first step uses *N*-bromosuccinimide for oxidative bromination and formation of bromoiodane **213**. Substitution with aqueous hydroxide formed the hydroxyiodane **214** before treatment with TREAT-HF furnished the desired fluoroiodane **210**. The authors discuss this method as a suitable choice for scale-up, as purification at each step is achieved by recrystallisation. It is also worth noting that the starting iodoalcohol (**211**) for Legault's and Stuart's route is the by-product of fluorination when using fluoroiodane **210**, therefore the material may be partially recycled. More recently, the radioactive variant [¹⁸F]-**210** has been synthesised by ¹⁸F anion exchange of a tosyl group using [¹⁸F]NBu₄ in just 5 minutes.²⁴

A Preparation of fluoroiodane reagent



B Example reactions using fluoroiodane reagent



Scheme 5.1 Preparation and use of fluoroiodane reagent

Its general use in fluorination reactions has been probed by many different types of reactions (Scheme 5.1B). Stuart and co-workers demonstrated its use in the classic fluorination of 1,3-dicarbonyl compounds showing selective monofluorination for β -ketoesters and selective difluorination for 1,3-diketones.²⁵ Szabó and co-workers presented a silver-mediated geminal-difluorination of styrenes.²⁶ In this work, it is proposed that one equivalent of fluoride comes from the fluoroiodane reagent and the other comes from the BF_4^- counterion following attack of a phenonium ion intermediate. The mechanism was elucidated by deuterium studies which gave evidence for the phenyl migration / phenonium ion formation by the regioselectivity outcome. Whilst this effect is not obvious on mono-substituted styrenes, Szabó and co-workers later extended to include α,α' -diaryl styrenes whereby the more electron rich aryl group always migrated.²⁷ Rh-catalysed geminal oxyfluorination of diazo carbonyl has also been shown using the fluoroiodane reagent with a reaction time of just 15 minutes possible for reactivity.²⁸ The fluoroiodane reagent also shows much greater activity in the reaction than Selectfluor.

5.1.3 Fluorocyclisation Using Fluoroiodane Reagent

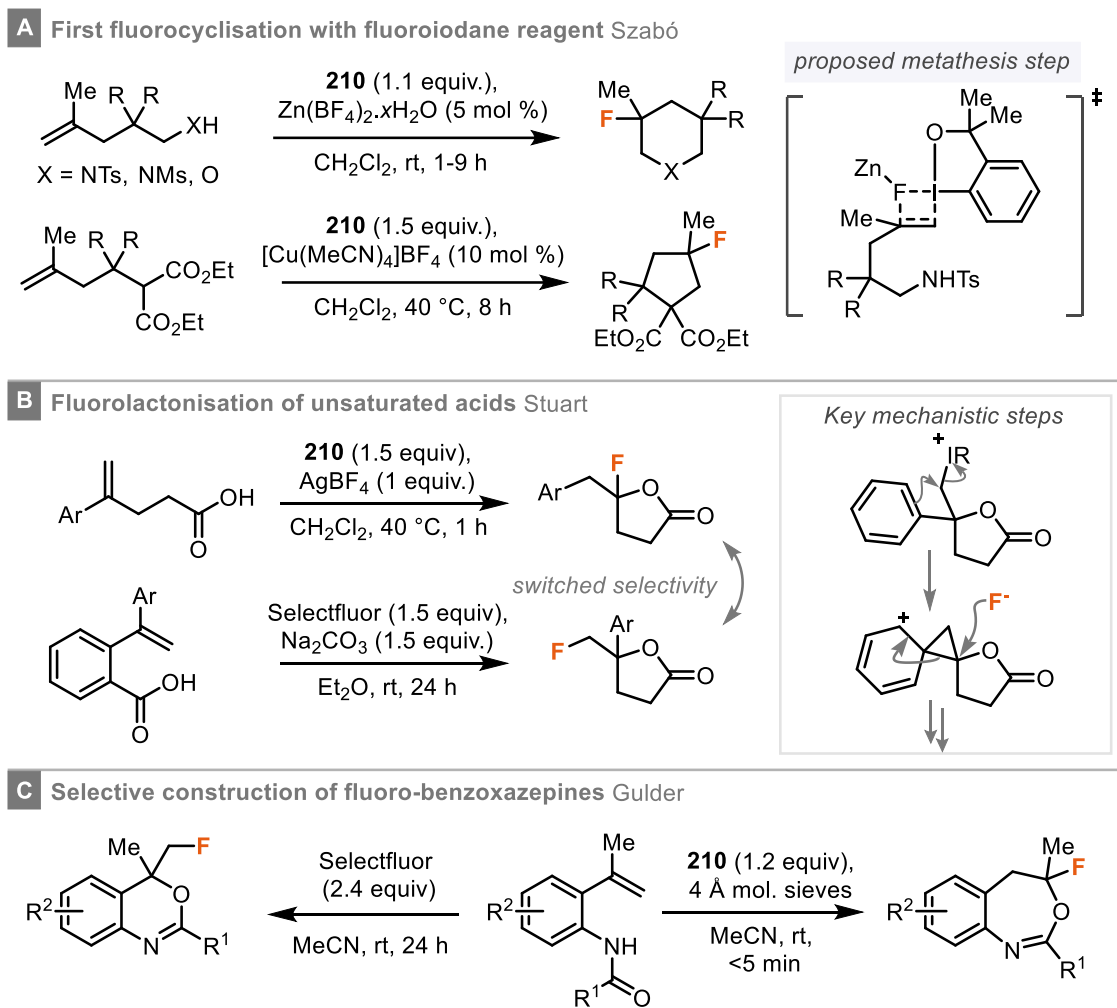
Fluoroiodane reagent **210** has found particular use in fluorocyclisation reactions. The first set of fluorocyclisation reaction was reported by Szabó and co-workers and gives examples of amino-, oxy-, and carbo-fluorocyclisation reactions (Scheme 5.2A).²⁹ A zinc-based Lewis acid is required where follow-up DFT studies suggest that the initial step is activation of the fluoroiodane by coordination of zinc cation to the fluorine atom.³⁰ It is then proposed that the reaction proceeds by a metathesis step between the activated reagent and alkene before ring closure.

In 2015, Stuart and co-workers reported a fluorolactonisation of unsaturated carboxylic acid to using the fluoroiodane reagent **210** to access a novel pathway for the synthesis of a range of γ -lactones bearing a tertiary alkyl fluoride in excellent yield (Scheme 5.2B).³¹ The selective formation of the tertiary fluoroalkyl lactones is divergent from reactivity observed upon reaction of the same or similar unsaturated acid with other fluorinating reagents such as Selectfluor,³² or *N*-fluoropentachloropyridinium triflate.³³ Key to the difference in the selectivity is the formation of a phenonium ion when using the fluoroiodane reagent allowing for phenyl migration.

Building upon this novel selectivity approach using **210**, Gulder and co-workers reported the fluorocyclisation reaction of *o*-styryl benzamides for the highly selective synthesis of 4-fluoro-1,3-benzoxazines bearing a tertiary alkyl fluoride (Scheme 5.2C).³⁴ The selectivity shown in this report once again demonstrated a different outcome to that observed using fluoraza reagents, whereby the reaction with Selectfluor selectively

5 - Mechanochemical Fluorocyclisations Using a Hypervalent Fluoroiodane Reagent

afforded the expected 6-exo-cyclisation product bearing a primary fluoromethyl motif. The proposed mechanism, supported by calculations from Cheng, suggests the reaction proceeds by a fluorination, aryl migration, and cyclisation cascade stating that the amide component is important for fluoroiodane activation.^{35,36} This methodology was later applied for the synthesis of fluoro-azabenzoxazepines.³⁷



Scheme 5.2 Fluorocyclisation reaction with the fluoroiodane reagent

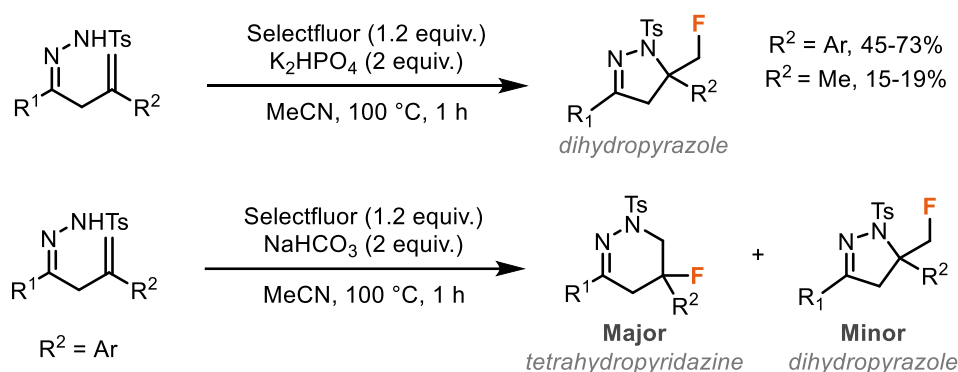
5.1.4 Fluorocyclisation of β,γ -unsaturated Hydrazones and Oximes

The halocyclisation reaction of β,γ -unsaturated hydrazones has previously been established for reliable assembly of brominated or iodinated dihydropyrazoles (an overall 5-exo-trig cyclisation).^{38,39} The introduced halide is not directly attached to the newly formed heterocycle but is instead a primary halide linked by a methylene group to the core heterocycle. The iodination reaction could also be performed effectively

enantioselectively using a bifunctional thiourea catalysed derived from *trans*-1,2-diaminocyclohexane (up to 92% *e.e.*).

Fluorocyclisation of β,γ -unsaturated tosyl hydrazones has been demonstrated by Liu and co-workers using Selectfluor as the fluorine source (Scheme 5.3).⁴⁰ In this study, the base controlled synthesis of fluorinated dihydropyrazoles and tetrahydropyridazines was shown. The scope of fluoromethyl dihydropyrazole synthesis was limited to α,α -disubstituted alkenes functionalised with aryl groups. When the alkene is substituted with a methyl group, a large drop in yield is seen (~70% to 15-19%). The construction of tetrahydropyridazines bearing a tertiary alkyl fluoride was also achieved by simply switching the base to NaHCO₃, allowing for a different mechanistic path whereby deprotonation occurs first. Whilst moderate to good yield were achieved (49-66%, 9 examples), the corresponding fluorinated dihydropyrazole was also observed in every case in varying amounts. The reaction is therefore not completely selective for 6-membered heterocycle formation. In addition, the tetrahydropyridazine reaction only proceeded when the alkene was substituted with an aryl group.

Base-controlled aminofluorocyclisation of β,γ -unsaturated hydrazones Liu



Scheme 5.3 Fluorocyclisation of β,γ -unsaturated hydrazones with Selectfluor

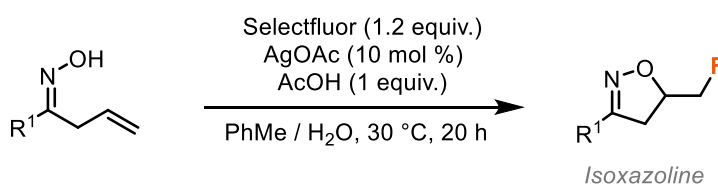
The fluorocyclisation reaction of β,γ -unsaturated oximes has also been achieved for the synthesis of fluoromethyl substituted isoxazolines (Scheme 5.4A).⁴¹ This was initially achieved by Li and co-workers using Selectfluor and catalytic silver (I) acetate. The fluorocyclisation proceeded in good yield for a range of oximes (60-72%) and showed complete selectivity for the 5-membered ring formation. A later report by Liu and co-workers, demonstrated a metal-free approach for fluorinated isooxazoline synthesis from β,γ -unsaturated oximes with an α,α -disubstituted alkene (Scheme 5.4B).⁴² In this report, the use of a base (NaHCO₃) promoted fluorocyclisation and gave typically slightly

5 - Mechanochemical Fluorocyclisations Using a Hypervalent Fluoroiodane Reagent

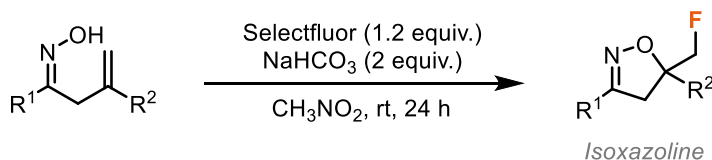
improved yields (65-85%) compared to the earlier report. Again, the reaction showed exclusive selectivity for the 5-membered heterocycle formation using Selectfluor.

Hypervalent iodine(III) reagents have also been employed previously for this oxyfluorination reaction. The use of bis(*tert*-butylcarbonyloxy)iodobenzene, PIDP, in combination with HF.pyridine provided a range of fluoromethyl-substituted dihydroisoxazoles in good yield (Scheme 5.4C, 40-86%).⁴³ The reaction only formed the 5-membered dihydroisoxazoles and 6-membered dihydrooxazines were not observed in any case, even when using oximes bearing disubstituted alkenes.

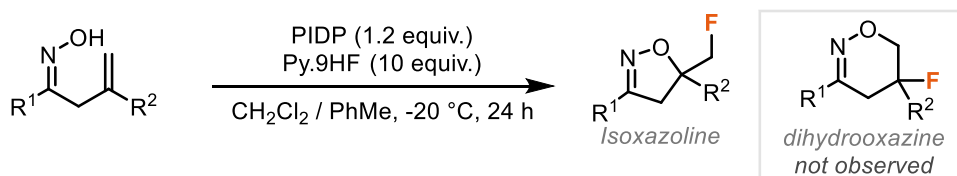
A Fluorocyclisation of β,γ -unsaturated oximes using Selectfluor Li - 2014



B Fluorocyclisation of β,γ -unsaturated oximes using Selectfluor Liu - 2017



C Fluorocyclisation of β,γ -unsaturated oximes using fluoroiodane Wang, Jiang & Xu - 2015



Scheme 5.4 Fluorocyclisations of β,γ -unsaturated oximes

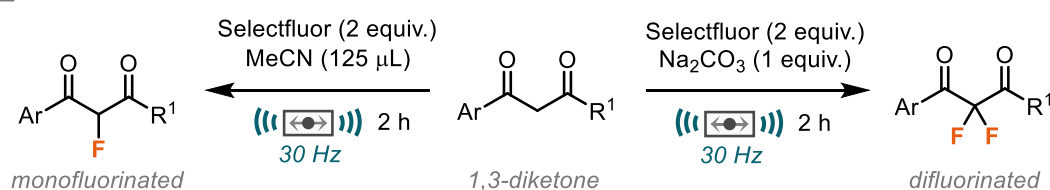
The selective fluorocyclisation of β,γ -unsaturated oximes to synthesise fluorinated dihydrooxazines bearing a tertiary alkyl fluoride has not yet been reported and remains a challenging prospect using conventional fluorinating agents due to the increased reaction rates of 5-*exo* cyclisation vs 6-*endo* cyclisation. Therefore, an alternative strategy and approach is required for fluorinated dihydrooxazine synthesis.

5.1.5 Mechanochemical Fluorination

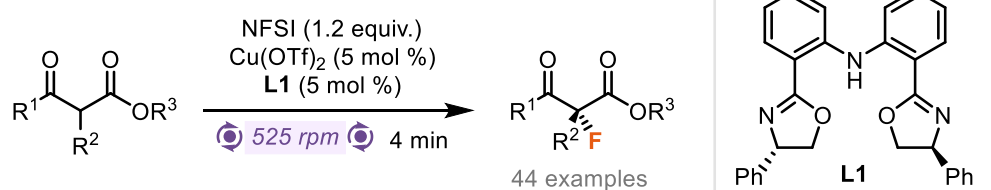
The use of ball-milling has emerged as a useful technique for the fluorination of organic materials. Using electrophilic fluorinating reagents such as Selectfluor, the mechanochemical fluorination of 1,3-dicarbonyl compounds has been explored in detail.

The first of these reports from Browne and co-workers in 2017 demonstrates outstanding control of mono vs di fluorination of 1,3-diketones by altering the additive used (Scheme 5.5A).⁴⁴ The monofluorinated product could selectively be formed (ratio mono /di = 50:1) with the use of acetonitrile as a LAG, and the difluorination was realised using sodium carbonate as base to help promote the second fluorination (ratio mono /di = 1:17). Browne and co-workers later adapted this protocol to the selective fluorination of liquid β -ketoesters, using sodium chloride as an additive to improve mass transfer.⁴⁵ An enantioselective fluorination of α -monofunctionalised β -ketoesters was also demonstrated by Xu and co-workers using NFSI as the electrophilic source of fluorine and a diphenylamine linked bis(oxazoline) copper (II) triflate complex as a catalyst to give excellent yields (85-99%) and high selectivity (>93% e.e. in all cases) for cyclic systems. Reduced yields were observed for acyclic 1,3-diketones (Scheme 5.5B).⁴⁶

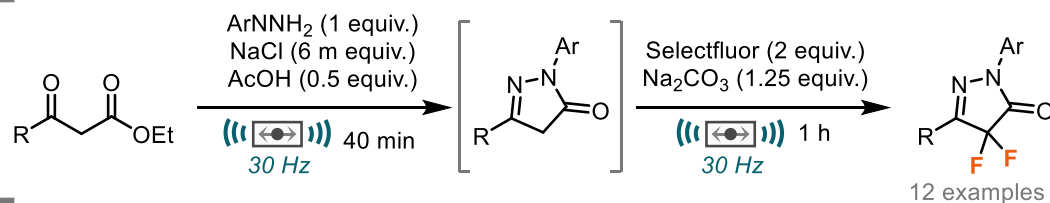
A Additive controlled mechanochemical fluorination of 1,3-dicarbonyls Browne - 2017



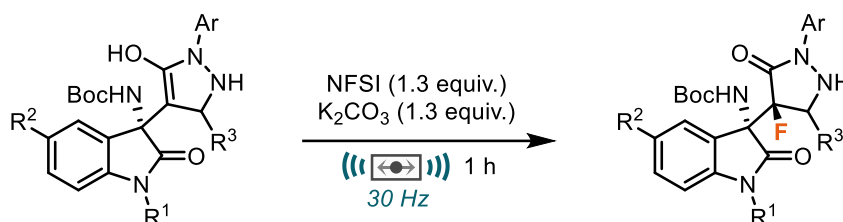
B Enantioselective fluorination of β -ketoesters Xu - 2017



C Fluorination of pyrazolones Browne - 2017



D Fluorination of pyrazolones Šebesta - 2020



Scheme 5.5 Mechanochemical fluorination

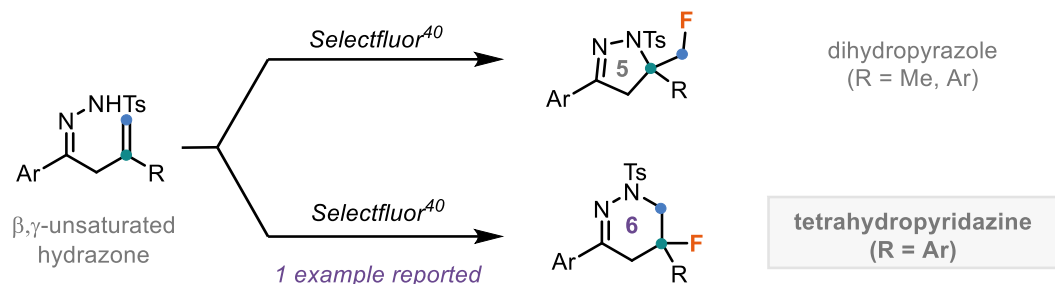
5 - Mechanochemical Fluorocyclisations Using a Hypervalent Fluoriodane Reagent

The fluorination of pyrazolones has also been shown under ball milling conditions. Firstly, difluorination of pyrazolones was achieved by Browne and co-workers as part of a 2-step, 1-pot procedure from β -ketoesters using Selectfluor as the fluorinating reagent (Scheme 5.5C).⁴⁷ Mechanochemical pyrazolone fluorination was also demonstrated as part of a sequential domino Mannich fluorination reaction whereby the stereospecific fluorination occurred using NFSI (Scheme 5.5D). Mechanochemical fluorination has also been applied to polymerisation chemistry, surface fluorination of cellulose, and the synthesis of inorganic fluorides.^{48–50}

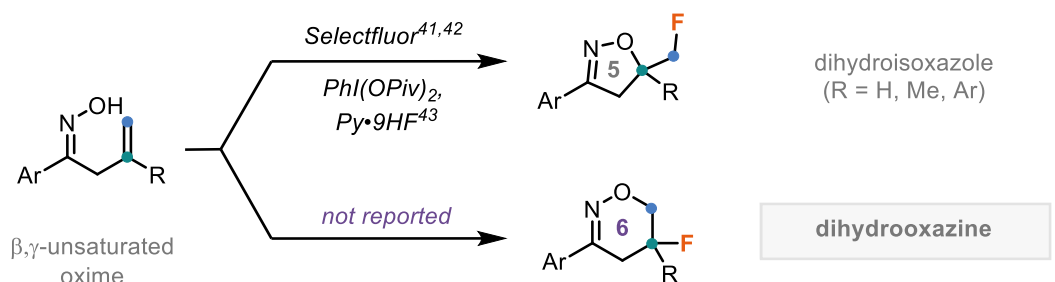
5.1.6 Outlook and Aims

An elegant method for fluorinated heterocycle synthesis is through fluorocyclisation. The fluorocyclisation of β,γ -unsaturated hydrazones and oximes has been previously explored for synthesis of 5-membered heterocycles (dihydropyrazoles and isoxazolines) bearing a fluoromethyl group. The fluorocyclisation of hydrazones to afford 6-membered tetrahydropyridazines has only been shown on one occasion, whereby the dihydropyrazole was also formed, showing that the reaction is not completely selective (Scheme 5.6A).⁴⁰ The fluorocyclisation of β,γ -unsaturated oximes to form fluorinated dihydrooxazines has not yet been reported (Scheme 5.6B).

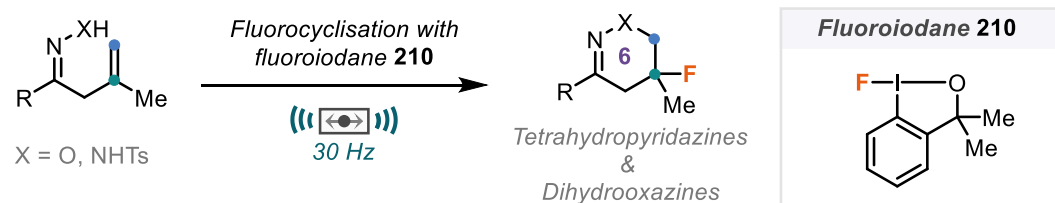
A Previous fluorocyclisation of β,γ -unsaturated hydrazones



B Previous fluorocyclisation of β,γ -unsaturated oximes



C Project aim - fluorinated tetrahydropyridazine and dihydrooxazine synthesis



Scheme 5.6 Overview and project aims

The hypervalent fluoroiodane reagent **210** has been shown to exhibit unique reactivity in solution based fluorocyclisation reactions, often allowing for switched selectivity compared to commonly employed electrophilic fluorinating reagents such as Selectfluor.

Mechanochemistry has emerged as a useful synthetic tool for fluorination chemistry and, through the controlled fluorination of 1,3-dicarbonyl compounds, has been shown to exhibit good selectivity in fluorination reactions.

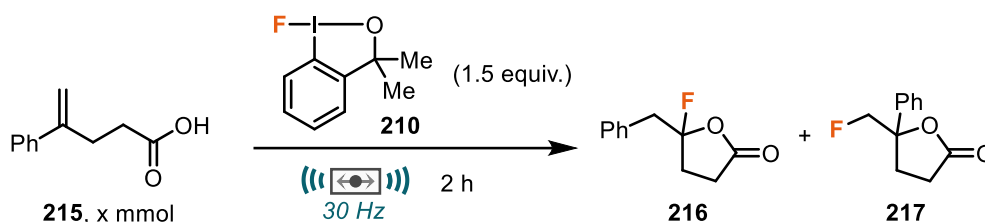
The aim of this project is to explore the use of **210** for the selective construction of fluorinated tetrahydropyridazines and dihydrooxazines (Scheme 5.6C). It is thought that the use of **210** will allow for a key ring expansion step, which in combination with ball-milling techniques will be used for the reaction to develop a solvent-free / minimised protocol whilst hopefully observing some of the unique benefits mechanochemistry has been shown to offer.

5.2 Results and Discussion

5.2.1 Initial Assessment of Fluoroiodane Reagent - Mechanochemical Fluorolactonisation of Carboxylic Acids

To provide a preliminary assessment of the reactivity and stability of the hypervalent fluoroiodane reagent under mechanochemical conditions and hence determine suitability towards the targeted fluorocyclisation, the fluorolactonisation of unsaturated carboxylic acids was investigated. This process was previously reported for solution-based conditions using CH_2Cl_2 as a solvent and hexafluoroisopropanol (HFIP) or silver tetrafluoroborate (AgBF_4) as an activator for the fluoroiodane reagent.^{31,51-54} In this report, the authors report exclusive selectivity for the tertiary fluoro γ -butyrolactone (**216**) over the primary fluoro γ -butyrolactone (observed with other fluorinating agents, **217**) where the key mechanistic step is the formation of a phenonium ion. Therefore, it is also interesting to consider the stability of such intermediates under mechanochemical conditions and if the same selectivity outcome is observed.

Table 5.1 Initial results: Investigation of scale



Entry	215 mmol	Jar size (mL)	Ball size (g)	Yield 216 (%) ^a	Yield 217 (%) ^a
1	0.5	10	2.5	23	0
2	0.25	10	2.5	16	0
3	0.25	10	1.5	24	0
4	0.125	10	1.5	14	0
5	0.125	10	0.5	9	0
6	0.125	5	1.5	11	0

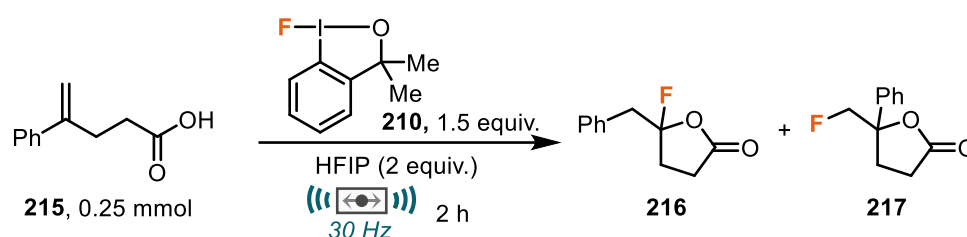
^a Yield determined by ^{19}F NMR spectroscopy using benzotrifluoride as an internal standard.

Studies commenced on a mechanochemical variant by adapting the previously reported conditions, starting with the neat milling reaction of 4-phenylpent-4-enoic acid (**215**, 0.5 mmol) with the fluoroiodane reagent (**210**, 1.5 equiv.) in a 10 mL milling jar loaded with

a 2.5 g milling ball. Under these initial conditions, a 23% of the targeted tertiary-fluoro γ -butyrolactone **216** was observed and no primary-alkyl fluoro product **217** was formed (Table 5.1, entry 1). Reducing the scale of the reaction to minimise consumption of the privileged fluoroiodane reagent saw a decreased yield of 16% at 0.25 mmol (Table 5.1, entry 2). However, this reduction was mitigated for by then reducing the mass of the ball to 1.5 g, allowing for a comparable yield (24%) to that observed initially (Table 5.1, entry 3). It is worth noting that lowering the scale again to 0.125 mmol resulted in diminished yields, both with a 1.5 g ball and a 0.5 g ball and in a smaller 5 mL milling jar (Table 5.1, entries 4-6).

Having established a 0.25 mmol scale was suitable (conditions as in Table 5.1, entry 3), optimisation continued through inclusion of HFIP as an activator for the fluoroiodane reagent. The addition of 2 equivalents of HFIP gave a significantly improved yield of the desired fluorolactonisation product **216** (55%, Table 5.2, entry 1). The yield remained consistent with the same loading of HFIP at a lower reaction time of 1 hour (57%), however diminution of yield was observed for a half hour reaction period (Table 5.2, entries 2-3). Again, the primary fluoroalkyl lactone product **217** that would arise from using other fluorinating agents was not observed in any case, demonstrating repeatability of the excellent selectivity achieved in solution for the mechanochemical variation. Satisfied that 1 h performed comparably to 2 h and allowed greater throughput of material, these conditions were taken forward as the optimised conditions

Table 5.2 Time studies of reaction with activator (HFIP)



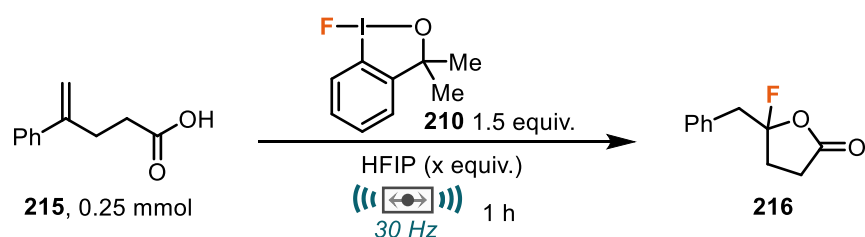
Entry	Time (h)	Yield 216 (%) ^a	Yield 217 (%) ^a
1	2	55	0
2	1	57	0
3	0.5	36	0

^a Yield determined by ¹⁹F NMR spectroscopy using benzotrifluoride as an internal standard.

5 - Mechanochemical Fluorocyclisations Using a Hypervalent Fluoroiodane Reagent

Having established that the inclusion HFIP as an activator is greatly beneficial to the reaction, optimisation continued to establish the optimal loading of HFIP (Table 3.3). To this end, different quantities of HFIP between 0 and 6 equivalents were added to the 1 hour milled reaction. The activator did not seem to take effect until a minimum of 2 equivalents was used. From this point, a distinct correlation was seen with higher loadings of HFIP providing higher yields of **216** up to a maximum of 96% when using 5 equivalents of HFIP (Table 5.2, entry 6). This is unsurprising given results from a recent report showing that HFIP, in combination with the hypervalent fluoroiodane reagent, forms a hydrogen-bonded adduct with the fluorine atom which elongates the I-F bond and gives an activated intermediate.⁵¹

Table 5.3 Loading of activator (HFIP)



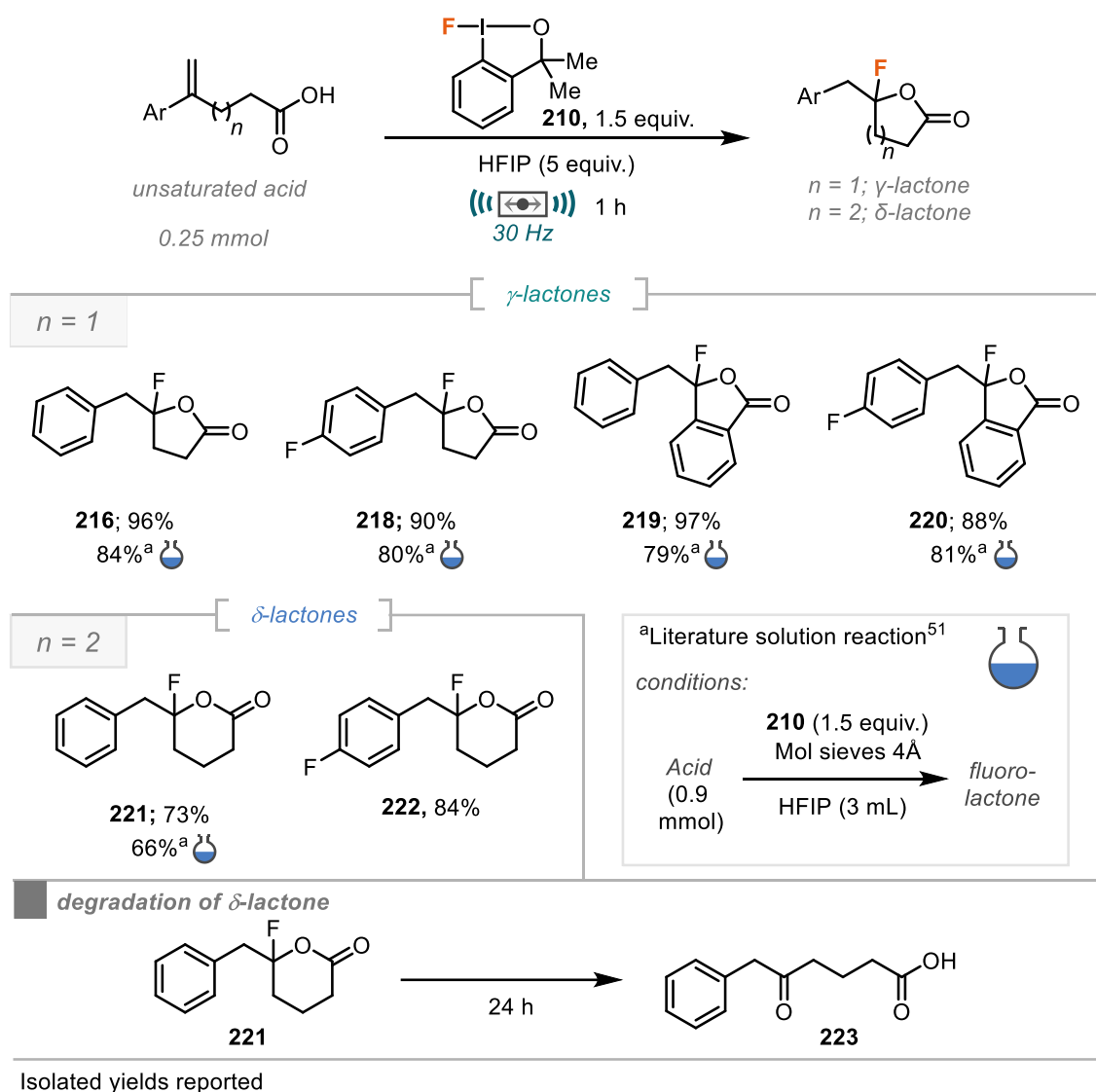
Entry	HFIP equiv.	Yield 216 (%) ^a
1	0	24
2	1	32
3	2	57
4	3	70
5	4	83
6	5	96 (92) ^b
7	6	95

^a Yield determined by ¹⁹F NMR spectroscopy using benzotrifluoride as an internal standard. ^b Isolated yield.

From the studies conducted, optimised conditions were identified as milling unsaturated acid (0.25 mmol), fluoroiodane (1.5 equiv.), and HFIP (5 equiv.) for 1 hour at 30 Hz in a 10 mL stainless steel milling jar with a 1.5 g stainless steel milling ball (Table 5.3, entry 6).

With optimal conditions for the fluorolactonisation reaction, application to a small range of unsaturated acids was demonstrated (Scheme 5.7). In all cases, fluorocyclisation of

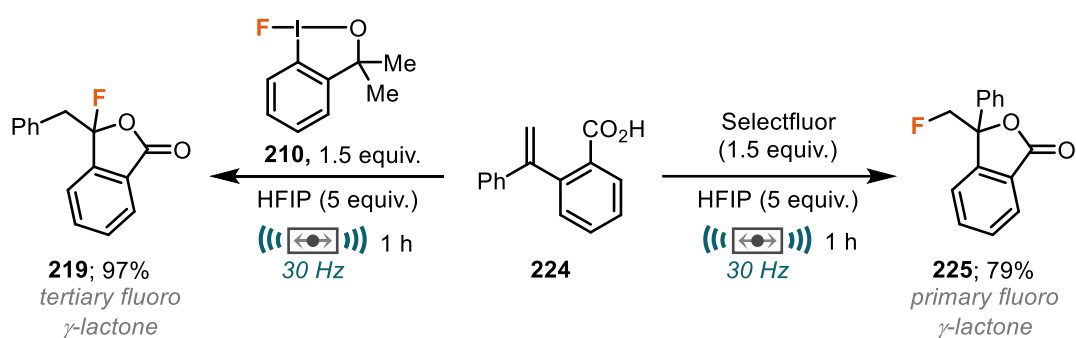
γ,δ -unsaturated carboxylic acid underwent fluorocyclisation to give the resulting tertiary-fluoro γ -butyrolactones in excellent isolated product yields (88-97%). The results obtained by ball-milling demonstrated increased yields (typically 10%) to that achieved by reported analogous solution conditions whereby HFIP is used in solvent quantity.⁵¹ In addition, δ,ϵ -unsaturated acids were found to be suitable substrates under the reaction conditions, successfully delivering fluorinated δ -lactones **221** and **222** in excellent yields (73 and 84%, respectively). It is worth noting that δ -lactone **221** did undergo partial degradation (~30%) after 2 hours *via* hydrodefluorinative ring-opening resulting in the formation of keto-acid **223**. After 24 hours, this degradation was quantitative with no fluorinated product remaining (Scheme 5.7, bottom).



Scheme 5.7 Scope of mechanochemical fluorolactonisation

5 - Mechanochemical Fluorocyclisations Using a Hypervalent Fluoriodane Reagent

Finally, the selectivity of the fluorocyclisation compared to a common electrophilic fluorinating agent, Selectfluor, was investigated. Under the mechanochemical fluoriodane conditions, 2-(1-phenylvinyl)benzoic acid (**224**) exclusively delivered the tertiary fluoro γ -lactone **219** in a 97% isolated yield. Taking the same substrate and milling with Selectfluor (1.5 equiv.) and HFIP (5 equiv.) for 1 hour the reversed selectivity with no tertiary fluoroalkyl product observed, and instead exclusively afforded 79% of the primary fluoro γ -lactone **225** (Scheme 5.8). These conditions for the Selectfluor-mediated conditions by ball-milling were not optimised and were derived simply by taking the fluoriodane conditions and replacing the fluorinated agent directly.



Scheme 5.8 Selectivity of fluorocyclisation under ball-milling conditions

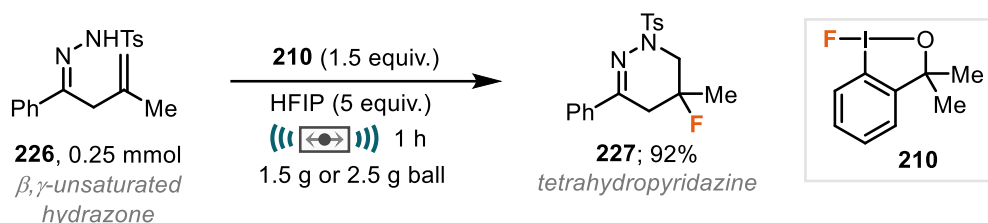
5.2.2 Mechanochemical Amino Fluorocyclisation (Tetrahydropyridazines)

With good reactivity established for the use of the hypervalent iodine reagent under ball-milling conditions by investigation of a fluorolactonisation reaction, attention turned to targeting the synthesis of novel fluorinated heterocycles. The first reaction to be explored was the fluorocyclisation of β,γ -unsaturated hydrazones for the construction of 5-fluorotetrahydropyridazines.

Initial studies carried out at Leicester University by Dr William Riley for the identification of conventional solution-based conditions determined that as was similarly displayed for the fluorolactonisation reaction, where the use of an activator such as HFIP showed promise for the hydrazone fluorocyclisation reactions.

With this information, the conditions previously shown to be optimal for the mechanochemical fluorolactonisation of unsaturated acids (Section 5.2.1) were employed as a starting point for the new hydrazone fluorocyclisation reaction. This initial model proved exceptionally successful for the fluorocyclisation of β,γ -unsaturated hydrazone **226**, producing 92% of the desired 6-membered fluorinated tetrahydropyridazine **227** exclusively with no 5-membered dihydropyrazole observed

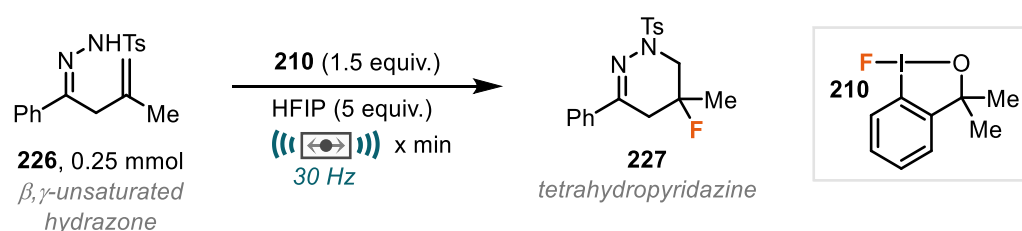
(Scheme 5.9). Pleasingly, the product showed excellent stability under milling conditions, demonstrating no evidence of HF elimination upon formation. Separate reactions containing a 1.5 g ball and 2.5 g ball resulted in identical yield (92%). A 2.5 g ball was to be used for following studies. The larger ball was initially attempted due to increased mass of the hydrazone starting material compared to the acids used in the previous studies, however this effect proved inconsequential.



Scheme 5.9 Initial results

After the initial success of the reaction showing efficient fluorocyclisation, lower reaction times were attempted to determine how quickly fluorocyclisation can occur (Table 5.4). Indeed, it was found that the milling time could be reduced to just 15 minutes with no detrimental effect on the yield (Table 5.4, entry 3). However, a shorter reaction period of 10 minutes resulted in a slightly reduced yield of 81% (Table 5.4, entry 4)

Table 5.4 Hydrazone fluorocyclisation time



Entry	Time (min)	Yield 227 (%) ^a
1	60	92
2	30	91
3	15	91
4	10	81

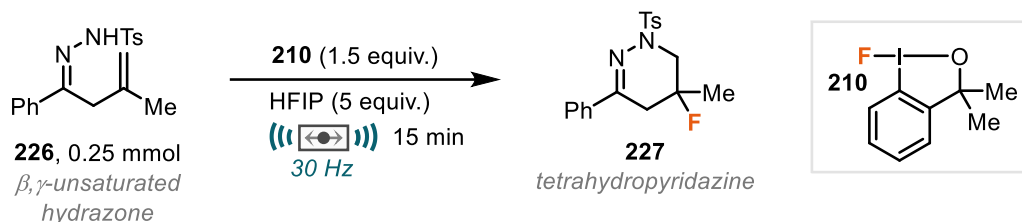
^a Yield determined by ¹⁹F NMR spectroscopy using benzotrifluoride as an internal standard.

With a greatly reduced reaction time still showing excellent yields for the fluorocyclisation, it was thought that the loading of activator could also be reduced. To this end, several reactions were run using between 1 and 5 equivalents of HFIP as

5 - Mechanochemical Fluorocyclisations Using a Hypervalent Fluoroiodane Reagent

activator (Table 5.5). The results showed that loading of HFIP could be reduced to 2 equivalents without any loss in yield (92%, Table 5.5, entry 5). In the absence of activator, fluorocyclisation still proceeds to give the desired tetrahydropyridazine, however a lower yield is obtained (52%, Table 5.5, entry 6).

Table 5.5 Optimisation of activator and fluoroiodane loading



Entry	210 equiv.	HFIP equiv.	Yield 227 (%) ^a
1	1.5	5	91
2	1.5	4	90
3	1.5	3	90
4	1.5	2	92(91) ^b
5	1.5	1	72
6	1.5	-	52
7	1.25	2	74

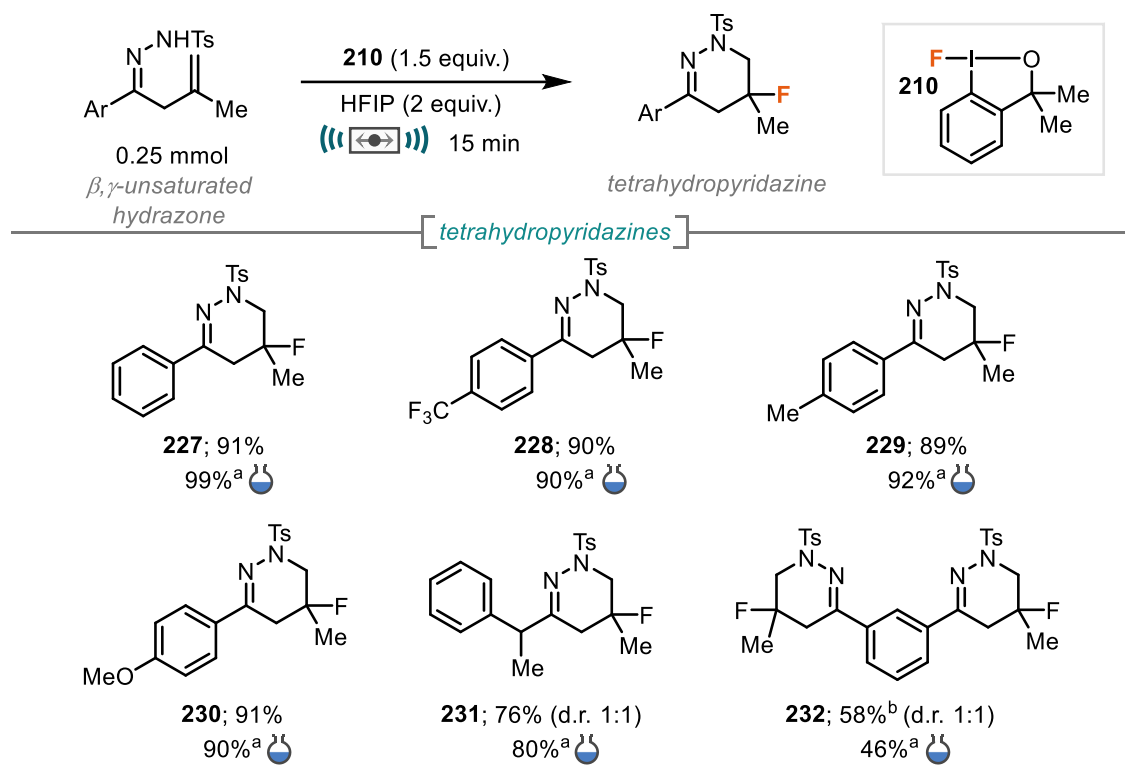
^a Yield determined by ¹⁹F NMR spectroscopy using benzotrifluoride as an internal standard. ^b Isolated yield.

Moving forward with 2 equivalents of HFIP, the stoichiometry of fluoroiodane reagent was discovered to have a significant impact on the reaction with a reduced loading of 1.25 equivalents giving a lower yield of 74% (Table 5.5, entry 7).

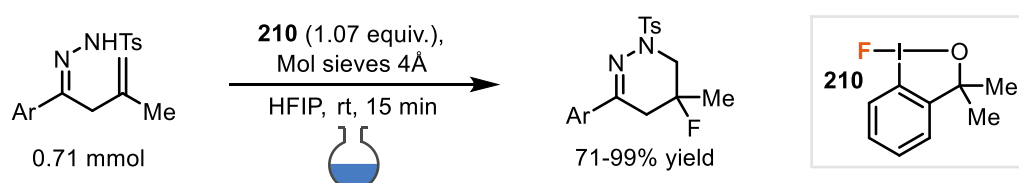
From the optimisation studies, optimal conditions were determined to be hydrazone (0.25 mmol), fluoroiodane (1.5 equiv.) and HFIP (2 equiv.) milled in a 10 mL jar with a 2.5 g ball for 15 minutes.

Having identified a set of conditions that gave excellent yield for the model reaction, their application to a small range of β,γ -unsaturated hydrazones was explored (Scheme 5.10). The reaction was tolerant to a series of aryl-substituted hydrazones bearing both

electron-withdrawing (**228**) and electron-donating groups (**230**). The fluorocyclisation also proved successful for a benzyl substituted hydrazone (76%, **231**). Bis-tetrahydropyridazine **232** was also prepared in a 58% yield by a double fluorocyclisation using twice as much fluoroiodane.



^aSolution reaction - performed by Dr William Riley, conditions:



Isolated yields reported. ^b 3 equiv. fluoroiodane **210**.

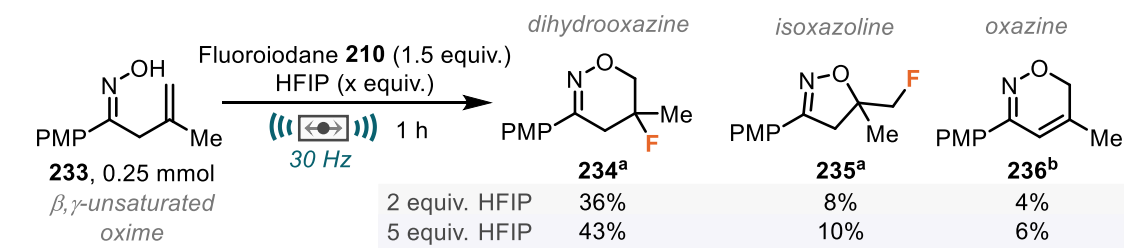
Scheme 5.10 Scope of mechanochemical β,γ -unsaturated hydrazone fluorocyclisation

In all cases, the solvent-minimised, mechanochemical reaction, gave comparable yields to the simultaneously developed solution reaction (developed by Dr William Riley). In the solution-based reaction, it was found that HFIP was required, either as a solvent, or as a stoichiometric reagent in conjunction with CH_2Cl_2 as a solvent. The mechanochemical reaction demonstrates option for a more sustainable approach for construction of these tetrahydropyridazines by eliminating (most of) the solvent. For the solution-based reaction that use HFIP, $1.69 \text{ mL mmol}^{-1}$ of HFIP was used as solvent with respect to

hydrazone starting material, whereas the mechanochemical reaction uses 0.21 mL mmol⁻¹ HFIP demonstrating over >8 fold reduction in the amount of solvent used.

5.2.3 Mechanochemical Oxy Fluorocyclisation (Dihydrooxazines)

After identification and assessment of conditions for the selective fluorocyclisation of β,γ -unsaturated hydrazones under mechanochemical conditions, attention next turned to targeting the synthesis of 6-membered 5-fluorodihydrooxazines, a motif that has previously not been reported. Studies began by assessing the reaction of β,γ -unsaturated oxime **233** with the hypervalent iodine reagent **210** using the standard conditions established for the hydrazone cyclisation i.e., 1.5 equivalents of fluoroiodane and 2 equivalents of HFIP with a 2.5 g milling ball. The initial reaction, which was milled for 1 hour, returned promising results demonstrating successful fluorocyclisation could be achieved to afford the desired 6-membered dihydrooxazine **234** in 36% yield (Scheme 5.11). However, the reaction was not entirely selective for the 6-membered product and underwent 5-exo-trig fluorocyclisation to give 8% of the 5-membered isoxazoline **235**. These reaction conditions also showed evidence for the elimination of HF from the target compound **233** with a small amount (4%) of oxazine **236** also present in the reaction outcome. Increasing the loading of HFIP to 5 equivalents gave increased yields of all 3 products with the remainder of the mixture comprising of starting material.



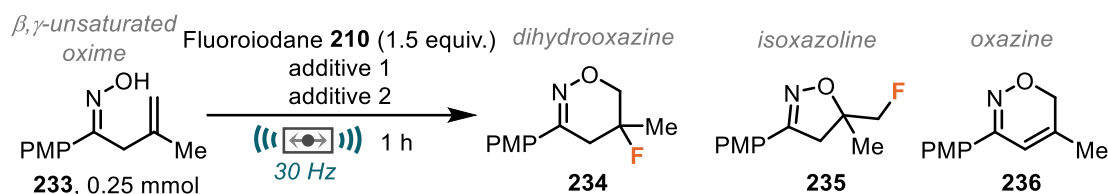
^aYield determined by ¹⁹F NMR spectroscopy using benzotrifluoride as an internal standard. ^bYield determined by ¹H NMR spectroscopy using benzotrifluoride as an internal standard.

Scheme 5.11 Initial results for β,γ -unsaturated oxime fluorocyclisation

At the same point in our collaborative project, whilst searching for conditions for the same fluorocyclisation reaction for solution-based synthesis, Dr William Riley presented conditions showing promising results by using an alternative activator, silver tetrafluoroborate (AgBF₄). This activator, along with other Lewis acids have been used previously for use with the hypervalent fluoroiodane reagents and DFT studies elucidated that activation occurs via coordination to the fluorine atom and hence elongating the I-F bond.^{31,52,53}

To test this activator for the mechanochemical reaction, HFIP was substituted by AgBF_4 , initially with 2 equivalents used. Preliminary results showed a reduced yield of 13% for the desired product **234**, however only a trace amount of 5-membered isoxazoline **235** was observed tentatively suggesting that the activator may have a role to play in controlling selectivity (Table 5.6, entry 1). Since all reagents in the reaction are solid, a liquid additive was thought to be a good proposition to aid with mixing. The first choice as LAG was HFIP due to its activating qualities previously demonstrated by ball-milling. Whilst the reaction including both activators did show a slightly increased yield of 26% (Table 5.6, entry 3) the production of the unwanted 5 membered product was again observed (5%), as was the case when previously using HFIP (Scheme 5.13). Since previous reports typically outline the use of AgBF_4 with CH_2Cl_2 as a solvent, this was next to be tried in mechanochemical reaction. Remarkably, using CH_2Cl_2 as a LAG (5 equiv.) gave a profound increased yield affording 84% of dihydrooxazine **234** in exclusive selectivity with only a trace amount of isoxazoline **235** and HF-elimination product **236** observed (Table 5.6, entry 3). Deviation from this ratio of the solid and liquid additive resulted in reduced yields (Table 5.6, entries 4-6).

Table 5.6 Optimisation of mechanochemical β,γ -unsaturated oxime fluorocyclisation



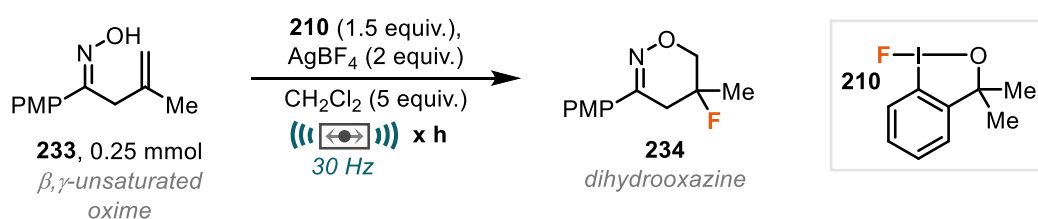
Entry	Additive 1	Additive 2	Yield (%) ^a		
			234	235	236
1	AgBF_4 (2 equiv.)	-	13	<2%	4
2	AgBF_4 (2 equiv.)	HFIP (5 equiv.)	26	5	<2
3	AgBF_4 (2 equiv.)	CH_2Cl_2 (5 equiv.)	84(80) ^b	<2%	<2
4	AgBF_4 (1 equiv.)	CH_2Cl_2 (5 equiv.)	53	<2	<2
5	AgBF_4 (3 equiv.)	CH_2Cl_2 (5 equiv.)	71	0	0
6	AgBF_4 (2 equiv.)	CH_2Cl_2 (2 equiv.)	47	<2	<2

^a Yield determined by ^{19}F NMR spectroscopy using benzotrifluoride as an internal standard. ^b Isolated yield.

5 - Mechanochemical Fluorocyclisations Using a Hypervalent Fluoroiodane Reagent

The optimal additives were therefore determined to be AgBF_4 as a fluoroiodane activator and CH_2Cl_2 as a LAG with a molar ratio of 2 and 5 respectively, shown to be optimal. From this point, the time of the reaction was altered. Firstly, since there was a small amount (~9%) of oxime starting material returned from the 1-hour reaction (Table 5.7, entry 1), a longer reaction time of 2 hours was attempted. The reaction yield remained similar (82%), and a comparable quantity of starting material was still observed (Table 5.7, entry 2). Reducing the reaction time to 30 minutes gave a reduction in yield to 68% product with 23% unsaturated oxime **233** also returned (Table 5.7, entry 3), showing that the reaction has not reached completion and that 1 hour is the optimal time for the fluorocyclisation of oximes. Although this a longer reaction time than was the case in the hydrazone fluorocyclisation (15 minutes), this may be attributed to the change in activator or the inherent nucleophilicity of nitrogen versus oxygen.

Table 5.7 Time optimisation of oxime fluorocyclisation



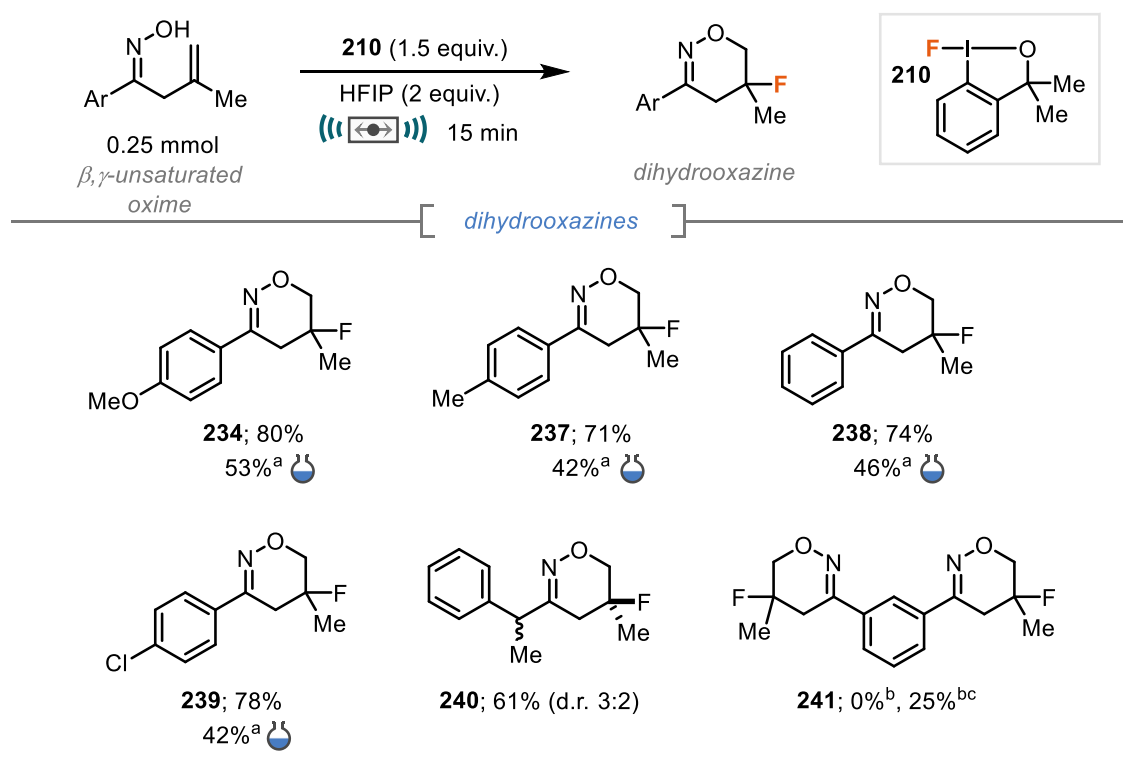
Entry	Time (h)	234 (%) ^a	SM 233 (%) ^a
1	1	84(80) ^b	9
2	2	82	8
3	0.5	68	23
4 ^c	1	83	8

^a Yield determined by ^{19}F NMR spectroscopy using benzotrifluoride as an internal standard. ^b Isolated yield. ^c 2 equiv. **210**.

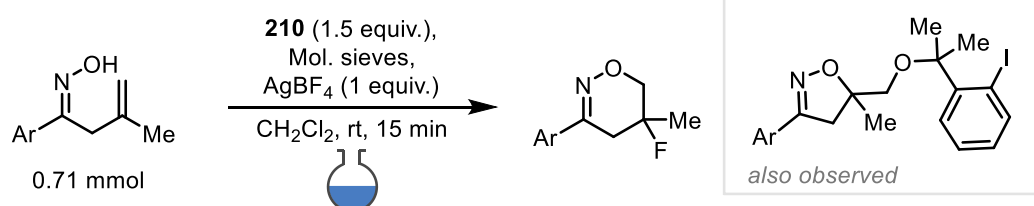
It was also established that an increased loading of fluoroiodane (2 equivalents) did not improve the yield (Table 5.6, entry 4). The optimised conditions for the mechanochemical fluorocyclisation of β,γ -unsaturated oximes were therefore considered to be oxime (0.25 mmol), fluoroiodane **210** (1.5 equiv.), AgBF_4 (2 equiv.) as a Lewis acid activator, and CH_2Cl_2 as a liquid additive for a 1 hour milling period.

With optimised conditions identified, a small range of β,γ -unsaturated oximes were examined for mechanochemical fluorocyclisation for the synthesis of novel 5-fluorodihydrooxazines (Scheme 5.12). Unsaturated oximes bearing aryl groups with

various functionality in the para position afforded the functionalised dihydrooxazines in very good yields (71-80%, Scheme 5.14, **234**, **237-239**). Interestingly a benzylic substituted oxime underwent fluorocyclisation in 61% to give **240** as 3:2 mixture of diastereoisomers. Whilst the major diastereomer was not fully confirmed, it would make sense that both methyl groups would be on the same side. This is due to the proposed mechanism (*vide supra*, section 5.2.4 featuring a carbocation intermediate and attack of fluoride as the stereochemical determining step). A bis-oxime did undergo double fluorocyclisation in 25% yield (**241**), giving a 1:1 mixture of diastereomers, however, isolation was not possible due to the presence of a small amount of the mono-cyclised product as well as the rapid elimination pathways of one or both dihydrooxazine fragments.



^aSolution reaction - performed by Dr William Riley, conditions:



Isolated yields reported. ^b 3 equiv. fluoroiodane **210**. ^c NMR yield reported

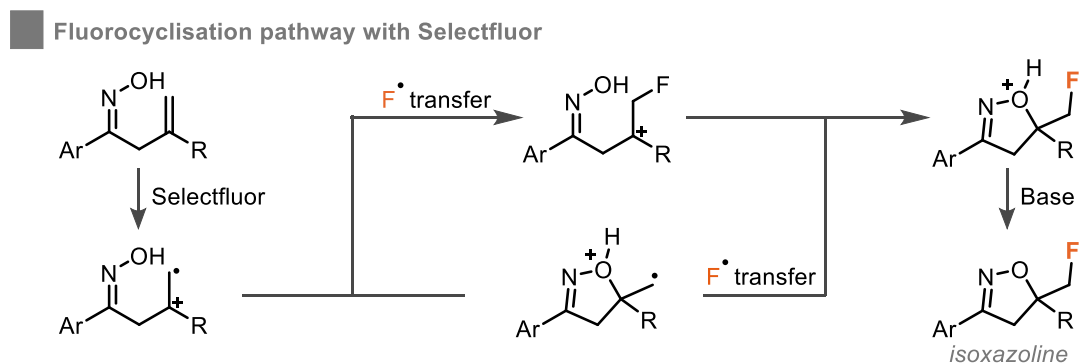
Scheme 5.12 Scope of mechanochemical β,γ -unsaturated oxime fluorocyclisation

5 - Mechanochemical Fluorocyclisations Using a Hypervalent Fluoroiodane Reagent

The mechanochemical oxime fluorocyclisation performed much better than the optimised solution counterpart (developed by Dr William Riley) with yields in solution being between 42 and 53%, whereas much higher yields (typically >70%) were observed under the ball-milling manifold. This is in part due to the presence of an adduct that arises from interception of the intermediate with the benzyl alcohol backbone of the fluoroiodane reagent in some cases. This iodoalcohol is the by-product from the fluorination reaction and was present in every reaction, however, the isoxazoline adduct observed in solution is intriguing given it was never observed in the mechanochemical set-up.

5.2.4 Proposed Mechanism for Heterocycle Construction

Previous fluorocyclisation reactions of β,γ -unsaturated hydrazones and oximes using typical fluorinating reagents such as Selectfluor are typically proposed to occur *via* fluorine radical transfer pathways (Scheme 5.13) or by simple addition of a nucleophile to 'F+'. The fast rate of the cyclisation drives the selectivity towards the 5 membered dihydropyrazoles / dihydroisoxazoles bearing a primary alkyl fluoride.

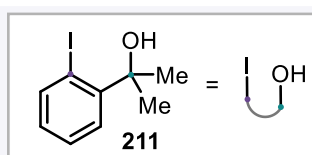
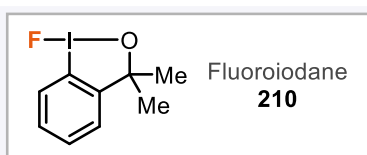
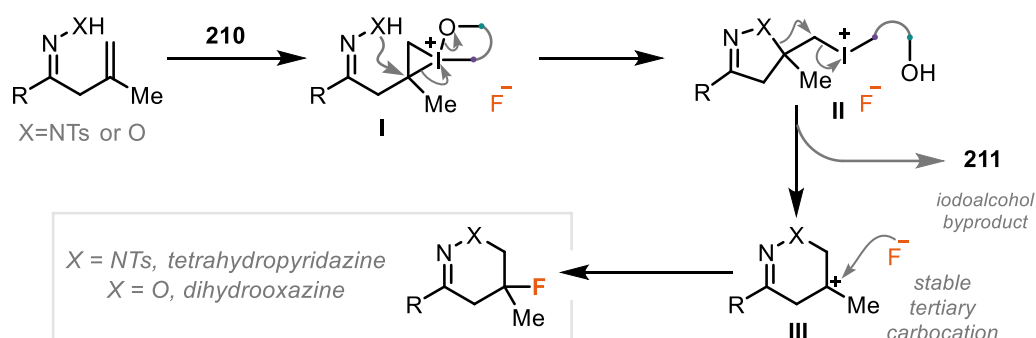


Scheme 5.13 Mechanism for fluorocyclisation with Selectfluor

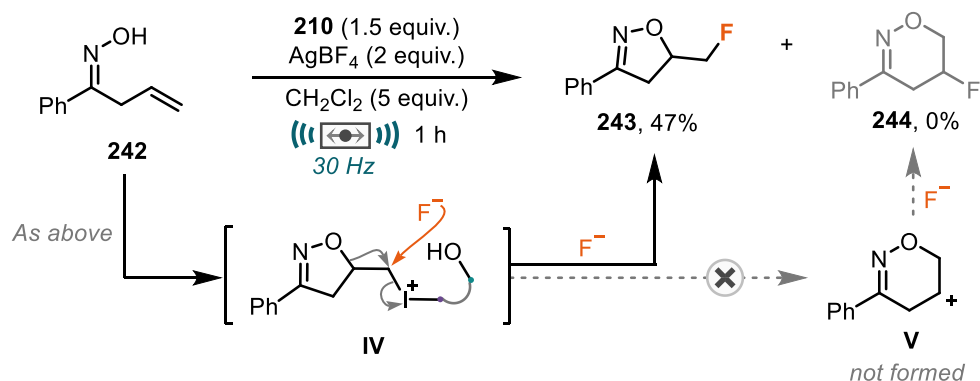
The application of the new hypervalent iodine fluorinating agent allows for the access of new chemical space and a different mechanistic pathway. The proposed mechanism for the synthesis of 6-membered fluorinated heterocycles begins with the activation of the fluoroiodane reagents. In the mechanochemical reactions, this is shown with HFIP for the hydrazone fluorocyclisation, and AgBF_4 for the oxime fluorocyclisation. Previous studies and DFT calculations detail the overall effect of both activators is to elongate the I-F bond, typically through coordination to the fluorine atom, thereby enhancing reactivity of the reagent. The alkene motif of the unsaturated hydrazone / oxime reacts with the activated fluoroiodane reagent, eliminating fluoride and forming an iodonium species (Scheme 5.14A, intermediate I). 5-Exo-tet cyclisation from the heteroatom then occurs, ring-opening the iodonium as well as breaking the weakened I-O bond to give a positively

charged iodine(I) species (Scheme 5.14A, intermediate **II**). The presence of the methyl group on the alkene component in the starting material allows for the key ring expansion step, whereby the iodoalcohol backbone (**211**) of the reagent is released resulting in the formation of a stable tertiary carbocation (Scheme 5.14A, intermediate **III**). Interception of this cation with the previously liberated fluoride then gives the final 6-membered fluorinated heterocycles.

A Fluorocyclisation pathway with hypervalent fluoroiodane reagent



B Reaction with mono-substituted unsaturated oxime



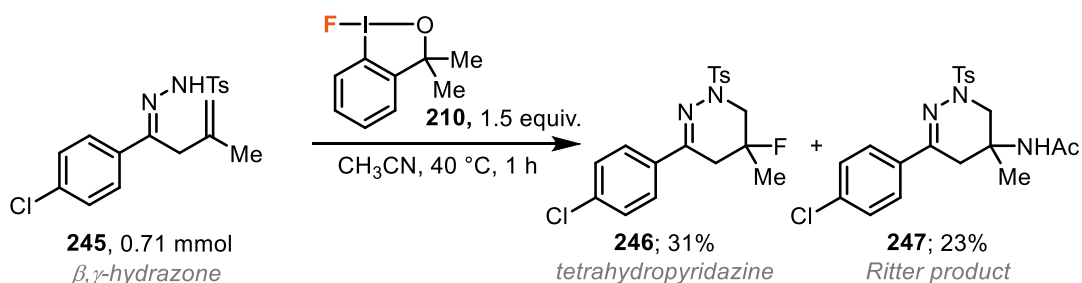
Scheme 5.14 Proposed mechanism for fluorocyclisation using fluoroiodane reagent

It was thought that the nature of the cation formed i.e., tertiary determines the excellent selectivity of the reaction. To probe this further, the mechanochemical fluorocyclisation of oxime **242** was examined (Scheme 5.14B). The result of this is that no 6-membered dihydrooxazine **244** was observed and the reaction instead furnished 47% of 5-membered isoxazoline **243**. The altered selectivity in this reaction can be attributed to the stability of the carbocation that is formed upon ring expansion (from intermediate **IV**).

5 - Mechanochemical Fluorocyclisations Using a Hypervalent Fluoriodane Reagent

Previously, using disubstituted alkenes, a stable tertiary carbocation is formed (Scheme 5.14A, intermediate **C**), however the monosubstituted oxime would result in a secondary carbocation (Scheme 5.14B, intermediate **V**), which has significantly reduced stability and evidently does not form. The reaction instead achieves the product that is typically seen when using Selectfluor (under a fluorine radical transfer pathway), although the formation of isoxazoline **243** is thought to occur via simple fluoride substitution of the charged iodine species in intermediate **IV** (Scheme 5.14B). The fluorocyclisation of oximes with a mono-substituted alkene for the synthesis of 5-membered heterocycles has previously been reported using a hypervalent iodine reagent $\text{PhI}(\text{O}i\text{Pr})_2$ in combination with $\text{HF}\cdot\text{pyridine}$ and these findings are in good agreement.⁴³

Evidence for carbocation formation is also given by the formation of a Ritter-type product **247** when using acetonitrile as the solvent under the solution based set up (performed by Dr William Riley), suggesting that once a carbocation is formed, it can be trapped by any available nucleophile (Scheme 5.15).



Scheme 5.15 Observation of Ritter product. Results by Dr William Riley

5.3 Conclusions and Comparisons

To conclude, this work demonstrates synthetic routes to novel fluorinated heterocycles via ball-milling. Taking advantage of an emerging hypervalent iodine fluoroiodane reagent, the construction of fluorinated tetrahydropyridazines and dihydrooxazines was achieved under mechanochemical conditions. This selectivity for 6-membered heterocycles is complementary to that previously achieved using typical fluorinating agents such as Selectfluor and is made possible by a ring expansion under the proposed mechanistic pathway.

The mechanochemical fluorocyclisation studies started through initial assessment of a known solution-based fluorolactonisation, in order to establish a default set of conditions and assess stability of the fluoroiodane under ball-milling conditions. HFIP was found to be a good activator for the fluorolactonisation of a small range of unsaturated carboxylic acids due to its Brønsted acidity.

β,γ -Unsaturated hydrazones were shown to participate in the mechanochemical fluorocyclisation much faster, furnishing a range of fluorinated tetrahydropyridazines in excellent yield after just 15 minutes of milling. The yields are comparable to that achieved by an analogous solution reaction, however the use of just 2 equivalents of HFIP allows for a solvent-minimised approach for the synthesis.

The mechanochemical fluorocyclisation of β,γ -unsaturated oximes proved to be a more challenging reaction, and initial assessment using HFIP as an activator demonstrated selectivity issues with undesired isooxazoline formation and elimination pathways being present alongside the targeted dihydrooxazine. This challenge was overcome by switching to a different known fluoroiodane activator, AgBF_4 , which in combination with CH_2Cl_2 as a liquid additive aided in furnishing a small range of fluorinated dihydrooxazines, prepared using a 1 hour milling reaction. The yields obtained by ball-milling were shown to be significantly higher than that achieved by an analogous solution reaction. (42-53% in solution vs 61-80% mechanochemically).

The reaction mechanism is proposed to proceed by initial formation of the 5-membered heterocycle from an iodonium intermediate, followed by ring expansion. The stable tertiary cation can then be intercepted by a fluoride anion. It is interesting to consider the opportunities for synthesis that this type of reagent and reaction manifold may allow access to. For example, alternative heterocycles such as dihydrothiazenes may be explored, or modification of the hypervalent iodine reagent to introduce alternative

5 - Mechanochemical Fluorocyclisations Using a Hypervalent Fluoroiodane Reagent

moieties. Derivatisation of these heterocycles, such as asymmetric imine reduction, may also provide further scope and potential application to therapeutics.

5.4 Bibliography

- 1 W. Riley, A. C. Jones, K. Singh, D. L. Browne and A. M. Stuart, *Chem. Commun.*, 2021, **57**, 7406–7409.
- 2 S. Purser, P. R. Moore, S. Swallow and V. Gouverneur, *Chem. Soc. Rev.*, 2008, **37**, 320–330.
- 3 M. Inoue, Y. Sumii and N. Shibata, *ACS Omega*, 2020, **5**, 10633–10640.
- 4 M. M. Alauddin, *Am. J. Nucl. Med. Mol. Imaging*, 2011, **2**, 55–76.
- 5 J. Petzold, Y. Lee, S. Pooseh, L. Oehme, B. Beuthien-Baumann, E. D. London, T. Goschke and M. N. Smolka, *Sci. Rep.*, 2019, **9**, 17927.
- 6 A. Harsanyi and G. Sandford, *Green Chem.*, 2015, **17**, 2081–2086.
- 7 L. N. Markovskij, V. E. Pashinnik and A. V. Kirsanov, *Synthesis*, 1973, **1973**, 787–789.
- 8 W. J. Middleton, *J. Org. Chem.*, 1975, **40**, 574–578.
- 9 H. Hayashi, H. Sonoda, K. Fukumura and T. Nagata, *Chem. Commun.*, 2002, 1618–1619.
- 10 P. Tang, W. Wang and T. Ritter, *J. Am. Chem. Soc.*, 2011, **133**, 11482–11484.
- 11 M. K. Nielsen, C. R. Ugaz, W. Li and A. G. Doyle, *J. Am. Chem. Soc.*, 2015, **137**, 9571–9574.
- 12 R. E. Banks, S. N. Mohialdin-Khaffaf, G. S. Lal, I. Sharif and R. G. Syvret, *J. Chem. Soc. Chem. Commun.*, 1992, 595–596.
- 13 J. J. Hart and R. G. Syvret, *J. Fluor. Chem.*, 1999, **100**, 157–161.
- 14 E. Differding and H. Ofner, *Synlett*, 1991, **1991**, 187–189.
- 15 T. Umemoto and G. Tomizawa, *Bull. Chem. Soc. Jpn.*, 1986, **59**, 3625–3629.
- 16 R. E. Banks, *J. Fluor. Chem.*, 1998, **87**, 1–17.
- 17 N. Srikanth Reddy, N. Ravi Kumar, D. Krishna Swaroop, N. Punna, G. Jitender Dev, N. Jagadeesh Babu and B. Narsaiah, *Eur. J. Org. Chem.*, 2019, **2019**, 2409–2413.
- 18 R. E. Banks, N. J. Lawrence and A. L. Popplewell, *J. Chem. Soc. Chem. Commun.*, 1994, 343–344.
- 19 P. T. Nyffeler, S. G. Durón, M. D. Burkart, S. P. Vincent and C.-H. Wong, *Angew. Chem. Int. Ed.*, 2005, **44**, 192–212.
- 20 R. Robidas and C. Y. Legault, *Helv. Chim. Acta*, 2021, **104**, e2100111.
- 21 S. V. Kohlhepp and T. Gulder, *Chem. Soc. Rev.*, 2016, **45**, 6270–6288.
- 22 C. Y. Legault and J. Prévost, *Acta Crystallogr. Sect. E Struct. Rep. Online*, 2012, **68**, o1238–o1238.
- 23 V. Matoušek, E. Pietrasiak, R. Schwenk and A. Togni, *J. Org. Chem.*, 2013, **78**, 6763–6768.
- 24 M. A. C. González, P. Nordeman, A. B. Gómez, D. N. Meyer, G. Antoni, M. Schou and K. J. Szabó, *Chem. Commun.*, 2018, **54**, 4286–4289.
- 25 G. C. Geary, E. G. Hope, K. Singh and A. M. Stuart, *Chem. Commun.*, 2013, **49**, 9263–9265.
- 26 N. O. Ilchenko, B. O. A. Tasch and K. J. Szabó, *Angew. Chem. Int. Ed.*, 2014, **53**, 12897–12901.
- 27 N. O. Ilchenko and K. J. Szabó, *J. Fluor. Chem.*, 2017, **203**, 104–109.
- 28 W. Yuan, L. Eriksson and K. J. Szabó, *Angew. Chem. Int. Ed.*, 2016, **55**, 8410–8415.
- 29 W. Yuan and K. J. Szabó, *Angew. Chem. Int. Ed.*, 2015, **54**, 8533–8537.
- 30 J. Zhang, K. J. Szabó and F. Himo, *ACS Catal.*, 2017, **7**, 1093–1100.
- 31 G. C. Geary, E. G. Hope and A. M. Stuart, *Angew. Chem. Int. Ed.*, 2015, **54**, 14911–14914.
- 32 D. Parmar, M. S. Maji and M. Rueping, *Chem. – Eur. J.*, 2014, **20**, 83–86.
- 33 M. Okada, Y. Nakamura, H. Horikawa, T. Inoue and T. Taguchi, *J. Fluor. Chem.*, 1997, **82**, 157–161.

5 - Mechanochemical Fluorocyclisations Using a Hypervalent Fluoriodane Reagent

- 34 A. Ulmer, C. Brunner, A. M. Arnold, A. Pöthig and T. Gulder, *Chem. – Eur. J.*, 2016, **22**, 3660–3664.
- 35 T. Yan, B. Zhou, X.-S. Xue and J.-P. Cheng, *J. Org. Chem.*, 2016, **81**, 9006–9011.
- 36 A. Andries-Ulmer, C. Brunner, J. Rehbein and T. Gulder, *J. Am. Chem. Soc.*, 2018, **140**, 13034–13041.
- 37 C. Brunner, A. Andries-Ulmer, G. M. Kiefl and T. Gulder, *Eur. J. Org. Chem.*, 2018, 2615–2621.
- 38 X.-Q. Hu, J.-R. Chen, Q. Wei, F.-L. Liu, Q.-H. Deng, Y.-Q. Zou and W.-J. Xiao, *Eur. J. Org. Chem.*, 2014, 3082–3086.
- 39 C. B. Tripathi and S. Mukherjee, *Org. Lett.*, 2014, **16**, 3368–3371.
- 40 J. Zhao, M. Jiang and J.-T. Liu, *Org. Chem. Front.*, 2018, **5**, 1155–1159.
- 41 Y.-Y. Liu, J. Yang, R.-J. Song and J.-H. Li, *Adv. Synth. Catal.*, 2014, **356**, 2913–2918.
- 42 J. Zhao, M. Jiang and J.-T. Liu, *Adv. Synth. Catal.*, 2017, **359**, 1626–1630.
- 43 W. Kong, Q. Guo, Z. Xu, G. Wang, X. Jiang and R. Wang, *Org. Lett.*, 2015, **17**, 3686–3689.
- 44 J. L. Howard, Y. Sagatov, L. Repousseau, C. Schotten and D. L. Browne, *Green Chem.*, 2017, **19**, 2798–2802.
- 45 J. L. Howard, Y. Sagatov and D. L. Browne, *Tetrahedron*, 2018, **74**, 3118–3123.
- 46 Y. Wang, H. Wang, Y. Jiang, C. Zhang, J. Shao and D. Xu, *Green Chem.*, 2017, **19**, 1674–1677.
- 47 J. L. Howard, W. Nicholson, Y. Sagatov and D. L. Browne, *Beilstein J. Org. Chem.*, 2017, **13**, 1950–1956.
- 48 B. R. Boswell, C. M. F. Mansson, J. M. Cox, Z. Jin, J. A. H. Romaniuk, K. P. Lindquist, L. Cegelski, Y. Xia, S. A. Lopez and N. Z. Burns, *Nat. Chem.*, 2021, **13**, 41–46.
- 49 X. Rao, S. Kuga, M. Wu and Y. Huang, *Cellulose*, 2015, **22**, 2341–2348.
- 50 G. Scholz, *ChemTexts*, 2021, **7**, 16.
- 51 H. K. Minhas, W. Riley, A. M. Stuart and M. Urbonaite, *Org. Biomol. Chem.*, 2018, **16**, 7170–7173.
- 52 Kita, Y., Tohma, H., Masanao, I., Hatanaka, K. & Yakura, T, *Tetrahedron Lett.*, **32**, 4321–4324
- 53 B. Zhou, T. Yan, X.-S. Xue and J.-P. Cheng, *Org. Lett.*, 2016, **18**, 6128–6131.
- 54 B. Zhou, X. Xue and J. Cheng, *Tetrahedron Lett.*, 2017, **58**, 1287–1291.

6 Experimental

6.1 General Information and Milling Equipment.....	175
6.2 A Robust Pd-PEPPSI Catalysed Carbon-Sulfur coupling by Ball-milling.....	177
6.1.1 General Experimental Procedures	177
6.2.2 Characterisation Data of Products.....	178
6.2.3 Comparison to Solution Reactions	188
6.2.4 Trace Metal Analysis.....	190
6.3 Cross-electrophile Coupling of Alkyl and Aryl Halides under Ball-milling Conditions.....	191
6.3.1 General Experimental Procedures	191
6.3.2 Synthesis of substrates	191
6.3.3 Characterisation data of products	193
6.3.4 Mechanistic Studies – Radical Clock and TEMPO Trapping	202
6.3.4 Scale-up Protocol.....	203
6.4 Mechanochemical Reductive Coupling of Activated Amides with Alkyl Halides	205
6.4.1 Synthesis of Starting Materials	205
6.4.2 Mechanochemical Reductive Cross-coupling Procedure and Characterisation Data of Products.....	213
6.4.3 Mechanistic studies	223
6.4.4 Scale up protocol	225
6.4.5 Other twisted amide reactivity by ball milling	226
6.5 Mechanochemical Fluorocyclisations Using a Hypervalent Fluoroiodane Reagent	228
6.5.1 Preparation of Fluoroiodane Reagent	228
6.5.2 Mechanochemical Fluorocyclisation of unsaturated Carboxylic Acids..	229
6.5.3 Mechanochemical Fluorocyclisation of β,γ -unsaturated Hydrazones	234
6.5.4 Mechanochemical Fluorocyclisation of β,γ -unsaturated Oximes	237
6.6 Bibliography	241

6.1 General Information and Milling Equipment

Thin layer chromatography (TLC) was carried out using Merck TLC silica gel 60 sheet and visualized with ultraviolet light or potassium permanganate stain. For Chapter 4, a 2,4-DNP stain was used for rapid visualisation of ketone products. Flash column chromatography (FCC) was performed with Sigma Aldrich silica gel 40-60 Å as the stationary phase and solvents employed were analytical grade. ^1H NMR spectra were recorded on a Bruker AVX500 (500 MHz) spectrometer at ambient temperature. ^{13}C NMR spectra were recorded on a Bruker AVX500 (126 MHz) spectrometer at ambient temperature. ^{19}F NMR spectra were recorded on a Bruker AVX500 (376 MHz) spectrometer at ambient temperature. ^1H and ^{13}C NMR spectra were referenced to residual protonated solvent (CDCl_3 : δ 7.26 ppm and 77.16 ppm respectively). Spin-spin coupling constants J are given in Hz and refer to apparent multiplicities rather than true coupling constants.

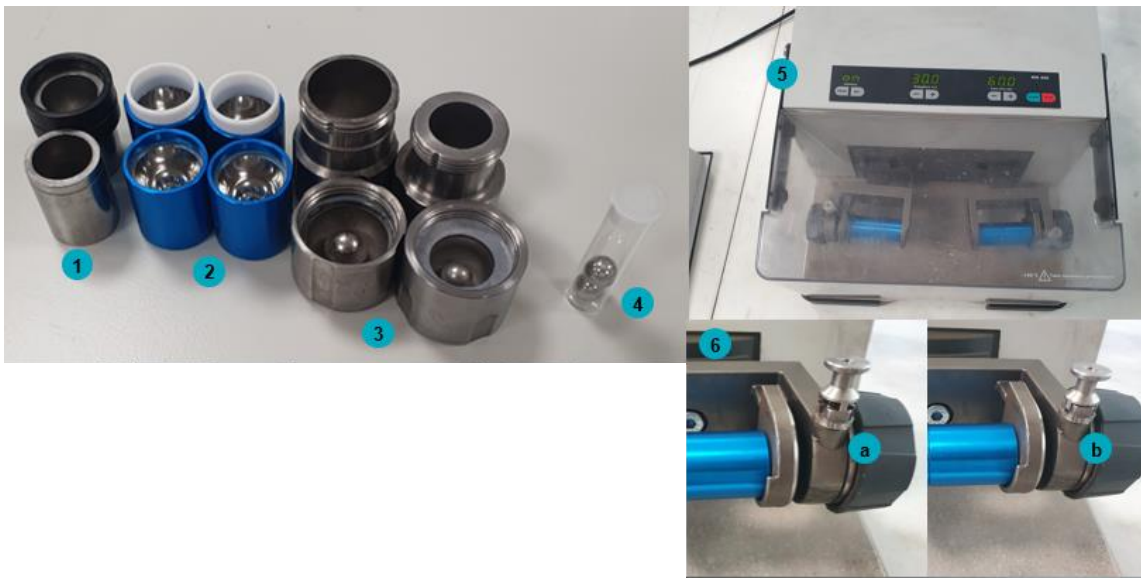
Melting points were measured on a Gallenkamp melting point apparatus and are reported corrected by linear calibration to benzophenone (47 - 49 °C) and benzoic acid (121 - 123 °C).

High resolution mass spectral (HRMS) data were obtained on a Waters MALDI-TOF mx in Cardiff University. Spectra were obtained using electron impact ionization (EI), chemical ionization (CI), positive electrospray (ES), pneumatically assisted electrospray (pESI) or atmospheric solids analysis probe (ASAP+). Inductively coupled plasma mass spectrometry (ICP-MS) data was obtained on an Agilent technologies 7900 ICP-MS. Infrared spectra were recorded on a Shimadzu IR-Affinity-1S FTIR spectrometer.

The ball mill used in all cases was a Retsch MM 400 mixer mill. The longest time this mill can be programmed to run is 99 minutes. Therefore, for reactions over 90 minutes, the mill was restarted after the initial 90 minute with the desired remaining time added. Milling balls were purchased from Bearingboys or Retsch.

Safety precaution: For experiments containing thiols in chapter 2, all equipment that came into contact with the thiol were soaked in a container filled with diluted bleach solution in a fume hood for at least 2 hours.

Milling equipment



- 1) IST milling jar 14 mL stainless steel with retaining collar
(<http://www.insolidotech.org/accessories.html>) – *Not used in this thesis*
- 2) FTS Smartsnap™ grinding jars, 15 mL stainless steel with PTFE retaining washer
(<https://formtechscientific.com/fts-1000-shaker-mill/products.html?section=accessories&accessory=smartsnap-grinding-jars>)
- 3) Retsch stainless steel milling jars 25 mL and 15 mL
(<https://www.retsch.com/products/milling/ball-mills/mixer-mill-mm-400/order-data-quote-request/>)
- 4) 4 g stainless steel milling balls from Retsch
(<https://www.retsch.com/products/milling/ball-mills/mixer-mill-mm-400/order-data-quote-request/>) (<https://www.bearingboys.co.uk/Ball-Bearings-Loose-1018-c>)
- 5) Retsch MM 400™ control panel and FTS Smartsnap™ grinding jars mounted
(<https://www.retsch.com/products/milling/ball-mills/mixer-mill-mm-400/function-features/>)
- 6) Retsch jar mounting with FTS Smartsnap™ grinding jars, (a) unlocked and (b) locked

6.2 A Robust Pd-PEPPSI Catalysed Carbon-Sulfur coupling by Ball-milling

6.1.1 General Experimental Procedures

Pd-PEPPSI Complexes

Pd-PEPPSI complexes used in this catalyst screen were synthesised according to a previously reported method.¹ Pd-PEPPSI-IPent was purchased from Sigma Aldrich (CAS No: 1158652-41-5).

General Procedure 1 (GP1): Mechanochemical C-S Coupling

To a 15 mL stainless steel jar (Form-Tech Scientific), a 3 g stainless steel milling ball was added. Aryl halide (1 mmol), thiol (1 mmol), sand (2 mass equivalents), potassium *tert*-butoxide (2 mmol, 0.2244 g) and Pd-PEPPSI-IPent (0.005 mmol, 0.0040 g) were added under an air atmosphere. The milling jar was then closed, and the mixture was milled at 30 Hz for 3 hours. After the desired reaction time, the black solid mixture was scraped out using a spatula and the jar was washed with EtOAc (~25-30 mL). The mixture was filtered and concentrated under reduced pressure. The crude product was purified by flash column chromatography using the noted solvent systems.

General Procedure 2 (GP2): Zinc-Assisted Mechanochemical C-S Coupling (used when large amounts of disulfide observed using GP1)

To a 15 mL stainless steel jar (Form-Tech Scientific), a 3 g stainless steel milling ball was added. Aryl halide (1 mmol), thiol (1 mmol), sand (2 mass equivalents), potassium *tert*-butoxide (2 mmol, 0.2244 g), Pd-PEPPSI-IPent (0.005 mmol, 0.0040 g) and zinc flake – 325 mesh (2.5 mmol, 0.1635 g) were added under an air atmosphere. The milling jar was then closed, and the mixture was milled at 30 Hz for 3 hours. After the desired reaction time, the black solid mixture was scraped out using a spatula and the jar was washed with EtOAc (~25-30 mL). The mixture was filtered and concentrated under reduced pressure. The crude product was purified by flash column chromatography using the noted solvent systems.

General Procedure 3 (GP3): To be Used for Cross-coupling Disulfides

To a 15 mL stainless steel jar (Form-Tech Scientific), a 3 g stainless steel milling ball was added. Disulfide (0.5 mmol), zinc flake – 325 mesh (2.5 mmol, 0.1635 g) and potassium *tert*-butoxide (2 mmol, 0.2244 g) were added under an air atmosphere. The milling jar was closed, and the mixture was milled at 30 Hz for 1 hour. The reaction vessel was then opened and aryl halide (1 mmol), sand (2 mass equivalents) and Pd-PEPPSI-

IPent (0.005 mmol, 0.0040 g) were added, and the jar was then closed. The reaction mixture was then milled for a further 3 hours at 30 Hz. After this period, the black solid was scraped out using a spatula and the jar was washed with EtOAc (~25-30 mL). The mixture was then filtered and concentrated under reduced pressure. The crude thioether products were purified by flash column chromatography using the noted solvent systems.

General procedure 4 (GP4): Phase-transition Induced Reactivity (used if one of the reactants is solid at room temperature but melts below 60 °C).

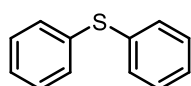
To a 15 mL stainless steel jar (Form-Tech Scientific), a 3 g stainless-steel ball was added. Aryl halide (1 mmol), thiol (1 mmol), sand (2 mass equivalents), potassium *tert*-butoxide (2 mmol, 0.2244 g) and Pd-PEPPSI-IPent (0.005 mmol, 0.0040 g) were added under an air atmosphere. The milling jar was then closed. The jar was modified by casing in cotton wool and surrounded by aluminium foil (see picture below) and the mixture was then milled at 30 Hz for 3 hours. After the desired reaction time, the black solid mixture was scraped out using a spatula and the jar was washed with EtOAc (~25-30 mL). The mixture was filtered and concentrated under reduced pressure. The crude product was purified by flash column chromatography using the noted solvent systems.



Figure 6.1 Insulated milling jar

6.2.2 Characterisation Data of Products

Diphenyl sulfide (44)

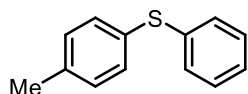


Prepared according to **GP1**. Purified by flash column chromatography (hexane) to give the title compound (0.172 g, 92%) as a colourless oil. **¹H NMR** (500 MHz, CDCl₃) δ 7.37 (d, *J* = 7.4 Hz, 4H), 7.32 (t, *J* = 7.6 Hz, 4H), 7.27 (d, *J* = 7.1 Hz, 2H). **¹³C NMR** (126 MHz, CDCl₃) δ 135.9, 131.2, 129.3, 127.2. **HRMS** (EI) *m/z*: [M]⁺ Calcd for C₁₂H₁₀S 186.0503, found: 186.0499. Characterisation data in accordance with literature report.²

6 - Experimental

Also prepared according to **GP3** by the 2 step reduction / coupling reaction of diphenyl disulfide (0.109 g, 0.5 mmol) and iodobenzene (0.2040, 1 mmol) to give the title compound (0.149 g, 80%).

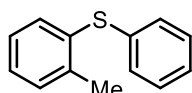
4-Methylphenyl phenyl sulfide (67)



Prepared according to **GP1**. Purified by flash column chromatography (hexane) to give the title compound (0.170 g, 85%) as a colourless oil. **¹H NMR** (500 MHz, CDCl₃) δ 7.33 – 7.30 (m, 2H), 7.29 – 7.26 (m, 4H), 7.22 – 7.18 (m, 1H), 7.16 – 7.13 (m, 2H), 2.35 (s, 3H). **¹³C NMR** (126 MHz, CDCl₃) δ 137.7, 137.3, 132.4, 131.4, 130.2, 129.9, 129.2, 126.5, 21.3. **HRMS** (EI) m/z: [M]⁺ Calcd for C₁₃H₁₂S 200.0660, found: 200.0653. Characterisation data in accordance with literature report.²

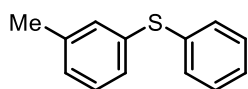
Also prepared according to **GP4** for the phase transition induced coupling of 4-methylthiophenol and iodobenzene to give the title compound (0.168 g, 84%).

2-Methylphenyl phenyl sulfide (68)



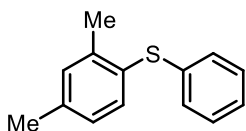
Prepared according to **GP1**. Purified by flash column chromatography (hexane) to give the title compound (0.164 g, 82%) as a colourless oil. **¹H NMR** (500 MHz, CDCl₃) δ 7.24 – 7.03 (m, 9H), 2.31 (s, 3H). **¹³C NMR** (126 MHz, CDCl₃) δ 140.1, 136.3, 133.9, 133.1, 130.7, 129.8, 129.3, 128.0, 126.9, 126.5, 20.7. **HRMS** (EI) m/z: [M]⁺ Calcd for C₁₃H₁₂S 200.0660, found: 200.0654. Characterisation data in accordance with literature report.²

3-Methylphenyl phenyl sulfide (69)



Prepared according to **GP1**. Purified by flash column chromatography (hexane) to give the title compound (0.166 g, 83%) as a colourless oil. **¹H NMR** (500 MHz, CDCl₃) δ 7.36 – 7.33 (m, 2H), 7.32 – 7.28 (m, 2H), 7.26 – 7.19 (m, 3H), 7.17 – 7.14 (m, 1H), 7.09 – 7.05 (m, 1H), 2.34 (s, 3H) **¹³C NMR** (126 MHz, CDCl₃) δ 139.2, 136.3, 135.4, 132.0, 130.9, 129.3, 129.2, 128.5, 128.2, 127.0, 21.4. **HRMS** (AP+) m/z: [M]⁺ Calcd for C₁₃H₁₂S 200.0660, found: 200.0652. Characterisation data in accordance with literature report.²

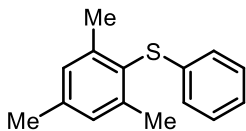
2,4-Dimethylphenyl phenyl sulfide (70)



Prepared according to **GP1**. Purified by flash column chromatography (hexane) to give the title compound (0.184 g, 86%) as a colourless oil. **¹H NMR** (500 MHz, CDCl₃) δ 7.32 (d, *J* = 7.8 Hz, 1H), 7.28 – 7.22 (m, 2H), 7.18 – 7.11 (m, 4H), 7.01 (d, *J* = 7.8 Hz, 1H), 2.36 (s, 3H), 2.35 (s, 3H). **¹³C NMR** (126 MHz, CDCl₃) δ 141.0, 138.7, 137.5, 134.6, 131.7, 129.4, 129.1, 128.4, 127.7, 125.8, 21.2, 20.7. **HRMS** (AP+) *m/z*: [M]⁺ Calcd for C₁₄H₁₄S 214.0816, found: 214.0812. Characterisation data in accordance with literature report.²

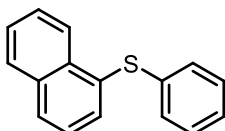
Also prepared according to **GP3** by the 2-step reduction / coupling reaction of 1,2-bis(2,4-dimethylphenyl) disulfide (0.137 g, 0.5 mmol) and iodobenzene (0.204 g, 1 mmol) to give the title compound (0.150 g, 70%).

2,4,6-Trimethylphenyl phenyl sulfide (71)



Prepared according to **GP1**. Purified by flash column chromatography (hexane) to give the title compound (0.164 g, 72%) as a colourless oil. **¹H NMR** (500 MHz, CDCl₃) δ 7.17 (t, *J* = 7.5 Hz, 2H), 7.08 – 7.03 (m, 1H), 7.02 (s, 2H), 6.92 (d, *J* = 7.7 Hz, 2H), 2.39 (s, 6H), 2.33 (s, 3H). **¹³C NMR** (126 MHz, CDCl₃) δ 143.9, 139.4, 138.5, 129.5, 129.0, 127.1, 125.6, 124.6, 21.8, 21.3. **HRMS** (EI) *m/z*: [M]⁺ Calcd for C₁₅H₁₆S 204.0409, found: 204.0413. Characterisation data in accordance with literature report.³

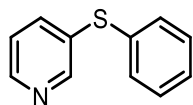
1-Naphthylphenyl sulfide (72)



Prepared according to **GP1**. Purified by flash column chromatography (hexane) to give the title compound (0.177 g, 76%) as a yellow oil. **¹H NMR** (500 MHz, CDCl₃) δ 8.44 – 8.34 (m, 1H), 7.93 – 7.83 (m, 2H), 7.67 (dd, *J* = 7.2, 1.2 Hz, 1H), 7.55 – 7.50 (m, 2H), 7.47 – 7.42 (m, 1H), 7.25 – 7.14 (m, 5H). **¹³C NMR** (126 MHz, CDCl₃) δ 137.1, 134.4, 133.7, 132.7, 131.4, 129.4, 129.2, 129.1, 128.7, 127.1, 126.6, 126.3, 126.0, 125.8.

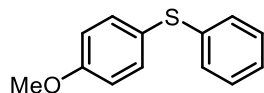
HRMS (EI) m/z : $[M]^+$ Calcd for $C_{16}H_{12}S$ 236.0660, found: 236.0669. Characterisation data in accordance with literature report.⁴

3-Pyridinyl phenyl sulfide (73)



Prepared according to **GP1**. Purified by flash column chromatography (petroleum ether / EtOAc : 9 / 1) to give the title compound (0.095 g, 51%) as a colourless oil. **¹H NMR** (500 MHz, $CDCl_3$) δ 8.56 (d, $J = 1.7$ Hz, 1H), 8.51 – 8.43 (m, 1H), 7.65 – 7.54 (m, 1H), 7.40 – 7.36 (m, 2H), 7.36 – 7.32 (m, 2H), 7.32 – 7.27 (m, 1H), 7.21 (ddd, $J = 8.0, 4.8, 0.8$ Hz, 1H). **¹³C NMR** (126 MHz, $CDCl_3$) δ 151.1, 147.9, 137.92, 133.9, 133.7, 131.8, 129.5, 127.9, 123.9. **HRMS** (EI) m/z : $[M]^+$ Calcd for $C_{11}H_9NS$ 187.0456, found: 187.0458. Characterisation data in accordance with literature report.²

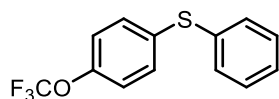
4-Methoxyphenyl phenyl sulfide (74)



Prepared according to **GP1**. Purified by flash column chromatography (hexane / EtOAc : 19 / 1) to give the title compound (0.203 g, 94%) as a colourless oil. **¹H NMR** (500 MHz, $CDCl_3$) δ 7.23 (d, $J = 8.1$ Hz, 2H), 7.04 (m, 2H), 7.01 – 6.96 (m, 2H), 6.94 (m, 1H), 6.71 (d, $J = 8.1$ Hz, 2H), 3.62 (s, 3H). **¹³C NMR** (126 MHz, $CDCl_3$) δ 159.9, 138.7, 135.5, 129.0, 128.3, 125.9, 124.4, 115.1, 55.5. **HRMS** (EI) m/z : $[M]^+$ Calcd for $C_{13}H_9S$ 216.0609, found: 216.0608. Characterisation data in accordance with literature report.²

Also prepared according to **GP3** by the 2 step reduction / coupling reaction of 1,2-bis(4-methoxyphenyl) disulfide (0.139 g, 0.5 mmol) and iodobenzene (0.204 g, 1 mmol) to give the title compound (0.153 g, 71%).

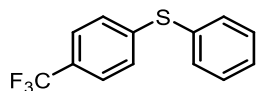
4-Trifluoromethoxyphenyl phenyl sulfide (75)



Prepared according to **GP1**. Purified by flash column chromatography (hexane) to give the title compound (0.165 g, 61%) as a colourless oil. **¹H NMR** (500 MHz, $CDCl_3$) δ 7.41 – 7.27 (m, 7H), 7.14 (d, $J = 8.6$ Hz, 2H). **¹³C NMR** (126 MHz, $CDCl_3$) δ 148.2 (q, $J = 1.8$ Hz), 135.2, 134.9, 131.9, 131.9, 129.6, 127.8, 121.8, 120.6 (q, $J = 257.5$ Hz). **¹⁹F{¹H}**

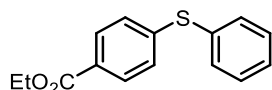
NMR (376 MHz, CDCl₃) δ -57.94. **HRMS** (AP+) m/z: [M]⁺ Calcd for C₁₃H₉OF₃S 270.0326, found: 270.0329. Characterisation data in accordance with literature report.⁵

4-Trifluoromethylphenyl phenyl sulfide (76)



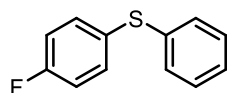
Prepared according to **GP1**. Purified by flash column chromatography (hexane) to give the title compound (0.217 g, 86%) as a white solid. M.p. 56-58 °C. **¹H NMR** (500 MHz, CDCl₃) δ 7.50 – 7.45 (m, 4H), 7.43 – 7.35 (m, 3H), 7.29 – 7.25 (m, 2H). **¹³C NMR** (126 MHz, CDCl₃) δ 143.0, 133.7, 132.7, 129.8, 128.8, 128.4, 128.2 (q, *J* = 32.7 Hz), 126.0 (q, *J* = 3.8 Hz), 124.2 (q, *J* = 271.8 Hz). **¹⁹F NMR** (471 MHz, CDCl₃) δ -62.48. **HRMS** (AP+) m/z: [M]⁺ Calcd for C₁₃H₉F₃S 254.0377, found: 270.0373. Characterisation data in accordance with literature report.²

Ethyl 4-(phenylthio)benzoate (77)

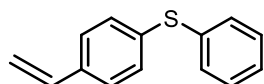


Prepared according to **GP1**. Purified by flash column chromatography (hexane) to give the title compound (0.140 g, 54%) as a colourless oil. **¹H NMR** (500 MHz, CDCl₃) δ 7.92 – 7.89 (m, 2H), 7.50 – 7.45 (m, 2H), 7.41 – 7.36 (m, 3H), 7.23 – 7.19 (m, 2H), 4.35 (q, *J* = 7.1 Hz, 2H), 1.37 (t, *J* = 7.1 Hz, 3H). **¹³C NMR** (126 MHz, CDCl₃) δ 166.4, 144.3, 133.7, 132.7, 130.2, 129.8, 128.7, 128.1, 127.8, 61.1, 14.5. **HRMS** (AP+) m/z: [M]⁺ Calcd for C₁₅H₁₅O₂S 259.0786, found: 259.0793. Characterisation data in accordance with literature report.³

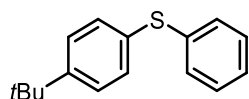
4-Fluorophenyl phenyl sulfide (78)



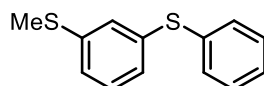
Prepared according to **GP1**. Purified by flash column chromatography (hexane) to give the title compound (0.170 g, 83%) as a colourless oil. **¹H NMR** (500 MHz, CDCl₃) δ 7.38 (m, 2H), 7.33 – 7.20 (m, 5H), 7.08 – 6.99 (m, 2H). **¹³C NMR** (126 MHz, CDCl₃) δ 162.6 (d, *J* = 247.7 Hz), 136.8 (s), 134.3 (d, *J* = 8.2 Hz), 130.4 (d, *J* = 3.4 Hz), 130.1, 129.3, 126.9, 116.6 (d, *J* = 22.0 Hz). **¹⁹F{¹H} NMR** (376 MHz, CDCl₃) δ -114.02. **HRMS** (EI) m/z: [M]⁺ Calcd for C₁₂H₉SF 204.0409, found: 204.0413. Characterisation data in accordance with literature report.²

4-Vinylphenyl phenyl sulfide (79)

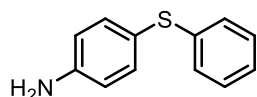
Prepared according to **GP1**. Purified by flash column chromatography (hexane) to give the title compound (0.178 g, 84%) as a colourless oil. **¹H NMR** (500 MHz, CDCl₃) δ 7.39 – 7.35 (m, 4H), 7.35 – 7.31 (m, 4H), 7.29 – 7.25 (m, 1H), 6.71 (dd, *J* = 17.6, 10.9 Hz, 1H), 5.76 (dd, *J* = 17.6, 0.8 Hz, 1H), 5.28 (dd, *J* = 10.9, 0.8 Hz, 1H). **¹³C NMR** (126 MHz, CDCl₃) δ 136.6, 136.2, 135.9, 135.3, 131.3, 131.2, 129.4, 127.2, 127.1, 114.4. **HRMS** (EI) *m/z*: [M]⁺ Calcd for C₁₄H₁₂S 212.0660, found: 212.0659. Characterisation data in accordance with literature report.⁶

4-Tert-butylphenyl phenyl sulfide (80)

Prepared according to **GP1**. Purified by flash column chromatography (hexane) to give the title compound (0.201 g, 83%) as a colourless oil. **¹H NMR** (500 MHz, CDCl₃) δ 7.37 – 7.26 (m, 8H), 7.22 (t, *J* = 7.1 Hz, 1H), 1.32 (s, 9H). **¹³C NMR** (126 MHz, CDCl₃) δ 150.7, 136.8, 131.8, 131.6, 130.4, 129.2, 126.7, 126.4, 34.7, 31.4. **HRMS** (EI) *m/z*: [M]⁺ Calcd for C₁₆H₁₈S 242.1129, found: 242.113. Characterisation data in accordance with literature report⁷

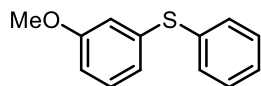
3-Methyl(phenylthio) phenyl sulfide (81)

Prepared according to **GP1**. Purified by flash column chromatography (hexane) to give the title compound (0.172 g, 74%) as a colourless oil. **¹H NMR** (500 MHz, CDCl₃) δ 7.32 – 7.27 (m, 2H), 7.24 (t, *J* = 7.6 Hz, 2H), 7.21 – 7.16 (m, 1H), 7.12 (t, *J* = 7.8 Hz, 2H), 7.05 – 6.96 (m, 2H), 2.35 (s, 3H). **¹³C NMR** (126 MHz, CDCl₃) δ 139.9, 137.1, 135.2, 131.6, 129.5, 129.4, 128.0, 127.5, 127.3, 125.1, 15.7. **HRMS** (EI) *m/z*: [M]⁺ Calcd for C₁₃H₁₂S₂ 232.0380, found: 232.0381. Characterisation data in accordance with literature report.⁸

4-Aminophenyl phenyl sulfide (82)

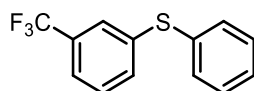
Prepared according to **GP1**. Purified by flash column chromatography (hexane / EtOAc : 19 / 1) to give the title compound (0.143 g, 71%) as a pale brown solid. M.p. 91-94 °C. **¹H NMR** (500 MHz, CDCl₃) δ 7.32 (d, *J* = 8.2 Hz, 2H), 7.21 (m, 2H), 7.16 – 7.06 (m, 3H), 6.68 (d, *J* = 8.2 Hz, 2H), 3.80 (br s, 2H). **¹³C NMR** (126 MHz, CDCl₃) δ 147.2, 139.8, 136.2, 128.9, 127.4, 125.4, 120.6, 116.0. **HRMS** (EI) *m/z*: [M]⁺ Calcd for C₁₂H₁₁NS 201.0612, found: 201.0620. Characterisation data in accordance with literature report.²

3-Methoxyphenyl phenyl sulfide (83)



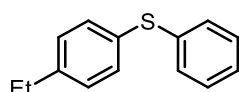
Prepared according to **GP1**. Purified by flash column chromatography (hexane) to give the title compound (0.134 g, 62%) as a colourless oil. **¹H NMR** (500 MHz, CDCl₃) δ 7.42 – 7.37 (m, 2H), 7.33 (t, *J* = 7.5 Hz, 2H), 7.29 – 7.25 (m, 1H), 7.22 (t, *J* = 7.8 Hz, 1H), 6.93 (d, *J* = 7.7 Hz, 1H), 6.89 (s, 1H), 6.79 (d, *J* = 8.3 Hz, 1H), 3.77 (s, 3H). **¹³C NMR** (126 MHz, CDCl₃) δ 160.2, 137.4, 135.4, 131.6, 130.1, 129.3, 127.4, 123.1, 116.0, 112.9, 55.4. **HRMS (EI)** *m/z*: [M]⁺ Calcd for C₁₃H₁₂OS 216.0609, found: 216.0610. Characterisation data in accordance with literature report.⁴

3-Trifluoromethylphenyl phenyl sulfide (84)



Prepared according to **GP1**. Purified by flash column chromatography (hexane) to give the title compound (0.140 g, 55%) as a colourless oil. **¹H NMR** (500 MHz, CDCl₃) δ 7.52 (d, *J* = 9.0 Hz, 1H), 7.48 – 7.31 (m, 8H). **¹³C NMR** (126 MHz, CDCl₃) δ 138.7, 133.7, 132.9, 132.6, 131.7 (q, *J* = 32.4 Hz), 129.7, 129.6, 128.3, 126.3 (q, *J* = 3.8 Hz), 123.9 (q, *J* = 272.6 Hz), 123.4 (q, *J* = 3.7 Hz). **¹⁹F{¹H} NMR** (376 MHz) δ -63.18. **HRMS (AP+)** *m/z*: [M]⁺ Calcd for C₁₃H₉F₃S 254.0372, found: 254.0377. Characterisation data in accordance with literature report.⁹

4-Ethylphenyl phenyl sulfide (85)

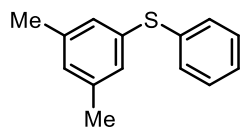


Prepared according to **GP2**. Purified by flash column chromatography (hexane) to give the title compound (0.191 g, 89%) as a colourless oil. **¹H NMR** (500 MHz, CDCl₃) δ 7.36 – 7.14 (m, 9H), 2.65 (q, *J* = 7.6 Hz, 2H), 1.25 (t, *J* = 7.6 Hz, 3H). **¹³C NMR** (126 MHz,

6 - Experimental

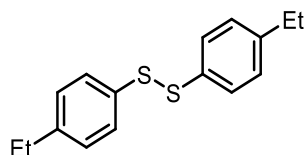
CDCl_3 δ 144.0, 137.1, 132.3, 131.7, 130.1, 129.2, 129.0, 126.6, 28.6, 15.6. **HRMS** (EI) m/z : $[\text{M}]^+$ Calcd for $\text{C}_{14}\text{H}_{14}\text{S}$ 214.0816, found: 214.0824.

3,5-Dimethylphenyl phenyl sulfide (86)



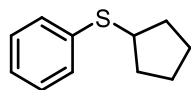
Prepared according to **GP2**. Purified by flash column chromatography (hexane) to give the title compound (0.150 g, 70%) as a colourless oil. **$^1\text{H NMR}$** (500 MHz, CDCl_3) δ 7.35 – 7.27 (m, 4H), 7.23 (m, 1H), 7.01 (s, 2H), 6.90 (s, 1H), 2.28 (s, 6H). **$^{13}\text{C NMR}$** (126 MHz, CDCl_3) δ 139.0, 136.5, 134.9, 130.7, 129.3, 129.3, 129.2, 126.8, 21.3. **HRMS** (EI) m/z : $[\text{M}]^+$ Calcd for $\text{C}_{16}\text{H}_{18}\text{S}$ 214.0816, found: 214.0810. Characterisation data in accordance with literature report.²

1,2-Bis(4-ethylphenyl)disulfide (88)



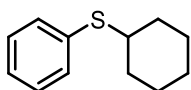
Received (0.115 g, 84%) after purification by flash column chromatography (hexane) as the major product in the reaction of iodobenzene (1 mmol) and 4-ethylthiophenol (1 mmol) using **GP1** attempting to form the cross-coupled product **XX** (above). **$^1\text{H NMR}$** (500 MHz, CDCl_3) δ 7.50-7.42 (m, 4H), 7.20 (d, J = 8.4 Hz, 4H), 2.64 (q, J = 7.6 Hz, 4H), 1.26 (t, J = 7.6 Hz, 6H). **$^{13}\text{C NMR}$** (126 MHz, CDCl_3) 143.9, 134.5, 128.9, 128.4, 28.7, 15.8. Characterisation data in accordance with literature report.¹⁰

Cyclopentyl phenyl sulfide (93)



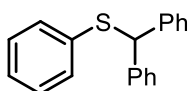
Prepared according to **GP2**. Purified by flash column chromatography (hexane) to give the title compound (0.118 g, 66%) as a colourless oil. **$^1\text{H NMR}$** (500 MHz, CDCl_3) δ 7.39 – 7.33 (m, 2H), 7.31 – 7.25 (m, 2H), 7.21 – 7.15 (m, 1H), 3.64 – 3.54 (m, 1H), 2.10 – 2.00 (m, 2H), 1.82 – 1.73 (m, 2H), 1.68 – 1.57 (m, 4H). **$^{13}\text{C NMR}$** (126 MHz, CDCl_3) δ 137.4, 130.1, 128.9, 125.0, 46.0, 33.7, 24.9. **HRMS** (EI) m/z : $[\text{M}]^+$ Calcd for $\text{C}_{11}\text{H}_{14}\text{S}$ 178.0816, found: 178.0818. Characterisation data in accordance with literature report.¹¹

Cyclohexyl phenyl sulfide (94)



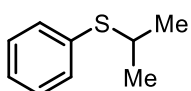
Prepared according to **GP2**. Purified by flash column chromatography (hexane) to give the title compound (0.119 g, 62%) as a colourless oil. **¹H NMR** (500 MHz, CDCl₃) δ 7.44 – 7.35 (m, 2H), 7.34 – 7.24 (m, 2H), 7.21 (m, 1H), 3.15 – 3.06 (m, 1H), 2.03 – 1.94 (m, 2H), 1.77 (m, 2H), 1.66 – 1.59 (m, 1H), 1.43 – 1.21 (m, 5H). **¹³C NMR** (126 MHz, CDCl₃) δ 135.3, 132.0, 128.9, 126.7, 46.7, 33.5, 26.2, 25.9. **HRMS** (EI) m/z: [M]⁺ Calcd for C₁₂H₁₆S 192.0973, found: 192.0980. Characterisation data in accordance with literature report.²

Benzhydryl phenyl sulfide (95)



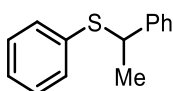
Prepared according to **GP2**. Purified by flash column chromatography (hexane) to give the title compound (0.190 g, 72%) as a white solid. M.p. 74-77 °C. **¹H NMR** (500 MHz, CDCl₃) δ 7.44 (d, *J* = 7.3 Hz, 4H), 7.32 (t, *J* = 7.5 Hz, 4H), 7.25 (m, 4H), 7.22 – 7.13 (m, 3H), 5.57 (s, 1H). **¹³C NMR** (126 MHz, CDCl₃) δ 141.1, 136.3, 130.6, 128.9, 128.7, 128.5, 127.4, 126.7, 57.6. **HRMS** (EI) m/z: [M]⁺ Calcd for C₁₉H₁₆S 276.0973, found: 276.0976. Characterisation data in accordance with literature report.¹²

Isopropyl phenyl sulfide (96)



Prepared according to **GP2**. Purified by flash column chromatography (hexane) to give the title compound (0.087 g, 57%) as a colourless oil. **¹H NMR** (500 MHz, CDCl₃) δ 7.41 (m, 2H), 7.32 – 7.27 (m, 2H), 7.25 – 7.20 (m, 1H), 3.38 (hept, *J* = 6.7 Hz, 1H), 1.30 (d, *J* = 6.7 Hz, 6H). **¹³C NMR** (126 MHz, CDCl₃) δ 135.6, 132.0, 128.9, 126.8, 38.3, 23.3. **HRMS** (EI) m/z: [M]⁺ Calcd for C₉H₁₂S 152.0660, found: 152.0666. Characterisation data in accordance with literature report.¹³

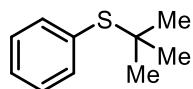
1-Phenylethyl phenyl sulfide (97)



6 - Experimental

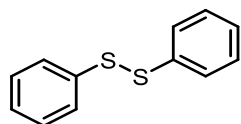
Prepared according to **GP2**. Purified by flash column chromatography (hexane) to give the title compound (0.135 g, 63%) as a colourless oil. **¹H NMR** (500 MHz, CDCl₃) δ 7.34 – 7.26 (m, 6H), 7.26 – 7.19 (m, 4H), 4.35 (q, *J* = 7.0 Hz, 1H), 1.64 (d, *J* = 7.0 Hz, 3H). **¹³C NMR** (126 MHz, CDCl₃) δ 143.3, 135.3, 132.6, 128.8, 128.5, 127.4, 127.3, 127.2, 48.1, 22.5. **HRMS** (EI) *m/z*: [M]⁺ Calcd for C₁₄H₁₄S 214.0816, found: 214.0808. Characterisation data in accordance with literature report.¹²

Tert-butyl phenyl sulfide (98)



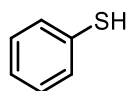
Prepared according to **GP2**. Purified by flash column chromatography (hexane) to give the title compound (0.133 g, 80%) as a colourless oil. **¹H NMR** (500 MHz, CDCl₃) δ 7.55 – 7.52 (m, 2H), 7.39 – 7.30 (m, 3H), 1.29 (s, 9H). **¹³C NMR** (126 MHz, CDCl₃) δ 137.6, 132.8, 128.8, 128.6, 46.0, 31.1. **HRMS** (EI) *m/z*: [M]⁺ Calcd for C₁₀H₁₄S 166.0816, found: 166.0811. Characterisation data in accordance with literature report.¹⁴

Thiol / disulfide interconversion - Diphenyl disulfide (5)



To a 15 mL stainless steel jar (Form-Tech Scientific), a 3 g stainless steel milling ball was added. Thiophenol (0.102 mL, 1 mmol) was added under an air atmosphere. The milling jar was then closed, and the mixture was milled at 30 Hz for 15 minutes. The material was washed from the jar with EtOAc (~15-20 mL). The solvent was evaporated to give the title compound (0.134 g, 98%) as a white solid. M.p. 64-66 °C. **¹H NMR** (500 MHz, CDCl₃) δ 7.44–7.42 (m, 4H), 7.24–7.21 (m, 4H), 7.17–7.14 (m, 2H). **¹³C NMR** (126 MHz, CDCl₃) δ 137.4, 129.4, 127.8, 127.4. Characterisation data in accordance with literature report.¹⁵

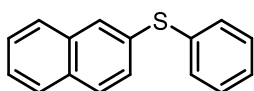
Thiol / disulfide interconversion – Thiophenol (63)



To a 15 mL stainless steel jar (Form-Tech Scientific), a 3 g stainless steel milling ball was added. Diphenyl disulfide (0.109 g, 0.5 mmol), zinc flake – 325 mesh (2.5 mmol, 0.164 g) and potassium *tert*-butoxide (2 mmol, 0.224 g) was added under an air atmosphere. The milling jar was then closed, and the mixture was milled at 30 Hz for 1

hour. The material was washed from the jar with EtOAc (~15-20 mL) into a conical flask. 1M HCl (15 mL) was added, and the layers separated. The aqueous phase was extracted with EtOAc (3 × 10 mL). The combined organic layers were washed with brine (30 mL), dried (MgSO₄), filtered, and concentrated under reduced pressure to give the title compound (0.107 g, 97%) as a colourless liquid. ¹H NMR (500 MHz, CDCl₃) δ 7.31-7.23 (m, 4H), 7.18-7.13 (m, 1H), 3.46 (s, 1H). ¹³C NMR (126 MHz, CDCl₃) 131.2, 129.6, 129.5, 116.0. Characterisation data in accordance with literature report.¹⁶

2-Naphthylphenyl sulfide (105 product)



Prepared according to **GP4** for the phase transition induced coupling of 2-bromonaphthalene and thiophenol. Purified by flash column chromatography (hexane) to give the title compound (0.113 g, 48%) as a white solid. M.p. 52-55 °C. ¹H NMR (500 MHz, CDCl₃) δ 7.84 (s, 1H), 7.82 – 7.71 (m, 3H), 7.52 – 7.44 (m, 2H), 7.43 – 7.36 (m, 3H), 7.32 (t, *J* = 7.3 Hz, 2H), 7.28 – 7.24 (m, 1H). ¹³C NMR (126 MHz, CDCl₃) δ 136.0, 133.9, 133.2, 132.4, 131.1, 130.0, 129.4, 129.0, 128.9, 127.9, 127.6, 127.2, 126.7, 126.4. **HRMS** (AP+) *m/z*: [M]⁺ Calcd for C₁₆H₁₂S 236.0652, found: 236.0660. Characterisation data in accordance with literature report.²

6.2.3 Comparison to Solution Reactions

Conventional Solution Method Under Air for Comparison.

To a 50 mL round bottom flask, potassium *tert*-butoxide (2 mmol, 0.224 g) and Pd-PEPPSI-IPent (0.005 mmol, 0.004 g) was added. Then a premixed solution of 1,4-dioxane (10 mL), 4-fluoro bromobenzene (1 mmol, 0.175 g), thiophenol (1 mmol, 0.110 g) and the internal standard benzotrifluoride (0.33 mmol, 41 μL) was added *via* syringe and the reaction was stirred at room temperature. The reaction was monitored by taking an aliquot and passing through a short plug of celite into an NMR tube. Yields were determined by ¹⁹F NMR referenced to benzotrifluoride.

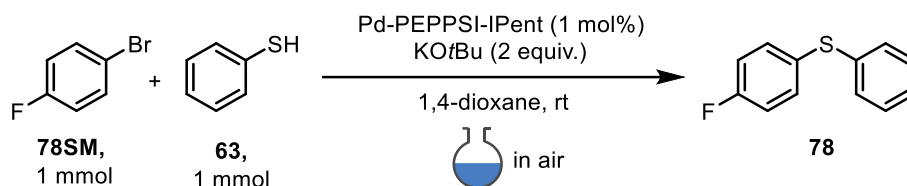
Conventional Solution Method under N₂ for Comparison

To a flame dried 50 mL round bottom flask, potassium *tert*-butoxide (2 mmol, 0.224 g) and Pd-PEPPSI-IPent (0.005 mmol, 0.004 g) was added. The flask was purged with N₂. Then a premixed solution of dry 1,4-dioxane (10 mL), 4-fluoro bromobenzene (1 mmol, 0.175 g), thiophenol (1 mmol, 0.110 g) and the internal standard benzotrifluoride (0.33 mmol, 41 μL) was added *via* syringe and the reaction was stirred at room temperature.

6 - Experimental

The reaction was monitored by taking an aliquot and passing through a short plug of celite into an NMR tube. Yields were determined by ^{19}F NMR referenced to benzotrifluoride.

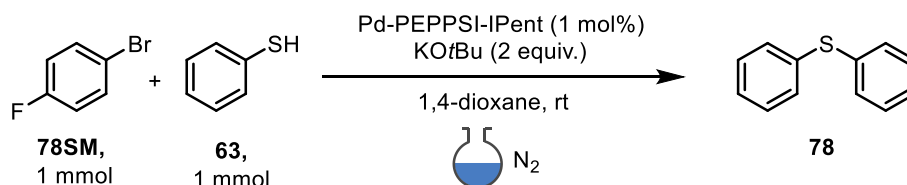
Table 6.1 Solution reaction under air



Entry	Time (h)	Consumption 78SM (%)	Yield 78 (%) ^a
1	0	0	0
2	0.5	19	1
3	1	22	2
4	2	24	2
5	4	26	3
6	6	26	3
8	24	26	4

^a Yield determined by ^{19}F NMR spectroscopy using benzotrifluoride as an internal standard.

Table 6.2 Solution reaction under nitrogen



Entry	Time (h)	Consumption 78SM (%)	Yield 78 (%) ^a
1	0	0	0
2	0.5	12	2
3	1	15	3
4	2	15	5
5	4	15	5
6	6	15	5
8	24	15	5

^a Yield determined by ^{19}F NMR spectroscopy using benzotrifluoride as an internal standard.

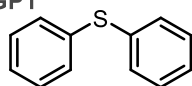
6.2.4 Trace Metal Analysis

Trace metal analysis was carried out to determine the levels of palladium and zinc present at the end of the reaction sequence.

Inductively coupled plasma mass spectrometry (ICP-MS) data was obtained on an Agilent technologies 7900 ICP-MS (detection limit ^{105}Pd = 0.01698 ppb, detection limit ^{66}Zn = 0.516 ppb).

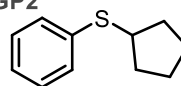
Trace metal analysis - ICP-MS

Following GP1



Pd = 0.07 ppb

Following GP2



Pd = 0.10 ppb
Zn = 31.84 ppb

Figure 6.2 Trace metal analysis

6.3 Cross-electrophile Coupling of Alkyl and Aryl Halides under Ball-milling Conditions

6.3.1 General Experimental Procedures

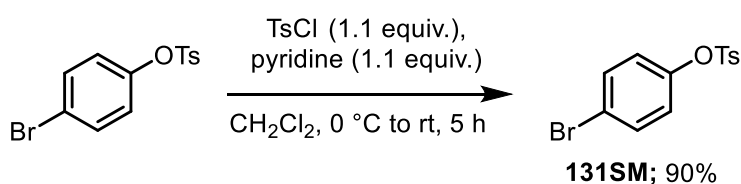
General Procedure 5 (GP5): Mechanochemical Cross-electrophile coupling of Aryl Halides with Alkyl Halides

To a 15 mL stainless steel jar, a 3 g stainless steel milling ball was added. Aryl halide (1 mmol), alkyl halide (1.5 mmol, 1.5 equiv.), NiCl₂•6H₂O (0.024 g, 0.1 mmol, 10 mol%), 1,10-phenanthroline (0.036 g, 0.2 mmol, 20 mol%), zinc granular (20-30 mesh, 0.130 g, 2 mmol, 2 equiv.) and *N,N*-dimethylacetamide (0.180 mL, 3 mmol, 3 equiv.) were all added to the jar (for alkyl bromide examples NaI (0.150 g, 1.0 mmol, 1.0 equiv.) was also added). The jar was closed and placed on the mixer mill. The reaction was milled at 30 Hz for 2 hours. After the milling period the jar was opened and rinsed from the jar into a conical flask using CH₂Cl₂ (~20 mL). 1 M HCl was added to the flask and stirred for 10 minutes. The resulting biphasic mixture was transferred to a separating funnel where the layers were separated. The aqueous layer was extracted with CH₂Cl₂ (2 × 15 mL). The combined organic layers were washed with brine (~40 mL), dried (MgSO₄), filtered, and concentrated under reduced pressure to give the crude product as a yellow/orange oil. The crude product was purified by flash column chromatography using the noted solvent systems to afford the cross-electrophile coupled product.

On some occasions when small quantities of homo-coupled biaryl products co-elute during column chromatography, the mixture can be further purified using Kugelrohr distillation (Büchi b-585 glass oven Kugelrohr) with the pressure and temperature ranges given where appropriate.

6.3.2 Synthesis of substrates

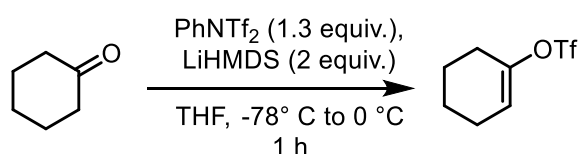
4-Bromophenyl 4-methylbenzenesulfonate (131SM)



Prepared according to a modified literature procedure.¹⁷ To a flame dried flask was added 5-bromophenol (0.855 g, 5 mmol) and CH₂Cl₂ (8 mL). The solution was cooled to 0 °C. Tosyl chloride (1.05 g, 5.5 mmol, 1.1 equiv.) was added followed by dropwise addition of pyridine (0.444 mL). The reaction mixture was warmed to room temperature

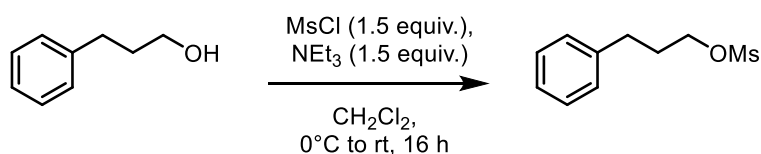
and stirred for 5 hours. Distilled water (~30 mL) and saturated aqueous NH_4Cl (~20 mL) were added, and the layers separated. The aqueous layer was extracted with CH_2Cl_2 (3 \times 25 mL). The combined organic fractions were washed with brine (~80 mL), dried (MgSO_4), filtered, and concentrated under reduced pressure to give the crude product. The crude material was purified by flash chromatography (hexane/ EtOAc : 9/1) to give the title compound (1.47 g, 90%) as a white solid. M.p. 75-77 °C. $^1\text{H NMR}$ (500 MHz, CDCl_3) δ 7.70 (d, J = 8.3 Hz, 2H), 7.41 (d, J = 8.5 Hz, 2H), 7.32 (d, J = 8.2 Hz, 2H), 6.91 (d, J = 7.9 Hz, 2H), 2.48 (s, 3H). $^{13}\text{C NMR}$ (126 MHz, CDCl_3) δ 148.8, 145.8, 132.9, 132.3, 130.0, 128.7, 124.4, 120.7, 21.9. Characterisation data in accordance with literature report.¹⁷

Cyclohex-1-en-1-yl trifluoromethanesulfonate (132SM)



Prepared according to a modified literature procedure.¹⁸ To a flame dried flask was added a solution of cyclohexanone (0.4910 g, 5 mmol) and PhNTf_2 (2.322 g, 1.3 equiv., 6.5 mmol) was slowly added LiHMDS (10 mL, 2 equiv., 10 mmol, 1 M in THF) at -78°C . The mixture was warmed to 0°C and stirred for 1 hour as monitored by TLC. Saturated aq. NH_4Cl (20 mL) was added to the reaction mixture. The organic layer was separated, and the aqueous layer was extracted with EtOAc (3 \times 20 mL). The combined organic phases were washed with brine (3 \times 20 mL), dried (MgSO_4), filtered, and concentrated under reduced pressure to give the crude product. The residue was purified using flash column chromatography (petroleum ether) to give the title compound (0.875 g, 76%) as a colourless oil. $^1\text{H NMR}$ (500 MHz, CDCl_3) δ 5.77 – 5.74 (m, 1H), 2.35 – 2.28 (m, 2H), 2.21 – 2.15 (m, 2H), 1.81 – 1.75 (m, 2H), 1.63 – 1.57 (m, 2H). $^{13}\text{C NMR}$ (126 MHz, CDCl_3) δ 149.5, 118.7 (q, J = 320.1 Hz), 118.6, 27.7, 24.0, 22.8, 21.1. $^{19}\text{F}\{^1\text{H}\}$ NMR (471 MHz, CDCl_3) δ -74.11. Characterisation data in accordance with literature report.¹⁸

3-Phenylpropyl methanesulfonate (150SM)

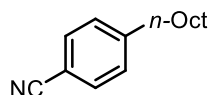


6 - Experimental

Prepared according to a literature procedure.¹⁹ To a flame dried flask was added 3-phenylpropan-1-ol (0.5 mmol, 0.681 mL), triethylamine (7.5 mmol, 1.05 mL) and CH₂Cl₂ (15 mL). Methanesulfonyl chloride (7.5 mmol, 0.393 mL) was added at 0 °C. The mixture was warmed to room temperature and stirred overnight. After completion of the reaction as indicated by TLC analysis (Product R_f ≈ 0.3, petroleum ether/ethyl acetate: 4/1), distilled water (15 mL) was added. The layers were separated, and the aqueous layer was extracted with CH₂Cl₂ (3 × 20 mL). The combined organic layers were washed with water (2 × 20 mL) and then brine (~20 mL). The combined organic phases were dried (MgSO₄), filtered, and concentrated under reduced pressure to afford the crude product. The crude product was then purified by flash column chromatography (petroleum ether/ethyl acetate: 4/1) to give the title compound (0.557 g, 52%) as a colourless oil. **¹H NMR** (500 MHz, CDCl₃) δ 7.35 – 7.28 (m, 2H), 7.24 – 7.15 (m, 3H), 4.23 (t, *J* = 6.3 Hz, 2H), 2.99 (s, 3H), 2.80 – 2.71 (m, 2H), 2.15 – 2.05 (m, 2H). **¹³C NMR** (126 MHz, CDCl₃) δ 140.4, 128.7, 128.6, 126.4, 69.3, 37.5, 31.7, 30.8. Characterisation data in accordance with literature report.¹⁹

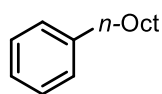
6.3.3 Characterisation data of products

4-Octylbenzonitrile (117)



Prepared according to **GP5**. Purified by flash column chromatography (petroleum ether/EtOAc: 49/1) to give the title compound (0.183 g, 85%) as a colourless oil. **¹H NMR** (500 MHz, CDCl₃) δ 7.52 (d, *J* = 8.3 Hz, 2H), 7.24 (d, *J* = 8.3 Hz, 2H), 2.66 – 2.59 (m, 2H), 1.63 – 1.54 (m, 2H), 1.32 – 1.19 (m, 10H), 0.85 (t, *J* = 7.0 Hz, 3H). **¹³C NMR** (126 MHz, CDCl₃) δ 148.7, 132.2, 129.3, 119.3, 109.5, 36.2, 31.9, 31.1, 29.4, 29.3, 29.3, 22.7, 14.2. **HRMS** (EI) *m/z*: [M]⁺ Calcd for C₁₅H₂₁N 215.1669, found: 215.1669. Characterisation data in accordance with literature report.²⁰

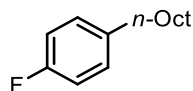
Octylbenzene (119)



Prepared according to **GP5**. Purified by flash column chromatography (hexane) to give the title compound (0.137 g, 72%) as a colourless oil. **¹H NMR** (500 MHz, CDCl₃) δ 7.29 – 7.26 (m, 2H), 7.20 – 7.15 (m, 3H), 2.63 – 2.58 (m, 2H), 1.65 – 1.58 (m, 2H), 1.36 – 1.24 (m, 10H), 0.88 (t, *J* = 7.0 Hz, 3H). **¹³C NMR** (126 MHz, CDCl₃) δ 143.1, 128.5, 128.4,

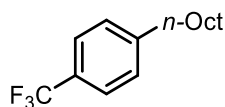
125.7, 36.2, 32.0, 31.7, 29.6, 29.5, 29.4, 22.8, 14.3. **HRMS** (EI) m/z : $[M]^+$ Calcd for $C_{14}H_{22}$ 190.1716, found: 190.1709. Characterisation data in accordance with literature report.²¹

1-Fluoro-4-octylbenzene (120)



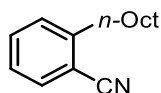
Prepared according to **GP5**. Purified by flash column chromatography (hexane) to give the title compound (0.148 g, 71%) as a colourless oil. **1H NMR** (500 MHz, $CDCl_3$) δ 7.16 – 7.08 (m, 2H), 6.98 – 6.91 (m, 2H), 2.60 – 2.52 (m, 2H), 1.64 – 1.51 (m, 2H), 1.35 – 1.20 (m, 10H), 0.88 (t, $J = 7.0$ Hz, 3H). **^{13}C NMR** (126 MHz, $CDCl_3$) δ 161.3 (d, $J = 242.8$ Hz), 138.6 (d, $J = 3.1$ Hz), 129.8 (d, $J = 7.7$ Hz), 115.0 (d, $J = 21.0$ Hz), 35.3, 32.0, 31.8, 29.6, 29.4, 29.4, 22.8, 14.3. **$^{19}F\{^1H\}$ NMR** (376 MHz, $CDCl_3$) δ -118.30. **HRMS** (EI) m/z : $[M]^+$ Calcd for $C_{14}H_{21}F$ 208.1622, found: 208.1616. Characterisation data in accordance with literature report.²²

1-Octyl-4-(trifluoromethyl)benzene (121)



Prepared according to **GP5**. Purified by flash column chromatography (hexane) to give the title compound (0.196 g, 76%) as a colourless oil. **1H NMR** (500 MHz, $CDCl_3$) δ 7.52 (d, $J = 7.9$ Hz, 2H), 7.28 (d, $J = 7.9$ Hz, 2H), 2.68 – 2.63 (m, 2H), 1.66 – 1.58 (m, 2H), 1.34 – 1.23 (m, 10H), 0.88 (t, $J = 7.0$ Hz, 3H). **^{13}C NMR** (126 MHz, $CDCl_3$) δ 147.1, 128.1 (q, $J = 32.3$ Hz), 127.1, 125.3 (q, $J = 3.8$ Hz), 124.6 (q, $J = 271.8$ Hz), 36.0, 32.0, 31.4, 29.6, 29.4 (q, $J = 0.8$ Hz), 22.8, 14.2. **HRMS** (EI) m/z : $[M]^+$ Calcd for $C_{15}H_{21}F_3$ 258.1590, found: 258.1589. Characterisation data in accordance with literature report.²³

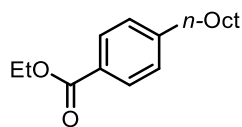
2-Octylbenzonitrile (122)



Prepared according to **GP5**. Purified by flash column chromatography (hexane/EtOAc: 9/1) to give the title compound (0.112 g, 52%) as a colourless oil. **1H NMR** (500 MHz, $CDCl_3$) δ 7.59 (dd, $J = 7.7, 1.0$ Hz, 1H), 7.50 (td, $J = 7.7, 1.4$ Hz, 1H), 7.34 – 7.30 (m, 1H), 7.27 (td, $J = 7.6, 1.2$ Hz, 1H), 2.86 – 2.80 (m, 2H), 1.72 – 1.63 (m, 2H), 1.41 – 1.23 (m, 10H), 0.89 (t, $J = 7.0$ Hz, 3H). **^{13}C NMR** (126 MHz, $CDCl_3$) δ 146.9, 132.7, 132.7, 129.5, 126.3, 118.1, 112.3, 34.6, 31.9, 31.0, 29.4, 29.3, 29.2, 22.7, 14.1. **HRMS** (EI) m/z :

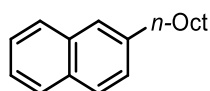
$[M]^+$ Calcd for $C_{15}H_{21}N$ 215.1674, found: 215.1671. Characterisation data in accordance with literature report.²⁴

Ethyl 4-octylbenzoate (123)



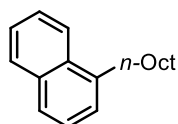
Prepared according to **GP5**. Purified by column chromatography (hexane/EtOAc: 19/1) to give the title compound (0.218 g, 83%) as a colourless oil. **¹H NMR** (500 MHz, $CDCl_3$) δ 7.95 (d, $J = 8.3$ Hz, 2H), 7.23 (d, $J = 8.4$ Hz, 2H), 4.36 (q, $J = 7.1$ Hz, 2H), 2.68 – 2.62 (m, 2H), 1.66 – 1.57 (m, 2H), 1.38 (t, $J = 7.1$ Hz, 3H), 1.33 – 1.23 (m, 5H), 0.88 (t, $J = 7.0$ Hz, 3H). **¹³C NMR** (126 MHz, $CDCl_3$) δ 166.9, 148.6, 129.7, 128.5, 128.1, 60.9, 36.2, 32.0, 31.3, 29.6, 29.4, 29.4, 22.8, 14.5, 14.2. The NMR data is consistent with the literature.²⁰ **HRMS** (EI) m/z : $[M]^+$ Calcd for $C_{17}H_{26}O_2$ 262.1927, found: 262.1925.

2-Octylnaphthalene (124)



Prepared according to **GP5**. Purified by flash column chromatography (hexane) to give the title compound (0.195 g, 81%) as a colourless oil. **¹H NMR** (500 MHz, $CDCl_3$) δ 7.83 – 7.73 (m, 3H), 7.62 (s, 1H), 7.47 – 7.39 (m, 2H), 7.34 (dd, $J = 8.4, 1.7$ Hz, 1H), 2.81 – 2.72 (m, 2H), 1.77 – 1.65 (m, 2H), 1.41 – 1.22 (m, 10H), 0.89 (t, $J = 6.9$ Hz, 3H). **¹³C NMR** (126 MHz, $CDCl_3$) δ 140.6, 133.7, 132.0, 127.8, 127.7, 127.6, 127.5, 126.4, 125.9, 125.1, 36.3, 32.0, 31.6, 29.7, 29.5, 29.4, 22.8, 14.3. **HRMS** (EI) m/z : $[M]^+$ Calcd for $C_{18}H_{24}$ 240.1873, found: 240.1873. Characterisation data in accordance with literature report.²⁵

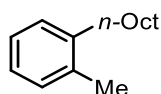
1-Octylnaphthalene (125)



Prepared according to general procedure **A**. Purified by flash column chromatography (hexane) and further purified by Kugelrohr distillation (95-100 °C at 0.001 mbar) to give the title compound (0.211 g, 88%) as a colourless oil. **¹H NMR** (500 MHz, $CDCl_3$) δ 8.06 (d, $J = 8.3$ Hz, 1H), 7.86 (dd, $J = 8.0, 0.8$ Hz, 1H), 7.71 (d, $J = 8.1$ Hz, 1H), 7.55 – 7.45 (m, 2H), 7.43 – 7.38 (m, 1H), 7.33 (d, $J = 6.7$ Hz, 1H), 3.10 – 3.05 (m, 2H), 1.81 – 1.71 (m, 2H), 1.49 – 1.41 (m, 2H), 1.39 – 1.24 (m, 8H), 0.90 (t, $J = 6.9$ Hz, 3H). **¹³C NMR** (126

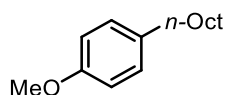
MHz, CDCl₃) δ 139.2, 134.0, 132.1, 128.9, 126.5, 126.0, 125.7, 125.7, 125.5, 124.1, 33.3, 32.1, 31.0, 30.0, 29.7, 29.5, 22.8, 14.3. **HRMS** (EI) m/z: [M]⁺ Calcd for C₁₈H₂₄ 240.1873, found: 240.1871. Characterisation data in accordance with literature report.²⁶

1-Methyl-2-octylbenzene (126)



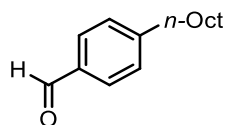
Prepared according to **GP5**. Purified by column chromatography (hexane) to give the title compound (0.145 g, 71%) as a colourless oil. **¹H NMR** (500 MHz, CDCl₃) δ 7.16 – 7.06 (m, 4H), 2.65 – 2.50 (m, 2H), 2.31 (s, 3H), 1.63 – 1.52 (m, 2H), 1.41 – 1.27 (m, 10H), 0.89 (t, *J* = 7.0 Hz, 3H). **¹³C NMR** (126 MHz, CDCl₃) δ 141.3, 136.0, 130.2, 128.9, 126.0, 125.8, 33.5, 32.1, 30.5, 29.9, 29.9, 29.7, 29.5, 22.8, 19.4, 14.3. **HRMS** (EI) m/z: [M]⁺ Calcd for C₁₅H₂₄ 204.1873, found: 204.1865. Characterisation data in accordance with literature report.²¹

1-Methoxy-4-octylbenzene (127)



Prepared according to **GP5**. Purified by column chromatography (hexane/Et₂O: 19/1) to give the title compound (0.130 g, 59%) as a colourless oil. **¹H NMR** (500 MHz, CDCl₃) δ 7.12 – 7.07 (m, 2H), 6.85 – 6.80 (m, 2H), 3.79 (s, 3H), 2.56 – 2.52 (m, 2H), 1.61 – 1.53 (m, 2H), 1.34 – 1.21 (m, 10H), 0.88 (t, *J* = 7.0 Hz, 3H). **¹³C NMR** (126 MHz, CDCl₃) δ 157.7, 135.2, 129.4, 113.8, 55.4, 35.2, 32.4, 31.9, 29.6, 29.4, 29.4, 22.8, 14.3. **HRMS** (EI) m/z: [M]⁺ Calcd for C₁₅H₂₄O 220.1821, found: 220.1820. Characterisation data in accordance with literature report.²⁷

4-Octylbenzaldehyde (128)

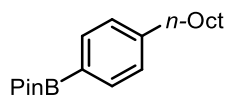


Prepared according to **GP5**. Purified by flash column chromatography (hexane/EtOAc: 19/1) to give the title compound (0.186 g, 85%) as a colourless oil. **¹H NMR** (500 MHz, CDCl₃) δ 9.97 (s, 1H), 7.80 (d, *J* = 8.2 Hz, 2H), 7.33 (d, *J* = 8.0 Hz, 2H), 2.70 – 2.65 (m, 2H), 1.67 – 1.58 (m, 2H), 1.35 – 1.21 (m, 10H), 0.87 (t, *J* = 7.0 Hz, 3H). **¹³C NMR** (126 MHz, CDCl₃) δ 192.3, 150.7, 134.5, 130.0, 129.2, 36.34, 32.0, 31.3, 29.6, 29.4, 29.4,

6 - Experimental

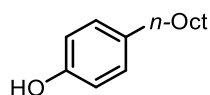
22.8, 14.3. **HRMS** (ES) m/z : $[MH]^+$ Calcd for $C_{15}H_{23}O$ 219.1749, found: 219.1748. Characterisation data in accordance with literature report.²⁸

4,4,5,5-Tetramethyl-2-(4-octylphenyl)-1,3,2-dioxaborolane (129)



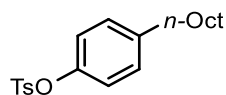
Prepared according to **GP5**. Purified by flash column chromatography (hexane/Et₂O: 19/1) to give the title compound (0.184 g, 58%) as a pale-yellow oil. **¹H NMR** (500 MHz, CDCl₃) δ 7.74 (d, J = 8.0 Hz, 2H), 7.21 (d, J = 8.0 Hz, 2H), 2.64 – 2.60 (m, 2H), 1.65 – 1.58 (m, 2H), 1.35 (s, 12H), 1.34 – 1.25 (m, 10H), 0.89 (t, J = 7.0 Hz, 3H). **¹³C NMR** (126 MHz, CDCl₃) δ 146.6, 134.9, 128.0, 83.7, 36.3, 32.0, 31.5, 29.8, 29.6, 29.4, 29.4, 25.0, 22.8, 14.3. **GC-MS** m/z (% relative intensity, ion): 316.26 (34%, M⁺), 301.23 (46%, M⁺-CH₃), 230.20 (100%, M⁺-C₅H₁₁O), 217.18 (33%, M⁺-C₇H₁₅). Characterisation data in accordance with literature report.²¹

4-Octylphenol (130)



Prepared according to **GP5**. Purified by flash column chromatography (petroleum ether/Et₂O: 9/1) to give the title compound (0.087 g, 42%) as a colourless oil. **¹H NMR** (500 MHz, CDCl₃) δ 7.06 – 7.01 (m, 2H), 6.78 – 6.72 (m, 2H), 4.62 (s, 1H), 2.59 – 2.43 (m, 2H), 1.61 – 1.52 (m, 2H), 1.34 – 1.24 (m, 10H), 0.88 (t, J = 7.0 Hz, 3H). **¹³C NMR** (126 MHz, CDCl₃) δ 153.5, 135.4, 129.6, 115.2, 35.2, 32.0, 31.9, 29.6, 29.4, 29.4, 22.8, 14.3. **HRMS** (EI) m/z : $[M]^+$ Calcd for $C_{14}H_{22}O$ 206.1665, found: 206.1664. Characterisation data in accordance with literature report.²⁹

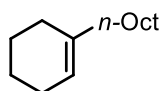
4-Octylphenyl 4-methylbenzenesulfonate (131)



Prepared according to **GP5**. Purified by flash column chromatography (hexane/EtOAc: 9/1) to give the title compound (0.220 g, 61%) as a colourless oil. **¹H NMR** (500 MHz, CDCl₃) δ 7.70 (d, J = 8.4 Hz, 2H), 7.30 (d, J = 8.2 Hz, 2H), 7.06 (d, J = 8.5 Hz, 2H), 6.86 (d, J = 8.6 Hz, 2H), 2.56 – 2.52 (m, 2H), 2.45 (s, 2H), 1.59 – 1.48 (m, 2H), 1.31 – 1.21 (m, 10H), 0.87 (t, J = 7.0 Hz, 3H). **¹³C NMR** (126 MHz, CDCl₃) δ 147.6, 145.3, 142.1, 132.6, 129.8, 129.5, 128.7, 122.2, 35.4, 32.0, 31.5, 29.6, 29.4, 29.4, 22.8, 21.9, 14.3.

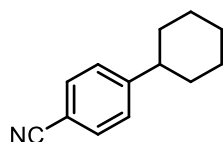
HRMS (ASAP) m/z : $[MH]^+$ Calcd for $C_{21}H_{29}O_3S$ 361.1837, found: 361.1837. Characterisation data in accordance with literature report.²⁷

1-Octylcyclohex-1-ene (132)



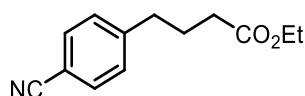
Prepared according to **GP5**. Synthesised from vinyl triflate. Purified by flash column chromatography (petroleum ether) to give the title compound (0.152 g, 78%) as a colourless oil. **¹H NMR** (500 MHz, $CDCl_3$) δ 5.40 – 5.35 (m, 1H), 2.03 – 1.95 (m, 2H), 1.93 – 1.87 (m, 4H), 1.64 – 1.57 (m, 2H), 1.58 – 1.50 (m, 2H), 1.41 – 1.32 (m, 2H), 1.32 – 1.23 (m, 10H), 0.88 (t, $J = 7.0$ Hz, 3H). **¹³C NMR** (126 MHz, $CDCl_3$) δ 138.3, 120.1, 38.3, 32.1, 29.9, 29.7, 29.6, 29.5, 28.5, 27.9, 25.4, 23.2, 22.8, 22.8, 14.3. **HRMS** (EI) m/z : $[M]^+$ Calcd for $C_{14}H_{26}$ 194.2029, found: 194.2028. Characterisation data in accordance with literature report.³⁰

4-Cyclohexylbenzonitrile (138)



Prepared according to **GP5**. Purified by flash column chromatography (petroleum ether/ Et_2O : 19/1) and further purified by Kugelrohr distillation (70-80 °C at 0.001 mbar) to give the title compound (0.148 g, 80%) as a colourless oil. **¹H NMR** (500 MHz, $CDCl_3$) δ 7.59 – 7.55 (m, 2H), 7.31 – 7.28 (m, 2H), 2.59 – 2.50 (m, 1H), 1.92 – 1.83 (m, 4H), 1.81 – 1.73 (m, 1H), 1.44 – 1.36 (m, 4H), 1.30 – 1.22 (m, 1H). **¹³C NMR** (126 MHz, $CDCl_3$) δ 153.6, 132.3, 127.8, 119.4, 109.7, 44.9, 34.1, 26.8, 26.1. **HRMS** (EI) m/z : $[M]^+$ Calcd for $C_{13}H_{15}N$ 185.1199, found: 185.1202. Characterisation data in accordance with literature report.³¹

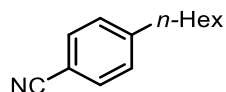
Ethyl 4-(4-cyanophenyl)butanoate (139)



Prepared according to **GP5**. Purified by flash column chromatography (petroleum ether/ Et_2O : 3/1) to give the title compound (0.163 g, 75%) as a colourless oil. **¹H NMR** (500 MHz, $CDCl_3$) δ 7.57 (d, $J = 8.1$ Hz, 2H), 7.29 (d, $J = 8.5$ Hz, 2H), 4.13 (q, $J = 7.1$ Hz, 2H), 2.86 – 2.62 (m, 2H), 2.32 (m, 2H), 2.00 – 1.91 (m, 2H), 1.25 (t, $J = 7.1$ Hz, 3H).

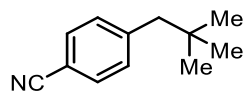
$^{13}\text{C NMR}$ (126 MHz, CDCl_3) δ 173.2, 147.3, 132.4, 129.4, 119.2, 110.1, 60.6, 35.4, 33.6, 26.1, 14.4.³² **HRMS** (ES) m/z : $[\text{MH}]^+$ Calcd for $\text{C}_{13}\text{H}_{16}\text{NO}_2$ 218.1181, found: 218.1178. Characterisation data in accordance with literature report.³²

4-Hexylbenzonitrile (140)



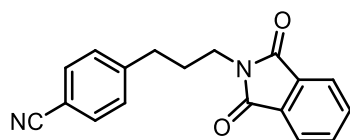
Prepared according to **GP5**. Purified by flash column chromatography (hexane/EtOAc: 9/1) to give the title compound (0.157 g, 84%) as a colourless oil. $^1\text{H NMR}$ (500 MHz, CDCl_3) δ 7.55 (d, $J = 8.2$ Hz, 2H), 7.26 (d, $J = 8.1$ Hz, 2H), 2.74 – 2.59 (m, 2H), 1.66 – 1.57 (m, 2H), 1.33 – 1.26 (m, 6H), 0.87 (t, $J = 6.8$ Hz, 3H). $^{13}\text{C NMR}$ (126 MHz, CDCl_3) δ 148.9, 132.3, 129.4, 119.4, 109.7, 36.4, 31.8, 31.2, 29.1, 22.8, 14.3. **HRMS** (EI) m/z : $[\text{M}]^+$ Calcd for $\text{C}_{13}\text{H}_{17}\text{N}$ 187.1356, found: 185.1356. Characterisation data in accordance with literature report.³³

4-Neopentylbenzonitrile (142)



Prepared according to **GP5**. Purified by flash column chromatography (petroleum ether/ Et_2O : 9/1) to give the title compound (0.151 g, 87%) as a colourless oil. $^1\text{H NMR}$ (500 MHz, CDCl_3) δ 7.56 (d, $J = 8.4$ Hz, 2H), 7.22 (d, $J = 8.4$ Hz, 2H), 2.54 (s, 2H), 0.90 (s, 9H). $^{13}\text{C NMR}$ (126 MHz, CDCl_3) δ 145.5, 131.5, 131.1, 119.3, 109.7, 50.3, 32.1, 29.3. **HRMS** (ES) m/z : $[\text{MH}]^+$ Calcd for $\text{C}_{12}\text{H}_{16}\text{N}$ 174.1283, found: 174.1281. Characterisation data in accordance with literature report.²⁸

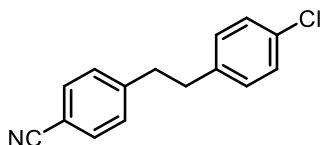
4-(3-(1,3-Dioxoisindolin-2-yl)propyl)benzonitrile (144)



Prepared according to **GP5**. Purified by flash column chromatography (petroleum ether/EtOAc: 4/1) to give the title compound (0.194 g, 67%) as a white solid. M.p. 134–138 °C. $^1\text{H NMR}$ (500 MHz, CDCl_3) δ 7.81 (dd, $J = 5.4, 3.0$ Hz, 2H), 7.71 (dd, $J = 5.5, 3.0$ Hz, 2H), 7.51 (d, $J = 8.3$ Hz, 2H), 7.29 (d, $J = 8.4$ Hz, 2H), 3.74 (t, $J = 7.0$ Hz, 2H), 2.80 – 2.70 (m, 2H), 2.09 – 2.00 (m, 2H). $^{13}\text{C NMR}$ (126 MHz, CDCl_3) δ 168.4, 146.7,

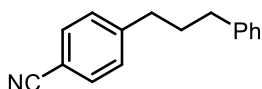
134.1, 132.2, 132.0, 129.1, 123.2, 118.9, 109.9, 37.5, 33.3, 29.2. **HRMS** (ES) m/z : $[MH]^+$
Calcd for $C_{18}H_{15}N_2O_2$ 291.1134, found: 291.1130.

4-(4-Chlorophenethyl)benzonitrile (145)



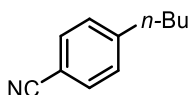
Prepared according to **GP5**. Purified by flash column chromatography (petroleum ether/EtOAc: 9/1) to give the title compound (0.193 g, 80%) as a white solid. M.p. 106-108 °C. **1H NMR** (500 MHz, $CDCl_3$) δ 7.55 (d, $J = 8.3$ Hz, 2H), 7.25 – 7.18 (m, 4H), 7.04 (d, $J = 8.3$ Hz, 2H), 3.00 – 2.92 (m, 2H), 2.93 – 2.83 (m, 2H). **^{13}C NMR** (126 MHz, $CDCl_3$) δ 146.8, 139.1, 132.3, 132.1, 129.9, 129.4, 128.7, 119.1, 110.1, 37.8, 36.6. **HRMS** (EI) m/z : $[M]^+$ Calcd for $C_{15}H_{24}$ 241.0653, found: 241.0651. Characterisation data in accordance with literature report.³¹

4-(3-Phenylpropyl)benzonitrile (146)



Prepared according to **GP5**. Purified by flash column chromatography (petroleum ether/ Et_2O : 4/1) to give the title compound (0.184 g, 83%) as a colourless oil. **1H NMR** (500 MHz, $CDCl_3$) δ 7.59 – 7.55 (m, 2H), 7.32 – 7.26 (m, 4H), 7.21 (m, 1H), 7.20 – 7.16 (m, 2H), 2.73 – 2.68 (m, 2H), 2.68 – 2.64 (m, 2H), 2.01 – 1.93 (m, 2H). **^{13}C NMR** (126 MHz, $CDCl_3$) δ 148.1, 141.7, 132.3, 129.3, 128.6, 128.5, 126.1, 119.2, 109.8, 35.6, 35.4, 32.5. **HRMS** (ES) m/z : $[MH]^+$ Calcd for $C_{16}H_{16}N$ 222.1283, found: 222.1281. Characterisation data in accordance with literature report.³⁴

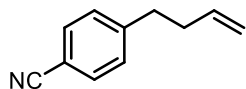
4-Butylbenzonitrile (147)



Prepared according to **GP5**. Purified by flash column chromatography (petroleum ether/EtOAc: 19/1) to give the title compound (0.126 g, 79%) as a colourless oil. **1H NMR** (500 MHz, $CDCl_3$) δ 7.55 – 7.51 (m, 2H), 7.27 – 7.23 (m, 2H), 2.67 – 2.62 (m, 2H), 1.62 – 1.54 (m, 2H), 1.38 – 1.28 (m, 2H), 0.91 (t, $J = 7.4$ Hz, 3H). **^{13}C NMR** (126 MHz, $CDCl_3$) δ 148.7, 132.2, 129.3, 119.4, 109.5, 35.9, 33.2, 22.4, 14.0. **HRMS** (ES) m/z : $[MH]^+$ Calcd

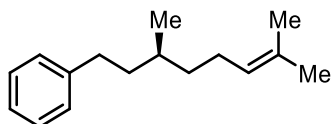
for $C_{11}H_{14}N$ 241.0653, found: 241.0651. Characterisation data in accordance with literature report.³³

4-(But-3-en-1-yl)benzonitrile (148)



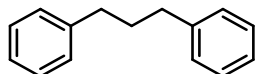
Prepared according to **GP5**. Purified by flash column chromatography (hexane/EtOAc: 49/1) to give the product the title compound (0.117 g, 74%) as a colourless oil. **¹H NMR** (500 MHz, $CDCl_3$) δ 7.59 – 7.56 (m, 2H), 7.30 – 7.26 (m, 2H), 5.86 – 5.75 (m, 1H), 5.05 – 4.96 (m, 2H), 2.80 – 2.75 (m, 2H), 2.42 – 2.35 (m, 2H). **¹³C NMR** (126 MHz, $CDCl_3$) δ 147.6, 137.1, 132.3, 129.4, 119.3, 115.9, 109.8, 35.6, 35.0. **HRMS** (ES) m/z : $[MH]^+$ Calcd for $C_{11}H_{12}N$ 158.0970, found: 158.0964. Characterisation data in accordance with literature report.³⁵

(S)-(3,7-Dimethyloct-6-en-1-yl)benzene (149)



Prepared according to **GP5**. Purified by flash column chromatography (petroleum ether) to give the title compound (0.132 g, 61%) as a colourless oil. **¹H NMR** (500 MHz, $CDCl_3$) δ 7.30 – 7.26 (m, 2H), 7.22 – 7.15 (m, 3H), 5.13 – 5.09 (m, 1H), 2.73 – 2.62 (m, 1H), 2.62 – 2.51 (m, 1H), 2.08 – 1.90 (m, 2H), 1.69 (d, $J = 1.1$ Hz, 3H), 1.67 – 1.63 (m, 1H), 1.61 (d, $J = 0.8$ Hz, 3H), 1.50 – 1.35 (m, 3H), 1.24 – 1.16 (m, 1H), 0.95 (d, $J = 6.4$ Hz, 3H). **¹³C NMR** (126 MHz, $CDCl_3$) δ 143.3, 131.3, 128.5, 128.4, 125.7, 125.0, 39.1, 37.1, 33.6, 32.3, 25.9, 25.6, 19.7, 17.8. **HRMS** (EI) m/z : $[M]^+$ Calcd for $C_{16}H_{24}$ 216.1873, found: 216.1872. Characterisation data in accordance with literature report.³⁶

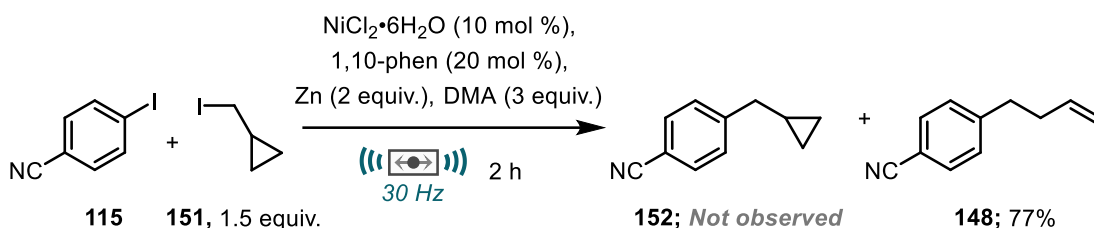
1,3-Diphenylpropane (150)



Prepared according to **GP5**. Purified by flash column chromatography (petroleum ether) to give the title compound (0.1078 g, 55%) as a colourless oil. **¹H NMR** (500 MHz, $CDCl_3$) δ 7.33 – 7.27 (m, 4H), 7.22 – 7.18 (m, 6H), 2.70 – 2.65 (m, 4H), 2.02 – 1.92 (m, 2H). **¹³C NMR** (126 MHz, $CDCl_3$) δ 142.4, 128.6, 128.4, 125.9, 35.6, 33.1. **HRMS** (EI) m/z : $[M]^+$ Calcd for $C_{15}H_{16}$ 196.1247, found: 196.1249. Characterisation data in accordance with literature report.³⁴

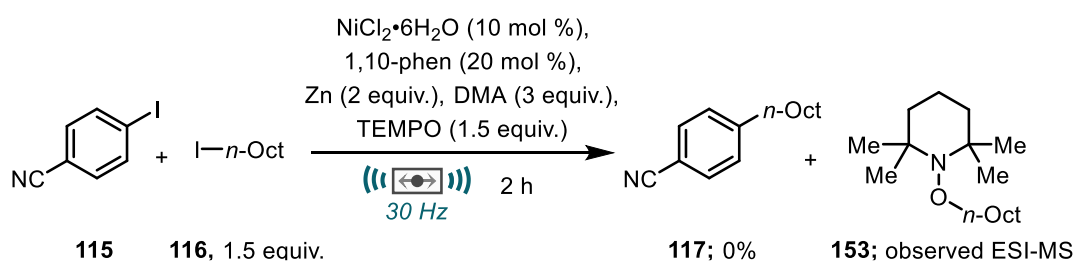
6.3.4 Mechanistic Studies – Radical Clock and TEMPO Trapping

Radical Clock Experiment



A 3 g stainless steel ball was added to a 15 mL stainless steel milling jar. 4-Iodobenzonitrile (0.229 g, 1 mmol), (iodomethyl)cyclopropyl (0.273 g, 1.5 mmol), $\text{NiCl}_2 \cdot 6\text{H}_2\text{O}$ (0.024 g, 0.1 mmol), 1,10-phenanthroline (0.036 g, 0.2 mmol), Zn (0.131 g, 2 mmol), *N,N*-dimethylacetamide (0.28 mL, 3 mmol) were all added to the milling jar. The reaction was then milled at 30 Hz for 2 hours. After the milling period, the mixture was washed from the jar with CH_2Cl_2 (~20 mL). 1 M HCl (~20 mL) was added, and the layers separated. The aqueous layer was extracted with CH_2Cl_2 (2 × 20 mL). The combined organic layers were washed with brine, dried (MgSO_4), filtered, and concentrated under reduced pressure to give the crude product. The crude product was purified by flash column chromatography (hexane/EtOAc: 19/1) to afford the ring opened product 4-(but-3-en-1-yl)benzonitrile **148** (0.090 g, 57%) as a colourless oil.

TEMPO Studies



A 3 g stainless steel ball was added to a 15 mL stainless steel milling jar. 4-Iodobenzonitrile (0.229 g, 1 mmol), 1-iodooctane (0.27 mL, 1.5 mmol, 1.5 equiv.), $\text{NiCl}_2 \cdot 6\text{H}_2\text{O}$ (0.024 g, 0.1 mmol), 1,10-phenanthroline (0.036 g, 0.2 mmol), Zn (0.131, 2 mmol), TEMPO (0.236 g, 1.5 mmol, 1.5 equiv.) and *N,N*-dimethylacetamide (0.28 mL, 3 mmol) were all added to the milling jar. The reaction was then milled at 30 Hz for 2 hours. After the milling period, the mixture was washed from the jar with CH_2Cl_2 (~20 mL) and filtered through a celite plug. The crude mixture was concentrated under reduced pressure. CDCl_3 was added and the yield of coupled product **117** was determined to be

6 - Experimental

0% by ^1H NMR. The sample was submitted for spectrometry analysis whereby the tempo adduct **153** was found by observed by ESI-MS.

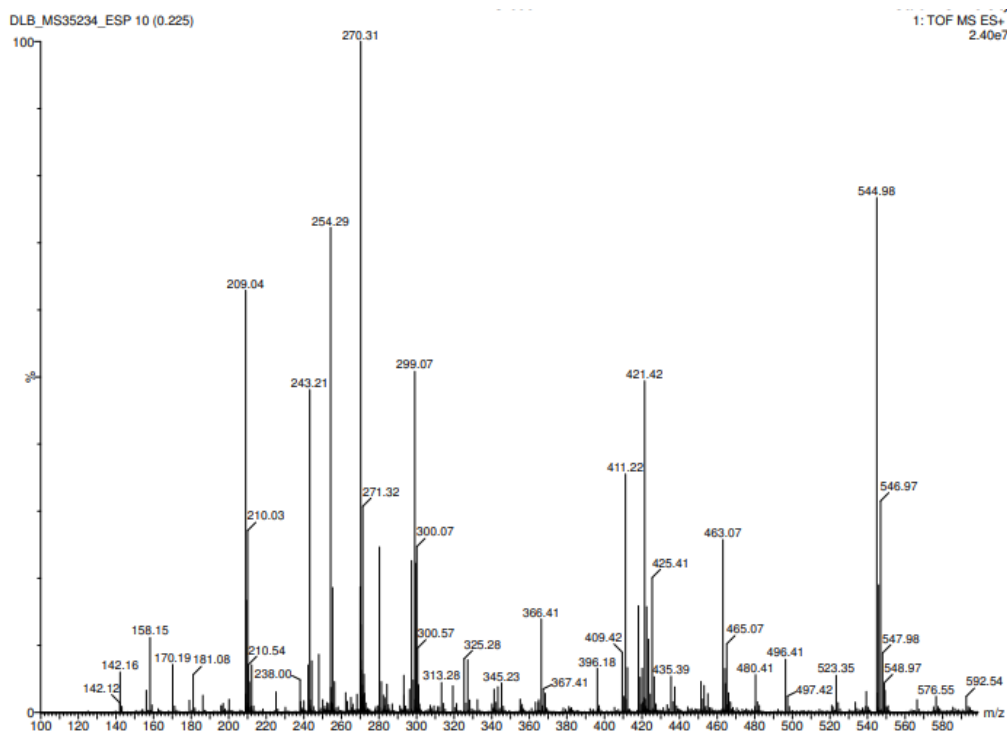
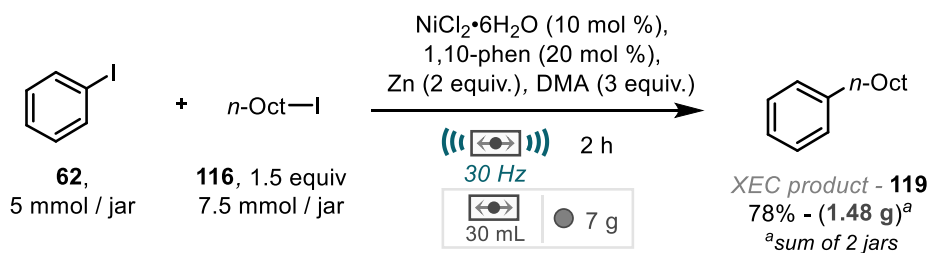


Figure 6.3 LRMS of TEMPO adduct

6.3.4 Scale-up Protocol



To two 30 mL stainless steel jars, a 7 g (12 mm) stainless steel ball was added to each. To each jar was then added zinc granular (20-30 mesh, 0.654 g, 10 mmol, 2 equiv.), $\text{NiCl}_2 \cdot 6\text{H}_2\text{O}$ (0.119 g, 0.5 mmol, 10 mol %) and 1,10-phenanthroline (0.180 g, 1 mmol, 20 mol %). Following, this *N,N*-dimethylacetamide (anhydrous, 1.39 mL, 15 mmol, 3 equiv.), 1-iodooctane (1.35 mL, 7.5 mmol, 1.5 equiv.) and iodobenzene (0.56 mL, 5 mmol, 1 equiv.) were added in quick succession. The jars were then sealed, and further secured with Teflon tape and then white electrical tape on top as an extra precaution. The jars were then placed on the mixer mill and milled at 30 Hz for 2 hours. After this time, the jars were removed and using CH_2Cl_2 (100 mL) and 1 M HCl (100 mL) the contents of both jars were transferred to a single conical flask. A stirrer bar was added,

and the mixture was stirred for ~10 minutes. The resulting biphasic mixture was then poured into a separating funnel, and the layers separated. The aqueous phase was then re-extracted with CH_2Cl_2 (2×100 mL). The combined organics were then washed with brine (100 mL), dried (MgSO_4), filtered, and concentrated under reduced pressure to form a deep orange/red oil. The crude residue was then purified *via* silica gel chromatography (hexane, product $R_f = 0.6$) to give *n*-octylbenzene **119** (1.46 g, 78%) as a colourless oil.

6.4 Mechanochemical Reductive Coupling of Activated Amides with Alkyl Halides

6.4.1 Synthesis of Starting Materials

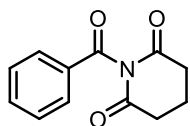
General Procedure 6 (GP6): Synthesis of *N*-acyl Glutarimides from Acid Chlorides

N-Acyl glutarimides were synthesised according to a modified literature procedure.³⁷ To a flask, glutarimide (1.131 g, 10 mmol), triethylamine (2.79 mL, 20 mmol, 2 equiv.), 4-dimethylaminopyridine (0.306 g, 2.5 mmol, 0.25 equiv.) and CH₂Cl₂ (15 mL) were added. Acyl chloride (11 mmol, 1.1 equiv.) was added dropwise over a period of 5 minutes at 0 °C with vigorous stirring. The reaction mixture was warmed to room temperature and stirred at this temperature overnight. After this period, the mixture was diluted with CH₂Cl₂ (~20 mL). The organic layer was then washed with 1 M HCl (~25 mL), water (~25 mL) and then brine (~25 mL). The organic layer was then dried (MgSO₄), filtered, and concentrated to afford the crude product as a brown solid. Unless stated otherwise, the crude product was purified by recrystallisation (toluene) to afford the pure *N*-acyl glutarimide.

General Procedure 7 (GP7): Synthesis of *N*-acyl Glutarimides from Carboxylic Acids

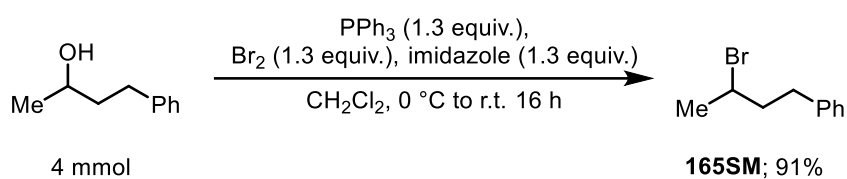
To a flask, carboxylic acid (10 mmol) and CH₂Cl₂ (15 mL) were added. Oxalyl chloride was added dropwise at 0 °C. A couple of drops of *N,N*-dimethylformamide were added and the reaction warmed to room temperature. The reaction was stirred until gas evolution ceased (typically 3 hours). After this period, the mixture was concentrated under reduced pressure to remove HCl and excess oxalyl chloride to give the corresponding acid chloride, which was used without further purification. In a different flask, glutarimide (7 mmol), triethylamine (14 mmol), 4-dimethylaminopyridine (1.75 mmol, 25 mol% with respect to glutarimide) and CH₂Cl₂ (15 mL) was added. The mixture was cooled to 0 °C and the acid chloride was added dropwise. The reaction mixture was warmed to room temperature and stirred for 16 h. After this period, the mixture was diluted with CH₂Cl₂ (~20 mL). The organic layer was then washed with 1 M HCl (~25 mL), water (~25 mL) and then brine (~25 mL). The organic layer was then dried (MgSO₄), filtered, and concentrated to afford the crude product as a brown solid. Unless stated otherwise, the crude product was purified by recrystallisation (toluene) to afford the pure *N*-acyl glutarimide.

1-Benzoylpiperidine-2,6-dione (155)



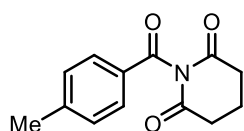
Prepared according to **GP6** to give the title compound (1.82 g, 84%) as a beige solid. M.p. 111-113 °C. $^1\text{H NMR}$ (500 MHz, CDCl_3) δ 7.88 – 7.84 (m, 2H), 7.66 – 7.62 (m, 1H), 7.52 – 7.46 (m, 2H), 2.78 (t, $J = 6.5$ Hz, 4H), 2.15 (p, $J = 6.5$ Hz, 2H). $^{13}\text{C NMR}$ (126 MHz, CDCl_3) δ 172.0, 170.9, 135.1, 131.9, 130.3, 129.3, 32.5, 17.6. **HRMS** (CI) m/z : $[\text{M}]^+$ Calcd for $\text{C}_{13}\text{H}_{11}\text{O}_3\text{N}$ 217.0733, found: 247.0734. Characterisation data in accordance with literature report.³⁷

(3-Bromobutyl)benzene (165SM)



To a flask was added 4-phenylbutan-2-ol (0.62 mL, 4 mmol), PPh_3 (1.36 g, 5.2 mmol, 1.3 equiv.), imidazole (0.354 g, 5.2 mmol, 1.3 equiv.) and dichloromethane (8 mL). Bromine (0.27 mL, 5.2 mmol, 1.3 equiv.) was added dropwise at 0 °C. The reaction was warmed to room temperature and stirred overnight. Upon completion of the reaction as monitored by TLC analysis, the mixture was quenched with saturated NaHCO_3 (10 mL). The layers were separated. The aqueous layer was extracted with CH_2Cl_2 (3×10 mL). The combined organic layers were washed with brine (~25 mL), dried (MgSO_4), filtered, and concentrated under reduced pressure. The crude product was purified by flash column chromatography (petroleum ether) to afford the title compound (0.772 g, 91%) as a colourless oil. $^1\text{H NMR}$ (500 MHz, CDCl_3) δ 7.33 – 7.27 (m, 2H), 7.23 – 7.19 (m, 3H), 4.13 – 4.05 (m, 1H), 2.90 – 2.84 (m, 1H), 2.79 – 2.72 (m, 1H), 2.19 – 2.10 (m, 1H), 2.10 – 2.00 (m, 1H), 1.74 (d, $J = 6.7$ Hz, 3H). $^{13}\text{C NMR}$ (126 MHz, CDCl_3) δ 141.1, 128.7, 128.6, 126.2, 51.0, 42.8, 34.1, 26.7. **HRMS** (CI) m/z : $[\text{MH}]^+$ Calcd for $\text{C}_{10}\text{H}_{13}^{79}\text{Br}$ 212.0195, found: 212.0913. The NMR data is consistent with the literature.⁴⁴

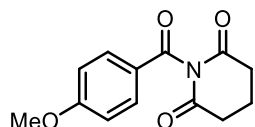
1-(4-Methylbenzoyl)piperidine-2,6-dione (169SM / 194)



6 - Experimental

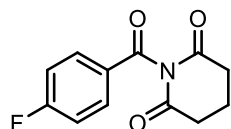
Prepared according to **GP6** to give the title compound (1.66 g, 72%) as an off-white solid. M.p. 168-170 °C. **¹H NMR** (500 MHz, CDCl₃) δ 7.75 (d, *J* = 8.2 Hz, 2H), 7.28 (d, *J* = 8.1 Hz, 2H), 2.77 (t, *J* = 6.5 Hz, 4H), 2.42 (s, 3H), 2.14 (p, *J* = 6.5 Hz, 2H). **¹³C NMR** (126 MHz, CDCl₃) δ 172.0, 170.5, 146.5, 130.5, 130.0, 129.3, 32.5, 22.0, 17.6. **HRMS** (CI) *m/z*: [M]⁺ Calcd for C₁₃H₁₃O₃N 231.0890, found: 231.0889. Characterisation data in accordance with literature report.³⁸

1-(4-Methoxybenzoyl)piperidine-2,6-dione (170SM)



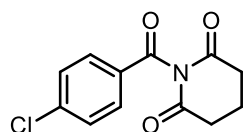
Synthesised according to **GP6** on a 5 mmol scale to give the title compound (1.00 g, 81%) as a beige solid. M.p. 150-152 °C. **¹H NMR** (500 MHz, CDCl₃) δ 7.84 – 7.80 (m, 2H), 6.97 – 6.91 (m, 2H), 3.87 (s, 3H), 2.76 (t, *J* = 6.6 Hz, 4H), 2.13 (p, *J* = 6.6 Hz, 2H). **¹³C NMR** (126 MHz, CDCl₃) δ 172.0, 169.6, 165.2, 132.9, 124.6, 114.6, 55.8, 32.6, 17.7. **HRMS** (CI) *m/z*: [M]⁺ Calcd for C₁₃H₁₃O₄N 247.0839, found: 247.0838. Characterisation data in accordance with literature report.³⁸

1-(4-Fluorobenzoyl)piperidine-2,6-dione (171SM)



Prepared according to **GP6** to give the title compound (1.76 g, 75%) as a beige solid. M.p. 169-172 °C. **¹H NMR** (500 MHz, CDCl₃) δ 7.89 (dd, *J* = 8.7, 5.3 Hz, 2H), 7.16 (app t, *J* = 8.5 Hz, 2H), 2.78 (t, *J* = 6.5 Hz, 4H), 2.15 (p, *J* = 6.5 Hz, 2H). **¹³C NMR** (126 MHz, CDCl₃) δ 171.9, 169.5, 166.7 (d, *J* = 258.4 Hz), 133.0 (d, *J* = 9.9 Hz), 128.3 (d, *J* = 2.8 Hz), 116.5 (d, *J* = 22.4 Hz), 32.4, 17.5. **¹⁹F NMR** (471 MHz, CDCl₃) δ -101.24 – -101.32 (m). **HRMS** (CI) *m/z*: [M]⁺ Calcd for C₁₂H₁₀O₃NF 235.0639, found: 235.0641. Characterisation data in accordance with literature report.³⁸

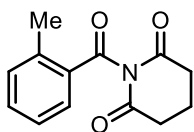
1-(4-Chlorobenzoyl)piperidine-2,6-dione (172SM)



Prepared according to the **GP6** to give the title compound (2.05 g, 82%) as a white solid. M.p. 167-169 °C. **¹H NMR** (500 MHz, CDCl₃) δ 7.81 – 7.77 (m, 2H), 7.48 – 7.45 (m, 2H),

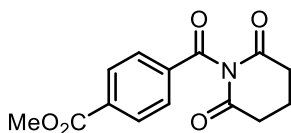
2.80 – 2.76 (m, 4H), 2.19 – 2.11 (m, 2H). ^{13}C NMR (126 MHz, CDCl_3) δ 172.0, 170.0, 141.8, 131.6, 130.4, 129.7, 32.5, 17.6. HRMS (EI) m/z : $[\text{M}]^+$ Calcd for $\text{C}_{12}\text{H}_{10}\text{O}_3\text{N}^{35}\text{Cl}$ 251.0344, found: 251.0346. The NMR data is consistent with the literature.³⁸

1-(2-Methylbenzoyl)piperidine-2,6-dione (173SM)



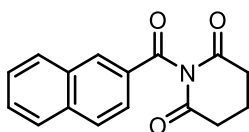
Prepared according to **GP6**. Purified by flash column chromatography (petroleum ether / EtOAc : 1/1) to give the title compound (1.70 g, 73%) as a pale yellow solid. M.p. 91-94°C. ^1H NMR (500 MHz, CDCl_3) δ 7.49 (dd, $J = 7.8, 1.3$ Hz, 1H), 7.46 (td, $J = 7.5, 1.4$ Hz, 1H), 7.33 – 7.31 (m, 1H), 7.27 – 7.23 (m, 1H), 2.75 (t, $J = 6.6$ Hz, 4H), 2.12 (p, $J = 6.6$ Hz, 2H). ^{13}C NMR (126 MHz, CDCl_3) δ 172.1, 170.8, 142.7, 133.9, 132.6, 131.3, 130.8, 126.3, 32.6, 22.0, 17.6. HRMS (EI) m/z : $[\text{M}]^+$ Calcd for $\text{C}_{13}\text{H}_{13}\text{O}_3\text{N}$ 231.0890, found: 231.0891. Characterisation data in accordance with literature report.³⁷

Methyl 4-(2,6-dioxopiperidine-1-carbonyl)benzoate (174SM)



Prepared according to **GP7** to give the title compound (1.65 g, 85%) as a beige solid. M.p. 93-94 °C. ^1H NMR (500 MHz, CDCl_3) δ 8.16 – 8.13 (m, 2H), 7.93 – 7.89 (m, 2H), 3.96 (s, 3H), 2.82 – 2.77 (m, 4H), 2.20 – 2.14 (m, 2H). ^{13}C NMR (126 MHz, CDCl_3) δ 172.0, 170.5, 165.9, 135.6, 135.3, 130.4, 130.1, 52.8, 32.6, 17.6. HRMS (EI) m/z : $[\text{M}]^+$ Calcd for $\text{C}_{14}\text{H}_{13}\text{O}_5\text{N}$ 275.0788, found: 275.0789. Characterisation data in accordance with literature report.³⁸

1-(2-Naphthoyl)piperidine-2,6-dione (175SM)

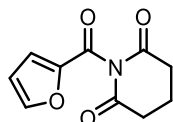


Prepared according to **GP6** to give title compound as a beige solid (2.10 g, 79%). M.p. 150-152 °C. ^1H NMR (500 MHz, CDCl_3) δ 8.34 (d, $J = 0.7$ Hz, 1H), 7.96 – 7.92 (m, 3H), 7.89 (dd, $J = 8.2, 0.6$ Hz, 1H), 7.64 (ddd, $J = 8.2, 6.9, 1.2$ Hz, 1H), 7.57 (ddd, $J = 8.1,$

6 - Experimental

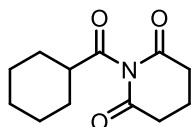
6.9, 1.2 Hz, 1H), 2.83 (t, $J = 6.6$ Hz, 4H), 2.21 (p, $J = 6.5$ Hz, 2H). ^{13}C NMR (126 MHz, CDCl_3) δ 172.1, 171.0, 136.6, 132.8, 132.6, 130.0, 129.7, 129.4, 129.3, 128.1, 127.3, 124.9, 32.6, 17.7. HRMS (EI) m/z : $[\text{M}]^+$ Calcd for $\text{C}_{16}\text{H}_{13}\text{O}_3\text{N}$ 267.0890, found: 267.0891. Characterisation data in accordance with literature report.³⁸

1-(Furan-2-carbonyl)piperidine-2,6-dione (176SM)



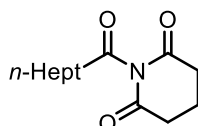
Prepared according to **GP6** to give the title compound (1.74 g, 84%) as a white solid. M.p. 104-105 °C. ^1H NMR (500 MHz, CDCl_3) δ 7.60 (s, 1H), 7.40 (d, $J = 2.8$ Hz, 1H), 6.61 (s, 1H), 2.76 (t, $J = 6.3$ Hz, 4H), 2.15 – 2.05 (m, 2H). ^{13}C NMR (126 MHz, CDCl_3) δ 171.8, 159.5, 148.4, 147.6, 122.3, 113.8, 32.5, 17.5. HRMS (EI) m/z : $[\text{M}]^+$ Calcd for $\text{C}_{10}\text{H}_9\text{O}_4\text{N}$ 207.0526, found: 207.0527. Characterisation data in accordance with literature report.³⁹

1-(Cyclohexanecarbonyl)piperidine-2,6-dione (177SM)



Prepared according to the **GP6** to give the title compound (1.92 g, 86%) as a white solid. M.p. 69-72 °C. ^1H NMR (500 MHz, CDCl_3) δ 2.68 – 2.58 (m, 5H), 2.05 – 1.95 (m, 1H), 1.84 – 1.77 (m, 4H), 1.68 – 1.62 (m, 2H), 1.52 – 1.41 (m, 1H), 1.31 – 1.17 (m, 3H). ^{13}C NMR (126 MHz, CDCl_3) δ 181.0, 172.0, 48.8, 32.5, 28.1, 25.7, 25.5, 17.5. HRMS (EI) m/z : $[\text{M}]^+$ Calcd for $\text{C}_{12}\text{H}_{17}\text{O}_3\text{N}$ 223.1203, found: 223.1205. Characterisation data in accordance with literature report.⁴⁰

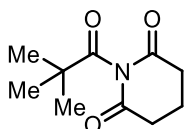
1-Octanoylpiperidine-2,6-dione (180SM)



Prepared according to **GP6**. Purified by flash column chromatography (petroleum ether/EtOAc: 1/1) to give the title compound (1.579 g, 66%) as a white solid. M.p. 34-36 °C. ^1H NMR (500 MHz, CDCl_3) δ 2.66 – 2.56 (m, 6H), 1.99 – 1.93 (m, 2H), 1.67 – 1.60 (m, 2H), 1.34 – 1.18 (m, 8H), 0.83 (t, $J = 7.0$ Hz, 3H). ^{13}C NMR (126 MHz, CDCl_3) δ

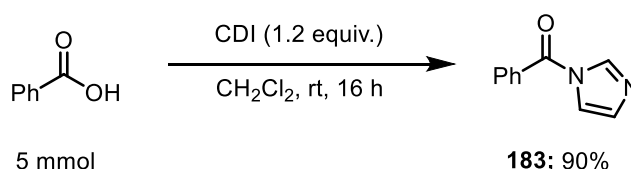
178.4, 171.7, 40.9, 32.2, 31.6, 28.89, 28.5, 23.4, 22.6, 17.3, 14.0. The NMR data is consistent with the literature.⁴¹

1-Pivaloylpiperidine-2,6-dione (181SM)



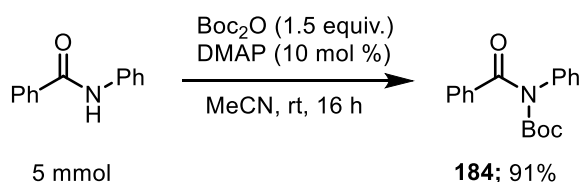
Prepared according to **GP6**. The crude mixture was dissolved in the minimum amount of CH_2Cl_2 and added dropwise to petroleum ether. The white precipitate was then filtered under vacuum to give 1-pivaloylpiperidine-2,6-dione (1.47 g, 75%) as a white solid. M.p. 49-51 °C. **¹H NMR** (500 MHz, CDCl_3) δ 2.65 (t, $J = 6.5$ Hz, 4H), 2.02 (p, $J = 6.6$ Hz, 2H), 1.26 (s, 9H). **¹³C NMR** (126 MHz, CDCl_3) δ 185.7, 172.0, 43.9, 32.3, 27.3, 17.6. **HRMS** (CI) m/z : $[\text{MH}]^+$ Calcd for $\text{C}_{10}\text{H}_{16}\text{O}_3\text{N}$ 198.1125, found: 198.1123. Characterisation data in accordance with literature report.⁴⁰

(1*H*-Imidazol-1-yl)(phenyl)methanone (183)



Prepared according to a literature procedure.⁴² To a solution of benzoic acid (0.61 g, 5 mmol) in CH_2Cl_2 (20 mL) was added *N,N'*-carbonyldiimidazole (0.972 g, 6 mmol, 1.2 equiv.). The mixture was stirred at room temperature overnight. Distilled water (~25 mL) was added, and the layers were separated. The organic layer was washed with water (2 \times 25 mL) and then brine (~30 mL). The organic phase was then dried (MgSO_4), filtered, and concentrated under reduced pressure to afford the title compound (0.774 g, 90%) as a colourless oil. **¹H NMR** (500 MHz, CDCl_3) δ 8.09 (s, 1H), 7.81 – 7.78 (m, 2H), 7.71 – 7.67 (m, 1H), 7.59 – 7.54 (m, 3H), 7.18 (s, 1H). **¹³C NMR** (126 MHz, CDCl_3) δ 166.3, 138.4, 133.8, 132.0, 131.6, 129.9, 129.1, 118.2. Characterisation data in accordance with literature report.⁴²

Tert-butyl benzoyl(phenyl)carbamate (184)

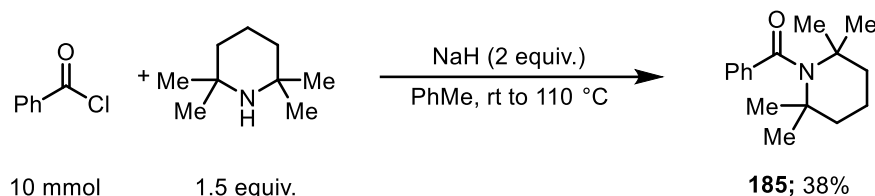


Prepared according to modified literature procedure. To a flame-dried flask was added,

6 - Experimental

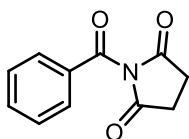
N-phenylbenzamide (0.985 g, 5 mmol), di-*tert*-butyl dicarbamate (1.64 g, 7.5 mmol, 1.5 equiv.), 4-dimethylaminopyridine (0.061 g, 10 mol %) and acetonitrile (25 mL). The mixture was stirred at room temperature for 16 hours. The reaction was quenched by addition of 1 M HCl (15 mL). CH₂Cl₂ (20 mL) was added, and the layers separated. The aqueous layer was extracted with CH₂Cl₂ (2 × 20 mL). The combined organic layers were dried (MgSO₄), filtered, and concentrated under reduced pressure to give the crude product. The crude material was purified by flash column chromatography (hexane/EtOAc: 1/1) to give the title compound (1.35 g, 91%) as a white solid. M.p. 96-98 °C. **¹H NMR (500 MHz, CDCl₃)** δ 7.75 – 7.71 (m, 2H), 7.54 – 7.50 (m, 1H), 7.46 – 7.40 (m, 4H), 7.37 – 7.32 (m, 1H), 7.28 – 7.26 (m, 2H), 1.23 (s, 9H). **¹³C NMR (126 MHz, CDCl₃)** δ 172.9, 153.5, 139.2, 137.1, 131.9, 129.4, 128.4, 128.3, 128.1, 127.9, 83.6, 27.6. Characterisation data in accordance with literature report.

Phenyl(2,2,6,6-tetramethylpiperidin-1-yl)methanone (185)



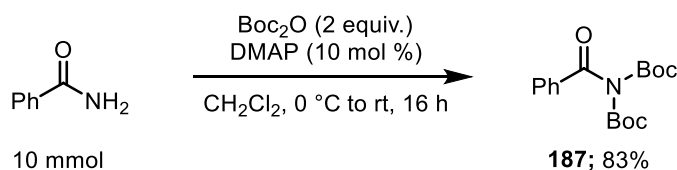
To a flame dried flask, 2,2,6,6-tetramethylpiperidine (2.55 mL, 15 mmol, 1.5 equiv.) was added to a solution of NaH (0.767 g, 60% dispersion in paraffin oil, 20 mmol, 2 equiv.) in toluene (20 mL). The mixture was stirred at room temperature for 10 minutes. Benzoyl chloride (1.16 mL, 10 mmol) was added dropwise, and the reaction was refluxed for 20 hours. The reaction was cooled to room temperature and EtOH (5 mL) was added to quench excess NaH followed by slow addition of water (10 mL). CH₂Cl₂ (25 mL) was added, and the layers were separated. The organic layer was washed with NaHCO₃ (2 × 20 mL) followed by brine (20 mL) to give the crude product as a yellow / brown oil. The crude product was purified by flash column chromatography (hexane/ethyl acetate, 9:1.) to give the title compound (0.875 g, 38%) as a white crystalline solid. M.p. 79-82 °C. **¹H NMR (500 MHz, CDCl₃)** δ 7.45 – 7.41 (m, 2H), 7.37 – 7.32 (m, 3H), 1.79 (s, 6H), 1.37 (s, 12H). **¹³C NMR (126 MHz, CDCl₃)** δ 176.9, 143.4, 129.5, 128.0, 56.7, 37.1, 30.6, 15.1. **HRMS (ES) m/z: [MH]⁺** Calcd for C₁₆H₂₄NO 246.1858, found: 246.1866. The NMR data is consistent with literature.³⁷

1-Benzoylpyrrolidine-2,5-dione (186)



To a flask was added succinimide (0.991 g, 10 mmol), triethylamine (2.79 mL, 20 mmol, 2 equiv.), 4-dimethylaminopyridine (0.306 g, 2.5 mmol, 0.25 equiv.) and CH₂Cl₂ (15 mL). Benzoyl chloride (1.27 mL, 11 mmol, 1.1 equiv.) was added dropwise over a period of 5 minutes at 0 °C with vigorous stirring. The reaction mixture was warmed to room temperature and stirred at this temperature overnight. After this period, the mixture was diluted with CH₂Cl₂ (~20 mL). The organic layer was then washed with 1 M HCl (~25 mL), water (~25 mL) and then brine (~25 mL). The organic layer was then dried (MgSO₄), filtered, and concentrated under reduced pressure to afford the crude product as a brown solid. The crude product was purified by recrystallization (toluene) to give the title compound (1.81 g, 89%) as a white solid. M.p. 118-120 °C. **¹H NMR** (500 MHz, CDCl₃) δ 7.87 – 7.83 (m, 2H), 7.67 (tt, *J* = 7.2, 1.2 Hz, 1H), 7.52 – 7.48 (m, 2H), 2.94 (s, 4H). **¹³C NMR** (126 MHz, CDCl₃) δ 174.8, 167.8, 135.3, 131.4, 130.7, 129.1, 29.2. **HRMS** (CI) *m/z*: [MH]⁺ Calcd for C₁₁H₁₀O₃N 204.0655, found: 204.0657. Characterisation data in accordance with literature report.³⁸

N,N-Bis(*tert*-butoxycarbonyl)benzamide (187)

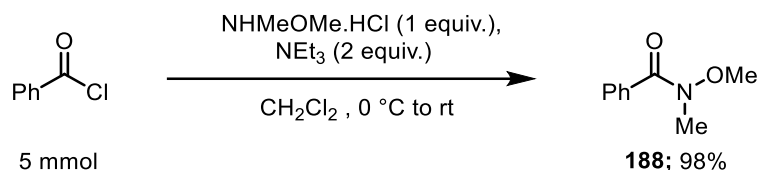


Synthesised according to a literature procedure.³⁸ To a flame dried flask was added benzamide (1.211 g, 10 mmol), 4-dimethylaminopyridine (0.122 g, 1 mmol, 0.1 equiv.), and CH₂Cl₂ (15 mL). Di-*tert*-butyl dicarbonate (4.37 g, 20 mmol, 2 equiv.) was added in portions at 0 °C with vigorous stirring. The reaction was warmed to room temperature and stirred for 16 hours. After this time, the reaction mixture was diluted with CH₂Cl₂ (~20 mL) The organic mixture was then washed with 1 M HCl (~20 mL), water (~20 mL), and then brine (~20 mL). The organic layer was then dried (MgSO₄), filtered, and concentrated under reduced pressure to afford the crude product as a brown liquid. The crude product was purified by column chromatography (hexane/EtOAc: 9/1) to give the title compound (2.67 g, 83%) as a colourless oil. **¹H NMR** (500 MHz, CDCl₃) δ 7.83 (m, 2H), 7.62 – 7.58 (m, 1H), 7.50 – 7.45 (m, 2H), 1.37 (s, 18H). **¹³C NMR** (126 MHz, CDCl₃) δ 169.5, 149.9, 134.3, 133.6, 129.2, 128.8, 84.4, 27.7. **HRMS** (ES) *m/z*: [2M+Na]⁺ Calcd

6 - Experimental

for $C_{34}H_{46}O_{10}N_2Na$ 665.3050, found: 665.3058. The NMR data is consistent with the literature.³⁸

N-Methoxy-*N*-methylbenzamide (188)



Prepared according to a modified literature procedure.⁴³ To a flame dried flask was added *N*-methoxymethylamine hydrochloride (0.388 g, 5 mmol) and CH_2Cl_2 (15 mL). The mixture was cooled to 0 °C and triethylamine (1.4 mL, 10 mmol) was added slowly. Benzoyl chloride (0.58 mL, 5 mmol) was added dropwise. After 10 minutes stirring at 0 °C, the mixture was warmed to room temperature and stirred for 1 hour. The reaction mixture was quenched with saturated aqueous $NaHCO_3$ (10 mL) and the layers separated. The organic phase was washed with 1 M HCl (2×10 mL) and brine (10 mL). The organic phase was then dried ($MgSO_4$), filtered, and concentrated under reduced pressure to afford the title compound (0.81 g, 98%) as a colourless oil. **¹H NMR** (500 MHz, $CDCl_3$) δ 7.68 – 7.64 (m, 2H), 7.47 – 7.42 (m, 1H), 7.41 – 7.37 (m, 2H), 3.55 (s, 3H), 3.36 (s, 3H). **¹³C NMR** (126 MHz, $CDCl_3$) δ 170.1, 134.2, 130.7, 128.3, 128.1, 61.2, 33.9. **HRMS** (CI) m/z : $[MH]^+$ Calcd for $C_9H_{12}O_2N$ 166.0863, found: 166.0862. Characterisation data in accordance with literature report.⁴³

6.4.2 Mechanochemical Reductive Cross-coupling Procedure and Characterisation Data of Products

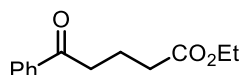
General Procedure 8 (GP8): Mechanochemical Reductive Coupling of Twisted Amides with Alkyl Halides

To a 15 mL stainless steel mixer mill jar (FormTech Scientific) was added a 2.5 g stainless steel milling ball. *N*-Acyl glutarimide (0.5 mmol), alkyl bromide (2 equiv.), $NiCl_2 \cdot 6H_2O$ (0.012 g, 10 mol %), 1,10-phenanthroline (0.018 g, 20 mol %), Mn powder (0.054 g, 2 equiv.) sodium chloride (0.029 g, 1 equiv.) and *N,N*-dimethylacetamide (0.140 mL, 3 equiv.) were all added to the milling jar under an air atmosphere. The milling jar was closed and placed on the mixer mill. The reaction was milled at 30 Hz for 2 hours. Upon completion of the milling period, the jar was opened, and the mixture was transferred to a conical flask using CH_2Cl_2 (~10 mL). 1 M HCl (~15 mL) was added, and the mixture was stirred for 2-3 minutes to quench metal salts. The mixture was then transferred to a separating funnel and the layers separated. The aqueous layer was

extracted with CH₂Cl₂ (2 × 15 mL). The combined organic layers were washed with brine (~30 mL), dried (MgSO₄), filtered, and concentrated under reduced pressure to afford the crude product as a yellow / orange oil. The crude product was purified by flash column chromatography using the noted solvent system to afford the pure ketone product.

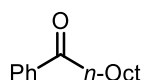
Unless stated otherwise, alkyl bromide was used as the alkyl halide coupling partner.

Ethyl 5-oxo-5-phenylpentanoate (156)



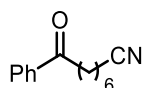
Prepared according to **GP8**. Purified by flash column chromatography (hexane/EtOAc: 9/1 to 4/1) to give the title compound (0.079 g, 72%) as a colourless oil. **¹H NMR** (500 MHz, CDCl₃) δ 7.97 – 7.94 (m, 2H), 7.57 – 7.53 (m, 1H), 7.47 – 7.43 (m, 2H), 4.13 (q, *J* = 7.1 Hz, 2H), 3.05 (t, *J* = 7.2 Hz, 2H), 2.42 (t, *J* = 7.2 Hz, 2H), 2.06 (app p, *J* = 7.2 Hz, 2H), 1.24 (t, *J* = 7.1 Hz, 3H). **¹³C NMR** (126 MHz, CDCl₃) δ 199.6, 173.4, 136.9, 133.2, 128.7, 128.1, 60.5, 37.6, 33.5, 19.5, 14.3. **HRMS** (CI) *m/z*: [M]⁺ Calcd for C₁₃H₁₆O₃ 220.1094, found: 220.1096. Characterisation data in accordance with literature report.⁴⁵

1-Phenylnonan-1-one (158)



Prepared according to **GP8** using 1-iodooctane as the alkyl halide. Purified by flash column chromatography (hexane/Et₂O: 19/1) to give the title compound (0.088 g, 81%) as a colourless oil. **¹H NMR** (500 MHz, CDCl₃) δ 7.97 – 7.94 (m, 2H), 7.57 – 7.53 (m, 1H), 7.48 – 7.44 (m, 2H), 2.98 – 2.93 (m, 2H), 1.79 – 1.69 (m, 2H), 1.41 – 1.24 (m, 10H), 0.88 (t, *J* = 7.0 Hz, 3H). **¹³C NMR** (126 MHz, CDCl₃) δ 200.8, 137.3, 133.0, 128.7, 128.2, 38.8, 32.0, 29.6, 29.5, 29.3, 24.5, 22.8, 14.3. **HRMS** (EI) *m/z*: [M]⁺ Calcd for C₁₅H₂₂O 218.1665, found: 218.1667. Characterisation data in accordance with literature report.⁴⁶

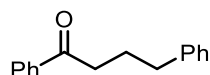
8-Oxo-phenyloctanenitrile (159)



6 - Experimental

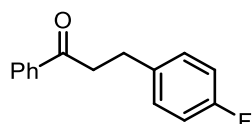
Prepared according to **GP8**. Purified by flash column chromatography (petroleum ether/EtOAc: 19/1) to give the title compound (0.087 g, 81%) as a colourless oil. **¹H NMR** (500 MHz, CDCl₃) δ 7.97 – 7.94 (m, 2H), 7.59 – 7.54 (m, 1H), 7.49 – 7.44 (m, 2H), 2.98 (t, *J* = 7.2 Hz, 2H), 2.35 (t, *J* = 7.1 Hz, 2H), 1.76 (m, 2H), 1.69 (m, 2H), 1.55 – 1.47 (m, 2H), 1.48 – 1.38 (m, 2H). **¹³C NMR** (126 MHz, CDCl₃) δ 200.3, 137.1, 133.2, 128.7, 128.2, 119.9, 38.4, 28.6, 28.6, 25.3, 23.9, 17.2. **HRMS** (CI) *m/z*: [MH]⁺ Calcd for C₁₄H₁₆ON 214.1226, found: 214.1225. Characterisation data in accordance with literature report.⁴⁵

1,4-Diphenylbutan-1-one (160)



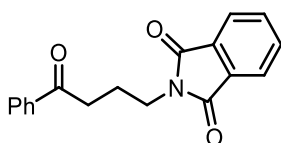
Prepared according to **GP8**. Purified by flash column chromatography (hexane/EtOAc: 19/1) to give the title compound (0.087 g, 78%) as a colourless oil. **¹H NMR** (500 MHz, CDCl₃) δ 7.94 – 7.90 (m, 2H), 7.57 – 7.53 (m, 1H), 7.48 – 7.42 (m, 2H), 7.32 – 7.27 (m, 2H), 7.23 – 7.15 (m, 3H), 2.98 (t, *J* = 7.3 Hz, 2H), 2.76 – 2.66 (m, 2H), 2.12 – 2.05 (m, 2H). **¹³C NMR** (126 MHz, CDCl₃) δ 200.3, 141.8, 137.2, 133.1, 128.7, 128.7, 128.6, 128.2, 126.1, 37.8, 35.3, 25.8. **HRMS** (EI) *m/z*: [M]⁺ Calcd for C₁₆H₁₆O 224.1196, found: 224.1194. Characterisation data in accordance with literature report.⁴²

3-(4-Fluorophenyl)-1-phenylpropan-1-one (161)



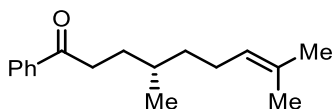
Prepared according to **GP8**. Purified by flash column chromatography (petroleum ether/EtOAc: 49/1 to 19/1) to give the title compound (0.080 g, 70%) as a white solid. M.p. 63-64 °C. **¹H NMR** (500 MHz, CDCl₃) δ 7.97 – 7.93 (m, 2H), 7.59 – 7.54 (m, 1H), 7.48 – 7.43 (m, 2H), 7.23 – 7.18 (m, 2H), 7.00 – 6.94 (m, 2H), 3.28 (t, *J* = 7.6 Hz, 2H), 3.05 (t, *J* = 7.6 Hz, 2H). **¹³C NMR** (126 MHz, CDCl₃) δ 199.2, 161.5 (d, *J* = 243.8 Hz), 137.0 (d, *J* = 3.2 Hz), 136.9, 133.3, 130.0 (d, *J* = 7.8 Hz), 128.8, 128.2, 115.4 (d, *J* = 21.1 Hz), 40.6, 29.4. **¹⁹F NMR** (471 MHz, CDCl₃) δ -117.23 – -117.31 (m). **HRMS** (CI) *m/z*: [M]⁺ Calcd for C₁₅H₁₃OF 228.0945, found: 228.0945. Characterisation data in accordance with literature report.⁴⁷

2-(4-Oxo-4-phenylbutyl)isoindoline-1,3-dione (162)



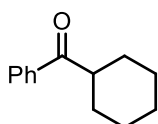
Prepared according to **GP8**. Purified by flash column chromatography (petroleum ether/EtOAc: 9/1 to 3/1) to give the title compound (0.089 g, 61%) as a white solid. M.p. 126-128 °C. **¹H NMR** (500 MHz, CDCl₃) δ 7.94 – 7.90 (m, 2H), 7.84 (dd, *J* = 5.4, 3.0 Hz, 2H), 7.71 (dd, *J* = 5.5, 3.0 Hz, 2H), 7.56 – 7.51 (m, 1H), 7.46 – 7.41 (m, 2H), 3.82 (t, *J* = 6.8 Hz, 2H), 3.06 (t, *J* = 7.3 Hz, 2H), 2.15 (app p, *J* = 7.0 Hz, 2H). **¹³C NMR** (126 MHz, CDCl₃) δ 199.0, 168.6, 136.9, 134.1, 133.2, 132.2, 128.7, 128.1, 123.4, 37.6, 35.9, 23.3. **HRMS** (ESI) *m/z*: [MH]⁺ Calcd for C₁₈H₁₆NO₃ 294.1130, found: 294.1335. Characterisation data in accordance with literature report.⁴⁸

(*S*)-4,8-Dimethyl-1-phenylnon-7-en-1-one (163)



Prepared according to **GP8**. Purified by flash column chromatography (petroleum ether/EtOAc: 1/0 to 9/1) to give (*S*)-4,8-dimethyl-1-phenylnon-7-en-1-one (0.068 g, 56%) as a colourless oil. **¹H NMR** (500 MHz, CDCl₃) δ 7.98 – 7.95 (m, 2H), 7.57 – 7.53 (m, 1H), 7.49 – 7.44 (m, 2H), 5.13 – 5.07 (m, 1H), 3.04 – 2.88 (m, 2H), 2.06 – 1.93 (m, 2H), 1.81 – 1.74 (m, 1H), 1.68 (d, *J* = 1.1 Hz, 3H), 1.60 (s, 3H), 1.59 – 1.51 (m, 2H), 1.43 – 1.35 (m, 1H), 1.25 – 1.16 (m, 1H), 0.94 (d, *J* = 6.5 Hz, 3H). **¹³C NMR** (126 MHz, CDCl₃) δ 201.0, 137.2, 133.0, 131.5, 128.7, 128.2, 124.8, 37.0, 36.5, 32.4, 31.5, 25.9, 25.7, 19.6, 17.8. **HRMS** (ES) *m/z*: [MH]⁺ Calcd for C₁₇H₂₅O 245.1905, found: 245.1910. Characterisation data in accordance with literature report.⁴⁹

Cyclohexyl(phenyl)methanone (164)

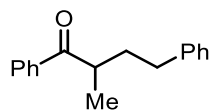


Prepared according to **GP8** with a reaction time of 3 hours. Purified by flash column chromatography (petroleum ether/EtOAc: 49/1 to 9/1) to give the title compound (0.045 g, 48%) as a white solid. M.p. 53-56 °C. **¹H NMR** (500 MHz, CDCl₃) δ 7.96 – 7.92 (m, 2H), 7.56 – 7.52 (m, 1H), 7.49 – 7.43 (m, 2H), 3.26 (m, 1H), 1.93 – 1.81 (m, 4H), 1.78 – 1.70 (m, 1H), 1.56 – 1.25 (m, 5H). **¹³C NMR** (126 MHz, CDCl₃) δ 204.1, 136.5, 132.9,

6 - Experimental

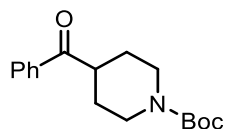
128.7, 128.4, 45.8, 29.6, 26.1, 26.0. **HRMS** (CI) m/z : $[MH]^+$ Calcd for $C_{13}H_{17}O$ 189.1274, found: 189.1274. Characterisation data in accordance with literature report.⁴²

2-Methyl-1,4-diphenylbutan-1-one (165)



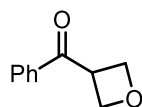
Prepared according to **GP8** with a reaction time of 3 hours. Purified by flash column chromatography (petroleum ether/EtOAc: 49/1 to 9/1) to give the title compound (0.061 g, 51%) as a colourless oil. **¹H NMR** (500 MHz, $CDCl_3$) δ 7.89 – 7.85 (m, 2H), 7.59 – 7.51 (m, 1H), 7.47 – 7.41 (m, 2H), 7.29 – 7.25 (m, 2H), 7.22 – 7.17 (m, 1H), 7.17 – 7.13 (m, 2H), 3.47 (app sex, $J = 6.8$ Hz, 1H), 2.69 – 2.60 (m, 2H), 2.21 – 2.13 (m, 1H), 1.79 – 1.70 (m, 1H), 1.24 (d, $J = 6.9$ Hz, 3H). **¹³C NMR** (126 MHz, $CDCl_3$) δ 204.3, 141.9, 136.6, 133.1, 128.8, 128.6, 128.5, 128.4, 126.1, 39.8, 35.3, 33.6, 17.4. **HRMS** (CI) m/z : $[MH]^+$ Calcd for $C_{17}H_{18}O$ 239.1430, found: 239.1429. Characterisation data in accordance with literature report.⁵⁰

Tert-butyl 4-benzoylpiperidine-1-carboxylate (166)



Prepared according to **GP8** with a reaction time of 3 hours. Purified by flash column chromatography (hexane/EtOAc: 19/1) to give the title compound (0.093 g, 64%) as a white solid. M.p. 93-95°C. **¹H NMR** (500 MHz, $CDCl_3$) δ 7.96 – 7.92 (m, 2H), 7.59 – 7.55 (m, 1H), 7.50 – 7.45 (m, 2H), 4.20 – 4.13 (m, 2H), 3.44 – 3.37 (m, 1H), 2.93 – 2.86 (m, 2H), 1.87 – 1.81 (m, 2H), 1.74 – 1.64 (m, 2H), 1.46 (s, 9H). **¹³C NMR** (126 MHz, $CDCl_3$) δ 202.2, 154.6, 136.0, 133.3, 128.9, 128.4, 79.8, 43.6, 43.4, 28.6, 28.5. **HRMS** (ES) m/z : $[M+Na]^+$. Calcd for $C_{17}H_{23}NO_3^{23}Na$ 312.1576, found: 312.1562. Characterisation data in accordance with literature report.⁴⁵

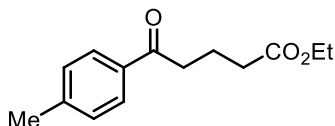
Oxetan-3-yl(phenyl)methanone (167)



Prepared according to **GP8** with a reaction time of 3 hours. Purified by flash column chromatography (petroleum ether/EtOAc: 9/1 to 3/1) to give the title compound (0.068 g, 84%) as a colourless oil. **¹H NMR** (500 MHz, $CDCl_3$) δ 7.80 – 7.77 (m, 2H), 7.62 – 7.57

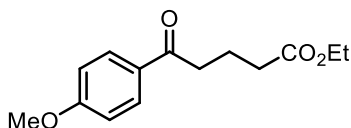
(m, 1H), 7.50 – 7.45 (m, 2H), 4.97 (d, $J = 7.8$ Hz, 4H), 4.64 (p, $J = 7.8$ Hz, 1H). $^{13}\text{C NMR}$ (126 MHz, CDCl_3) δ 197.2, 135.0, 133.8, 129.1, 128.3, 72.9, 42.3. **HRMS** (ES) m/z : $[\text{MH}]^+$ Calcd for $\text{C}_{10}\text{H}_{11}\text{O}$ 163.0759, found: 163.0753. **FTIR** (neat) ν_{max} , 2914, 2854, 1672, 1583, 1212, 1080, 801 cm^{-1} .

Ethyl 5-oxo-5-(*p*-tolyl)pentanoate (169)



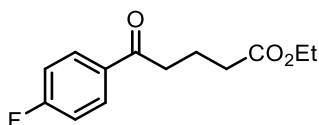
Prepared according to **GP8**. Purified by flash column chromatography (petroleum ether/EtOAc: 9/1) to give the title compound (0.098 g, 84%) as a white solid. M.p. 37–38 °C. $^1\text{H NMR}$ (500 MHz, CDCl_3) δ 7.88 – 7.82 (m, 2H), 7.26 – 7.22 (m, 2H), 4.13 (q, $J = 7.1$ Hz, 2H), 3.02 (t, $J = 7.2$ Hz, 2H), 2.43 – 2.39 (m, 5H), 2.06 (app p, $J = 7.2$ Hz, 2H), 1.25 (t, $J = 7.1$ Hz, 3H). $^{13}\text{C NMR}$ (126 MHz, CDCl_3) δ 199.2, 173.4, 144.0, 134.5, 129.4, 128.3, 60.5, 37.5, 33.6, 21.8, 19.6, 14.4. **HRMS** (ES) m/z : $[\text{MH}]^+$ Calcd for $\text{C}_{14}\text{H}_{19}\text{O}_3$ 235.1334, found: 235.1340. Characterisation data in accordance with literature report.⁵¹

Ethyl 5-(4-methoxyphenyl)-5-oxopentanoate (170)



Prepared according to **GP8**. Purified by flash column chromatography (petroleum ether/EtOAc: 9/1 to 3/1) to give the title compound (0.111 g, 89%) as a white solid. M.p. 54–56 °C. $^1\text{H NMR}$ (500 MHz, CDCl_3) δ 7.97 – 7.91 (m, 2H), 6.94 – 6.90 (m, 2H), 4.13 (q, $J = 7.1$ Hz, 2H), 3.86 (s, 3H), 2.99 (t, $J = 7.2$ Hz, 2H), 2.42 (t, $J = 7.2$ Hz, 2H), 2.05 (app p, $J = 7.2$ Hz, 2H), 1.25 (t, $J = 7.1$ Hz, 3H). $^{13}\text{C NMR}$ (126 MHz, CDCl_3) δ 198.2, 173.5, 163.6, 130.4, 130.1, 113.8, 60.5, 55.6, 37.3, 33.6, 19.8, 14.4. **HRMS** (ES) m/z : $[\text{MH}]^+$ Calcd for $\text{C}_{14}\text{H}_{19}\text{O}_4$ 251.1283, found: 251.1289. Characterisation data in accordance with literature report.⁵²

Ethyl 5-(4-fluorophenyl)-5-oxopentanoate (171)

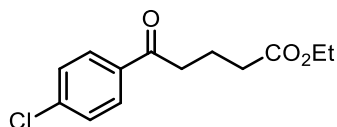


Prepared according to **GP8**. Purified by flash column chromatography (petroleum ether/EtOAc: 19/1) to give the title compound (0.083 g, 70%) as a colourless oil. $^1\text{H NMR}$

6 - Experimental

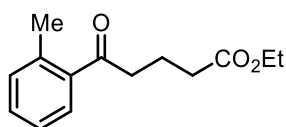
(500 MHz, CDCl₃) δ 8.02 – 7.95 (m, 2H), 7.15 – 7.10 (m, 2H), 4.14 (q, J = 7.1 Hz, 2H), 3.02 (t, J = 7.2 Hz, 2H), 2.43 (t, J = 7.1 Hz, 2H), 2.06 (app p, J = 7.2 Hz, 2H), 1.25 (t, J = 7.1 Hz, 3H). **¹³C NMR** (126 MHz, CDCl₃) δ 198.0, 173.4, 165.9 (d, J = 254.6 Hz), 133.4 (d, J = 3.0 Hz), 130.8 (d, J = 9.3 Hz), 115.8 (d, J = 21.8 Hz), 60.6, 37.5, 33.5, 19.5, 14.4. **HRMS** (ES) m/z : [MH]⁺ Calcd for C₁₃H₁₆O₃F 239.1083, found: 239.1085. Characterisation data in accordance with literature report.⁵³

Ethyl 5-(4-chlorophenyl)-5-oxopentanoate (172)



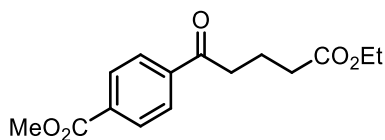
Prepared according to **GP8**. Purified by flash column chromatography (petroleum ether/EtOAc: 49/1 to 19/1) to give the title compound (0.086 g, 68%) as a white solid. M.p. 50-52 °C. **¹H NMR** (500 MHz, CDCl₃) δ 7.92 – 7.88 (m, 2H), 7.45 – 7.41 (m, 2H), 4.14 (q, J = 7.1 Hz, 2H), 3.02 (t, J = 7.2 Hz, 2H), 2.43 (m, 2H), 2.06 (app p, J = 7.2 Hz, 2H), 1.25 (t, J = 7.2 Hz, 3H). **¹³C NMR** (126 MHz, CDCl₃) δ 198.4, 173.4, 139.7, 135.3, 129.6, 129.1, 60.6, 37.6, 33.4, 19.4, 14.4. **HRMS** (ES) m/z : [MH]⁺ Calcd for C₁₃H₁₆O₃Cl 255.0788, found: 255.0785. Characterisation data in accordance with literature report.⁵⁴

Ethyl-5-oxo-5-(*o*-tolyl)pentanoate (173)



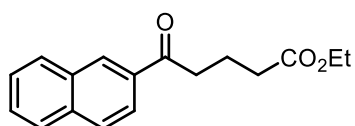
Prepared according to **GP8**. Purified by flash column chromatography (petroleum ether/EtOAc: 19/1 to 9/1) to give the title compound (0.084 g, 72%) as a colourless oil. **¹H NMR** (500 MHz, CDCl₃) δ 7.63 (d, J = 7.8 Hz, 1H), 7.36 (td, J = 7.5, 1.3 Hz, 1H), 7.27 – 7.22 (m, 2H), 4.13 (q, J = 7.1 Hz, 2H), 2.97 (t, J = 7.2 Hz, 2H), 2.49 (s, 3H), 2.41 (t, J = 7.2 Hz, 2H), 2.04 (app p, J = 7.2 Hz, 2H), 1.25 (t, J = 7.1 Hz, 3H). **¹³C NMR** (126 MHz, CDCl₃) δ 203.7, 173.4, 138.2, 138.0, 132.1, 131.4, 128.6, 125.8, 60.5, 40.5, 33.6, 21.4, 19.7, 14.4. **HRMS** (ES) m/z : [M+Na]⁺ Calcd for C₁₄H₁₈O₃Na 257.1154, found: 257.115. Characterisation data in accordance with literature report.⁵⁴

Methyl 4-(5-ethoxy-5-oxopentanoyl)benzoate (174)



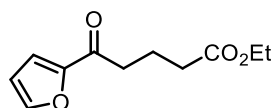
Prepared according to **GP8**. Purified by flash column chromatography (petroleum ether/EtOAc: 19/1 to 9/1) to give the title compound (0.104 g, 75%) as a white solid. M.p. 96-98 °C. **¹H NMR** (500 MHz, CDCl₃) δ 8.13 – 8.10 (m, 2H), 8.02 – 7.99 (m, 2H), 4.14 (q, *J* = 7.1 Hz, 2H), 3.95 (s, 3H), 3.08 (t, *J* = 7.2 Hz, 2H), 2.44 (t, *J* = 7.1 Hz, 2H), 2.08 (app p, *J* = 7.2 Hz, 2H), 1.25 (t, *J* = 7.1 Hz, 3H). **¹³C NMR** (126 MHz, CDCl₃) δ 199.1, 173.4, 166.4, 140.1, 134.0, 130.0, 128.1, 60.6, 52.6, 38.0, 33.4, 19.4, 14.4. **HRMS** (ES) *m/z*: [MH]⁺ Calcd for C₁₅H₁₉O₅ 279.1232, found: 279.1227. **FTIR** (neat) *v*_{max} 2930, 2842, 1731, 1680, 1262, 1196, 692 cm⁻¹.

Ethyl 5-(naphthalen-2-yl)-5-oxopentanoate (175)

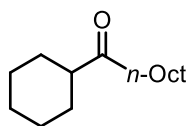


Prepared according to **GP8**. Purified by flash column chromatography (petroleum ether/EtOAc: 9/1 to 3/1) to give the title compound (0.086 g, 64%) as a white solid. M.p. 61-62 °C. **¹H NMR** (500 MHz, CDCl₃) δ 8.48 (s, 1H), 8.03 (dd, *J* = 8.6, 1.7 Hz, 1H), 7.96 (d, *J* = 8.0 Hz, 1H), 7.91 – 7.86 (m, 2H), 7.63 – 7.53 (m, 2H), 4.15 (q, *J* = 7.1 Hz, 2H), 3.19 (t, *J* = 7.2 Hz, 2H), 2.48 (t, *J* = 7.2 Hz, 2H), 2.14 (app p, *J* = 7.2 Hz, 2H), 1.26 (t, *J* = 7.1 Hz, 3H). **¹³C NMR** (126 MHz, CDCl₃) δ 199.6, 173.5, 135.7, 134.3, 132.7, 129.9, 129.7, 128.6, 128.6, 127.9, 126.9, 124.0, 60.5, 37.7, 33.6, 19.7, 14.4. **HRMS** (ES) *m/z*: [MH]⁺ Calcd for C₁₇H₁₉O₃ 271.1334, found: 271.1339. Characterisation data in accordance with literature report.⁵⁵

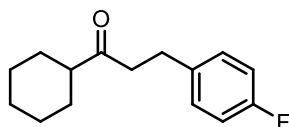
Ethyl 5-(furan-2-yl)-5-oxopentanoate (176)



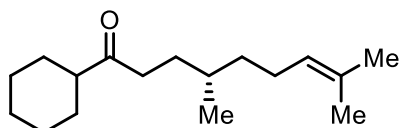
Prepared according to **GP8**. Purified by flash column chromatography (petroleum ether/EtOAc: 9/1) to give the title compound (0.061 g, 58%) as a colourless oil. **¹H NMR** (500 MHz, CDCl₃) δ 7.59 – 7.56 (m, 1H), 7.20 (d, *J* = 3.6 Hz, 1H), 6.53 (dd, *J* = 3.5, 1.7 Hz, 1H), 4.13 (q, *J* = 7.1 Hz, 2H), 2.90 (t, *J* = 7.3 Hz, 2H), 2.41 (t, *J* = 7.2 Hz, 2H), 2.05 (app p, *J* = 7.3 Hz, 2H), 1.25 (t, *J* = 7.1 Hz, 3H). **¹³C NMR** (126 MHz, CDCl₃) δ 188.7, 173.2, 152.6, 146.3, 117.0, 112.2, 60.4, 37.3, 33.4, 19.3, 14.2. **HRMS** (ES) *m/z*: [M+Na]⁺ Calcd for C₁₁H₁₄O₄Na 233.0790, found: 233.0786. Characterisation data in accordance with literature report.⁵⁴

1-Cyclohexylnonan-1-one (177)

Prepared according to **GP8**. Purified by flash column chromatography (petroleum ether/EtOAc: 49/1 to 19/1) to give the title compound (0.057 g, 51%) as a colourless oil. **¹H NMR** (500 MHz, CDCl₃) δ 2.43 – 2.29 (m, 3H), 1.86 – 1.73 (m, 3H), 1.70 – 1.63 (m, 1H), 1.57 – 1.51 (m, 2H), 1.37 – 1.16 (m, 15H), 0.87 (t, *J* = 6.9 Hz, 3H). **¹³C NMR** (126 MHz, CDCl₃) δ 214.7, 51.0, 43.0, 40.8, 32.0, 29.6, 29.5, 29.3, 28.7, 26.0, 25.9, 23.9, 22.8, 14.2. **HRMS** (EI) *m/z*: [MH]⁺ Calcd for C₁₅H₂₈O 224.2135, found: 224.2134. Characterisation data in accordance with literature report.⁵⁶

1-Cyclohexyl-3-(4-fluorophenyl)propan-1-one (178)

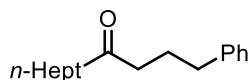
Prepared according to **GP8**. Purified by flash column chromatography (petroleum ether/EtOAc: 49/1 to 19/1) to give the title compound (0.049 g, 42%) as a colourless oil. **¹H NMR** (500 MHz, CDCl₃) δ 7.14 – 7.10 (m, 2H), 6.98 – 6.92 (m, 2H), 2.85 (t, *J* = 7.5 Hz, 2H), 2.73 (t, *J* = 7.4 Hz, 2H), 2.33 – 2.25 (m, 1H), 1.82 – 1.72 (m, 3H), 1.68 – 1.58 (m, 2H), 1.35 – 1.15 (m, 5H). **¹³C NMR** (126 MHz, CDCl₃) δ 213.1, 161.5 (d, *J* = 243.6 Hz), 137.2 (d, *J* = 3.2 Hz), 129.9 (d, *J* = 7.8 Hz), 115.3 (d, *J* = 21.1 Hz), 51.1, 42.4, 29.0, 28.5, 26.0, 25.8. **¹⁹F NMR** (471 MHz, CDCl₃) δ -117.42 – -117.50 (m). **HRMS** (EI) *m/z*: [M]⁺ Calcd for C₁₅H₁₉OF 234.1414, found: 234.1416. Characterisation data in accordance with literature report.⁵⁷

(S)-1-Cyclohexyl-4,8-dimethylnon-7-en-1-one (179)

Prepared according to **GP8**. Purified by flash column chromatography (petroleum ether/EtOAc: 49/1 to 19/1) to give the title compound (0.059 g, 47%) as a colourless oil. **¹H NMR** (500 MHz, CDCl₃) δ 5.11 – 5.05 (m, 1H), 2.49 – 2.30 (m, 3H), 2.04 – 1.89 (m, 2H), 1.86 – 1.73 (m, 3H), 1.70 – 1.54 (m, 8H), 1.44 – 1.11 (m, 10H), 0.87 (d, *J* = 6.2 Hz, 3H). **¹³C NMR** (126 MHz, CDCl₃) δ 214.8, 131.4, 124.9, 51.0, 38.5, 37.0, 32.3, 30.8, 28.7,

28.7, 26.0, 25.9, 25.6, 19.5, 17.8. **HRMS** (EI) m/z : $[M]^+$ Calcd for $C_{17}H_{39}O$ 250.2291, found: 250.2293. **FTIR** (neat) 2926, 2854, 1706, 1450, 1377, 1145, 987, 822 cm^{-1} .

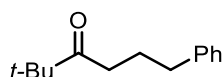
1-Phenylundecan-4-one (180)



Prepared according to **GP8**. Purified by flash column chromatography (petroleum ether/EtOAc: 1/0 to 49/1) to give the title compound (0.060 g, 49%) as a colourless oil.

1H NMR (500 MHz, $CDCl_3$) δ 7.30 – 7.27 (m, 2H), 7.21 – 7.15 (m, 3H), 2.64 – 2.59 (m, 2H), 2.41 (t, $J = 7.4$ Hz, 2H), 2.36 (t, $J = 7.5$ Hz, 2H), 1.96 – 1.87 (m, 2H), 1.59 – 1.50 (m, 2H), 1.32 – 1.22 (m, 8H), 0.88 (t, $J = 7.0$ Hz, 3H). **^{13}C NMR** (126 MHz, $CDCl_3$) δ 211.3, 141.8, 128.6, 128.5, 126.0, 43.0, 42.0, 35.3, 31.8, 29.3, 29.2, 25.4, 24.0, 22.7, 14.2. **HRMS** (ES) m/z : $[MH]^+$ Calcd for $C_{17}H_{27}O$ 247.2062, found: 247.2054. Characterisation data in accordance with literature report.⁵⁸

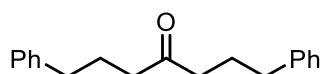
2,2-Dimethyl-6-phenylhexan-3-one (181)



Prepared according to **GP8**. Purified by flash column chromatography (petroleum ether/EtOAc: 1/0 to 33/1) to give the title compound (0.033 g, 32%) as a colourless oil.

1H NMR (500 MHz, $CDCl_3$) δ 7.30 – 7.26 (m, 2H), 7.21 – 7.16 (m, 3H), 2.61 (t, $J = 7.4$ Hz, 2H), 2.50 (t, $J = 7.2$ Hz, 2H), 1.90 (p, $J = 7.4$ Hz, 2H), 1.12 (s, 9H). **^{13}C NMR** (126 MHz, $CDCl_3$) δ 215.9, 142.0, 128.6, 128.5, 126.0, 44.26, 35.8, 35.3, 26.6, 25.5. **HRMS** (EI) m/z : $[M]^+$ Calcd for $C_{14}H_{20}O$ 204.1509, found: 204.1512. Characterisation data in accordance with literature report.⁵⁹

1,7-Diphenylheptan-4-one (182)



Obtained as a side product using **GP8** to form **XX**. Purified by flash column chromatography (petroleum ether/EtOAc: 1/0 to 33/1) to give the title compound (0.011 g, 8%) as a colourless oil. **1H NMR** (500 MHz, $CDCl_3$) δ 7.39 – 7.21 (m, 4H), 7.19 – 7.04 (m, 6H), 2.61 (t, $J = 7.5$ Hz, 4H), 2.39 (t, $J = 7.4$ Hz, 4H), 1.90 (app p, $J = 7.4$ Hz, 4H). **^{13}C NMR** (126 MHz, $CDCl_3$) 210.7, 141.8, 128.6, 128.5, 126.1, 42.1, 35.3, 25.4. **HRMS** (EI) m/z : $[M]^+$ Calcd for $C_{19}H_{22}O$ 266.1670, found: 266.1668. Characterisation data in accordance with literature report.⁵⁶

A 2.5 g stainless steel ball was added to a 15 mL stainless steel milling jar. 1-benzoylpiperidine-2,6-dione **155** (0.109 g, 0.5 mmol), ethyl 4-bromobutyrate **141** (0.194 g, 2, equiv. 1 mmol), NiCl₂•6H₂O (0.012 g, 10 mol %), 1,10-phenanthroline (0.018 g, 20 mol %), Mn powder (0.054 g, 2 equiv. 1 mmol), sodium chloride (0.029 g, 1 equiv., 0.5 mmol), *N,N*-dimethylacetamide (0.140 mL, 3 equiv., 1.5 mmol) and TEMPO (0.156 g, 2 equiv., 1 mmol) were all added to the jar. The reaction was then milled at 30 Hz for 2 hours. After the milling period, the mixture was washed from the jar with CH₂Cl₂ (~20 mL) and filtered under vacuum through a short pad of celite. The crude mixture was concentrated under reduced pressure. CDCl₃ was added and the yield of coupled product **156** was determined to be 0% by ¹H NMR spectroscopy. The sample was submitted for spectrometry analysis whereby the tempo adduct **192** was found by observed by ESI-MS.

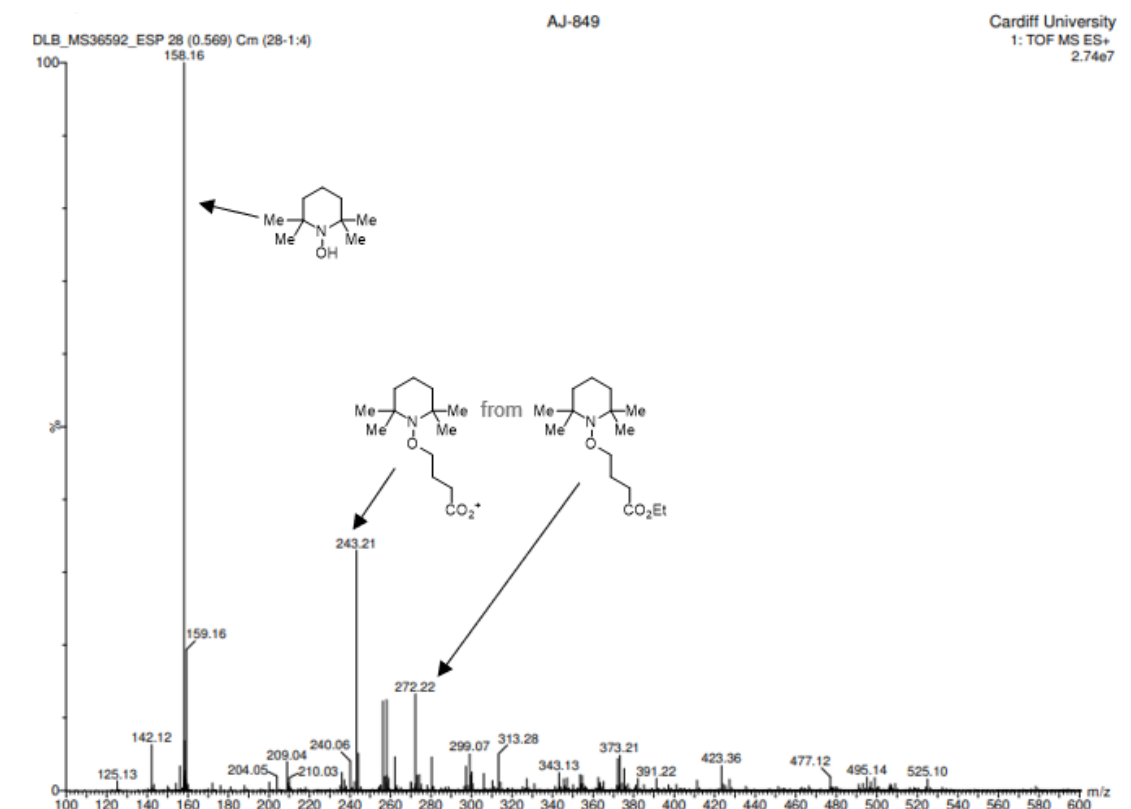


Figure 6.4 LRMS of TEMPO adduct

Organomanganese generation

A 2.5 g stainless steel milling ball was added to a 15 mL stainless steel milling jar. 4-Ethylbromobutyrate **141** (0.097 g, 0.5 mmol), Mn powder (0.054 g, 1 mmol, 2 equiv.) and *N,N*-dimethylacetamide (0.140 mL, 1.5 mmol, 3 equiv.) were added and the reaction was milled at 30 Hz for 2-6 hours. After the reaction period, the material was washed from the jar into a conical flask using CH₂Cl₂ (~10 mL). 2 M HCl (~15 mL) was added, and the

6 - Experimental

biphasic mixture was stirred for 20 minutes to hydrolyse any organometallics formed. The layers were separated, and the aqueous layer was extracted with CH_2Cl_2 (2×10 mL). The combined organic layers were washed with brine (~40 mL), dried (MgSO_4), filtered, and concentrated under reduced pressure. Mesitylene (23 μL , 0.166 mmol) was added as an internal standard, and then CDCl_3 . The yield of protodehalogenated product **193** and starting material **141** was determined by ^1H NMR spectroscopy using mesitylene as an internal standard.

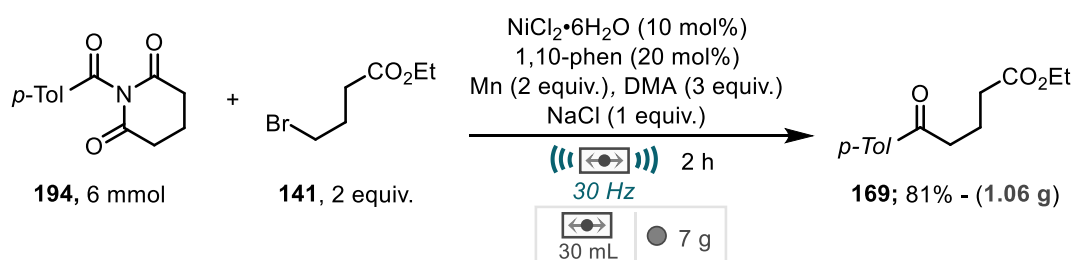
Table 6.2 Probing Organomanganese formation

Entry	Time (h)	Remaining 141 (%)	Yield 193 (%) ^a
1	2	98	0
2	4	97	0
3	6	98	0

^a Yield determined by ^1H NMR spectroscopy using mesitylene as an internal standard.

6.4.4 Scale up protocol

Ethyl 5-oxo-5-(*p*-tolyl)pentanoate (**169**)

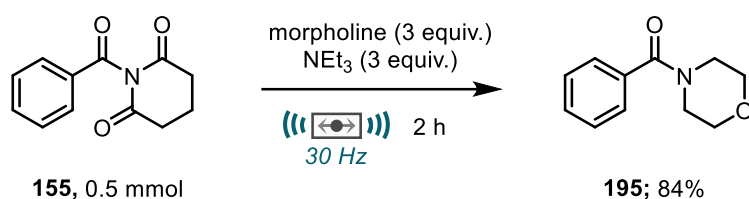


To a 25 g stainless steel milling jar (Retsch) was added a 7 g stainless steel milling ball. 1-(4-Methylbenzoyl)piperidine-2,6-dione **194** (1.39 g, 6 mmol), ethyl 4-bromobutyrate **141** (2.33 g, 12 mmol, 2 equiv.), $\text{NiCl}_2 \cdot 6\text{H}_2\text{O}$ (0.144 g, 10 mol %), 1,10-phenanthroline (0.216 g, 20 mol %), Mn powder (0.648 g, 12 mmol, 2 equiv.) sodium chloride (0.348 g, 6 mmol, 1 equiv.) and *N,N*-dimethylacetamide (1.68 mL, 18 mmol, 3 equiv.) were all added to the milling jar under an air atmosphere. The milling jar was closed and placed on the mixer mill. The reaction was milled at 30 Hz for 2 hours. Upon completion of the milling period, the jar was opened, and the mixture was transferred to a conical flask

using CH₂Cl₂ (~30 mL). 1 M HCl (~40 mL) was added, and the mixture was stirred for 5 minutes to quench metal salts. The mixture was then transferred to a separating funnel and the layers separated. The aqueous layer was extracted with CH₂Cl₂ (2 × 30 mL). The combined organic layers were washed with brine (~100 mL), dried (MgSO₄), filtered, and concentrated under reduced pressure to afford the crude product as a yellow / orange oil. The crude material was purified by flash column chromatography (petroleum ether/EtOAc: 9/1) to give the title compound (1.06 g, 81%) as a white solid.

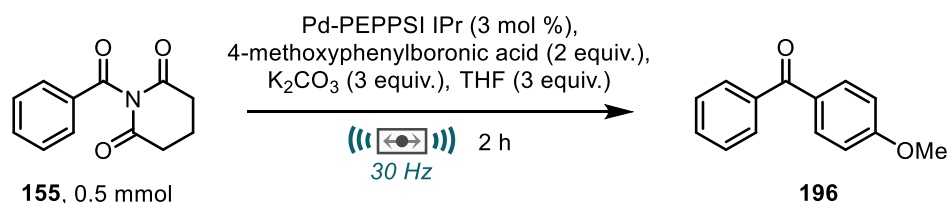
6.4.5 Other twisted amide reactivity by ball milling

Transamidation - morpholino(phenyl)methanone (195)



A 2.5 g stainless steel milling ball was added to a 15 mL stainless steel milling jar (FormTech Scientific). 1-benzoylpiperidine-2,6-dione **155** (0.218 g, 1 mmol), morpholine (0.259 mL, 3 mmol) and triethylamine (0.369 mL, 3 mmol) were all added to the jar under air. The jar was closed and placed on the mixer mill. The reaction was milled at 30 Hz for 2 hours. After the milling period, the reaction mixture was rinsed from the jar with EtOAc (~20 mL). 1 M HCl (~15 mL) was added, and the layers separated. The aqueous layer was extracted with EtOAc (3 × 15 mL). The combined organic layers were washed with brine (~50 mL), dried (MgSO₄), filtered, and concentrated under reduced pressure to afford the crude product as a yellow oil. The crude product was purified by flash column chromatography (petroleum ether/EtOAc: 1/1) to give the title compound (0.160 mg, 84%) as a white solid. M.p. 64-67 °C. ¹H NMR (500 MHz, CDCl₃) δ 7.43 – 7.38 (m, 5H), 3.86 – 3.37 (m, 8H). ¹³C NMR (126 MHz, CDCl₃) δ 170.7, 135.5, 130.1, 128.8, 127.3, 67.1, 48.4, 42.8. HRMS (ES) m/z: [MH]⁺ Calcd for C₁₁H₁₄NO₂ 192.1025, found: 192.1033. Characterisation data in accordance with literature report.⁴⁰

Suzuki coupling – (4-methoxyphenyl)(phenyl)methanone (196)



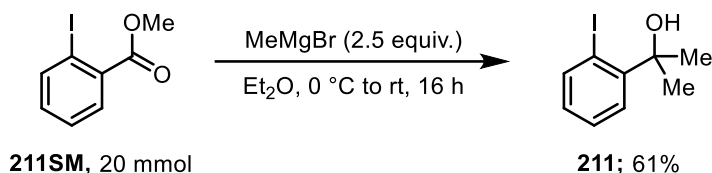
6 - Experimental

A 2.5 g stainless steel milling ball was added to a 15 mL stainless steel milling jar (FormTech Scientific). 1-benzoylpiperidine-2,6-dione **155** (0.218 g, 1 mmol), 4-methoxyphenylboronic acid (0.304 g, 2 mmol), Pd-PEPPSI IPr (0.020 g, 3 mol %), K₂CO₃ (0.414 g, 3 mmol) and THF (0.244 mL, 3 mmol) were all added to the jar under air. The jar was closed and placed on the mill. The reaction was milled at 30 Hz for 2 hours. After the milling time, the reaction was rinsed from the jar using CH₂Cl₂ (~20 mL). The resulting mixture was filtered through a short pad of celite and concentrated under reduced pressure to afford the crude product as an orange liquid. The crude product was purified by flash column chromatography (petroleum ether/EtOAc: 19/1 to 9/1) to afford the title compound (0.076 g, 36%) as a white solid. M.p. 59-62 °C. **¹H NMR** (500 MHz, CDCl₃) δ 7.83 (d, *J* = 9.0 Hz, 2H), 7.78 – 7.74 (m, 2H), 7.60 – 7.55 (m, 1H), 7.49 – 7.44 (m, 2H), 6.97 (d, *J* = 9.0 Hz, 2H), 3.89 (s, 3H). **¹³C NMR** (126 MHz, CDCl₃) δ 195.7, 163.4, 138.4, 132.7, 132.0, 130.3, 129.9, 128.3, 113.7, 55.6. **HRMS** (ES) *m/z*: [MH]⁺ Calcd for C₁₄H₁₃O₂ 213.0914, found: 213.0916. Characterisation data in accordance with literature report.⁶¹

6.5 Mechanochemical fluorocyclisations using a hypervalent fluoroiodane reagent

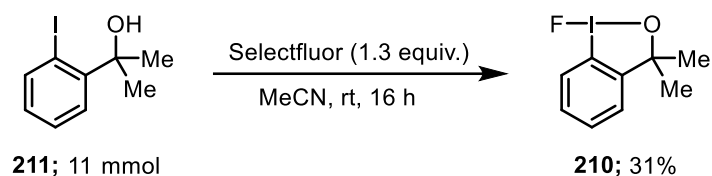
6.5.1 Preparation of Fluoroiodane Reagent

2-(2-Iodophenyl)propan-2-ol (**211**)



Prepared according to a modified literature procedure.⁶² To a flame dried flask, ethyl 2-iodobenzoate (5.52 g, 20 mmol) and Et₂O (90 mL) were added. The solution was cooled to 0 °C. Methyl magnesium bromide (16.7 mL, 50 mmol, 2.5 equiv., 3 M in Et₂O) was added slowly. The mixture was warmed to room temperature and stirred overnight. Saturated aqueous NH₄Cl (50 mL) was added slowly to quench the reaction and the layers separated. The aqueous layer was extracted with Et₂O (2 × 40 mL). The combined organic phases were dried (MgSO₄), filtered, and concentrated under reduced pressure to give the crude product. The crude material was purified by flash column chromatography (hexane/EtOAc: 3.1) to give the title compound (3.19 g, 61%) as a yellow oil. **¹H NMR** (500 MHz, CDCl₃) δ 8.01 – 7.97 (m, 1H), 7.67 – 7.63 (m, 1H), 7.37 – 7.33 (m, 1H), 6.95 – 6.90 (m, 1H), 1.79 (s, 6H). **¹³C NMR** (126 MHz, CDCl₃) δ 148.6, 142.9, 128.8, 128.3, 126.9, 93.3, 73.7, 29.9. Characterisation data in accordance with literature report.⁶²

1-Fluoro-3,3-dimethyl-1,3-dihydro-1λ³-benzo[d][1,2]iodaoxole – Fluoroiodane (**210**)



Prepared according to a modified literature procedure.⁶³ To a flask, 2-(2-iodophenyl)propan-2-ol **211** (2.882 g, 11 mmol) and acetonitrile (40 mL) were added. Selectfluor (5.06 g, 14.3 mmol, 1.3 equiv.) was added, and the reaction was stirred at room temperature for 16 hours. The mixture was concentrated under reduced pressure to give a white solid. The solid was dissolved in CH₂Cl₂ (~30 mL) and washed with water (3 × 25 mL). The organic phase was concentrated under reduced pressure and further

6 - Experimental

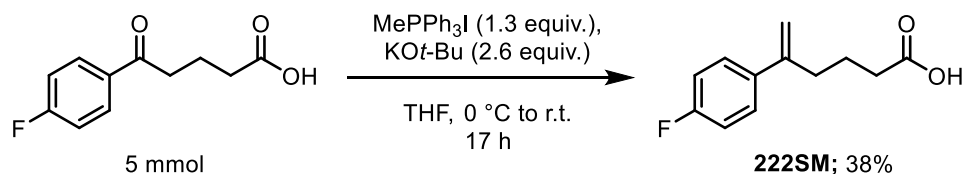
dried under high vacuum to give the crude product as a yellow solid. The crude material was recrystallised (hexane) to give the title compound (0.955 g, 31%) as a pale-yellow solid. M.p. 80-82 °C. $^1\text{H NMR}$ (500 MHz, CDCl_3) δ 7.78 (d, $J = 8.1$ Hz, 1H), 7.55 (t, $J = 7.5$ Hz, 1H), 7.47 (t, $J = 7.3$ Hz, 1H), 7.17 (dd, $J = 7.5, 1.2$ Hz, 2H), 1.52 (s, 6H). $^{13}\text{C NMR}$ (126 MHz, CDCl_3) δ 148.6, 130.7, 130.3, 128.7, 126.1, 116.1, 85.3, 29.1. $^{19}\text{F}\{^1\text{H}\}$ NMR (471 MHz, CDCl_3) δ -142.33. Characterisation data in accordance with literature report.⁶³

Alternatively, fluoroiodane reagent was synthesised by Dr William Riley following a literature procedure.⁶⁴

6.5.2 Mechanochemical Fluorocyclisation of Unsaturated Carboxylic Acids

γ,δ -unsaturated carboxylic acid starting materials were synthesised by Dr William Riley at Leicester University following a literature procedure with the exception of **222SM**.⁶⁵

5-(4-Fluorophenyl)hex-5-enoic acid (**222SM**)



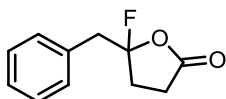
A suspension of methyltriphenylphosphonium iodide (2.63 g, 6.5 mmol, 1.3 equiv.) in dry THF (10 mL) was cooled to 0 °C. Potassium *tert*-butoxide* (1.46 g, 13 mmol, 2.6 equiv.) was added in one portion and the mixture was stirred for 30 min at 0 °C. 5-(4-Fluorophenyl)-5-oxopentanoic acid (0.1051 g, 5 mmol) was added slowly and the reaction mixture was warmed to room temperature and stirred for 16 hours. NaOH (1 M) was added to quench the reaction. CH_2Cl_2 (~25 mL) was added, and the layers separated. The aqueous layer was acidified to pH 2 using HCl (12 M) and the product was then extracted into dichloromethane (3 \times 20 mL), dried (MgSO_4), filtered, and concentrated under reduced pressure to give the title compound (0.394 g, 38 %) as a white solid. M.p. 91-93 °C $^1\text{H NMR}$ (500 MHz, CDCl_3) δ 7.40 – 7.33 (m, 2H), 7.06 – 6.97 (m, 2H), 5.26 (s, 1H), 5.07 (s, 1H), 2.55 (t, $J = 7.4$ Hz, 2H), 2.38 (t, $J = 7.3$ Hz, 2H), 1.84 – 1.74 (m, 2H). $^{13}\text{C NMR}$ (126 MHz, CDCl_3) δ 177.7, 162.5 (d, $J = 246.5$ Hz), 146.5, 136.9 (d, $J = 3.0$ Hz), 127.8 (d, $J = 7.9$ Hz), 115.3 (d, $J = 21.3$ Hz), 113.2, 34.7, 33.0, 23.1. $^{19}\text{F}\{^1\text{H}\}$ NMR (376 MHz, CDCl_3) δ -115.16. Characterisation data in accordance with literature report.⁶⁶

* KOt-Bu was sublimed under vacuum before use (<1 mbar, 180 °C)

General Procedure 9 (GP9): Mechanochemical Fluorolactonisation of Unsaturated Carboxylic Acids

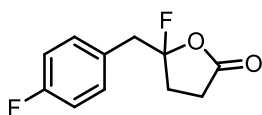
To a 10 mL stainless steel jar (Retsch), a 2.5 g stainless steel milling ball was added. Unsaturated carboxylic acid (0.25 mmol), 1-fluoro-3,3-dimethyl-1,3-dihydro-1 λ^3 -benzo[d][1,2]iodoxole (Fluoroiodane **210**) (0.1050 g, 0.375 mmol) and 1,1,1,3,3,3-hexafluoro-2-propanol (130 μ L, 1.25 mmol) were added under an air atmosphere. The milling jar was then screwed closed and milled at 30 Hz for 1 hour. After the desired reaction time, the mixture was transferred to a flask with CHCl_3 (~2-5 mL). Crude NMR yield was determined by adding benzotrifluoride (10 μ L, 0.083 mmol) as an internal standard. The crude product was concentrated under reduced pressure and purified by flash column chromatography using the noted solvent systems.

5-Benzyl-5-fluorodihydrofuran-2(3H)-one (**216**)



Prepared according to **GP9**. Purified by flash column chromatography (CH_2Cl_2) to give the title compound (0.0466 g, 96%) as a colourless oil. $^1\text{H NMR}$ (500 MHz, CDCl_3) δ 7.37 – 7.27 (m, 5H), 3.29 (d, J = 14.4 Hz, 2H), 2.82 – 2.69 (m, 1H), 2.46 – 2.37 (m, 1H), 2.31 – 2.15 (m, 2H). $^{13}\text{C NMR}$ (126 MHz, CDCl_3) δ 174.8, 133.1 (d, J = 5.6 Hz), 130.5, 128.8, 127.8, 119.3 (d, J = 230.4 Hz), 42.8 (d, J = 28.2 Hz), 31.0 (d, J = 27.6 Hz), 27.1. $^{19}\text{F}\{^1\text{H}\}$ **NMR** (376 MHz, CDCl_3) δ -97.07. **HRMS** (EI) m/z : $[\text{M}-\text{F}]^+$ Calcd for $\text{C}_{11}\text{H}_{10}\text{O}_2$ 174.0673, found: 176.0676. Characterisation data in accordance with literature report.⁶⁷

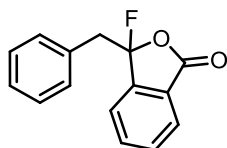
5-Fluoro-5-(4-fluorobenzyl)dihydrofuran-2(3H)-one (**218**)



Prepared according to **GP9**. Purified by flash column chromatography (hexane/EtOAc: 9/1) to give the title compound (0.0477 g, 90%) as a colourless oil. $^1\text{H NMR}$ (500 MHz, CDCl_3) δ 7.30 – 7.21 (m, 2H), 7.02 (t, J = 8.7 Hz, 2H), 3.25 (d, J = 14.6 Hz, 2H), 2.75 (m, 1H), 2.45 (m, 1H), 2.34 – 2.13 (m, 2H). $^{13}\text{C NMR}$ (126 MHz, CDCl_3) δ 174.7 (d, J = 1.2 Hz), 162.5 (d, J = 246.4 Hz), 132.1 (dd, J = 8.1, 0.8 Hz), 128.8 (dd, J = 5.3, 3.4 Hz), 119.0 (dd, J = 230.4, 1.4 Hz), 115.7 (d, J = 21.4 Hz), 42.0 (d, J = 28.5 Hz), 31.1 (d, J = 27.7 Hz), 27.1. $^{19}\text{F}\{^1\text{H}\}$ **NMR** (376 MHz, CDCl_3) δ -97.79, -114.82. **HRMS** (EI) m/z : $[\text{M}]^+$

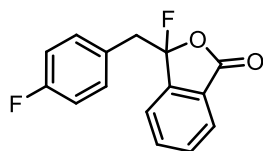
Calcd for $C_{11}H_{10}O_2F_2$ 212.0643, found: 212.0643. Characterisation data in accordance with literature report.⁶⁷

3-Benzyl-3-fluoroisobenzofuran-1(3H)-one (219)



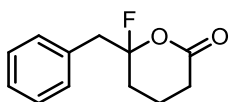
Prepared according to **GP9**. Purified by flash column chromatography (hexane/EtOAc: 19/1) to give the title compound (0.059 g, 97%) as a white solid. M.p. 50-52 °C. **¹H NMR** (500 MHz, $CDCl_3$) δ 7.82 (dd, $J = 7.6, 0.8$ Hz, 1H), 7.69 (t, $J = 7.5$ Hz, 1H), 7.63 – 7.58 (m, 1H), 7.36 (d, $J = 7.6$ Hz, 1H), 7.30 – 7.25 (m, 3H), 7.25 – 7.20 (m, 2H), 3.68 – 3.61 (m, 1H), 3.58 – 3.50 (m, 1H). **¹³C NMR** (126 MHz, $CDCl_3$) δ 166.7 (d, $J = 1.9$ Hz), 144.8 (d, $J = 21.2$ Hz), 134.8 (d, $J = 1.9$ Hz), 132.2 (d, $J = 5.4$ Hz), 131.7 (d, $J = 2.1$ Hz), 130.8 (d, $J = 0.8$ Hz), 128.6, 127.8, 126.5 (d, $J = 1.8$ Hz), 125.9 (d, $J = 0.9$ Hz), 123.29, 115.3 (d, $J = 232.0$ Hz), 42.5 (d, $J = 31.0$ Hz). **¹⁹F {¹H} NMR** (376 MHz, $CDCl_3$) δ -100.76. **HRMS** (EI) m/z : $[M-(F+2H)]^+$ Calcd for $C_{15}H_{10}O_2$ 222.0673, found: 222.0676. Characterisation data in accordance with literature report.⁶⁷

3-Fluoro-3-(4-fluorobenzyl)isobenzofuran-1(3H)-one (220)



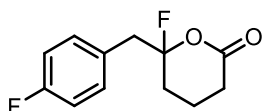
Prepared according to **GP9**. Purified by flash column chromatography (hexane/EtOAc: 19/1) to give the title compound (0.0572 g, 88%) as a white solid. M.p. 48-51 °C. **¹H NMR** (500 MHz, $CDCl_3$) δ 7.81 (m, 1H), 7.69 (m, 1H), 7.60 (m, $J = 7.5, 1.1$ Hz, 1H), 7.38 – 7.36 (m, 1H), 7.17 (dd, $J = 8.3, 5.4$ Hz, 2H), 6.98 – 6.90 (m, 2H), 3.60 – 3.48 (m, 2H). **¹³C NMR** (126 MHz, $CDCl_3$) δ 166.5 (d, $J = 1.9$ Hz), 162.5 (d, $J = 246.5$ Hz), 144.6 (d, $J = 21.2$ Hz), 134.9 (d, $J = 1.9$ Hz), 132.3 (d, $J = 8.1$ Hz), 131.8 (d, $J = 2.1$ Hz), 127.9 (dd, $J = 5.7, 3.4$ Hz), 126.4 (d, $J = 1.7$ Hz), 126.0 (s, $J = 0.8$ Hz), 123.1 (s), 115.5 (d, $J = 21.4$ Hz), 115.1 (d, $J = 232.0$ Hz), 41.7 (d, $J = 31.4$ Hz). **¹⁹F {¹H} NMR** (376 MHz, $CDCl_3$) δ -101.11, -114.61. **HRMS** (ASAP) m/z : $[MH]^+$ Calcd for $C_{15}H_{11}O_2F_2$ 261.0727, found: 261.0733. The NMR data is consistent with the literature.⁶⁷

6-Benzyl-6-fluorotetrahydro-2H-pyran-2-one (221)



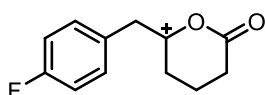
Prepared according to **GP9**. Purified by flash column chromatography (hexane/EtOAc: 19/1) to give the title compound (0.0380 g, 73%) as a colourless oil. **¹H NMR** (500 MHz, CDCl₃) δ 7.40 – 7.27 (m, 5H), 3.24 – 3.18 (m, 2H), 2.69 (m, 1H), 2.41 (m, 1H), 2.12 – 1.96 (m, 2H), 1.83 – 1.61 (m, 2H). **¹³C NMR** (126 MHz, CDCl₃) δ 169.0, 133.6 (d, *J* = 5.6 Hz), 130.6, 128.6, 127.6, 115.6 (d, *J* = 227.3 Hz), 45.4 (d, *J* = 26.6 Hz), 29.2, 29.0 (d, *J* = 26.3 Hz), 14.9 (d, *J* = 3.0 Hz). **¹⁹F {¹H} NMR** (376 MHz, CDCl₃) δ -96.78. HRMS data not obtained as product degraded to **XX** in 2-3 hours. Characterisation data in accordance with literature report.⁶⁷

6-Fluoro-6-(4-fluorobenzyl)tetrahydro-2H-pyran-2-one (222)

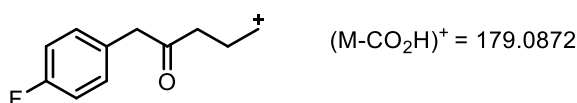
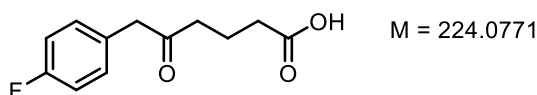


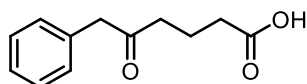
Prepared according to **GP9**. Purified by flash column chromatography (hexane/EtOAc: 19/1) to give the title compound (0.0475 g, 84%) as a colourless oil. **¹H NMR** (500 MHz, CDCl₃) δ 7.29 – 7.21 (m, 2H), 7.04 – 6.97 (m, 2H), 3.17 (d, *J* = 14.9 Hz, 2H), 2.69 (m, 1H), 2.46 – 2.36 (m, 1H), 2.12 – 1.95 (m, 2H), 1.84 – 1.63 (m, 2H). **¹³C NMR** (126 MHz, CDCl₃) δ 168.8 (d, *J* = 1.4 Hz), 162.4 (d, *J* = 246.1 Hz), 132.1 (d, *J* = 8.1 Hz), 129.3 (dd, *J* = 5.5, 3.4 Hz), 115.5 (d, *J* = 21.3 Hz), 115.4 (dd, *J* = 227.2, 1.4 Hz), 44.5 (d, *J* = 26.9 Hz), 29.2 (s), 29.0 (d, *J* = 26.3 Hz), 14.9 (d, *J* = 2.9 Hz). **¹⁹F {¹H} NMR** (376 MHz, CDCl₃) δ -97.38, -115.17. (ASAP) *m/z* 207.0820 ((M-F)⁺, C₁₂H₁₂FO₂ requires 207.0821, 37%), 179.0876 ((4-F-PhCHCOCH₂CH₂CH₂)⁺ requires 179.0872, 100%).

(M-F)⁺ 207.0821

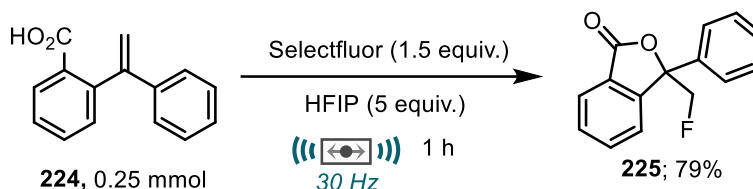


Degradation product



5-Oxo-6-phenylhexanoic acid (223)

6-Benzyl-6-fluorotetrahydro-2H-pyran-2-one (**221**) decomposed *via* hydrodefluorinative ring-opening after a few hours to give the title compound as a white solid in quantitative conversion. ¹H NMR (500 MHz, CDCl₃) δ 7.35 – 7.31 (m, 2H), 7.29 – 7.25 (m, 1H), 7.21 – 7.18 (m, 2H), 3.69 (s, 2H), 2.55 (t, *J* = 7.1 Hz, 2H), 2.34 (t, *J* = 7.2 Hz, 2H), 1.88 (p, *J* = 7.2 Hz, 2H). ¹³C NMR (126 MHz, CDCl₃) δ 207.6, 178.7, 134.2, 129.5, 128.9, 127.2, 50.4, 40.6, 32.9, 18.7. HRMS (ASAP) *m/z*: [M-(OH)]⁺ Calcd for C₁₂H₁₂O 189.0916, found: 189.0912. Characterisation data in accordance with literature report.⁶⁷

Mechanochemical intramolecular fluorolactonisation with Selectfluor - 3-(fluoromethyl)-3-phenylisobenzofuran-1(3H)-one (225)

To a 10 mL stainless steel jar (Retsch) was added a 2.5 g stainless steel milling ball. 2-(1-Phenylvinyl)benzoic acid **224** (0.056 g, 0.25 mmol), Selectfluor (0.1329 g, 0.375 mmol) and 1,1,1,3,3,3-hexafluoro-2-propanol (130 μL, 1.25 mmol) were added under an air atmosphere. The milling jar was then screwed closed and milled at 30 Hz for 1 hour. After the desired reaction time, the mixture was transferred to a flask with CHCl₃ (~2-5 mL). The reaction mixture was filtered to remove insoluble salts. The crude product was concentrated under reduced pressure and purified by flash column chromatography (hexane/EtOAc: 19/1) to give the title compound (0.048 g, 79%) as a white solid. M.p. 100-102 °C. ¹H NMR (500 MHz, CDCl₃) δ 7.95 (d, *J* = 7.7 Hz, 1H), 7.77 – 7.71 (m, 1H), 7.68 (d, *J* = 7.7 Hz, 1H), 7.62 – 7.54 (m, 3H), 7.43 – 7.36 (m, 3H), 4.84 (m, 2H). ¹³C NMR (126 MHz, CDCl₃) δ 169.2, 148.5, 148.5, 134.4, 130.0, 129.3, 129.0, 126.2, 125.7, 125.7, 123.0, 87.63 (d, *J* = 19.6 Hz), 84.8 (d, *J* = 185.1 Hz). ¹⁹F NMR (471 MHz, CDCl₃) δ -222.04 (t, *J* = 47.0 Hz). HRMS (ESI) *m/z*: [MH]⁺ Calcd for C₁₅H₁₂FO₂ 243.0821, found: 243.0833. Characterisation data in accordance with literature report.⁶⁸

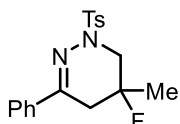
6.5.3 Mechanochemical Fluorocyclisation of β,γ -unsaturated Hydrazones

β,γ -unsaturated hydrazone starting materials were synthesised by Dr William Riley at Leicester University following a literature procedure.⁶⁹

General Procedure 10 (GP10): Mechanochemical Fluorolactonisation of β,γ -Unsaturated Hydrazones

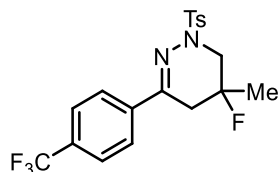
To a 10 mL stainless steel jar (Retsch) was added a 2.5 g stainless steel milling ball. Unsaturated hydrazone (0.25 mmol), 1-fluoro-3,3-dimethyl-1,3-dihydro-1 λ^3 -benzo[d][1,2]iodoxole (0.105 g, 0.375 mmol) and 1,1,1,3,3,3-hexafluoro-2-propanol (52 μ L, 0.5 mmol) were added under an air atmosphere. The milling jar was then screwed closed and milled at 30 Hz for 15 minutes. After the desired reaction, the mixture was transferred to a flask with CHCl_3 (~2-5 mL). Crude NMR yield was determined by adding benzo-trifluoride (10 μ L, 0.083 mmol) as an internal standard. The crude product was concentrated under reduced pressure and purified by flash column chromatography using the noted solvent systems.

5-Fluoro-5-methyl-3-phenyl-1-tosyl-1,4,5,6-tetrahydropyridazine (227)



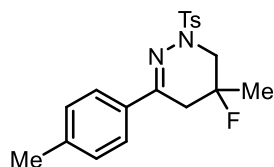
Prepared according to **GP10**. Purified by flash column chromatography (hexane/EtOAc: 4/1) to give the title compound (0.079 g, 91%) as a white solid. M.p. 157-158 °C. **¹H NMR** (500 MHz, CDCl_3) δ 7.85 (d, J = 8.0 Hz, 2H), 7.70 – 7.66 (m, 2H), 7.39 – 7.35 (m, 3H), 7.30 (d, J = 8.0 Hz, 2H), 3.77 – 3.68 (m, 2H), 3.23 (dd, J = 22.7, 11.7 Hz, 1H), 2.86 (app t, J = 18.2, 1H), 2.59 (ddd, J = 25.5, 18.3, 1.7 Hz, 1H), 2.40 (s, 3H), 1.56 (d, J = 20.6 Hz, 3H). **¹³C NMR** (126 MHz, CDCl_3) δ 147.4 (d, J = 2.0 Hz), 144.4, 136.0, 133.3, 129.9, 129.7, 128.6, 128.6, 125.6, 88.0 (d, J = 175.9 Hz), 50.6 (d, J = 25.9 Hz), 35.3 (d, J = 25.5 Hz), 25.0 (d, J = 24.2 Hz), 21.8. **¹⁹F {¹H} NMR** (376 MHz, CDCl_3) δ -141.90. **HRMS** (ESI) m/z : $[\text{MH}]^+$ Calcd for $\text{C}_{18}\text{H}_{20}\text{N}_2\text{O}_2\text{FS}$ 347.1230, found: 347.1223.

5-Fluoro-5-methyl-1-tosyl-3-(4-(trifluoromethyl)phenyl)-1,4,5,6-tetrahydropyridazine (228)



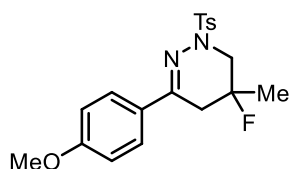
Prepared according to **GP10**. Purified by flash column chromatography (hexane/EtOAc: 4/1) to give the title compound (0.093 g, 90%) as a white solid. M.p. 197- 198 °C. **¹H NMR** (500 MHz, CDCl₃) δ 7.83 (d, *J* = 8.1 Hz, 2H), 7.78 (d, *J* = 7.8 Hz, 2H), 7.62 (d, *J* = 8.2 Hz, 2H), 7.31 (d, *J* = 8.0 Hz, 2H), 3.84 (m, 1H), 3.24 (dd, *J* = 24.1, 11.8 Hz, 1H), 2.86 (app t, *J* = 17.6 Hz, 1H), 2.58 (dd, *J* = 27.2, 18.9 Hz, 1H), 2.41 (s, 3H), 1.58 (d, *J* = 20.6 Hz, 3H). **¹³C NMR** (126 MHz, CDCl₃) δ 145.3 (d, *J* = 0.9 Hz), 144.5, 139.2, 133.3, 131.4 (q, *J* = 32.6 Hz), 129.7, 128.4, 125.7, 125.4 (q, *J* = 3.8 Hz), 123.9 (q, *J* = 273.6 Hz), 87.4 (d, *J* = 176.3 Hz), 50.3 (d, *J* = 25.5 Hz), 35.0 (d, *J* = 25.6 Hz), 24.8 (d, *J* = 24.1 Hz), 21.6. **¹⁹F{¹H} NMR** (376 MHz, CDCl₃) δ -62.73, -142.36. **HRMS** (ESI) *m/z*: [MH]⁺ Calcd for C₁₉H₁₉N₂F₄S 377.1335, found: 377.1330.

5-Fluoro-5-methyl-3-(p-tolyl)-1-tosyl-1,4,5,6-tetrahydropyridazine (229)



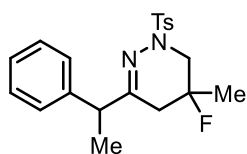
Prepared according to **GP10**. Purified by flash column chromatography (hexane/EtOAc: 4/1) to give the title compound (0.080 g, 89%) as a white solid. M.p. 161-163 °C. **¹H NMR** (500 MHz, CDCl₃) δ 7.88 – 7.79 (m, 2H), 7.59 – 7.56 (m, 2H), 7.31 – 7.28 (m, 1H), 7.21 – 7.14 (m, 1H), 3.69 (ddd, *J* = 11.6, 7.6, 1.9 Hz, 1H), 3.26 – 3.16 (m, 1H), 2.88 – 2.78 (m, 1H), 2.58 (ddd, *J* = 25.1, 18.3, 1.7 Hz, 1H), 2.39 (s, 3H), 2.36 (s, 3H), 1.55 (d, *J* = 20.7 Hz, 3H). **¹³C NMR** (126 MHz, CDCl₃) δ 147.5 (d, *J* = 2.1 Hz), 144.3, 140.1, 133.3, 129.7, 129.3, 128.6, 125.5, 88.2 (d, *J* = 175.7 Hz), 50.6 (d, *J* = 26.1 Hz), 35.4 (d, *J* = 25.5 Hz), 25.1 (d, *J* = 24.2 Hz), 21.7, 21.5 (2 x C). **¹⁹F{¹H} NMR** (376 MHz, CDCl₃) δ -141.76. **HRMS** (ESI) *m/z*: [MH]⁺ Calcd for C₁₉H₂₂N₂O₂FS 361.1386, found: 361.1386.

5-Fluoro-3-(4-methoxyphenyl)-5-methyl-1-tosyl-1,4,5,6-tetrahydropyridazine (230)



Prepared according to **GP10**. Purified by flash column chromatography (hexane/EtOAc: 4/1) to give the title compound (0.086 g, 91%) as a white solid. M.p. 162-164 °C. **¹H NMR** (500 MHz, CDCl₃) δ 7.84 (d, *J* = 7.7 Hz, 2H), 7.63 (d, *J* = 7.8 Hz, 2H), 7.30 (d, *J* = 7.7 Hz, 2H), 6.87 (d, *J* = 7.8 Hz, 2H), 3.83 (s, 3H), 3.72 – 3.61 (m, 1H), 3.22 (dd, *J* = 22.0, 11.7 Hz, 1H), 2.82 (app t, *J* = 18.3 Hz, 1H), 2.63 – 2.48 (m, 1H), 2.40 (s, 3H), 1.55 (d, *J* = 20.7 Hz, 3H). **¹³C NMR** (126 MHz, CDCl₃) δ 161.0, 147.3 (d, *J* = 2.1 Hz), 144.3, 133.3, 129.7, 128.7, 128.6, 127.1, 113.9, 88.3 (d, *J* = 175.8 Hz), 55.5, 50.7 (d, *J* = 26.1 Hz), 35.4 (d, *J* = 25.4 Hz), 25.1 (d, *J* = 24.3 Hz), 21.7. **¹⁹F{¹H} NMR** (376 MHz, CDCl₃) δ - 141.63. **HRMS** (ESI) *m/z*: [MH]⁺ Calcd for C₁₉H₂₂N₂OFS 377.1335, found: 377.1330.

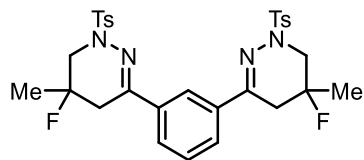
5-Fluoro-5-methyl-3-(1-phenylethyl)-1-tosyl-1,4,5,6-tetrahydropyridazine (231)



Prepared according to **GP10**. Purified by flash column chromatography (hexane/EtOAc: 4/1) to give the title compound (0.075 g, 80%) as a white solid with both diastereoisomers present. M.p. 130-133 °C. **¹H NMR** (500 MHz, CDCl₃) δ 7.83 (d, *J* = 8.0 Hz, 2H), 7.34 (d, *J* = 7.9 Hz, 2H), 7.24 – 7.18 (m, 3H), 7.05 – 6.96 (m, 2H), 3.64 – 3.40 (m, 2H), 3.11 – 2.90 (m, 1H), 2.47 (s, 3H), 2.23 – 2.07 (m, 1H), 2.00 – 1.85 (m, 1H), 1.44 – 1.26 (m, 6H). **¹⁹F{¹H} NMR** (376 MHz, CDCl₃) δ -142.64, -142.76 (Both diastereomers). **HRMS** (ESI) *m/z*: [MH]⁺ Calcd for C₂₀H₂₄FN₂O₂S 375.1543, found: 375.1542.

Diastereoisomer 1: **¹³C NMR** (126 MHz, CDCl₃) δ 154.8 (d, *J* = 1.7 Hz), 144.1, 142.3, 132.9, 129.4, 128.7 (2 x C) 127.4, 127.0, 87.9 (d, *J* = 175.5 Hz), 50.8, 47.0, 36.2 (d, *J* = 25.0 Hz), 24.4 (d, *J* = 24.4 Hz), 21.6, 18.6,

Diastereoisomer 2: **¹³C NMR** (126 MHz, CDCl₃) δ 154.? (d, *J* = 1.7 Hz), 144.1, 142.1, 132.9, 129.3, 128.67, 128.65, 127.4, 126.9, 87.8 (d, *J* = 175.9 Hz), 50.8, 46.7, 35.8 (d, *J* = 25.6 Hz), 24.5 (d, *J* = 24.2 Hz), 21.6, 18.6.

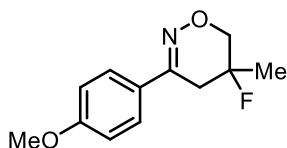
1,3-Bis(5-fluoro-5-methyl-1-tosyl-1,4,5,6-tetrahydropyridazin-3-yl)benzene (232)

Prepared according to **GP10**. Purified by flash column chromatography (hexane/EtOAc: 4/1) to give the title compound (0.089 g, 58%) as a white solid with both diastereoisomers present. M.p. 177-178 °C. **¹H NMR** (500 MHz, CDCl₃) δ 8.07 – 8.03 (m, 1H), 7.89 – 7.85 (m, 4H), 7.64 – 7.60 (m, 2H), 7.37 – 7.31 (m, 5H), 3.84 – 3.73 (m, 2H), 3.24 (dd, *J* = 23.5, 11.8 Hz, 2H), 3.22 (dd, *J* = 23.6, 11.9 Hz, 2H), 2.86 (t, *J* = 18.1 Hz, 2H), 2.62 (d, *J* = 18.4 Hz, 1H), 2.56 (d, *J* = 18.5 Hz, 1H), 2.39 (s, 7H), 1.59 (d, *J* = 20.6 Hz, 7H). **¹³C NMR** (126 MHz, CDCl₃) δ 146.7, 144.6, 136.3, 133.3, 129.9 (d, *J* = 1.5 Hz), 128.7, 128.6, 126.7, 122.7, 87.9 (d, *J* = 176.1 Hz), 50.6 (d, *J* = 25.8 Hz), 41.0, 35.3 (d, *J* = 25.6 Hz), 25.1 (d, *J* = 24.2 Hz), 21.8 (s). **¹⁹F NMR** (376 MHz, CDCl₃) δ -141.87, -141.91. (Both diastereoisomers). **HRMS** (ESI) *m/z*: [MH]⁺ Calcd for C₃₀H₃₃F₂N₄O₄S₂ 615.1911, found: 615.1909.

6.5.4 Mechanochemical Fluorocyclisation of β,γ-unsaturated Oximes**General Procedure 11 (GP11): Mechanochemical Fluorolactonisation of β,γ-Unsaturated Oximes**

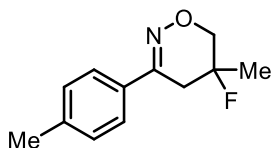
To a 10 mL stainless steel jar (Retsch) was added a 2.5 g stainless steel milling ball. Unsaturated hydrazone (0.25 mmol), 1-fluoro-3,3-dimethyl-1,3-dihydro-1λ³-benzo[*d*][1,2]iodoxole (0.105 g, 0.375 mmol) and 1,1,1,3,3,3-hexafluoro-2-propanol (52 μL, 0.5 mmol) were added under an air atmosphere. The milling jar was then screwed closed and milled at 30 Hz for 15 minutes. After the desired reaction, the mixture was transferred to a flask with CHCl₃ (~2-5 mL). Crude NMR yield was determined by adding benzotrifluoride (10 μL, 0.083 mmol) as an internal standard. The crude product was concentrated under reduced pressure and purified by flash column chromatography using the noted solvent systems.

5-Fluoro-3-(4-methoxyphenyl)-5-methyl-5,6-dihydro-4H-1,2-oxazine (234)



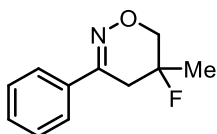
Prepared according to **GP11**. Purified by flash column chromatography (hexane/EtOAc: 4/1) followed by trituration with hexane to give the title compound (0.045 g, 80%) as a white solid. M.p. 105-107 °C. **¹H NMR** (500 MHz, CDCl₃) δ 7.64 (d, *J* = 8.8 Hz, 2H), 6.91 (d, *J* = 8.8 Hz, 2H), 4.06 (ddd, *J* = 11.5, 7.8, 1.9 Hz, 1H), 3.73 (dd, *J* = 23.3, 11.6 Hz, 3H), 2.88 (app t, *J* = 18.7 Hz, 1H), 2.66 (ddd, *J* = 25.8, 18.2, 1.2 Hz, 1H), 1.54 (d, *J* = 20.7 Hz, 3H). **¹³C NMR** (126 MHz, CDCl₃) δ 161.2, 153.5, 127.4, 127.0, 114.1, 87.6 (d, *J* = 174.0 Hz), 71.1 (d, *J* = 24.6 Hz), 55.5, 33.6 (d, *J* = 25.9 Hz), 23.7 (d, *J* = 24.8 Hz). **¹⁹F {¹H} NMR** (376 MHz, CDCl₃) δ -146.79. **HRMS** (ESI) *m/z*: [MH]⁺ Calcd for C₁₂H₁₅O₂F 224.1087, found: 224.1080.

5-Fluoro-5-methyl-3-(p-tolyl)-5,6-dihydro-4H-1,2-oxazine (237)



Prepared according to **GP11**. Purified by flash column chromatography (hexane/EtOAc: 4/1) to give the title compound (0.037 g, 71%) as a white solid. M.p. 100-102 °C. **¹H NMR** (500 MHz, CDCl₃) δ 7.58 (d, *J* = 8.4 Hz, 2H), 7.20 (d, *J* = 8.0 Hz, 2H), 4.07 (ddd, *J* = 11.6, 7.7, 2.0 Hz, 1H), 3.79 – 3.69 (m, 1H), 2.94 – 2.84 (m, 1H), 2.67 (ddd, *J* = 25.8, 18.3, 1.7 Hz, 1H), 2.37 (s, 3H), 1.54 (d, *J* = 20.7 Hz, 3H). **¹³C NMR** (126 MHz, CDCl₃) δ 153.7, 140.2, 132.0, 129.3, 125.4, 87.4 (d, *J* = 174.0 Hz), 71.0 (d, *J* = 24.6 Hz), 33.5 (d, *J* = 26.0 Hz), 23.6 (d, *J* = 24.7 Hz), 21.3. **¹⁹F {¹H} NMR** (376 MHz, CDCl₃) δ -146.91. **HRMS** (ESI) *m/z*: [MH]⁺ Calcd for C₁₂H₁₅OF 208.1138, found: 208.1143.

5-Fluoro-5-methyl-3-phenyl-5,6-dihydro-4H-1,2-oxazine (238)

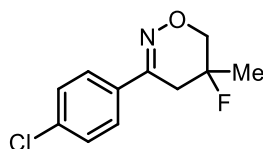


Prepared according to **GP11**. Purified by flash column chromatography (hexane/EtOAc: 4/1) and then trituration with hexane to give the title compound (0.036 g, 74%) as a white solid. M.p. 62-65 °C. **¹H NMR** (500 MHz, CDCl₃) δ 7.64 – 7.60 (m, 2H), 7.36 – 7.31 (m,

6 - Experimental

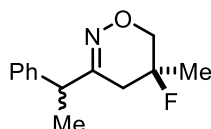
3H), 4.02 (ddd, $J = 11.6, 7.8, 2.3$ Hz, 1H), 3.73 – 3.63 (m, 1H), 2.93 – 2.78 (m, 1H), 2.62 (ddd, $J = 26.1, 18.3, 1.7$ Hz, 1H), 1.48 (d, $J = 20.6$ Hz, 3H). $^{13}\text{C NMR}$ (126 MHz, CDCl_3) δ 153.8, 134.9, 130.2, 128.8, 125.6, 87.3 (d, $J = 174.0$ Hz), 71.1 (d, $J = 24.5$ Hz), 33.6 (d, $J = 26.0$ Hz), 23.7 (d, $J = 24.6$ Hz). $^{19}\text{F}\{^1\text{H}\}$ NMR (376 MHz, CDCl_3) δ -147.10. HRMS (EI) m/z : $[\text{M}]^+$ Calcd for $\text{C}_{11}\text{H}_{12}\text{OF}$ 193.0897, found: 193.0897.

3-(4-Chlorophenyl)-5-fluoro-5-methyl-5,6-dihydro-4H-1,2-oxazine (239)



Prepared according to **GP11**. Purified by flash column chromatography (hexane/EtOAc: 4/1) and then trituration with hexane to give the title compound (0.044 g, 78%) as a white solid. M.p. 95-98 °C. $^1\text{H NMR}$ (500 MHz, CDCl_3) δ 7.63 (d, $J = 8.3$ Hz, 2H), 7.37 (d, $J = 8.3$ Hz, 2H), 4.14 – 4.06 (m, 1H), 3.75 (dd, $J = 23.9, 11.8$ Hz, 1H), 2.87 (app t, $J = 18.4$ Hz, 1H), 2.64 (dd, $J = 26.8, 18.3$ Hz, 1H), 1.55 (d, $J = 20.5$ Hz, 3H). $^{13}\text{C NMR}$ (126 MHz, CDCl_3) δ 152.6, 136.2, 133.4, 129.0, 126.9, 87.1 (d, $J = 174.1$ Hz), 71.1 (d, $J = 24.3$ Hz), 33.4 (d, $J = 26.0$ Hz), 23.6 (d, $J = 24.6$ Hz). $^{19}\text{F}\{^1\text{H}\}$ NMR (376 MHz, CDCl_3) δ -147.40. HRMS (EI) m/z : $[\text{M}]^+$ Calcd for $\text{C}_{11}\text{H}_{11}\text{ON}^{35}\text{ClF}$ 227.0508, found: 227.0508.

5-Fluoro-5-methyl-3-(1-phenylethyl)-5,6-dihydro-4H-1,2-oxazine (240)



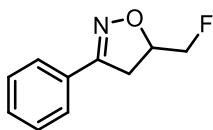
Prepared according to **GP11**. Purified by flash column chromatography (hexane/EtOAc: 4/1). The product was then further purified by vacuum kugelrohr distillation (80-85 °C) to give the title compound (0.021 g, 47%) as a colourless oil with a d.r. of 3:2.

Data for major diastereomer: $^1\text{H NMR}$ (500 MHz, CDCl_3) δ 7.36 – 7.32 (m, 2H), 7.28 – 7.24 (m, 3H), 3.99 – 3.86 (m, 1H), 3.73 – 3.51 (m, 2H), 2.35 – 1.89 (m, 2H), 1.50 (d, $J = 7.1$ Hz, 3H), 1.33 (d, $J = 20.7$ Hz, 3H). $^{13}\text{C NMR}$ (126 MHz, CDCl_3) δ 159.8, 141.7, 129.0, 127.6, 127.3, 87.6 (d, $J = 174.0$ Hz), 71.1 (d, $J = 24.7$ Hz), 45.4, 33.1 (d, $J = 25.9$ Hz), 23.4 (d, $J = 24.8$ Hz), 18.0. $^{19}\text{F}\{^1\text{H}\}$ NMR (376 MHz, CDCl_3) δ -147.30.

Data for minor diastereomer: $^1\text{H NMR}$ (500 MHz, CDCl_3) (selected) δ 1.31 (d, $J = 20.7$ Hz, 3H). $^{13}\text{C NMR}$ (126 MHz, CDCl_3) δ 159.5, 142.0, 129.0, 127.6, 127.3, 87.6 (d, $J = 173.7$ Hz), 71.1 (d, $J = 24.4$ Hz), 46.0, 33.7 (d, $J = 25.7$ Hz), 23.3 (d, $J = 24.8$ Hz), 18.3. $^{19}\text{F}\{^1\text{H}\}$ NMR (376 MHz, CDCl_3) δ -147.48.

Mixture: **FTIR** (ν_{\max} cm^{-1} , thin film): 2974, 2929, 1492, 1452, 1382, 1282, 1107, 1007, 851, 802, 760, 697. **HRMS** (ESI) m/z : $[\text{MH}]^+$ Calcd for $\text{C}_{13}\text{H}_{17}\text{NOF}$ 222.1924, found: 222.1298.

5-(Fluoromethyl)-3-phenyl-4,5-dihydroisoxazole (243)



Prepared according to **GP11**. Purified by flash column chromatography (hexane/EtOAc: 9/1) and then trituration with hexane to give the title compound (0.021 g, 47%) as a white solid. M.p. 40-42 °C. **^1H NMR** (500 MHz, CDCl_3) δ 7.71 – 7.65 (m, 2H), 7.44 – 7.40 (m, 3H), 5.04 – 4.88 (m, 1H), 4.62 – 4.47 (m, 2H), 3.47 (dd, $J = 16.7, 11.0$ Hz, 1H), 3.30 (dd, $J = 16.7, 7.3$ Hz, 1H). **^{13}C NMR** (126 MHz, CDCl_3) δ 156.3, 130.5, 128.9, 126.9, 83.0 (d, $J = 174.9$ Hz), 78.8 (d, $J = 20.4$ Hz), 36.4 (d, $J = 6.0$ Hz). **^{19}F $\{^1\text{H}\}$ NMR** (376 MHz, CDCl_3) δ -230.57. **HRMS** (ESI) m/z : $[\text{MH}]^+$ Calcd for $\text{C}_{10}\text{H}_{11}\text{NOF}$ 180.0825, found: 180.0825.

6.6 Bibliography

- 1 Q. Cao, W. I. Nicholson, A. C. Jones and D. L. Browne, *Org. Biomol. Chem.*, 2019, **17**, 1722–1726.
- 2 V. P. Reddy, K. Swapna, A. V. Kumar and K. R. Rao, *J. Org. Chem.*, 2009, **74**, 3189–3191.
- 3 Y.-C. Wong, T. T. Jayanth and C.-H. Cheng, *Org. Lett.*, 2006, **8**, 5613–5616.
- 4 N. Park, K. Park, M. Jang and S. Lee, *J. Org. Chem.*, 2011, **76**, 4371–4378.
- 5 C. Liu and M. Szostak, *Org. Chem. Front.*, 2021, **8**, 4805–4813.
- 6 Y. Lin, M. Cai, Z. Fang and H. Zhao, *Tetrahedron*, 2016, **72**, 3335–3343.
- 7 J. Mao, T. Jia, G. Frensch and P. J. Walsh, *Org. Lett.*, 2014, **16**, 5304–5307.
- 8 X. Wu and G. Yan, *Synlett*, 2015, **26**, 537–542.
- 9 X. Wang, G. D. Cuny and T. Noël, *Angew. Chem. Int. Ed.*, 2013, **52**, 7860–7864.
- 10 H. Li, C. Tao, Y. Xie, A. Wang, Y. Chang, H. Yu, S. Yu and Y. Wei, *Green Chem.*, 2021, **23**, 6059–6064.
- 11 J. Zhao, H. Fang, J. Han, Y. Pan and G. Li, *Adv. Synth. Catal.*, 2014, **356**, 2719–2724.
- 12 K. Colas, R. Martín-Montero and A. Mendoza, *Angew. Chem. Int. Ed.*, 2017, **56**, 16042–16046.
- 13 N. Kennedy, P. Liu and T. Cohen, *Angew. Chem. Int. Ed.*, 2016, **55**, 383–386.
- 14 K. D. Jones, D. J. Power, D. Bierer, K. M. Gericke and S. G. Stewart, *Org. Lett.*, 2018, **20**, 208–211.
- 15 A. Tota, S. St John-Campbell, E. L. Briggs, G. O. Estévez, M. Afonso, L. Degennaro, R. Luisi and J. A. Bull, *Org. Lett.*, 2018, **20**, 2599–2602.
- 16 H.-J. Xu, Y.-F. Liang, Z.-Y. Cai, H.-X. Qi, C.-Y. Yang and Y.-S. Feng, *J. Org. Chem.*, 2011, **76**, 2296–2300.
- 17 D. Dheer, C. Behera, D. Singh, M. Abdulla, G. Chashoo, S. B. Bharate, P. N. Gupta and R. Shankar, *Eur. J. Med. Chem.*, 2020, **207**, 112813.
- 18 H.-F. Wang, S.-Y. Wang, T.-Z. Qin and W. Zi, *Chem. – Eur. J.*, 2018, **24**, 17911–17914.
- 19 J. Duan, Y.-F. Du, X. Pang and X.-Z. Shu, *Chem. Sci.*, 2019, **10**, 8706–8712.
- 20 O. Vechorkin, V. Proust and X. Hu, *J. Am. Chem. Soc.*, 2009, **131**, 9756–9766.
- 21 D. A. Everson, R. Shrestha and D. J. Weix, *J. Am. Chem. Soc.*, 2010, **132**, 920–921.
- 22 T. Iwasaki, X. Min, A. Fukuoka, H. Kuniyasu and N. Kambe, *Angew. Chem. Int. Ed.*, 2016, **55**, 5550–5554.
- 23 S. KC, P. Basnet, S. Thapa, B. Shrestha and R. Giri, *J. Org. Chem.*, 2018, **83**, 2920–2936.
- 24 W. Xu and N. Yoshikai, *Chem. Sci.*, 2017, **8**, 5299–5304.
- 25 S. Thapa, S. K. Gurung, D. A. Dickie and R. Giri, *Angew. Chem. Int. Ed.*, 2014, **53**, 11620–11624.
- 26 B. Shrestha, S. Thapa, S. K. Gurung, R. A. S. Pike and R. Giri, *J. Org. Chem.*, 2016, **81**, 787–802.
- 27 R. Agata, H. Takaya, H. Matsuda, N. Nakatani, K. Takeuchi, T. Iwamoto, T. Hatakeyama and M. Nakamura, *Bull. Chem. Soc. Jpn.*, , DOI:10.1246/bcsj.20180333.
- 28 J. W. Hilborn, E. MacKnight, J. A. Pincock and P. J. Wedge, *J. Am. Chem. Soc.*, 1994, **116**, 3337–3346.
- 29 X. Lu, B. Xiao, L. Liu and Y. Fu, *Chem. – Eur. J.*, 2016, **22**, 11161–11164.
- 30 Y. Sumida, T. Sumida and T. Hosoya, *Synthesis*, 2017, **49**, 3590–3601.
- 31 Q. Cao, J. L. Howard, E. Wheatley and D. L. Browne, *Angew. Chem. Int. Ed.*, 2018, **57**, 11339–11343.
- 32 D. A. Everson, B. A. Jones and D. J. Weix, *J. Am. Chem. Soc.*, 2012, **134**, 6146–6159.

- 33 G. Dilauro, C. S. Azzollini, P. Vitale, A. Salomone, F. M. Perna and V. Capriati, *Angew. Chem. Int. Ed.*, 2021, **60**, 10632–10636.
- 34 D. J. Charboneau, E. L. Barth, N. Hazari, M. R. Uehling and S. L. Zultanski, *ACS Catal.*, 2020, **10**, 12642–12656.
- 35 A. J. Challinor, M. Calin, G. S. Nichol, N. B. Carter and S. P. Thomas, *Adv. Synth. Catal.*, 2016, **358**, 2404–2409.
- 36 C.-T. Yang, Z.-Q. Zhang, Y.-C. Liu and L. Liu, *Angew. Chem. Int. Ed.*, 2011, **50**, 3904–3907.
- 37 G. Meng and M. Szostak, *Org. Biomol. Chem.*, 2016, **14**, 5690–5707.
- 38 F. Bie, X. Liu, Y. Shi, H. Cao, Y. Han, M. Szostak and C. Liu, *J. Org. Chem.*, 2020, **85**, 15676–15685.
- 39 F. Bie, X. Liu, H. Cao, Y. Shi, T. Zhou, M. Szostak and C. Liu, *Org. Lett.*, 2021, **23**, 8098–8103.
- 40 Y. Liu, M. Achtenhagen, R. Liu and M. Szostak, *Org. Biomol. Chem.*, 2018, **16**, 1322–1329.
- 41 K. Govindan and W.-Y. Lin, *Org. Lett.*, 2021, **23**, 1600–1605.
- 42 J. Zhuo, Y. Zhang, Z. Li and C. Li, *ACS Catal.*, 2020, **10**, 3895–3903.
- 43 W. J. Kerr, A. J. Morrison, M. Pazicky and T. Weber, *Org. Lett.*, 2012, **14**, 2250–2253.
- 44 Y. Li, Y. Li, L. Peng, D. Wu, L. Zhu and G. Yin, *Chem. Sci.*, 2020, **11**, 10461–10464.
- 45 P. Zhang, C. “Chip” Le and D. W. C. MacMillan, *J. Am. Chem. Soc.*, 2016, **138**, 8084–8087.
- 46 D. Wang and Z. Zhang, *Org. Lett.*, 2003, **5**, 4645–4648.
- 47 F. Jafarpour, S. Rajai-Daryasarei and M. H. Gohari, *Org. Chem. Front.*, 2020, **7**, 3374–3381.
- 48 D. G. Kohler, S. N. Gockel, J. L. Kennemur, P. J. Waller and K. L. Hull, *Nat. Chem.*, 2018, **10**, 333–340.
- 49 G. Blay, I. Fernández, B. Monje and J. R. Pedro, *Molecules*, 2004, **9**, 365–372.
- 50 L. Zhang, X. Si, Y. Yang, S. Witzel, K. Sekine, M. Rudolph, F. Rominger and A. S. K. Hashmi, *ACS Catal.*, 2019, **9**, 6118–6123.
- 51 D. Stevanović, A. Pejović, I. S. Damljanović, M. D. Vukićević, G. Dobrikov, V. Dimitrov, M. S. Denić, N. S. Radulović and R. D. Vukićević, *Helv. Chim. Acta*, 2013, **96**, 1103–1110.
- 52 H. Nambu, K. Hata, M. Matsugi and Y. Kita, *Chem. – Eur. J.*, 2005, **11**, 719–727.
- 53 D. M. Fialho, E. Etemadi-Davan, O. C. Langner, B. S. Takale, A. Gadakh, G. Sambasivam and B. H. Lipshutz, *Org. Lett.*, 2021, **23**, 3282–3286.
- 54 X.-H. Yang, J.-H. Xie, W.-P. Liu and Q.-L. Zhou, *Angew. Chem. Int. Ed.*, 2013, **52**, 7833–7836.
- 55 D. Guijarro, Ó. Pablo and M. Yus, *J. Org. Chem.*, 2013, **78**, 3647–3654.
- 56 R. Shi and X. Hu, *Angew. Chem. Int. Ed.*, 2019, **58**, 7454–7458.
- 57 G. S. Lee, J. Won, S. Choi, M.-H. Baik and S. H. Hong, *Angew. Chem. Int. Ed.*, 2020, **59**, 16933–16942.
- 58 T. Hunt, A. F. Parsons and R. Pratt, *Synlett*, 2005, **2005**, 2978–2980.
- 59 M. Das, M. D. Vu, Q. Zhang and X.-W. Liu, *Chem. Sci.*, 2019, **10**, 1687–1691.
- 60 S. Nicolai, R. Sedigh-Zadeh and J. Waser, *J. Org. Chem.*, 2013, **78**, 3783–3801.
- 61 P. Lei, G. Meng, Y. Ling, J. An and M. Szostak, *J. Org. Chem.*, 2017, **82**, 6638–6646.
- 62 F. Chahdoura, S. Mallet-Ladeira and M. Gómez, *Org. Chem. Front.*, 2015, **2**, 312–318.
- 63 C. Y. Legault and J. Prévost, *Acta Crystallogr. Sect. E Struct. Rep. Online*, 2012, **68**, o1238–o1238.
- 64 G. C. Geary, E. G. Hope, K. Singh and A. M. Stuart, *Chem. Commun.*, 2013, **49**, 9263–9265.

6 - Experimental

- 65 G. C. Geary, E. G. Hope and A. M. Stuart, *Angew. Chem. Int. Ed.*, 2015, **54**, 14911–14914.
- 66 M. Aursnes, J. E. Tungen and T. V. Hansen, *J. Org. Chem.*, 2016, **81**, 8287–8295.
- 67 G. C. Geary, E. G. Hope and A. M. Stuart, *Angew. Chem. Int. Ed.*, 2015, **54**, 14911–14914.
- 68 J.-F. Zhao, X.-H. Duan, H. Yang and L.-N. Guo, *J. Org. Chem.*, 2015, **80**, 11149–11155.
- 69 W. Riley, A. C. Jones, K. Singh, D. L. Browne and A. M. Stuart, *Chem. Commun.*, 2021, **57**, 7406–7409.